Appendix A. Proposed LRFD Bridge Design Pier Protection Specifications

PROPOSED PRELIMINARY LRFD BRIDGE PIER PROTECTION GUIDELINES

3.6.5 – Vehicular Collision Force: *CT*

3.6.5.1 – Protection of Structures

Unless the Owner determines that site conditions indicate otherwise, abutments and piers located within ~~a distance of 30.0 ft to the edge of roadway~~ the clear zone as defined by the Roadside Design Guide shall be investigated for collision. Collision shall be addressed by either providing structural resistance or by redirecting or absorbing the collision load. The provisions of Article 2.3.2.2.1 shall apply as appropriate.

Where the design choice is to provide structural resistance, the pier or abutment shall be designed for an equivalent static force of 600 kips, which is assumed to act in a direction of zero to 15 degrees with the edge of the pavement in a horizontal plane, at a distance between 2.0 and 5.0 ft above the ground, whichever produces the critical shear or moment in the pier component and the connections to the foundation or pier cap.

Each of the following substructure components are considered to have adequate structural resistance to bridge collapse due to vehicular impacts:

1. Substructure components that are backed by soil (e.g., abutments)
2. Reinforced concrete pier components that are at least 3-ft thick and have a concrete cross-sectional area greater than 30 ft^2 as measured in the horizontal plane at all elevations from the top of the pier foundation to a height of at least 5.0 ft above the grade.
3. Pier systems with three or more columns where the designer shows by calculation that the superstructure will not collapse with one column missing when subjected to the full dead load with a 1.1 load factor and the live load in the permanent travel lanes with a load factor of 1.0.
4. Piers supporting a bridge superstructure where it is shown by calculation that the superstructure will not collapse with one column missing when subjected to the full dead load with a 1.1 load factor and the live load in the permanent travel lanes with a load factor of 1.0.
5. Pier walls and struts between columns that have been designed and detailed as MASH TL-5 longitudinal traffic barriers according to Section 13.

C3.6.5.1

Where an Owner chooses to make an assessment of site conditions for the purpose of implementing this provision, input from highway or highway safety engineers and structural engineers should be part of that assessment.

The equivalent static force of 600 kips is based on full-scale crash tests of rigid columns impacted by 80.0-kip tractor trailers at 50 mph as well as finite element simulations of 80.0-kip tractor trailer trucks striking pier columns with a variety of typical diameters and reinforcement details. For individual column shafts, the 600-kips load should be considered a point load. Field observations indicate shear failures are one important ~~the primary~~ mode of failure for individual columns but field observations have also indicated that flexural failures and failures between the column and cap or the column and foundation can sometimes occur depending on the detailing. The designer should examine not only the shear capacity of the column but should also verify by calculation that the flexural capacity and connections are sufficient for the 600-kip design impact load. ~~and columns~~ Columns that are 30.0 in. in diameter and smaller are the most vulnerable to impacts. For wall piers, the load may be considered to be a point load or may be distributed over an area deemed suitable for the size of the structure and the anticipated impacting vehicle, but not greater than 5.0 ft wide by 2.0 ft high centered around the assumed impact point. These dimensions were determined by considering the size of a truck frame.

Requirements for train collision loads found in previous editions have been removed. Designers are encouraged to consult the AREMA Manual for Railway Engineering or local railroad company guidelines for train collision requirements.

For the purpose of this Article, a barrier may be considered structurally independent if it does not transmit loads to the bridge.

Where the design choice is to redirect or absorb the collision load, protection shall consist of one of the following:

- ~~An embankment;~~
- ~~A structurally independent, crashworthy ground-mounted 54.0 in high barrier, located within 10.0 ft from the component being protected; or~~
- ~~A 42.0 in. high barrier located at more than 10.0 ft from the component being protected.~~
- For new or retrofit construction, a minimum 42.0-inch high MASH crash tested rigid TL-5 barrier located such that the top edge of the traffic face of the barrier is 3.25 ft. or more from the edge of the lane to the nearest traffic face of the pier component being protected.
- For retrofit construction, a minimum 42.0-inch high MASH crash tested rigid TL-5 barrier may be placed closer than 3.25 ft from the top edge of the traffic face of the barrier to the nearest traffic face of the pier component being protected when there is no other practical option.

Such rigid barriers shall be structurally and geometrically capable of surviving the crash test for MASH Test Level 5 as specified in Section 13.

3.6.5.2 – Vehicle Collision with Barriers

The provisions of Section 13 shall apply for assessing the strength and geometry of a rigid barrier used for pier component protection. The provisions of Article 2.3.2.2.1 shall apply as appropriate except if an independently supported rigid MASH TL-5 barrier is used it shall be placed such that there is at least 3.25 ft between the traffic face of the barrier and the nearest face of the pier component. Barriers used for pier protection shall be MASH crashed TL-5 rigid concrete barriers.

Barriers should be placed on the site according to the recommendations of the AASHTO Roadside Design Guide. The MASH TL-5 rigid shielding barrier must be at least 42 inches tall. A minimum barrier length of 60 ft upstream of the leading edge of the pier system plus the entire length of the pier system shall be shielded.

~~Full-scale crash tests have shown that some vehicles have a greater tendency to lean over or partially cross over a 42.0 in. high barrier than a 54.0 in. high barrier. This behavior would allow a significant collision of the vehicle with the component being protected if the component is located within a few ft of the barrier. If the component is more than about 10.0 ft behind the barrier, the difference between the two barrier heights is no longer important.~~ Prior guidance indicated that if pier components were located closer than 10.0 ft from the shielding barrier a 54.0 in. tall barrier should be used. Recent full-scale crash tests and finite element simulations indicate that the modern trailer suspensions result in much more stable impacts than was the case in crash tests of older trailer suspensions. If a trailer does lean over the barrier and contact a pier component, the interaction will not involve the entire mass of the vehicle and is unlikely to develop sufficient impact forces to put the pier system at risk of failure. It is preferable to allow 3.25 ft of space between the top traffic face of the barrier and the face of the nearest pier component to minimize contact with a heavy vehicle. In some retrofit situations, however, it may be impossible to provide this amount of space given the existing pier location and arrangement of the roadway. In such cases it is permissible to place the barrier closer to the face of at-risk pier components.

One way to determine whether site conditions qualify for exemption from protection is to evaluate the annual frequency of bridge collapse ~~impact~~ from impacts with heavy vehicles. With approval of the Owner, the expected annual frequency ~~for a bridge pier to be hit by a heavy vehicle, AF_{HPB},~~ of bridge collapse, AF_{BC}, can be calculated ~~by~~ as follows:

1. Identify each approach direction i where a pier component is at risk of an impact from approaching traffic.
2. Calculate the annual frequency of bridge collapse as follows:

$$AF_{BC} = \sum_{i=1}^{m} N_i \cdot HVE_i \cdot P(C|HVE_i) \cdot P(Q_{CT} > R_{CPC}|C)$$ (C3.5.6.1-1)

where:

N_i = The site-specific adjustment factor, Ni, from Table C3.6.5.1-1.

HVE_i = The heavy vehicle base encroachment frequency from Table C3.6.5.1-2.

$P(C| HVE_i)$ = The probability of a collision given a heavy vehicle encroachment from Table C3.6.5.1-3.

$P(Q_{CT}>R_{CPC}|C)$ = The probability of the worst-case collision force, Q_{CT}, exceeding the critical pier component capacity, R_{CPC}, from Table C3.6.5.1-4.

~~$AF_{HBP} = 2(ADTT)(P_{HBP})365$ (C3.5.6.1-1)~~

~~where:~~

~~ADTT = the number of trucks per day in one direction~~

~~P_{HBP} = the annual probability for a bridge pier to be hit by a heavy vehicle~~

~~Table C.3.6.1.4.2-1 may be used to determine ADTT from available ADT date.~~

~~P_{HBP} = 3.457×10^{-9} for undivided roadways in tangent and horizontally curved sections~~

~~1.090×10^{-9} for divided roadways in tangent sections~~

~~2.184×10^{-9} for divided roadways in horizontally curved sections~~

Design for vehicular collision force is not required if ~~AF_{HBP}~~ the annual frequency of bridge collapse, AF_{BC}, is less than 0.0001 for critical or essential bridges or 0.001 for typical bridges. If the annual frequency of bridge collapse, AF_{BC}, is greater than or equal to 0.0001 for critical or essential bridges or 0.001 for typical bridges and the pier components are not designed to resist vehicular collision forces, then the pier system must be shielded as described in Article 3.6.5.1.

~~The determination of annual frequency for a bridge pier to be hit by a heavy vehicle, AF_{HBP}, is derived from limited statistical studies performed by the Texas Transportation Institute. Due to limited data, no distinction has been made between tangent sections and horizontally curved sections for undivided roadways.~~ The target values for ~~AF_{HBP}~~ AF_{BC} mirror those for vessel collision force found in Article 3.14.5.

~~Table C3.6.5.1-1 provides typical resulting values for AF_{HBP}.~~

Table 1. Proposed Table C3.6.5.1-1: Site Specific Adjustment Factor, N_i.

Major Accesses‡			**Lane Width**			**Horizontal Curve Radius †**	
Number of Access Points within 300 ft upstream of the pier system.	Undivided	Divided and One-way	Avg. Lane Width in feet	Undivided	Divided and One-way	Horizontal Curve Radius at Centerline in feet	All Highway Types
0	1.0	1.0	≤9	1.50	1.25	AR> 10,000	1.00
1	1.5	2.0	10	1.30	1.15	10,000≥AR>432	Exp(474.4/AR)
2≤	2.2	4.0	11	1.05	1.03	432≥AR>0	3.00
			≥12	1.00	1.00	TR>10,000	1.00
						10,000≥TR>432	Exp(173.6/TR)
						432≥TR>0	1.50
f_{ACC}=			f_{LW}=			f_{HC}=	
Lanes in One Direction			**Posted Speed Limit ¶**			**Grade Approaching the Pier System††**	
No. of Through Lanes in One Direction	Undivided	Divided and One-way	Posted Speed Limit	Undivided	Divided and One-way	Percent Grade	All Highway Types
1	1.00	1.00	<65	1.42	1.18	-6 ≥ G	2.00
2	0.76	1.00	≥65	1.00	1.00	-6<G<-2	0.5-G/4
≥3	0.76	0.91				-2≤G	1.00
f_{LN}=			f_{PSL}=			f_G=	
$N_i = f_{ACC} \cdot f_{LN} \cdot f_{LW} \cdot f_G \cdot f_{HC} \cdot f_{PSL}$ =							

‡ Major accesses include ramps and intersections. Commercial and residential driveways should not be included as access points unless they are signalized or stop-sign controlled.

† The horizontal curve radius may either curve away (AR) from the pier system under consideration or toward it (TR). When the driver is turning the wheel of the vehicle away from the pier, the AR adjustments shall be used. When the driver is turning the wheel of the vehicle toward the pier, the TR adjustments should be used. This adjustment must be considered for each direction of travel (i) where an encroaching vehicle could approach the pier system.

†† The grade approaching the pier system must be considered for each direction of travel, i. Positive grades indicate an uphill grade and negative values indicate a downhill grade.

¶ For roads with unposted speed limits, use the adjustment for <65 mi/hr.

Table 2. Proposed Table C3.5.6.1-2: Base Annual Heavy Vehicle Encroachments in Direction *i* (HVE_i). †

Two-Way AADT	**Undivided Highways**							
	Percent Trucks (PT)							
veh/day	**5**	**10**	**15**	**20**	**25**	**30**	**35**	**≥40**
0	0.0000	0.0000	0.0000	0.0000	0.0000	0.0000	0.0000	0.0000
1,000	0.0009	0.0017	0.0019	0.0020	0.0021	0.0022	0.0022	0.0023
2,000	0.0014	0.0028	0.0031	0.0033	0.0034	0.0035	0.0036	0.0037
3,000	0.0017	0.0034	0.0038	0.0040	0.0042	0.0043	0.0044	0.0045
4,000	0.0019	0.0037	0.0041	0.0043	0.0045	0.0046	0.0048	0.0049
5,000-41,000	0.0019	0.0038	0.0042	0.0044	0.0046	0.0047	0.0048	0.0049
42,000	0.0020	0.0039	0.0043	0.0045	0.0047	0.0049	0.0050	0.0051
43,000	0.0020	0.0040	0.0044	0.0047	0.0048	0.0050	0.0051	0.0052
44,000	0.0020	0.0041	0.0045	0.0048	0.0049	0.0051	0.0052	0.0054
45,000	0.0021	0.0042	0.0046	0.0049	0.0051	0.0052	0.0054	0.0055
≥46,000	0.0021	0.0043	0.0047	0.0050	0.0052	0.0053	0.0055	0.0056
Two-Way AADT	**Divided Highways**							
	Percent Trucks (PT)							
veh/day	**5**	**10**	**15**	**20**	**25**	**30**	**35**	**≥40**
1000	0.0006	0.0006	0.0006	0.0006	0.0007	0.0007	0.0007	0.0007
5000	0.0026	0.0026	0.0027	0.0027	0.0028	0.0028	0.0028	0.0028
10000	0.0042	0.0043	0.0044	0.0045	0.0045	0.0045	0.0046	0.0046
15000	0.0051	0.0053	0.0054	0.0054	0.0055	0.0055	0.0056	0.0056
20000	0.0055	0.0057	0.0058	0.0059	0.0060	0.0060	0.0060	0.0061
24000-47,000	0.0056	0.0058	0.0059	0.0060	0.0061	0.0061	0.0062	0.0062
50000	0.0060	0.0062	0.0064	0.0065	0.0065	0.0066	0.0066	0.0067
55000	0.0066	0.0069	0.0070	0.0071	0.0072	0.0072	0.0073	0.0073
60000	0.0072	0.0075	0.0076	0.0077	0.0078	0.0079	0.0079	0.0080
65000	0.0078	0.0081	0.0083	0.0084	0.0085	0.0085	0.0086	0.0087
70000	0.0084	0.0087	0.0089	0.0090	0.0091	0.0092	0.0093	0.0093
75000	0.0090	0.0094	0.0095	0.0097	0.0098	0.0099	0.0099	0.0100
80000	0.0096	0.0100	0.0102	0.0103	0.0104	0.0105	0.0106	0.0107
85000	0.0102	0.0106	0.0108	0.0110	0.0111	0.0112	0.0113	0.0113
≥ 90000	0.0108	0.0112	0.0115	0.0116	0.0117	0.0118	0.0119	0.0120

† Encroachment data is not available for one-way roadways. One-way roadways shall be evaluated using the encroachment model for divided highways where the one-way AADT value should be multiplied by 2 and used to determine HVE_i for use in the calculations.

Table 3. Proposed Table C3.6.5.1-3: Probability of a Heavy Vehicle Collision given a Heavy-Vehicle Encroachment as a Function of Pier Column Diameter or Wall Thickness and Offset from the Direction of Travel, $P(C|HVE_i)$.

Offset ‡ (ft)	**Pier Column Size** (ft) †				
	1	2	3	4	6
2	0.1763	0.1868	0.1978	0.2093	0.2337
4	0.1650	0.1750	0.1855	0.1964	0.2198
6	0.1543	0.1638	0.1738	0.1842	0.2064
8	0.1442	0.1532	0.1626	0.1725	0.1937
10	0.1347	0.1432	0.1521	0.1614	0.1816
15	0.1131	0.1204	0.1282	0.1363	0.1539
20	0.0946	0.1009	0.1075	0.1145	0.1297
25	0.0789	0.0842	0.0899	0.0958	0.1088
30	0.0656	0.0701	0.0749	0.0799	0.0910
35	0.0544	0.0582	0.0622	0.0665	0.0758
40	0.0450	0.0482	0.0515	0.0551	0.0630

$$P(C|HVE_i) = \frac{e^{-0.0398\,P_i+0.0709\,D_i-1.5331}}{1+e^{-0.0398\,P_i+0.0709\,D_i-1.5331}}$$

‡ P_i = Offset to critical pier component in direction i in ft where the distance is from the face of the critical pier component to the closest edge of travel lane i.

† D_i = Size of the critical component of the pier in direction i where size is either the diameter of the critical circular column or the smallest cross-sectional dimension of a rectangular column.

Table 4. Proposed Table C3.6.5.1-4: Probability of Impact Force (Q_{CT}) Exceeding Critical Pier Component Nominal Lateral Resistance (R_{CPC}).

	Rural Interstates and Primaries							**Rural Collectors**						
	Posted Speed Limit (mi/hr)							Posted Speed Limit (mi/hr)						
R_{CPC}	≤45	50	55	60	65	70	≥75	≤45	50	55	60	65	70	≥75
100	0.9999	1.0000	1.0000	1.0000	1.0000	1.0000	1.0000	1.0000	1.0000	1.0000	1.0000	1.0000	1.0000	1.0000
150	0.9939	0.9989	0.9999	1.0000	1.0000	1.0000	1.0000	0.9817	0.9969	0.9993	1.0000	1.0000	1.0000	1.0000
200	0.9063	0.9629	0.9890	0.9966	0.9992	0.9996	0.9999	0.6980	0.8826	0.9609	0.9892	0.9960	0.9994	0.9998
250	0.8058	0.8422	0.9049	0.9565	0.9824	0.9935	0.9974	0.3710	0.5055	0.7018	0.8602	0.9431	0.9792	0.9930
300	0.7931	0.7928	0.8125	0.8566	0.9116	0.9533	0.9771	0.3322	0.3429	0.4023	0.5462	0.7134	0.8523	0.9283
350	0.7892	0.7884	0.7907	0.7996	0.8279	0.8684	0.9142	0.3302	0.3315	0.3350	0.3657	0.4455	0.5800	0.7291
400	0.7584	0.7832	0.7886	0.7902	0.7978	0.8079	0.8370	0.3179	0.3294	0.3300	0.3374	0.3464	0.3897	0.4873
450	0.6440	0.7550	0.7820	0.7887	0.7931	0.7914	0.7990	0.2720	0.3177	0.3280	0.3358	0.3327	0.3357	0.3622
500	0.4232	0.6620	0.7552	0.7817	0.7912	0.7894	0.7901	0.1797	0.2770	0.3163	0.3328	0.3313	0.3296	0.3360
550	0.1964	0.4754	0.6731	0.7570	0.7843	0.7879	0.7888	0.0817	0.1993	0.2837	0.3213	0.3290	0.3285	0.3323
600	0.0597	0.2628	0.5216	0.6903	0.7602	0.7810	0.7870	0.0254	0.1086	0.2163	0.2895	0.3183	0.3261	0.3313
650	0.0125	0.1054	0.3292	0.5582	0.6999	0.7584	0.7790	0.0056	0.0432	0.1397	0.2356	0.2942	0.3174	0.3287
700	0.0016	0.0312	0.1614	0.3816	0.5883	0.7076	0.7586	0.0008	0.0130	0.0657	0.1645	0.2463	0.2956	0.3193
750	0.0002	0.0067	0.0584	0.2132	0.4338	0.6144	0.7095	0.0000	0.0028	0.0253	0.0916	0.1833	0.2550	0.2998
800	0.0000	0.0008	0.0177	0.0958	0.2706	0.4781	0.6263	0.0000	0.0005	0.0070	0.0429	0.1129	0.1975	0.2666
850	0.0000	0.0001	0.0048	0.0361	0.1390	0.3246	0.5072	0.0000	0.0001	0.0016	0.0158	0.0610	0.1343	0.2167
900	0.0000	0.0000	0.0007	0.0098	0.0594	0.1934	0.3692	0.0000	0.0000	0.0003	0.0048	0.0269	0.0796	0.1571
950	0.0000	0.0000	0.0001	0.0024	0.0224	0.0988	0.2362	0.0000	0.0000	0.0001	0.0012	0.0107	0.0400	0.0998
1000	0.0000	0.0000	0.0000	0.0006	0.0065	0.0431	0.1363	0.0000	0.0000	0.0001	0.0002	0.0033	0.0165	0.0559
1050	0.0000	0.0000	0.0000	0.0000	0.0018	0.0155	0.0670	0.0000	0.0000	0.0000	0.0000	0.0010	0.0063	0.0260
1100	0.0000	0.0000	0.0000	0.0000	0.0006	0.0054	0.0285	0.0000	0.0000	0.0000	0.0000	0.0002	0.0018	0.0117
1150	0.0000	0.0000	0.0000	0.0000	0.0001	0.0015	0.0102	0.0000	0.0000	0.0000	0.0000	0.0000	0.0005	0.0042
1200	0.0000	0.0000	0.0000	0.0000	0.0000	0.0001	0.0034	0.0000	0.0000	0.0000	0.0000	0.0000	0.0002	0.0014
1250	0.0000	0.0000	0.0000	0.0000	0.0000	0.0000	0.0011	0.0000	0.0000	0.0000	0.0000	0.0000	0.0001	0.0004
1300	0.0000	0.0000	0.0000	0.0000	0.0000	0.0000	0.0002	0.0000	0.0000	0.0000	0.0000	0.0000	0.0000	0.0001

	Urban Interstates and Primaries							**Urban Collectors**						
	Posted Speed Limit (mi/hr)							Posted Speed Limit (mi/hr)						
R_{CPC}	≤45	50	55	60	65	70	≥75	≤45	50	55	60	65	70	≥75
100	1.0000	1.0000	1.0000	1.0000	1.0000	1.0000	1.0000	1.0000	1.0000	1.0000	1.0000	1.0000	1.0000	1.0000
150	0.9924	0.9986	0.9996	0.9999	1.0000	1.0000	1.0000	0.9798	0.9961	0.9996	0.9997	0.9999	1.0000	1.0000
200	0.8599	0.9419	0.9813	0.9947	0.9987	0.9995	0.9998	0.6462	0.8638	0.9551	0.9870	0.9969	0.9990	0.9996
250	0.7093	0.7597	0.8573	0.9322	0.9743	0.9903	0.9966	0.2676	0.4239	0.6550	0.8368	0.9350	0.9763	0.9908
300	0.6915	0.6837	0.7196	0.7815	0.8663	0.9264	0.9673	0.2228	0.2396	0.3082	0.4745	0.6701	0.8248	0.9155
350	0.6876	0.6769	0.6858	0.6962	0.7394	0.7954	0.8723	0.2211	0.2260	0.2274	0.2599	0.3610	0.5123	0.6816
400	0.6622	0.6728	0.6832	0.6832	0.6890	0.7054	0.7587	0.2129	0.2245	0.2228	0.2237	0.2410	0.2901	0.3987
450	0.5611	0.6504	0.6791	0.6816	0.6826	0.6795	0.6997	0.1798	0.2166	0.2210	0.2216	0.2258	0.2295	0.2579
500	0.3724	0.5678	0.6562	0.6764	0.6812	0.6764	0.6869	0.1187	0.1887	0.2139	0.2199	0.2248	0.2223	0.2245
550	0.1718	0.4055	0.5845	0.6542	0.6758	0.6751	0.6850	0.0552	0.1377	0.1914	0.2128	0.2227	0.2211	0.2208
600	0.0513	0.2231	0.4522	0.5932	0.6544	0.6681	0.6833	0.0161	0.0742	0.1486	0.1932	0.2151	0.2191	0.2200
650	0.0110	0.0886	0.2836	0.4795	0.6024	0.6485	0.6775	0.0029	0.0284	0.0937	0.1574	0.1975	0.2134	0.2180
700	0.0010	0.0252	0.1410	0.3302	0.5068	0.6042	0.6589	0.0003	0.0079	0.0461	0.1071	0.1666	0.1998	0.2118
750	0.0002	0.0051	0.0529	0.1847	0.3724	0.5194	0.6170	0.0000	0.0019	0.0172	0.0592	0.1246	0.1741	0.1992
800	0.0000	0.0005	0.0155	0.0851	0.2344	0.4050	0.5437	0.0000	0.0003	0.0054	0.0266	0.0758	0.1356	0.1761
850	0.0000	0.0001	0.0038	0.0315	0.1200	0.2770	0.4387	0.0000	0.0000	0.0012	0.0100	0.0417	0.0924	0.1435
900	0.0000	0.0000	0.0008	0.0092	0.0529	0.1636	0.3200	0.0000	0.0000	0.0003	0.0026	0.0182	0.0554	0.1055
950	0.0000	0.0000	0.0001	0.0022	0.0184	0.0836	0.2076	0.0000	0.0000	0.0000	0.0005	0.0067	0.0279	0.0698
1000	0.0000	0.0000	0.0000	0.0003	0.0055	0.0356	0.1186	0.0000	0.0000	0.0000	0.0001	0.0018	0.0116	0.0411
1050	0.0000	0.0000	0.0000	0.0000	0.0016	0.0138	0.0584	0.0000	0.0000	0.0000	0.0000	0.0006	0.0041	0.0210
1100	0.0000	0.0000	0.0000	0.0000	0.0004	0.0042	0.0252	0.0000	0.0000	0.0000	0.0000	0.0001	0.0015	0.0088
1150	0.0000	0.0000	0.0000	0.0000	0.0000	0.0010	0.0104	0.0000	0.0000	0.0000	0.0000	0.0000	0.0004	0.0038
1200	0.0000	0.0000	0.0000	0.0000	0.0000	0.0001	0.0031	0.0000	0.0000	0.0000	0.0000	0.0000	0.0002	0.0013
1250	0.0000	0.0000	0.0000	0.0000	0.0000	0.0000	0.0008	0.0000	0.0000	0.0000	0.0000	0.0000	0.0000	0.0004
1300	0.0000	0.0000	0.0000	0.0000	0.0000	0.0000	0.0002	0.0000	0.0000	0.0000	0.0000	0.0000	0.0000	0.0001

Appendix B. Proposed RDG Occupant Protection Guidelines

PRELIMINARY RDG OCCUPANT PROTECTION GUIDELINES

These guidelines are applicable to all bridge pier components. Users should first determine if a MASH TL-5 rigid barrier is needed to protect the structure from heavy-vehicle impacts based on Article 3.6.5 of the AASHTO LRFD Bridge Design Specification's risk-based pier protection procedure. If so, no further analysis is needed for passenger vehicle occupant protection since a barrier is already needed for pier protection. If a barrier is not required by Article 3.6.5 of the AASHTO LRFD Bridge Design Specifications, then the following procedure should be used to assess if shielding for passenger-vehicle occupant protection is needed.

Unlike the AASHTO LRFD Bridge Design Specification, the RDG does not contain a single section that is applicable only to impacts with bridge piers. Instead, bridge piers are treated like any other fixed object in the clear zone. As such, revised language for the RDG regarding bridge piers is suggested in four parts of the RDG:

1. New RDG Section 4.10 – The 4th edition of the RDG addresses narrow fixed objects in Chapter 4. A variety of narrow fixed objects are addressed in specific sections (e.g., 4.5 luminaire supports, 4.7 traffic signal supports, 4.8 utility poles, 4.9 trees, etc.) but, there is currently no separate section on bridge piers. A proposed new section 4.10 for bridge piers is presented below.
2. Revised Section 5.5.2 – the 4th edition of the RDG provides some guidance in Section 5.5.2 regarding the zone of intrusion and placement of barriers in front of bridge piers. A proposed revised version of Section 5.5.2 appears below.
3. Revised Figure 5-46 – Figure 5-46 and the accompanying text in the 4th edition of the RDG is a barrier layout example for a shielding a bridge pier. A revised Figure and accompanying text is provided below.
4. Revisions to Section 6.6.2 – Some minor revisions to this section of the 4th edition are proposed for bridge piers located in medians.

NCHRP project 15-65 was recently initiated with the objective to "develop safety performance-based guidance to address high-priority needs that support quantitative design decisions, and that promote consistency in interpretation and implementation" in anticipation of re-writing a future edition of the RDG. [Ray17b] The proposed procedures included herein are consistent with the objective of NCHRP Project 15-65 in that they use the risk of a severe or fatal injury crash to quantify the roadside design goal. The NCHRP 15-65 is anticipated to be presented in a workbook fashion, therefore, these procedures have been presented in the same manner anticipated for NCHRP 15-65.

PROPOSED PRELIMINARY RDG GUIDELINES

NEW RDG SECTION 4.10: BRIDGE PIERS

The Process

The procedure for evaluating the need for shielding of bridge piers for passenger vehicle occupant protection, as outlined in Table 1, involves finding four values:

N_i = The site-specific adjustment factor is found using Table 2 and the characteristics of the site.

PVE_i = The expected annual number of passenger vehicle encroachments in direction i is found using Table 3 knowing the highway type, traffic volume and percent of trucks.

$P(C|PVE_i)$ = The probability of a crash given an encroachment in direction i is found by using Table 4 knowing the nearest pier component offset and size in each direction i.

$P(KA_{CUSPi}|C)$ = The probability of a severe injury or fatal crash with an unshielded bridge pier component given that a crash occurs is found using Table 5 based on the posted speed limit of the roadway.

The product of these four values and a multiplier for the number of piers in the system results in the estimated annual frequency of severe and fatal injury crashes involving the unshielded pier system. If this value is less than 0.0001 annual fatal and severe injury crashes, the pier system need not be shielded for vehicle occupant protection. If this value is greater than or equal to 0.0001 annual fatal and severe injury crashes, the pier system should be shielded with a MASH TL-3 w-beam guardrail.

The following procedure includes four steps: (1) determine site and traffic conditions at the site; (2) estimate the expected number of passenger-vehicle encroachments, (3) estimate the probability of striking the pier if an encroachment occurs and (4) estimate the annual frequency of severe injury and fatal crashes for the existing conditions. The assessment process is detailed in Table 1 and shown as a flowchart in Figure 1. A description of each step follows the flow chart.

Table 1. Process for Evaluating the Need for Shielding of Bridge Piers for Occupant Safety

FIND:	The annual frequency of severe and fatal passenger-vehicle collisions with an unshielded pier system (i.e., $AF_{KA\ CUSP}$). This step is not necessary if it has already been determined that a MASH TL-5 rigid barrier is needed to protect the structure from heavy-vehicle impacts based on Article 3.6.5 of the AASHTO LRFD Bridge Design Specification's risk-based pier protection procedure.
GIVEN:	The following traffic and site characteristics for each approach direction where a pier component is exposed to approaching traffic: • The highway type (i.e., divided, undivided, or one-way). • The number of columns in the pier system (n). • Site-specific characteristics like the number of lanes, lane width, major access points, posted speed limit, radius of horizontal curvature and the grade of the highway. • Total two-way average annual daily traffic (AADT) in vehicles/day. • Percent trucks (PT_i) as a percentage in each approach direction. • Perpendicular distance in ft from the edge of the travel for each direction of travel to the face of the nearest pier component (P_i). • Diameter in ft for circular pier columns, the smallest cross-sectional dimension for rectangular pier columns or the thickness of a pier wall (D_i) nearest to relative direction of travel where the offset (P_i) is measured perpendicular from nearest edge of the lane for the travel direction under consideration to the face of the pier.
PROCEDURE:	Calculate the annual frequency of severe and fatal passenger vehicle collisions with an unshielded pier ($AF_{KA\ CUSP}$) using the following process: 1) Collect traffic and site characteristics. **{Worksheet A}** 2) Calculate annual frequency of severe and fatal passenger-vehicle collisions with an unshielded pier system ($AF_{KA\ CUSP}$). a) Use Table 2 to find the segment-specific encroachment adjustment factor for each approach direction, N_i. Note for horizontal curve direction and grade the values may be different for each direction of travel. **{Worksheet B}** b) Use Table 3 to estimate annual number of passenger vehicle encroachments (PVE_i) per direction. **{Worksheet C}** c) Use Table 4 to estimate the probability of a crash given an encroachment by direction, $P(C|PVE_i)$. **{Worksheet C}** d) Use Table 5 to estimate the probability of a severe injury or fatality given a crash, $P(KA_{CUSPi}|C)$. **{Worksheet C}** e) Calculate $AF_{KA\ CUSP}$ where: $AF_{KA\ CUSP} = \sum_{i=1}^{m} \left[\frac{(n+2)}{3}\right] \cdot N_i \cdot PVE_i \cdot P(C|PVE_i) \cdot P(KA_{CUSPi}|C)$ **{Worksheet C}** 3) Determine if shielding is required for occupant safety. a) If $AF_{KA\ CUSP} \geq 0.0001$ shield with a MASH TL-3 guardrail. b) If $AF_{KA\ CUSP} < 0.0001$ the pier system may remain unshielded.

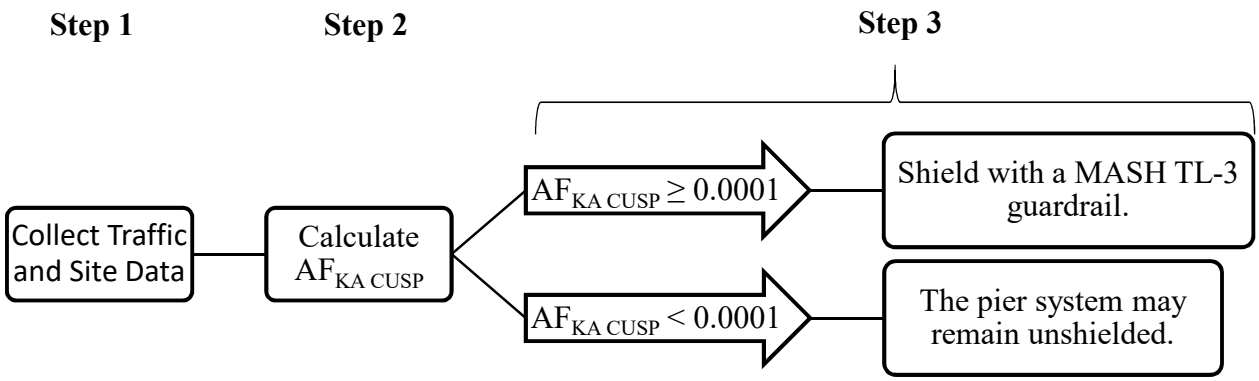

Figure 1. Flowchart of $AF_{KA\ CUSP}$ Process for Bridge Pier Shielding

Site Specific Encroachment Adjustment Factors: N_i

Use Table 2 to find the site-specific encroachment adjustment factor with respect to each possible approach direction. Multiply the adjustments together to obtain the site-specific encroachment adjustment factor for each approach direction, N_i. Each site-specific encroachment adjustment (N_i) should be calculated for each direction of possible encroachment direction, i. The direction number (e.g., i = 1, 2, etc.) is arbitrary but the site-specific encroachment adjustment must always be matched to the offset (P_i) and traffic characteristics that are also associated with that same direction of travel in later steps. Directions of travel are illustrated in Figure 2 for a two-lane undivided highway.

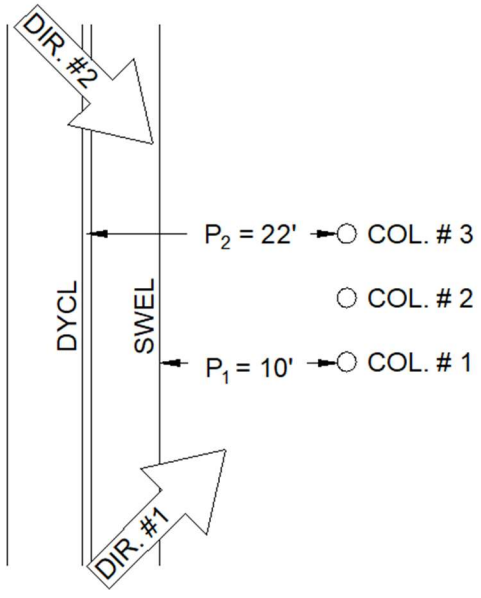

Figure 2. Example of Two Possible Directions of Travel and Measurement of Offset.

Table 2. Site Specific Adjustment Factor: N_i.

Major Accesses‡			Lane Width			Horizontal Curve Radius †	
Number of Access Points within 300 ft upstream of the pier system.	Undivided	Divided and One-way	Avg. Lane Width (ft)	Undivided	Divided and One-way	Horizontal Curve Radius at Centerline (ft)	All Highway Types
0	1.0	1.0	≤9	1.50	1.25	AR > 10,000	1.00
1	1.5	2.0	10	1.30	1.15	10,000 ≥ AR > 432	Exp(474.4/AR)
2≤	2.2	4.0	11	1.05	1.03	432 ≥ AR > 0	3.00
			≥12	1.00	1.00	TR > 10,000	1.00
						10,000 ≥ TR > 432	Exp(173.6/TR)
						432 ≥ TR > 0	1.50
Lanes in One Direction			**Posted Speed Limit ¶**			**Grade Approaching the Pier System††**	
No. of Through Lanes in One Direction	Undivided	Divided and One-way	Posted Speed Limit (mph)	Undivided	Divided and One-way	Percent Grade	All Highway Types
1	1.00	1.00	<65	1.42	1.18	-6 ≥ G	2.00
2	0.76	1.00	≥65	1.00	1.00	-6 < G < -2	0.5-(G/4)
≥3	0.76	0.91				-2 ≤ G	1.00

‡ Major accesses include ramps and intersections. Commercial and residential driveways should not be included as access points unless they are signalized or stop-sign controlled.

† The horizontal curve radius may either curve away (AR) from the pier system under consideration or toward it (TR). When the driver is turning the wheel of the vehicle away from the pier, the AR adjustments shall be used. When the driver is turning the wheel of the vehicle toward the pier, the TR adjustments should be used. This adjustment must be considered for each direction of travel (i) where an encroaching vehicle could approach the pier system.

†† The grade approaching the pier system must be considered for each direction of travel, i. Positive grades indicate an uphill grade and negative values indicate a downhill grade.

¶ For roads with unposted speed limits, use the design or observed speed.

Passenger Vehicle Encroachment Frequency: PVE_i

The expected annual number of passenger vehicle encroachments in direction i is found using Table 3 knowing the highway type, two-way traffic volume and percent of trucks. Linear interpolation may be used if the specific values are not displayed in the table.

Table 3. Base Annual Passenger Vehicle Encroachments in Direction i: PVE_i.†

Two-Way AADT	Undivided Highways							
	Percent Trucks (PT)							
veh/day	5	10	15	20	25	30	35	40
1,000	0.0165	0.0157	0.0148	0.0139	0.0130	0.0122	0.0113	0.0104
2,000	0.0268	0.0254	0.0240	0.0226	0.0212	0.0198	0.0183	0.0169
3,000	0.0326	0.0309	0.0292	0.0275	0.0258	0.0240	0.0223	0.0206
4,000	0.0353	0.0334	0.0316	0.0297	0.0279	0.0260	0.0241	0.0223
5,000-41,000	0.0358	0.0339	0.0320	0.0301	0.0282	0.0264	0.0245	0.0226
42,000	0.0371	0.0351	0.0332	0.0312	0.0293	0.0273	0.0254	0.0234
43,000	0.0380	0.0360	0.0340	0.0320	0.0300	0.0280	0.0260	0.0240
44,000	0.0389	0.0368	0.0348	0.0327	0.0307	0.0286	0.0266	0.0245
45,000	0.0397	0.0377	0.0356	0.0335	0.0314	0.0293	0.0272	0.0251
≥46,000	0.0406	0.0385	0.0364	0.0342	0.0321	0.0299	0.0278	0.0257
Two-Way AADT	**Divided Highways**							
	Percent Trucks (PT)							
veh/day	**5**	**10**	**15**	**20**	**25**	**30**	**35**	**40**
1,000	0.0114	0.0108	0.0102	0.0096	0.0090	0.0084	0.0078	0.0072
5,000	0.0485	0.0459	0.0434	0.0408	0.0383	0.0357	0.0332	0.0306
10,000	0.0789	0.0747	0.0706	0.0664	0.0623	0.0581	0.0540	0.0498
15,000	0.0962	0.0912	0.0861	0.0810	0.0760	0.0709	0.0658	0.0608
20,000	0.1044	0.0989	0.0934	0.0879	0.0824	0.0769	0.0714	0.0659
24,000-47,000	0.1062	0.1006	0.0950	0.0894	0.0838	0.0782	0.0727	0.0671
50,000	0.1143	0.1082	0.1022	0.0962	0.0902	0.0842	0.0782	0.0722
55,000	0.1257	0.1191	0.1125	0.1058	0.0992	0.0926	0.0860	0.0794
60,000	0.1371	0.1299	0.1227	0.1155	0.1082	0.1010	0.0938	0.0866
65,000	0.1485	0.1407	0.1329	0.1251	0.1173	0.1094	0.1016	0.0938
70,000	0.1600	0.1515	0.1431	0.1347	0.1263	0.1179	0.1094	0.1010
75,000	0.1714	0.1624	0.1533	0.1443	0.1353	0.1263	0.1173	0.1082
80,000	0.1828	0.1732	0.1636	0.1540	0.1443	0.1347	0.1251	0.1155
85,000	0.1942	0.1840	0.1738	0.1636	0.1533	0.1431	0.1329	0.1227
≥ 90,000	0.2057	0.1948	0.1840	0.1732	0.1624	0.1515	0.1407	0.1299

$$PVE_i = \left[\frac{ENCR_{BASE}}{4}\right] \cdot \left[\frac{300}{5280}\right] \cdot \left[1 - \left[\frac{PT}{100}\right]\right]$$

† Encroachment data is not available for one-way roadways. Traditionally, one-way roadways are evaluated using the encroachment model for divided highways. The one-way AADT value should be multiplied by 2 and used to determine PVE_i for use in the remaining calculations.

Probability of a Crash: P(C|PVE$_i$)

Find the probability of a crash given an encroachment in direction i by using Table 4 knowing the pier component offset and size in each direction i. Linear interpolation may be used if the specific values are not displayed in the table.

Table 4. Probability of a Collision given a Passenger-Vehicle Encroachment: P(C|PVE$_i$).

Offset, P_i ‡ (ft)	Pier Column Size, D_i (ft) †				
	1	2	3	4	6
2	0.1125	0.1242	0.1369	0.1507	0.1818
4	0.1066	0.1178	0.1300	0.1432	0.1730
6	0.1011	0.1117	0.1233	0.1360	0.1646
8	0.0957	0.1059	0.1170	0.1291	0.1565
10	0.0907	0.1004	0.1109	0.1225	0.1487
15	0.0790	0.0876	0.0970	0.1073	0.1307
20	0.0688	0.0763	0.0846	0.0937	0.1146
25	0.0598	0.0664	0.0737	0.0817	0.1002
30	0.0519	0.0577	0.0641	0.0712	0.0875
35	0.0450	0.0501	0.0557	0.0619	0.0762
40	0.0390	0.0434	0.0483	0.0537	0.0663

$$P(C|PVE_i) = \frac{e^{-0.0300\,P_i + 0.1122\,D_i - 2.1177}}{1 + e^{-0.0300\,P_i + 0.1122\,D_i - 2.1177}}$$

‡ P_i is the offset to the nearest pier component in direction i in ft where the distance is measured from the face of the critical pier component to the closest edge of travel lane in direction i.

† D_i is the size of the nearest component of the pier in direction i where the size is either the diameter of the critical circular column, the smallest cross-sectional dimension of a rectangular column, or the thickness of a pier wall.

Probability of Severe Injury or Fatality Given a Crash: P(KA$_{CUSPi}$|C)

The probability of a severe injury or fatal crash with a bridge pier component given that a crash occurs is found from Table 5 based on the posted speed limit of the roadway.

Table 5. Probability of Severe or Fatal Injury given that a Crash with an Unshielded Pier Component Occurs: P(KA$_{CUSPi}$|C).

Posted Speed Limit (mi/hr)	P(KA$_{CUSPi}$|C)	Posted Speed Limit (mi/hr)	P(KA$_{CUSPi}$|C)
≥75	0.1008	50	0.0299
70	0.0820	45	0.0218
65	0.0656	40	0.0153
60	0.0516	35	0.0102
55	0.0398	30	0.0065
		≤25	0.0037

$$P(KA_{CUSPi}|C) = 2.3895 \cdot 10^{-7} \cdot PSL_i^3$$

Annual Frequency of Severe Injury and Fatal Passenger-Vehicle Collisions with an Unshielded Pier System: $AF_{KA\ CUSP}$

The total annual frequency of severe and fatal passenger vehicle collisions with an unshielded pier ($AF_{KA\ CUSP}$) is calculated using Equation 1 where m is the total number of directions of interest and n is the number of pier columns.

$$AF_{KA\ CUSP} = \sum_{i=1}^{m} \left[\frac{(n+2)}{3}\right] \cdot N_i \cdot PVE_i \cdot P(C|PVE_i) \cdot P(KA_{CUSPi}|C) \qquad \textbf{Equation 1}$$

Evaluate Need for Shielding Based on $AF_{KA\ CUSP}$

If $AF_{KA\ CUSP} \geq 0.0001$ shield the bridge pier with a MASH TL-3 guardrail, however, if $AF_{KA\ CUSP} < 0.0001$ the pier system may remain unshielded.

Worksheets

Worksheets have been developed to assist users in collecting data and calculating the components of the process for evaluating the need for shielding of bridge piers for occupant safety.

Worksheet A

General Information		**Location Information**	
Analyst		Roadway	
Agency		Bridge ID	
Date Performed		Jurisdiction	
		Analysis Year	

Input Data	**Base Condition**			**Direction 1**	**Direction 2**
Divided, undivided or one-way	D	U	O		
Number of columns in pier system	--				
Number of access points	0				
Lane width (ft)	≥12				
Radius of curvature (ft)	>1000				
Curve away from the pier?	--				
Number of lanes (in one direction)	≤2	1	≤2		
Posted speed limit (mph)	≥65				
Grade	≥-2				
AADT	--				
Percent trucks (PT)	--				
Nearest pier column size (ft)	--				
Offset to face of nearest pier column (ft)	--				

Worksheet B – Encroachment Adjustment Factors

Direction	(1) Access Points	(2) Lane Width	(3) Horizontal Curve	(4) Number of Lanes	(5) Posted Speed Limit	(6) Percent Grade	(7) Encroach Adjustment Factor
	f_{ACC}	f_{LW}	f_{HC}	f_{LN}	f_{PSL}	f_G	N_i
	from Table 2	from Table 2	from Table 2	from Table 2	from Table 2	from Table 2	See Note 1
1							
2							

Note 1: $N_i = (1) * (2) * (3) * (4) * (5) * (6)$

Worksheet C

Direction	(1) Number of Columns in the Pier System	(2) Encroachment Adjustment Factor	(3) Annual Encroachments	(4) Probability of Crash Given an Encroachment by Direction
	n	N_i	PVE_i	$P(C\|PVE_i)$
	from Worksheet A	(7) from Worksheet B	from Table 3	from Table 4
1				
2				

Worksheet C continued

Direction	(5) Probability of Severe Injury or Fatality Given a Crash	(6) Avg. Annual Frequency of Severe Injury or Fatal Crash with an Unshielded Pier from Each Direction	(7) Avg. Annual Frequency of Injury Crash with an Unshielded Pier for All Directions
	$P(KA_{CUSPi}\|C)$	$AF_{KA\ CUSPi}$	$AF_{KA\ CUSP}$
	from Table 5	See Note 1	See Note 2
1			
2			

Note 1: $AF_{KA\ CUSP} = \sum_{i=1}^{m} \left[\frac{((1)+2)}{3}\right] \cdot (2) \cdot (3) \cdot (4) \cdot (5)$

Note 2: If (7) ≥ 0.0001 shield with a MASH TL-3 guardrail, however, if (7) < 0.0001 the pier system may remain unshielded.

Example Problem #1

The layout for Example Problem #1 is shown in Figure 3 and the user-supplied input information is shown in Worksheet A. Example Problem #1 represents a three-column pier system on the right side of the primary direction of an undivided two-lane rural collector with 10,000 vehicles/day, 5 percent trucks and a posted speed limit of 45 mi/hr. The three pier columns are parallel with the roadway and all three columns are two feet in diameter. The user wishes to evaluate the need for pier protection in order to protect vehicle occupants in the case of a crash.

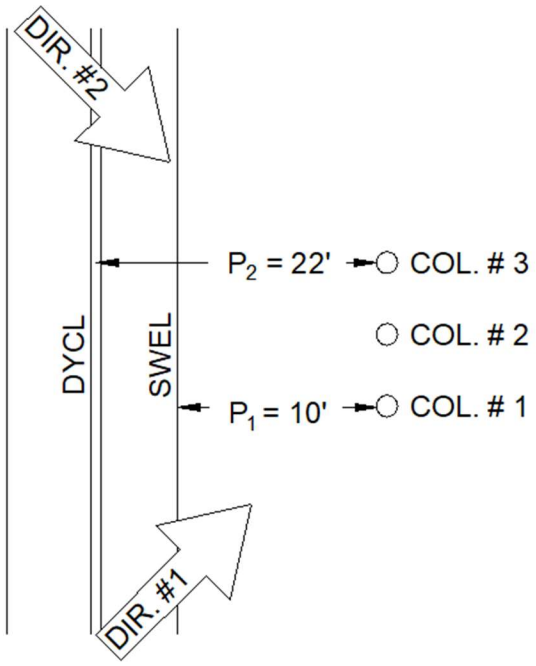

Figure 3. Example Problem #1 Roadway Layout.

Worksheet A

General Information		**Location Information**	
Analyst		Roadway	
Agency		Bridge ID	
Date Performed		Jurisdiction	
		Analysis Year	

Input Data	**Base Condition**			**Direction 1**	**Direction 2**
Divided, undivided or one-way	D	U	O	Undivided	Undivided
Number of columns in pier system	--			3	3
Number of access points	0			2	2
Lane width (ft)	≥12			12	12
Radius of curvature (ft)	>1000			Tangent	Tangent
Curve away from the pier?				N/A	N/A
Number of lanes (in one direction)	≤2	1	≤2	1	1
Posted speed limit (mph)	≥65			45	45
Grade	≥-2			Flat	Flat
AADT	--			10,000	10,000
Percent trucks (PT)	--			5	5
Nearest pier column size (ft)	--			2.0	2.0
Offset to face of nearest pier column (ft)	--			10	22

Worksheet B – Encroachment Adjustment Factors

Direction	(1) Access Points	(2) Lane Width	(3) Horizontal Curve	(4) Number of Lanes	(5) Posted Speed Limit	(6) Percent Grade	(7) Encroach Adjustment Factor
	f_{ACC}	f_{LW}	f_{HC}	f_{LN}	f_{PSL}	f_G	N_i
	from Table 2	from Table 2	from Table 2	from Table 2	from Table 2	from Table 2	See Note 1
1	2.20	1.00	1.00	1.00	1.42	1.00	3.12
2	2.20	1.00	1.00	1.00	1.42	1.00	3.12

Note 1: $N_i = (1) * (2) * (3) * (4) * (5) * (6)$

Worksheet C

Direction	(1) Number of Columns in the Pier System	(2) Encroachment Adjustment Factor	(3) Annual Encroachments	(4) Probability of Crash Given an Encroachment by Direction
	n	N_i	PVE_i	$P(C\|PVE_i)$
	from Worksheet A	(7) from Worksheet B	from Table 3	from Table 4
1	3	3.12	0.0358	0.1004
2	3	3.12	0.0358	0.0722

Worksheet C continued

Direction	(5) Probability of Severe Injury or Fatality Given a Crash	(6) Avg. Annual Frequency of Severe Injury or Fatal Crash with an Unshielded Pier from Each Direction	(7) Avg. Annual Frequency of Injury Crash with an Unshielded Pier for All Directions
	$P(KA_{CUSPi}\|C)$	$AF_{KA\ CUSPi}$	$AF_{KA\ CUSP}$
	from Table 5	See Note 1	See Note 2
1	0.0218	0.00041	0.00070
2	0.0218	0.00029	

Note 1: $AF_{KA\ CUSP} = \sum_{i=1}^{m} \left[\frac{((1)+2)}{3}\right] \cdot (2) \cdot (3) \cdot (4) \cdot (5)$

Note 2: If (7) ≥ 0.0001 shield with a MASH TL-3 guardrail, however, if (7) < 0.0001 the pier system may remain unshielded.

The annual expected frequency of severe or fatal injury crashes involving passenger vehicles and this pier system with these traffic and site characteristics is 0.00070 severe or fatal crashes/yr. Another way to view this is that if traffic conditions remined the same forever, one severe injury or fatal crash could be expected every 1,429 years. Since the goal is to limit severe injury and fatal crashes to less than 0.0001 per pier system per year, this site requires shielding for occupant protection.

REVISED RDG SECTION 5.5.2

The following section presents a proposed edited portion of Section 5.5.2 of the RDG. The existing text is shown in a regular faced font, text recommended for deletion is shown in a crossed-out font and text recommended for inclusion is shown with an underlined font.

Paragraph 3

The designer should also be aware that a truck or similar high-center-of-gravity vehicles may lean over the barrier upon impact, which could require an increased offset to lessen the likelihood of contact with the shielded object. Also, the designer may need to consider the use of a more rigid system if the placement of the barrier is such that the available space is less than the predicted deflection of a less rigid barrier system. ~~The designer may need to consider the use of a taller barrier where the lean of the vehicle over the rail is a concern for larger trucks.~~ Prior guidance indicated that if bridge pier components were located closer than 10.0 ft from the shielding barrier a 54.0 in. tall barrier should be used. Unfortunately, there are at present no MASH TL-5 crash tested rigid barriers that are taller than 42.0 in. While rigid barriers taller than 42.0 in. are likely to reduce the roll of articulated trucks, recent full-scale crash tests and finite element simulations indicate that the modern trailer suspensions result in much more stable impacts than was the case in crash tests of older trailer suspensions. If a trailer does lean over the barrier and contact a pier component, the interaction will not involve the entire mass of the vehicle and is unlikely to develop sufficient impact forces to put the pier system at risk of failure. It is preferable to allow at least 3.25 ft of space between the top traffic face of the barrier and the face of the nearest pier component to minimize contact with a heavy vehicle. In some retrofit situations, however, it may be impossible to provide this amount of space given the existing pier location and arrangement of the roadway. In such cases it is permissible to place the barrier closer to face of at-risk pier components.

Paragraph 5-7

When placing the bridge pier beyond the clear zone is impractical at overpass structures, a longitudinal roadside barrier is typically provided to shield an errant vehicle and its occupants from a collision with the bridge pier. One way to determine whether site conditions qualify for shielding for occupant safety is to evaluate the annual frequency of fatal and severe injury crashes using the procedure described in Section 4.10. From a roadside safety perspective, a TL-3 barrier is typically sufficient to shield the passenger-vehicle motorists from a pier located within the clear zone. However, structural protection of the bridge may call for the need for a higher test level barrier, not based on roadside safety criterion. The *AASHTO LRFD Bridge Design Specification (14)* specify that bridge piers that are within 9 m [30 ft.] of the traveled way should be designed to withstand a large impact load or be shielded with a specified barrier system. The following height guidelines from the *AASHTO LRFD Bridge Design Specifications* are based on offset from the traveled way to the face of the pier:

- ~~A 1370-mm [54-in.] high barrier located 3 m [10 ft] or less from the pier, or~~
- ~~A 1070-mm [42-in.] high barrier located more than 3 m [10 ft.] from the pier~~
- For new or retrofit construction, a 42.0-inch or higher MASH crash tested rigid TL-5 barrier located 3.25 ft or more from the top edge of the traffic face of the barrier to the nearest traffic face of the pier component being protected.

- For retrofit construction, a 42.0-inch high or higher MASH crash tested rigid TL-5 barrier may be placed closer than 3.25 ft from the top edge of the traffic face of the barrier to the nearest traffic face of the pier component being protected when there is no other feasible option.

Such rigid barriers shall be structurally and geometrically capable of surviving the crash test for MASH Test Level 5 as specified in *AASHTO LRFD Bridge Design Specifications*.

Typically, a barrier would be extended to provide advance shielding based on the length-of-need (see Sections 5.6.4). ~~However, at this time, the appropriate length-of-need for this application is unknown. Therefore,~~ t To address the criteria reflected in the LRFD specifications, it is recommended that the MASH TL-5 rigid barrier ~~tall wall~~ be extended a minimum of 18 m [60 ft] in advance of the piers. Beyond this point, the length-of-need as described in Section 5.6 should be provided also with a MASH TL-5 rigid barrier. Another option to accommodate bridge piers not designed to withstand impact loads is to shield the piers with a separate crash wall to accommodate the LRFD impact loads and then shield this system with a TL-3 longitudinal roadside barrier. Significant research is needed to develop more specific criteria to warrant the use of this tall barrier for pier protection. Transportation agencies can develop their own criteria based on factors such as project scope, route classification, ADT, geometry, bridge type, barrier offset, barrier/pier impact history, bridge type and configuration, and the roadway alignment.

On construction projects with an existing bridge pier system, transportation agencies can evaluate the adequacy of the existing bridge pier and the appropriate test level barrier system to provide based on factors such as offset, roadway geometry, traffic composition, bridge type and configuration and crash history. ~~The implementation of AASHTO LRFD specifications regarding this extreme column loading and barrier requirements may not be appropriate for existing bridges that were not originally designed using the AASHTO LRFD specifications.~~ Each state can develop their own criteria for existing bridges to fit their conditions.

REVISED RDG FIGURE 5-46

Example Problem #1 from section 4.10 is continued here to determine shielding barrier layout. Since shielding is only required for vehicle occupant protection, a MASH crash tested TL-3 strong-post w-beam guardrail will be used at the site. Vehicles can approach from either direction on this undivided roadway, so the guardrail will extend in both directions #1 and #2. For purposes of this example, it is assumed that the owner agency prefers a tangent rather than a flared installation.

RDG Table 5-7 recommends a shy-line offset (L_S) of 6 ft for a roadway with a 45 mi/hr posted speed limit. The offset to the nearest pier component is 10 ft from the edge of the travelled way and a w-beam guardrail is a little less than 2 ft wide depending on the particular design. RDG Table 5-6 shows that in both finite element simulations and crash tests, MASH TL-3 strong-post w-beam guardrails (i.e., the MGS single w-beam with 6.25-ft post spacing) generally deflects about 3.5 ft so there is not adequate deflection distance behind the guardrail if it is placed at the edge of the 6-ft shy line (i.e., 10 - 2 – 3.5 = 4.5 < 6). While placing the w-beam inside the shy line is acceptable, a better alternative would be to use the MGS with half post spacings (i.e., 3.125 ft) which would have a deflection of less than 2 ft. The barrier should, therefore, be placed at the edge of the shy line, 6 ft from the edge of the lane (i.e., L_2 = 6 ft) such that there is at least 3 ft of deflection space.

RDG Table 5-10(b) recommends runout lengths (L_R) for roadways with traffic volumes between 5,000 and 10,000 vehicles/day of 130 ft for a 40 mi/hr and 190 ft for 50 mi/hr. Interpolating to the site condition of a 45 mi/hr posted speed limit results in a 160 ft runout length. The parameters needed to find the length of need (X) of the guardrail are summarized for both directions in Table 6 recognizing that the lateral extent of the area of concern (L_A) is simply the lateral offset to the face of the pier column (P_i=10 ft) plus the diameter of the pier column (D_i=2 ft). The lateral area of concern (L_A) is the distance from the edge of lane to the back face of the pier column so it is 10 ft plus the 2-ft diameter of the column (12 ft) in Direction #1 and the 12-ft lane width plus the 10-ft lateral offset to the face of the pier plus the 2-ft diameter of the column (24 ft) for Direction #2. RDG Equation 5-2 is used to determine the length of need for a tangent guardrail as shown in Table 7.

Table 6. Barrier Layout Parameters from the Roadside Design Guide for Example Problem #1.

RDG Table	Parameter		Direction	
			#1	#2
5-7	L_S	Shy-Line Offset (ft)	6.0	6.0
5-9	a/b	Flare Rate	--	--
5-10(b)	L_R	Runout Length (ft)	160	160
	L_1	Tangent Length (ft)	--	--
	L_2	Barrier Offset (ft)	6	6
	L_A	Lateral Extent of Area of Concern	12.0	24.0

Table 7. Required Length of Need for Tangent Guardrail Shielding Pier for Example Problem #1.

$X = \frac{L_R(L_A - L_2)}{L_A}$	
Direction #1	Direction #2
$X = \frac{160\ ((10+2)-6)}{(10+2)} = 80$	$X = \frac{160\ ((22+2)-18)}{(22+2)} = 40$

The values in Table 7 show the necessary length of need to shield the pier columns from passenger vehicles in Example #1 should extend 80 ft upstream of Column #1 and 40 ft downstream of Column #3 as shown in Figure 4. These distances are measured to the length of need of the guardrail terminal which is generally at post 3 so the end of the terminal would be another 12.5 ft up and down stream.

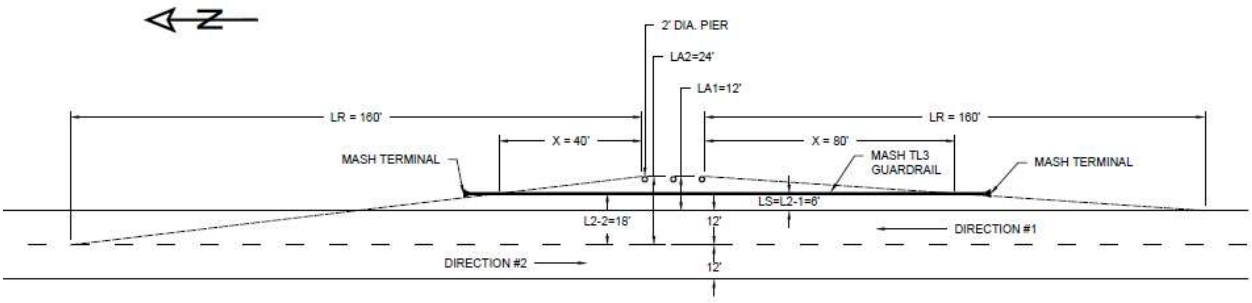

Figure 4. Occupant Protection Shielding Barrier for Example Problem #1.

REVISED RDG SECTION 6.6.2

In many locations, an obstacle such as a rigid object may be located in a median. If a median barrier is not being installed and the object is outside of the clear zone for one direction of traffic, the barrier should be treated as a roadside barrier (see Chapter 5). Appropriate flare rates should be used for the approaching traffic side of the barrier and, if the deflection distance for the barrier cannot be provided, a transition may be necessary to stiffen the barrier in advance of the object. In addition, when the object is within the clear zone for both directions, the object and back side of the barrier need to be shielded as well.

Typical examples of objects that often are located in the median are bridge piers and overhead sign support structures. If shielding for both directions of travel is necessary and if the median is flat (i.e. side slopes less than approximately 1V:10H), two means of protection are suggested. In the first case, the designer should investigate the possible use of a crash cushion to shield the object. The second suggestion is to employ either semi-rigid or rigid barriers with crash cushions or end treatments to shield the barrier ends as illustrated in Figure 6-20. If semi-rigid systems are used, the distance from the barrier to the obstruction should be greater than the dynamic deflection of the barrier. If a concrete barrier is used, ~~the barrier can be placed adjacent to the obstruction unless there is a concern that a high-center-of-gravity vehicle will strike the obstruction because its contact with the barrier causes the top of the vehicle to lean over the railing.~~ it is preferable to allow 3.25 ft of space between the top traffic face of the barrier and the face of the nearest pier component to minimize contact with a heavy vehicle.

Appendix C. Survey of Practice

RESULTS OF SURVEY OF PRACTICE

INTRODUCTION

A survey was conducted of the State Departments of Transportation, practitioners, and researchers to ascertain current practices for bridge pier shielding. The survey examined situations in which pier protection is and is not used. The survey also asked for respondent feedback on the strengths and weaknesses of current policy. The distribution list included members of the AASHTO Subcommittee for Bridges and Structures, the AASHTO Subcommittee on Roadside Design, and the TRB AFB20 Roadside Design committee and subcommittees such that the recipients of the survey should be knowledgeable about pier shielding practice. A complete copy of the questionnaire can be found in at the end of this appendix. The survey was assembled using the on-line tool surveymonkey.com (i.e., www.surveymonkey.com) and distributed through electronic mail. The survey was distributed on February 26, 2013. Reminders were sent on August 21, 2013. Sixty-four responses were received and are included in this summary.

Question 1: Please provide the following optional information about yourself.

Respondents were asked to provide their demographic information. Approximately 90 percent of the respondents provided this information. Respondents represent a variety of countries including the United States, Canada, United Kingdom, and New Zealand. Representatives from thirty-six states responded (listed below), however, not all of these respondents represent the State Department of Transportation (DOT). Three international responses were received; the remaining 53 were from the United States. Some respondents are consultants, researchers, or manufactures who have knowledge of local and regional design guidance regarding bridge pier protection.

Arkansas	Nebraska
California	New Hampshire
Connecticut	New Jersey
Delaware	New York
Florida	North Carolina
Georgia	Ohio
Hawaii	South Dakota
Iowa	Tennessee
Kansas	Texas
Louisiana	Utah
Maryland	Virginia
Massachusetts	Washington
Minnesota	Wisconsin
Mississippi	Wyoming
Missouri	

This wide variety of respondents provides a good cross-section geographically, allowing for different regional and international perspectives to be reflected in the results of this survey.

Question 2: Please check the box that best describes your work.

Respondents were asked the type of work they are engaged in and instructed to check all categories that apply. A respondent, for example, may work in both bridge design and bridge research so a respondent may have checked more than one field. The results are shown in Figure 1. One interesting observation is that over 60 percent of the respondents identified themselves as working as bridge designers. Policy work and roadside design were identified by about 30 percent of respondents while highway design was identified by less than ten percent of the respondents. The respondents who describe themselves as doing "other" work included design, manufacturing and sales of roadside safety hardware, and international experts in roadside standard development. The NJDOT collected responses from within the department divisions, indicating the responses include: "Bridge Design, Bridge Inspection, Maintenance, Roadway, and Construction."

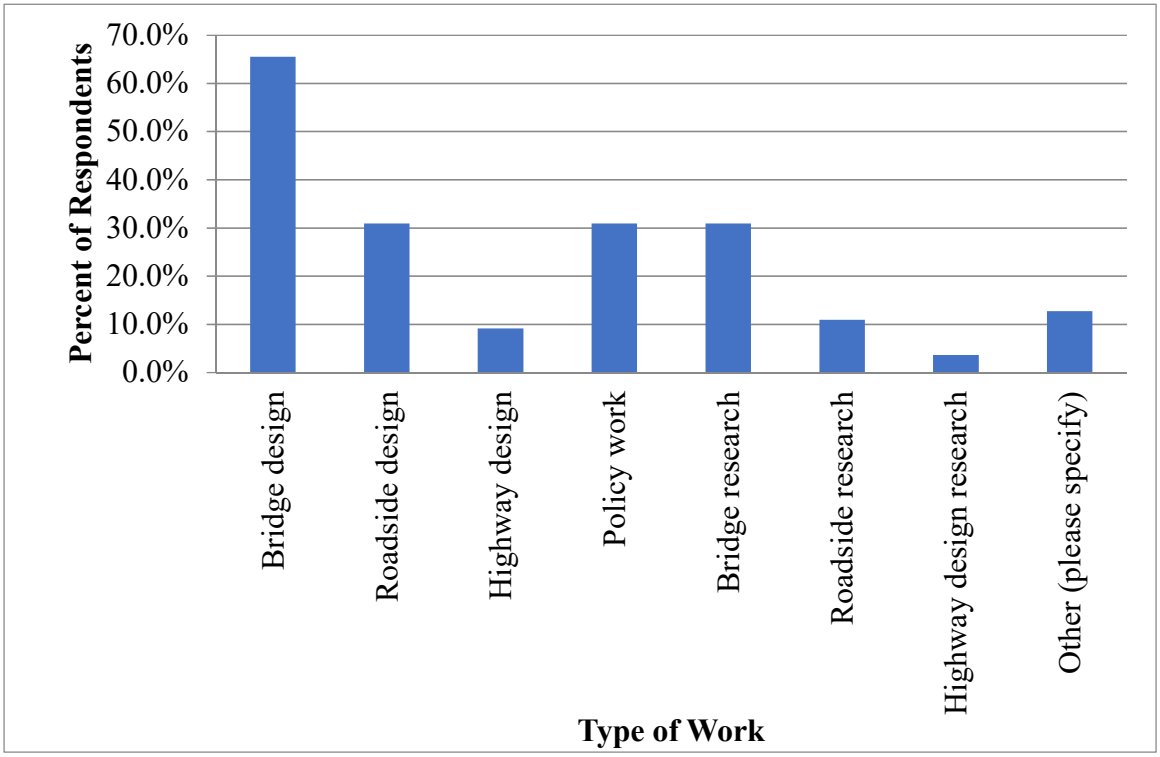

Figure 1. Distribution of Responses to Survey Question Two.

Question 3: In the conduct of your work, have you used guidelines for the placement of longitudinal barriers to protect piers?

Approximately 60 percent of the respondents indicated that they have used the LRFD specifications for designing the placement of longitudinal barriers, while forty percent indicated they have also used supplemental guidance. Twenty-two percent of the respondents noted that they have used something other than the LRFD specifications, including state and ministry standards. The Florida DOT notes that the LRFD was used to develop Florida DOT Design Standard Index 410. Iowa DOT's Road Design Manual discusses protection of bridge piers with longitudinal barriers in an online publication: http://www.iowadot.gov/design/dmanual/08A-04.pdf. The New Jersey DOT Roadway Design Manual Section 8 for guide rail and median

barriers currently discusses pier protection; however, the New Jersey DOT is developing a policy which will separate pier protection for new bridges and existing bridges. One respondent noted "we felt the LRFD Requirements were too prescriptive and rigid for a few cases, so we developed requirements on a case-by-case basis." Another noted impact resistance is "not critical too us; we design for non-collapse during a seismic event and don't skimp on confinement of longitudinal column reinforcing." This respondent indicated the following is done within their state: "we design new piers for the collision force such that longitudinal barriers are not used for this purpose. We have not retrofitted existing piers with longitudinal barriers that meet LRFD specifications or guidance."

Question 4: Which characteristics do you use in the decision to protect piers?

Respondents were asked what traffic, highway and bridge characteristics are used in making the decision to protect bridge piers and asked to check all characteristics that apply. In addition to site characteristics, the list also includes some methods like "engineering judgment" or "cost/benefit analysis" to provide some indication of how the decision was made. The results are shown in Table 1. Engineering judgment is the most prominent deciding factor, closely followed by traffic volumes, design speed, and horizontal alignment. Land use around the structure and the cost/benefit of the decision received the least attention.

Table 1. Summary of Question 4 Results.

Answer Options	Response Percent	Response Count
Engineering judgment	65.1%	28
ADT	53.5%	23
Percentage of Trucks	46.5%	20
Posted Speed Limit	37.2%	16
Design Speed	53.5%	23
Number of lanes	23.3%	10
Accident data	48.8%	21
Cost/benefit	20.9%	9
Roadway type	41.9%	18
Horizontal alignment	58.1%	25
Vertical alignment	23.3%	10
Land use around structure	18.6%	8
Other (please specify)	37.2%	16

Respondents provided some additional items that were not on the list that affected the decision to protect piers including:

- Lateral load capacity,
- Criticality of bridge,
- Clear zone,
- Redundancy of the piers (number of pier columns), and/or
- Continuity of the bridge super structure.

Also considered is whether or not the bridge is a new bridge design project or a 3R project (resurfacing, restoration, rehabilitation). These results seem to imply that there is a strong reliance on engineering judgment and on post-construction decisions (i.e., crash data), indicating that additional guidance is needed during the design development of new bridges and maintenance of areas around existing bridges.

Question 5: Does your organization have a policy for identifying unprotected piers that should have protection?

Almost sixty-three percent of the respondent indicated that their organization does not have a policy to identify unprotected piers that should be protected. Some of the respondents who noted that their organization does have a policy included information on it or where to find it. Some policies include protecting any pier within the clear zone, any pier within thirty feet of the edge of traveled way, or other formal policies with information provided by respondents as follows:

- WIDOT Facility Development Manual and Bridge Manual at:
  http://roadwaystandards.dot.wi.gov/standards/fdm/11-35.pdf
  http://roadwaystandards.dot.wi.gov/standards/fdm/11-45.pdf#fd11-45
  http://on.dot.wi.gov/dtid_bos/extranet/structures/LRFD/BridgeManual/Ch-13.pdf
- FDOT Design Standard Index 411,Pier Protection Barrier,
  http://www.dot.state.fl.us/rddesign/DS/13/IDx/00411.pdf"
- FDOT Structures Design Guidelines, Section 2.6 which can be obtained at this website:
  http://www.dot.state.fl.us/Structures/StructuresManual/CurrentRelease/StructuresManual.shtm
- http://www.dot.state.oh.us/Divisions/Engineering/Structures/standard/Bridges/BDM/BDB2007_01-18-13.pdf
- See page 21 of Roadway Design Manual
  https://connect.ncdot.gov/projects/Roadway/Roadway%20Design%20Manual/03.%20Guardrail,%20Barriers%20and%20Attenuators.pdf"

The Minnesota DOT published policy currently "does not speak much about existing piers in regard to protection requirements. Existing piers are identified only when a bridge or roadway rehab project occurs. Our policy states 'For Bridge Improvement and Bridge Rehabilitation projects that include substructure widening, designers should meet the requirements of this policy. Other bridge repair projects generally will not require upgrading.' We are working on updating our policy. Adding pier protection to existing piers will still be considered only during rehab projects and for the most part will still be considered on a case-by-case basis, but additional factors are being added for consideration."

The South Dakota DOT "…has a research project in progress that is anticipated to provide guidance on unprotected piers: SD2012-02 'Evaluation and Mitigation of Vehicle Impact Hazards for Overpasses.'" Some DOT respondents noted that "for the projects which involve only Resurfacing, Restoring and Rehabilitation, the protection of existing bridge structures may be exempted on a project-by-project basis, based on the factors in question four above."

Question 6: Does your organizations have a policy for the length of need of barriers when protecting the piers is warranted?

Fifty-seven percent of the respondents indicated that their organization has a policy for the length of need of barriers when protecting piers is warranted. Some respondents indicated that this policy is not "official," some reference the AASHTO Roadside Design Guide, while others provided information on how to obtain the specific policy. For example:

- FDOT Design Standard Index 400: http://www.dot.state.fl.us/rddesign/DS/13/IDx/00400.pdf"
- Iowa DOT's Road Design Manual discusses length of need for longitudinal barriers in general: http://www.iowadot.gov/design/dmanual/08b-06.pdf
- NJDOT Roadway Design Manual Section 8 Guidelines for Guide Rail Design and Median Barriers.
- SDDOT Road Design Manual: www.sddot.com/business/design/forms/roaddesign
- See guidance in New York Highway Design Manual: https://www.dot.ny.gov/divisions/engineering/design/dqab/hdm/hdm-repository/rev_64_HDM_Ch10.pdf
- "See page 21 of Roadway Design Manual (link below)
- https://connect.ncdot.gov/projects/Roadway/Roadway%20Design%20Manual/03.%20Guardrail,%20Barriers%20and%20Attenuators.pdf"
- The information is noted in Manual of the Structure and Bridge Division, Volume V - Part 2, Chapter 15, and the standards noted in Manual of the Structure and Bridge Division, Volume V - Part 3.
- Georgia Standards 4000W, 4010, and 4948 are available online at http://standarddetails.dot.ga.gov/stds_dtls/"
- http://www.dot.state.mn.us/bridge/manuals/LRFD/pdf/memo/Memo2007-01.pdf

Having a policy in place for the warranting of barrier absent of the length of need of the warranted barrier has the potential to allow for barriers which will not serve their purpose (e.g., barrier is too short and a vehicle can travel around and behind barrier to hit a bridge pier). Establishing guidance on the length of need for pier protection or an appropriate reference should be a priority of this research.

Question 7: Does your organization have a default longitudinal barrier used for pier protection?

Roughly half (i.e., 44 percent) of the respondents indicated that their organization has a default longitudinal barrier for pier protection. One respondent noted it "depends on type of protection needed (i.e., structural or vehicle protection), room available for barrier installation, roadway and other factors." Some respondents noted specific barriers that (e.g., New Jersey shaped barrier, F-shaped barrier, Single Slope concrete barrier, thrie beam guardrail and w-beam guardrail) are used as the default barrier for pier protection.

Question 8: Are there any reasons for not installing pier protection?

About sixty percent of the respondents indicate there are reasons for not installing pier protection. Many referenced situations where piers are outside the clear zone or satisfying the LRFD specifications. Some other examples given include:

- For some roadways it is not possible to get large vehicles up to an appropriate speed to cause a 600 KIP impact (e.g. bridge has roundabouts on both sides).
- There are alternative routes.
- Posted Speeds are less than 35 MPH.
- Drifting snow complicating snow removal operations.
- Tall barrier may limit sight distance.
- Pier protection may not be cost-effective.
- 3R projects are based on site-specific conditions and accident history.

These special situations, while limited in number, should be considered in the development of new guidelines.

Question 9: Have you experienced any issues with these policies or specifications discussed above?

The representative sample of the respondents' comments regarding the issues experienced are shown below:

- "Question came up in Bridge Design Manual Committee meeting on embankment protection. What dimensions should embankment be to qualify? How high, how wide, what slope?? No guidance is available, to our knowledge."
- "Where shielding with a barrier is required, no information is given on the minimum length of such a barrier necessary to protect the pier."
- "No guidance is given as to whether the requirements apply to existing bridges that were designed using specifications other than LRFD."
- "We have concerns that the LRFD requirements for pier protection are too strict for all cases."
- "Sometimes there is not enough space between the bridge pier and the road track. So it can be difficult to find a solution to contain the vehicle without any load transfer to the pier."
- "The AASHTO LRFD Specifications have changed rapidly and significantly, evidently without considering ramifications."
- "The current AASHTO LRFD specs require 42" or 54" high barriers, even if the zone of intrusion would not allow vehicle to hit the piers."
- "Guidelines are so vague and not mandatory."
- "The current LRFD collision load will result in excessive large pier or extensive work on barrier protection."
- "LRFD appears to be quite conservative and very prescriptive."
- "Yes. At first it was thought that placing a barrier in front of the piers would be the best choice for pier protection, but it was found that width in roadway corridors is at a premium and the barrier itself can be a hazard to traffic. Therefore, in most cases, the pier columns are designed for the crash load and/or a crash strut is constructed."
- "The revised AASHTO Specs do not consider design speed."

The representative comments above suggest clarification is needed regarding the appropriate application of the specification to new and reconstructed bridges, situations where roadway width is limited, embankments and length-of-need. Expanding the options for roadside barriers may also be needed.

Question 10: Are you aware of any specific cases in your State where a bridge pier was damaged in a crash?

Approximately fifty percent of the respondents provided anecdotal evidence of piers damaged by crashes. Below is a sample of these cases and the repairs made:

- "My experience revolves around a tanker truck that crashed into a pier and took the entire structure out of service (Tampa, FL). The bridge was repaired as a design-build contract using the existing bridge plans for plan documentation."
- "June 2007: A bridge pier was heavily damaged by a truck impact in Belgium. The highway was blocked for several days."
- "HGV hit a ramped end to a concrete barrier, rode on the top of the barrier and hit a bridge pier. This was on the M25 motorway in the UK about 5-6 years ago."
- "I know we have had bridge piers impacted by vehicles, and I am aware of at least one case where a loaded semi-trailer hit a pier. I am not, however, aware of any damage to said piers, other than I am certain the bridges remained standing."
- "We have seen minor damage rarely. No piers have been damaged in crashes where piers are protected with guide rail."
- "A few cases of relatively minor fire related damage resulting from a post-crash vehicular fire."
- "Oct 1998 a tractor trailer carrying mail strayed from travel lane and hit the closest of three 3' square columns on the Merrimack 114/140 bridge. Due to the loss of column support, the 3' x 3' horizontal pier cap also failed at the face of the middle column, although it did not collapse."
- "Semi hit large round column. Column was encased in steel, had grout pumped into voids, and was painted to match other columns."
- "Semi-truck took out a single column of a multi-column support. The structure was quickly shored up, column replaced and opened to traffic."
- "We had a truck crash thru a pier. Bridge was a grade separation on a ramp over an interstate. The pier had 3 columns. 2 columns were not effective in carrying loads. Pier cap came to rest on truck. ODOT jacked up the bridge, supported on temporary bents, and rebuilt the pier. Bridge is still in service."
- "We have several cases where trucks have impacted bridge piers. The piers/columns are either replace or encased. details are not readily available."
- "Minnesota has 2 instances of pier hits. We can provide details."

Recall this survey includes respondents from four countries and thirty-six states, however, only two of the cases provided as a response to this question resulted in the bridge collapsing. While not statically meaningful, it appears that catastrophic failure of a bridge is a relatively rare event.

Question 11: As part of this work, the research team is collecting in-service crash records for bridge piers. If you or your agency has data available to help with the development of these guidelines, please list the best way to contact you and the nature of the data in the box below. Thank you.

Approximately 65 percent of the respondents skipped this question and 12 percent indicated that data is not available. In other words, more than three-quarters of those responding do not have data available on pier crashes. Eleven respondents provided contact information,

suggesting data may be available and these respondents would help track down that data. The research team has contacted these respondents and already received data from the state of Wyoming. The state of New Jersey has replied that they will collect crash data for use in this project. The state of Ohio has made their road inventory and crash data available for use in this research. The State of Delaware is compiling data and will make it available. The state of Minnesota has been contacted.

Question 12: Has your State sponsored any in-service performance studies of barriers protecting piers or unprotected piers?

Approximately 93 percent of the respondents indicated that their state has not sponsored a study of the barriers protecting piers or unprotected piers. This lack of in-service study indicates the understanding of existing performance is based on assumptions and anecdotal information, not a scientific analysis of field performance. Assumptions can be clouded by one or two media-grabbing events or, conversely, a lack of "media worthy" events.

Question 13: Are you aware of new construction or maintenance costs available for bridge piers?

All of the respondents to this question responded with some variations of "…pier costs vary with the size and height of the pier, there is no standard cost." Costs are "…calculated from our unit prices for concrete and reinforcing steel. Concrete piers typically require little maintenance." One respondent included the unit costs for concrete from their state: $1,100 per cubic yard for high performance concrete and $950 per cubic yard for non-high-performance concrete.

Question 14: Are you aware of crash repair or replacement costs available for bridges and piers?

None of the respondents currently have this information. One respondent indicated that a crash repair project will be let in the summer of 2013. The research team will follow up with this respondent in the fall of 2013.

Question 15: Do you have any additional comments or suggestions about what should be contained in the guidelines for bridge pier protection?

The suggestions received in response to this question are provided here:

- "Bridge pier protection should include protection of the pier and protection of road users."
- "They should be realistic and based not in what COULD happen, but what does."
- "Definitely want to see a risk-based approach that considers most of the factors the survey listed at the outset."
- "Guidelines should be reasonable and consider cost vs. risk."
- "Please include redundancy in the pier… superstructure redundancy...ADTT… and horizontal alignment."
- "FLEXIBILITY - both in regard to which piers need to be shielded, as well as the type of barrier necessary for a pier to be considered protected."
- "Preventing a pier collapse certainly is a safety issue, but it's not the only safety issue. Considering only one issue doesn't seem to be the best approach, and changes to the bridge specifications seem to have been rushed. Cleaning up the specifications is likely to result in more turmoil unless all safety issues are considered."

- "Guidance is needed for existing bridges, as well as new bridges to reduce conservatively of these criteria."

Respondents from Florida and Kansas suggest reviewing the guidance from those DOTs which supplements the LRFD specification to understand the issues those states have addressed.

SUMMARY

The results of this survey suggest that there is a strong reliance on engineering judgment both regionally and internationally in the protection of piers. Many respondents indicated that clarification is needed during the design development and additional guidance is necessary for 3R projects.

Improving the references to Roadside Design Guide may clarify some of the issues discussed by respondents regarding length of need, however, the issues regarding barrier selection options should be directly addressed during this research effort. When considering barrier options, the special situations pointed out by respondents should be addressed in addition to highway geometrics, including:

- Reasonable travel speed.
- 3R projects.
- Available alternative routes.
- Potential for barrier to limit sight distance.
- Snow removal operations.
- Embankments.

There is a severe lack of available crash and cost data, which would explain why many respondents suggested cost-benefit analysis should be the driver behind pier protection, however, few respondents use cost-benefit analysis when selecting pier protection systems.

Appendix D. Lateral Impact Loads on Pier Columns

DETERMINING AN EQUIVALENT QUASI-STATIC IMPACT LOAD

Assessing the structural resistance of piers to heavy-vehicle impacts requires knowing the nominal lateral resistance and estimating the likely range of real-world impact forces. The first is discussed in detail in Appendix E (Nominal Resistance to Lateral Impacts of Pier Columns) and the former is discussed here. Since impact loads are dynamic, the loading is best characterized as kinetic energy. It is the kinetic energy of the moving vehicle that results in the impact loading to the pier system so appreciating the range and probability of kinetic energies is an important aspect of assessing the risk of pier failure. Kinetic energy in the context of highway vehicles involves the weight and speed of the moving vehicle. The distribution of weights for each of the FHWA vehicle classifications are addressed in Appendix F (Heavy Vehicle Mix and Properties) and speeds is discussed in the next section. These data will be used to develop a probable distribution of impact energy that will then be used to estimate the worst-case loadings caused by heavy-vehicle impacts with piers.

Unfortunately, the dynamic impact energy calculated is not directly comparable to the quasi-static forces calculated by the bridge designer. It is necessary, therefore, to find a method for determining the equivalent load that results from a heavy-vehicle impact so that it can be compared to the calculated design load.

The finite element code LS-DYNA was used to evaluate the static and impact response of the five baseline column designs to determine their strength and capacity. Three loading conditions were evaluated: quasi-static loading with rigid cylinder, 20-mph loading with rigid cylinder and an impact with an 80,000-lbs tractor-trailer truck model impacting the column head-on at 50 mph.

In order to gain confidence in the model results, it was necessary to validate the model predictions against physical test results. There have been no full-scale impact tests with bridge piers, thus the validation of the concrete model was based on comparison to pendulum impact tests. The validation of the tractor-trailer model was based on comparison of a full-scale crash test of an 80,000-lb tractor-trailer impacting a 36-inch diameter rigid steel column. The validation procedures presented in NCHRP Web Document 179 were used to assess the fidelity of the model. [Ray10] The basic approach included:

1. Validate FE model of scaled spiral and square bridge pier columns
    - Develop and construct scaled down versions of spiral and square column pier designs.
    - Perform material characterization tests on cored samples to calibrate material properties.
    - Perform impact tests on the scaled column designs.
    - Develop an LS-DYNA finite element model of the scaled impact experiments and compare/validate the finite element model to the impact experiments.
2. Validate FE model of tractor-trailer
    - Revise the tractor-trailer model developed by NCAC/Battelle/ORNL for head-on high energy impacts.
    - Validate the model by simulating a full-scale tractor-trailer test into a 36” diameter rigid column and comparing results.

3. Develop LS-DYNA models of representative bridge piers and perform quasi-static and dynamic impact analyses to determine capacity in terms of force and energy (and/or impulse).
    - Perform finite element analyses of full-scale column designs using displacement control lateral loading of columns. The columns are to be loaded to failure at two different loading rates: 2 mi/hr (quasi-static) and 20 mi/hr (dynamic).
    - Perform full-scale crash simulations with tractor-trailer model to evaluate strength performance of column under MASH Test Level 5 impact conditions (i.e., head-on impact at 50 mi/hr with impact at center-line of tractor).

The following sections discuss the physical test program for the scaled impact tests, development and validation of the finite element models and the analysis of the selected bridge pier designs to determine capacity.

IMPACT CONDITIONS

Johnson conducted a study on heavy vehicle posted and travel speed for the American Transportation Research Institute in 2008 and the results were presented at the 2010 Annual Transportation Research Board Meeting. [Johnson10] Johnson chose 21 rural interstate highways located throughout the United States with a range of posted speed limits. All the sites were relatively flat and straight for two miles in either direction of the speed measurement location. Travel speed was gathered using on-board vehicle GPS units that recorded the speed when subject vehicles travelled through these road segments. Table 1 shows the roadways used by Johnson, the posted speed limit (PSL) and statistics of the observed travel speeds.

As expected, the distribution of speeds is a normal distribution. The relative 85^{th} percentile speed to the passenger vehicle PSL and a relative mean speed to the PSL were calculated for each site. These calculations were then weighted by the sample size and averaged to find the following linear model with respect to passenger vehicle posted speed limits:

- $1.01 \cdot$ PSL to find the 85^{th} percentile travel speed of trucks,
- $0.96 \cdot$ PSL to find the mean travel speed of trucks and
- The standard deviation of the truck travel speed distribution is $0.05 \cdot$ PSL.

Weigh-in-motion data was used to determine the speed distribution of heavy vehicles at two WIM data collection stations as described in Appendix F (Heavy Vehicle Mix and Properties). Both WIM stations are on rural principal arterials with 70 mi/hr posted speed limits.

Table 1. Heavy Vehicle Posted and Travel Speeds for Interstate Highways. [after Johnson10]

State	Hwy	Posted Speed Limit (PSL)	Sample Size	Average Speed (mph)	85th Percentile Speed	Relative	
						85th/PSL	Mean/PSL
CA	I-5	55	277	61.2	65	1.18	0.87
IL	I-57	55	262	64.2	68	1.24	0.99
OR	I-5	55	273	60.9	64	1.16	0.94
WA	I-5 †	60	139	63.3	67	1.12	0.90
WA	I-5	60	154	64.5	67	1.12	0.92
WA	I-90	60	246	62.9	66	1.10	0.90
CT	I-395	65	184	66.4	70	1.08	1.02
CT	I-84*	65	156	66.0	69	1.06	1.02
CT	I-95	65	212	66.1	70	1.08	1.02
SC	I-85*	65	433	67.2	71	1.09	1.03
AR	I-40	65	169	66.7	70	1.08	0.95
SC	I-26	70	276	69.0	73	1.04	0.99
MO	I-44	70	247	68.6	73	1.04	0.98
TX	I-40	70	131	68.6	72	1.03	0.98
OK	I-40	70	168	69.4	72	1.03	0.99
NM	I-25	75	36	68.9	75	1.00	0.92
NM	I-40	75	276	68	73	0.97	0.91
SD	I-90	75	193	67	71	0.95	0.89
WY	I-90	75	140	69.8	75	1.00	0.93

† Six-lane highways. All others are four lanes.

As shown in Table 2, the ratios of the mean and 85th percentile travel speed of all heavy vehicles to the PSL is somewhat less than that predicted by Johnson for the Lodi, CA WIM site but almost identical for the Brevard County, FL WIM site. Table 2 shows that the ratio is somewhat different for the different vehicle classes at the Lodi site but more similar across all heavy vehicle classes at the Brevard County, FL WIM site. The WIM data indicate that the model based on the Johnson data is a reasonable model of how heavy vehicle travel speed varies with respect to the posted passenger vehicle speed limit.

Table 2. Travel Speed Percentiles by Vehicle Class for Two WIM Stations.

Vehicle Category	FHWA Vehicle Class	Samples	50th/PSL	85th/PSL	99th/PSL
Lodi, CA WIM Site					
Bus	4	31,738	0.97	1.03	1.14
Single-Unit Truck	5	923,192	0.96	1.06	1.20
	6	81,671	0.86	0.91	1.03
	7	1,077	0.82	0.88	0.96
Single-Trailer Truck	8	133,074	0.84	0.90	1.00
	9	2,334,096	0.84	0.89	0.97
	10	18,879	0.84	0.89	0.95
Multi-Trailer Truck	11	375,456	0.84	0.89	0.96
	12	42,648	0.84	0.89	0.97
	13	3,515	0.82	0.87	0.94
Unknown		112,203	0.84	0.90	1.18
Weighted average of all heavy vehicles		4,057,549	0.87	0.93	1.03
Brevard Co., FL WIM Site					
Bus	4	25,285	1.01	1.07	1.17
Single-Unit Truck	5	232,322	0.99	1.06	1.20
	6	82,296	0.99	1.06	1.14
	7	13,716	0.98	1.06	1.13
Single-Trailer Truck	8	99,175	0.97	1.03	1.11
	9	1,633,972	0.99	1.06	1.14
	10	16,071	1.00	1.06	1.15
Multi-Trailer Truck	11	60,334	0.91	0.97	1.03
	12	18,869	0.96	1.02	1.09
	13	3,717	0.98	1.05	1.18
Unknown		72,254	0.99	1.09	1.49
Weighted average of all heavy vehicles		2,258,011	0.98	1.06	1.16

The vehicle properties recommended for use in this research effort are shown in Appendix F (Heavy Vehicle Mix and Properties). The kinetic energy of a moving heavy vehicle is given by:

$$KE = \frac{1}{2}\left[\frac{W}{32.2}\right]\left[V \times \frac{5280}{3600}\right]^2$$

where: W = Weight of vehicle in kips,

V = Travel speed of the vehicle in mi/hr and

KE = Kinetic energy of the vehicle in kip-ft.

In a series of two crash tests involving an 80,000 lbs Class 9 tractor trailer trucks striking a rigid pole at 50 mi/hr, Buth concluded that the peak force experienced by the pier column was approximately 600 kips. While the validity of this value is the subject of a later section, the 600 kips observed force would be correlated with the impact kinetic energy of the tractor trailer truck in the crash test; $0.5 \cdot (80/32.2)(50 \cdot 5280/3600)^2 = 6{,}680$ ft-kips. In selecting vehicle properties and impact conditions for the development of pier design and protection guidelines, the distribution of properties chosen should be able to produce impacts with more than 6,680 ft-kips of kinetic energy in order to subject the piers to failure producing loads. The WIM data from Lodi, CA and Brevard County, FL were examined to determine if the speeds and weights of heavy vehicles at these sites included vehicles with sufficient kinetic energy to pose a serious risk of failure to piers. The distributions of the kinetic energy at the two WIM sites are summarized in Table 3 where cells that exceeded 6,680 ft-kips are shown in a bold font.

Generally speaking, most of the tractor trailer classes of heavy vehicles (i.e., classes 8-13) had an 85th percentile energy greater than 6,680 ft-kips, the energy associated with the 600-kip design load. In some of the tractor trailer truck cases, even the mean energy was above this load limit. This indicates that roughly 15 percent of the heavy vehicles on at least these two rural principal arterials have sufficient energy to cause an impact load of 600 kips if the bridge pier were struck. The energies tabulated in Table 3 should be viewed as the energy when the vehicle first encroaches rather than impact energies since the vehicle will lose some energy as it traverses the roadside or median prior to striking the pier. The closer the pier is to the roadside, however, the smaller the amount of energy that will be lost so this value is an upper bound.

Table 4 shows the list of recommended heavy vehicles to use in developing bridge pier design and protection guidelines. The speed needed to produce 6,680 ft-lbs of kinetic energy was back calculated using the equation above and the vehicle weight for each type of vehicle. As shown in Table 4, it is highly unlikely that the light or average weight SUT will ever have sufficient speed to generate more than 6,680 ft-lbs of kinetic energy. On the other hand, the extra heavy SUT and all the tractor trailers except the light (i.e., empty) weight category can have sufficient kinetic energy at what may be considered typical highway speeds (e.g., 50 to 65 mi/hr). The extra heavy tractor trailer truck, which represents the 99th percentile truck weight, has sufficient energy even at a relatively low speed of 44 mi/hr.

Table 3. Kinetic Energy Percentiles by Vehicle Class for Two WIM Stations.

Vehicle Category	FHWA Vehicle Class	Percentile of Kinetic Energy (ft-kips)				
		50th	85th	90th	95th	99th
Lodi, CA WIM Station						
Bus	4	5,279	7,532	7,866	8,346	**9,355**
Single-Unit Truck	5	1,761	2,656	2,949	3,409	4,266
	6	2,498	4,439	5,010	5,768	**7,192**
	7	6,536	**7,672**	**8,050**	**8,434**	**9,903**
Single-Trailer Truck	8	3,689	5,150	5,529	6,127	**7,389**
	9	**6,847**	**9,232**	**9,600**	**10,123**	**11,337**
	10	**7,024**	**9,189**	**9,643**	**10,308**	**12,012**
Multi-Trailer Truck	11	6,667	**9,187**	**9,633**	**10,232**	**11,367**
	12	6,544	**8,839**	**9,275**	**9,897**	**11,130**
	13	**11,093**	**19,397**	**20,632**	**22,384**	**25,385**
Unknown		3,232	**8,364**	**8,972**	**9,842**	**12,718**
Brevard Co., FL CA WIM Station						
Bus	4	4,776	**6,559**	**6,945**	**7,618**	**8,970**
Single-Unit Truck	5	2,375	3,235	3,469	3,848	4,683
	6	3,695	5,518	6,066	**6,841**	**8,269**
	7	8,200	**10,095**	**10,620**	**11,363**	**12,830**
Single-Trailer Truck	8	4,587	6,171	6,592	**7,241**	**8,766**
	9	6,937	**9,983**	**10,623**	**11,536**	**13,300**
	10	7,836	**11,512**	**12,324**	**13,469**	**15,695**
Multi-Trailer Truck	11	**6,965**	**8,466**	**8,799**	**9,279**	**10,214**
	12	**7,088**	**9,242**	**9,790**	**10,559**	**12,104**
	13	**10,050**	**15,659**	**16,780**	**18,357**	**21,117**
Unknown		3,777	**7,533**	**8,675**	**10,244**	**13,462**

Note: Cells with bold font indicate that the energy is greater than 6,680 ft-kips which was shown in crash tests to generate a rigid-pole peak force of 600 kips.

Table 4. Minimum Travel Speed for Encroachment Energy of 6,680 ft-kips for the Recommended Analysis Vehicles.

Vehicle Group	FHWA Vehicle Class	Weight	Min. Speed
		lbs	mi/hr
Light SUT	5-7	11,500	132
Average SUT	5-7	15,000	116
Heavy SUT	5-7	22,000	95
Extra Heavy SUT	5-7	50,600	63
Light TT	8-9	27,000	86
Average TT	8-13	50,000	63
Heavy TT	8-13	80,000	50
Extra Heavy TT	8-13	105,000	44

REPRESENTATIVE PIER DESIGNS.

Pier designs using columns appear to be the most at-risk type of pier designs due to the relatively small size of the columns and the exposure of the leading columns to vehicle impacts. Pier walls, whether full-road width walls or walls supporting hammerheads, are so large as to be unlikely to fail. The purpose of choosing representative designs for evaluation in this project is not to replicate what might be common on the roadside but, rather, to choose a range of designs that encompass pier components that are likely to fail under impact loading to those that are unlikely to fail in impact loadings. The five baseline pier column designs proposed for use in developing the guidelines are listed in Table 5.

Table 5. Representative Pier Column Designs for Evaluation (Baseline).

Diameter (inches)	Design Capacity (LRFD 5.8.3.4.2) (kips)	Longitudinal Bars (number and size)	Shear Reinforcement (size and spiral pitch)
24	253	5 #9	#3 w/ 2.25-inch pitch
30	349	8 #9	#3 w/ 2.25-inch pitch
36	461	9 #10	#4 w/ 4.00-inch pitch
48	710	15 #10	#4 w/ 4.00-inch pitch
54	872	11 #14	#5 w/ 6.00-inch pitch

Note: f'_c = 4 ksi, f_y= 60 ksi and concrete cover = 3 inches for all the designs listed.

Each of the pier column designs listed in Table 5 would meet the 6th edition of the LRFD Bridge Design Specifications with respect to shear if the concrete cover were 1.5 inches or less. The bridge design guidelines in most States, however, require 3 inches of concrete cover for

bridge piers (e.g., Ohio). To meet the LRFD specifications for a 3-inch concrete cover requires an increase in the amount of shear steel (e.g., increase in bar size and/or reduced pitch). For example, Table 6 lists the LRFD compliant designs for the five bridge pier diameters shown in Table 5 for the case of a 3-inch concrete cover. The increase in the amount of shear steel results in higher shear capacities for each given column diameter; however, the research team is unaware of any state's bridge pier designs that meet these requirements (except maybe those states in earthquake zones). Throughout the remainder of this report, the designs listed in Table 5 will be designated with a "b" indicating they are baseline designs (e.g., representative pier 24b is listed in the first column of Table 5).

Table 6. Representative Pier Column Designs for Evaluation (Alternate).

Diameter (inches)	**Design Capacity** (LRFD 5.8.3.4.2) (kips)	**Longitudinal Bars** (number and size)	**Shear Reinforcement** (size and spiral pitch (in))
24	468	5 #9	#4 w/ 1.75-inch pitch
30	624	8 #19	#4 w/ 1.75-inch pitch
36	744	9 #10	#5 w/ 3.00-inch pitch
48	1095	15 #10	#5 w/ 3.00-inch pitch
54	1283	11 #14	#5 w/ 3.00-inch pitch

The shear capacities shown in Tables 5 and 6 were computed using the General Procedures of Article 5.8.3.4.2 of the 6th edition of the AASHTO LRFD Bridge Design Specifications. [AASHTO12] Of course, there are many pier columns on the highway network that do not meet the 6th Edition requirements but their capacities can be determined using the 6th Edition procedures.

Regarding the baseline designs shown in Table 5, one has a capacity of only 254 kips which would be very vulnerable to impacts and another has a capacity less than 400 kips which was a critical value in the previous LRFD specifications. Two of the designs in Table 5 are well above the current design guideline of 600 kips and should have a relatively low risk of failure. This selection of representative designs should, therefore, provide the necessary range for examining the implications of setting the design capacity at a variety of values.

FULL-SCALE IMPACT WITH A RIGID POLE

Buth *et al* performed a full-scale crash test involving an 80,000-lbs tractor trailer truck striking a rigid instrumented pole in order to determine the load characteristics of a heavy-vehicle striking a bridge pier. [Buth11] The test was performed in order to measure the impact force resulting from the collision of an 80,000-lb tractor/box-trailer impacting a rigid 36-in diameter column. The rigid column was 14 feet tall and was instrumented in the longitudinal direction with two load cells. The test vehicle was a 2001 Freightliner FLD tractor and a 1983 utility van-trailer as shown in Figure 1. The vehicle was ballasted to a gross-static weight of 79,640-lb using bags of sand placed on pallets and distributed throughout the length of the

trailer. The geometric dimensions and mass inertial measurements of the test vehicle are provided in Figure 2.

The vehicle struck the rigid column head-on at 48.4 mi/hr with the centerline of the vehicle aligned with the center of the rigid column, as shown in Figure 1. At 0.2 seconds after impact, the front of the engine compartment contacted the pier reaching a peak 10-msec force of 980 kips at 0.3 seconds. By 0.125 sec, the cab stopped forward motion, but the truck-frame continued around the rigid column. The front of the trailer contacted the rear of the cab at 0.187 seconds and began to crush the cab of the truck. At 0.276 seconds a peak 10-msec load of 465 kips occurred as the front wall of the trailer failed. The king-pin remained intact while the ballast continued to move forward pushing the (failed) front-wall of the trailer. At 0.380 sec the ballast again began to compress the cabin, and at 0.393 sec a 10-msec peak force of 460 kips occurred as the front-wall of the trailer, along with the ballast material, made direct contact with the rigid column. The trailer creased forward motion at 0.452 sec.

Figure 1. Vehicle and Instrumented Rigid Column Used in Test 429730-2. [Buth11]

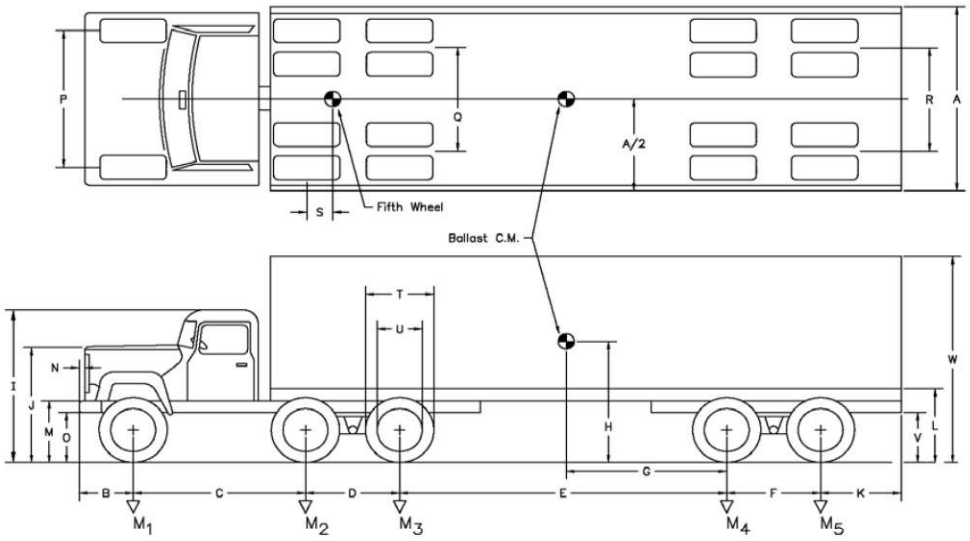

Vehicle Geometry -mm

	Test Vehicle	FE Model	Error %		Test Vehicle	FE Model	Error %		Test Vehicle	FE Model	Error %		Test Vehicle	FE Model	Error %
A	96.00	102.40	6.7	G		208.90		N	0.75			T	41.00	39.50	-3.7
B	45.00	45.00	0.0	H		61.00		O	17.25	20.40	18.3	U	23.00	23.30	1.3
C	208.00	191.80	-7.8	J	73.25	68.50	-6.5	P	80.25	75.90	-5.4	V	36.50	36.50	0.0
D	51.00	50.00	-2.0	K	67.00	61.10	-8.8	Q	73.00	75.00	2.7	W	153.00	153.30	0.2
E	356.00	391.00	9.8	L	52.00	51.30	-1.3	R	71.00	80.50	13.4				
F	49.00	49.00	0.0	M	31.00	28.60	-7.7	S	26.00	18.10	-30.4				

Mass -Properties

		Curb			Test Inertial			Gross Static		
		Test Vehicle	FE Model	Error %	Test Vehicle	FE Model	Error %	Test Vehicle	FE Model	Error %
M_1	(lb)	8,780	-	-	-	-	-	-	-	-
$M_2 + M_3$	(lb)	14,900	-	-	-	-	-	-	-	-
$M_4 + M_5$	(lb)	12,480	-	-	-	-	-	-	-	-
M_{Total}	(lb)	36,160	29,872	-17.4	79,640	79,918	0.3	79,640	79,918	0.3
I_{xx}	(kip - ft^2)	-	-	-	-	587	-	-	587	-
I_{yy}	(kip - ft^2)	-	-	-	-	23,566	-	-	23,566	-
I_{zz}	(kip - ft^2)	-	-	-	-	23,641	-	-	23,641	-

Figure 2. Properties for the Vehicle for Test No. 429730-2 and FE Model. [Buth11]

Figure 3. Post-Test Photos of TTI Test 429730-2. [Buth11]

SCALED IMPACT EXPERIMENTS WITH CONCRETE COLUMNS

Dynamic pendulum impact tests were performed to measure the failure characteristics of axially loaded reinforced concrete columns when subjected to lateral impact loads. The impact tests were conducted at the Federal Outdoor Impact Laboratory (FOIL) at the Turner-Fairbank Highway Research Center located in McLean, Virginia. The test matrix included scale-models of four reinforced concrete bridge pier designs, including three circular-spiral column designs and one square-tied column design. The tests were set up to excite failure in the columns representative of typical of real-world bridge column failures.

The size of the test specimens were limited by the maximum amount of impact energy that could be achieved in the pendulum tests (i.e., 58 kip-ft) and the minimum diameter spiral that could be achieved for the shear reinforcing steel (e.g., ≈ 9 inches).

TEST ARTICLES

The test specimens were generally 1/3 scale models of some typical bridge pier columns based largely on those found by Buth *et al*. [Buth10] The design parameters for the four design cases tested are listed in Table 7 and images of the four designs are shown in Figure 4. The steel reinforcing was fabricated by Harris Rebar located in Canaan, New Hampshire; and the columns were poured by Precast of Maine located in Topsham, Maine. Designs I, II and IV meet both the ACI and LRFD specifications; while Design III involves a spiral-pitch that is greater than currently allowed by ACI or the LRFD. [AASHTO12] Bridge piers with such large pitch designs were observed quite frequently in the real-world crash cases investigated by Buth (e.g., #2 bar with 6-inch pitch); so apparently there are numerous spiral columns already in the field that have relatively low shear-steel-to-concrete ratios that a probably reflective of earlier design standards.[Buth10]

The test program included five samples of Design I, and three each of Designs II through IV for a total of 14 samples. The additional samples for Design I were used in preliminary tests for calibrating impact conditions and finalizing data collection procedures. The selected design cases allow for comparing:

(1) The effect of the number of longitudinal bars (e.g., Design I and Design II),
(2) The effect of the spiral pitch (e.g., Design II to Design III) and
(3) The effect of shape (e.g., Design III and Design IV).

Table 7. Four Scale Model Designs Used in the Test Program.

	Design			
	I	**II**	**III**	**IV**
Size/Shape	12-inch Dia.	12-inch Dia.	12-inch Dia.	12-inch Sq.
Longitudinal Steel	6 #4	11 #3	11 #3	8 #4
Shear Steel	#3 Spirals @ 1-3/8" pitch	#3 Spirals @ 1-3/8" pitch	#3 Spirals @ 8-5/8" pitch	#3 Ties @ 8" spacing
Ratio of Longitudinal Steel to concrete	1.04%	1.07%	1.07%	1.09%
Ratio of Shear Steel to concrete core	1.9%	1.9%	0.30%	0.39%

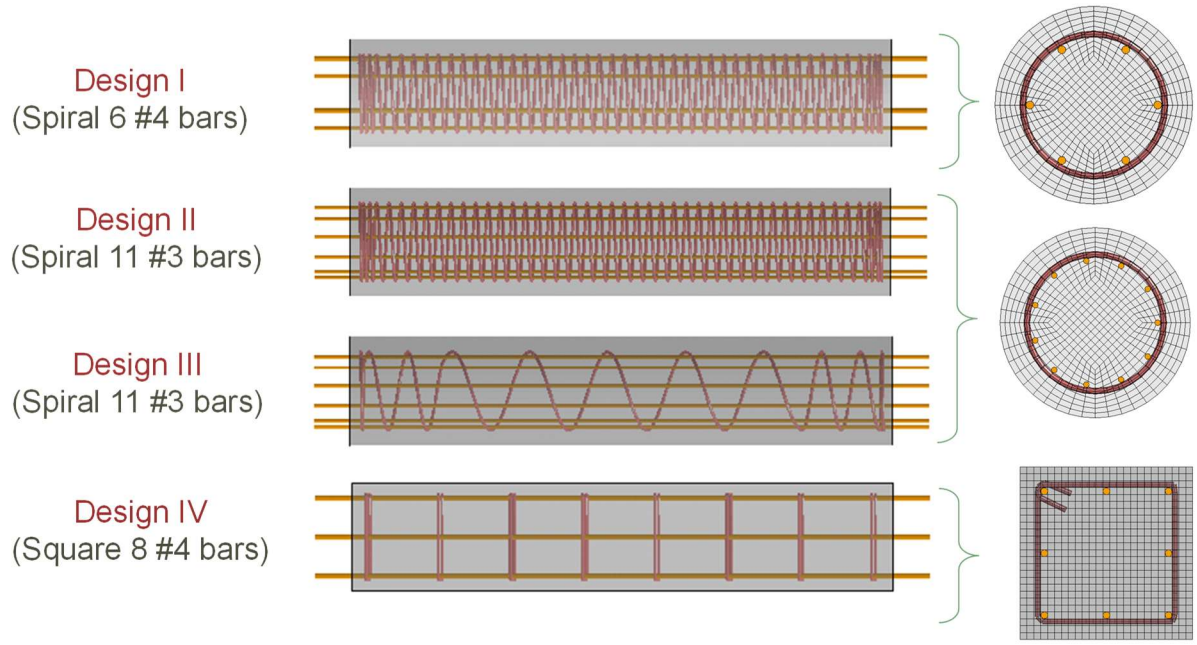

Figure 4. Images of the Four Design Cases for the Test Program.

STRENGTH PROPERTIES OF CONCRETE

The unconfined design strength of the concrete was specified to be 5 ksi. During fabrication of the concrete column specimens, eight test cylinders were poured with dimensions 4-inch diameter by 8 inches long. These cylinders were tested at the Tuner-Fairbanks Highway Research Center (TFHRC) laboratory using a uniaxial-load machine to measure the actual unconfined compression strength of the concrete. These tests were performed within ± 5 days of the dynamic impact tests on the concrete columns. The results for each of unconfined compression tests are shown in Table 8; the mean value was 7.88 ksi with a standard deviation of 0.47 ksi.

Table 8. Unconfined Compression Test Results for Concrete Cylinders - Measured at TFHRC Laboratory.

Specimen Identification	Specimen Diameter top (in)	Specimen Diameter Bottom (in)	Area (in^2)	Force at Failure (kip)	Strength (ksi)
15-113 / 56D / 8-5	4.0	4.01	12.60	91.67	7.28
15-114 / 56 D / 8-6	4.0	4.01	12.60	89.8	7.13
15-115 / 56D / 8-7	4.0	4.01	12.60	102.86	8.16
15-116 / 56D / 8-10	4.0	4.01	12.60	100.52	7.98
15-117 / 56D / 8-11	4.0	4.01	12.60	102.22	8.11
15-118 / 56D / 8-12	4.0	4.01	12.60	98.92	7.85
15-119 / 56D / 8-13	4.0	4.01	12.60	100.22	7.96
15-121 / 56D / 8-17	4.0	4.01	12.60	108.09	8.58

Average Strength =	**7.88 ksi**
Standard Deviation =	**0.47 ksi**

In addition to the eight poured cylinders, a 12x12x6 inch concrete slab was also poured during the column fabrication process. This slab was used to extract six cored samples which were tested by to measure various strength properties for the concrete. The dimensions of the cored samples were 1.86 inches diameter by 3.75 inches long. The tests included two unconfined compression tests, two triaxial compression tests with 21.8 ksi confining pressure and two triaxial tests with 43.5 ksi confining pressure.

The results for the unconfined compression tests are shown in Table 9. The mean value was 6.93 ksi with a standard deviation of 1.02 ksi. Test UNC-S2B15 yielded a similar result to those measured at TFHRC. It was assumed that the low value for unconfined compressive strength measured in Test UNC-S2A15 resulted from a premature failure of the specimen. The plots for true stress vs. true strain for the three test cases are shown in Figures 5, 6 and 7. The plot for true stress vs. pressure is shown in Figure 8.

Table 9. Unconfined Compression Test Results for Concrete Cores - Measured at ARA Laboratory.

Specimen Identification	Specimen Diameter top (in)	Specimen Diameter Bottom (in)	Area (in^2)	Strength (ksi)
UNC-S2A15	1.86	1.86	2.72	6.21
UNC-S2B15	1.86	1.86	2.72	7.65

Average Strength =	**6.93 ksi**
Standard Deviation =	**1.02 ksi**

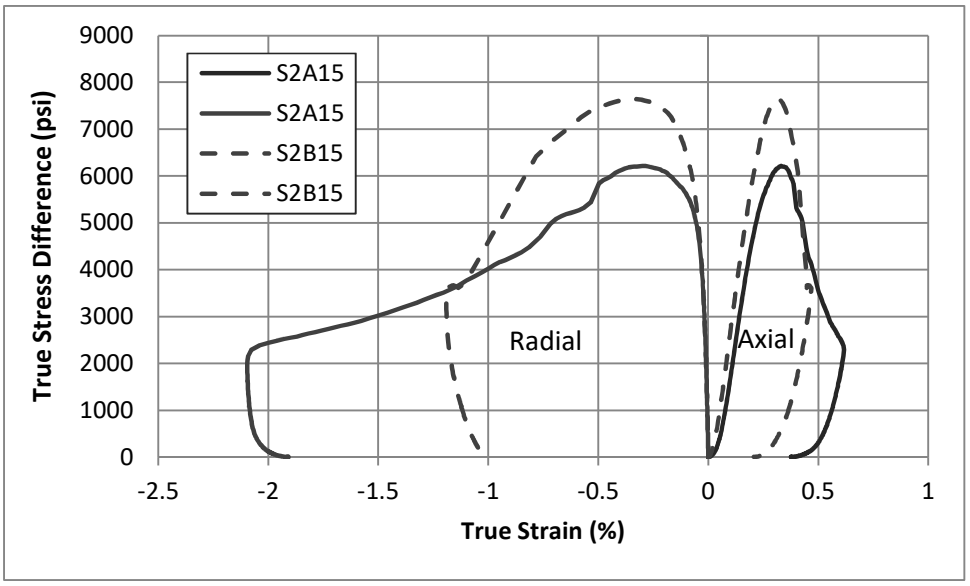

Figure 5. Stress Difference versus Strain for ARA Unconfined Compression Tests.

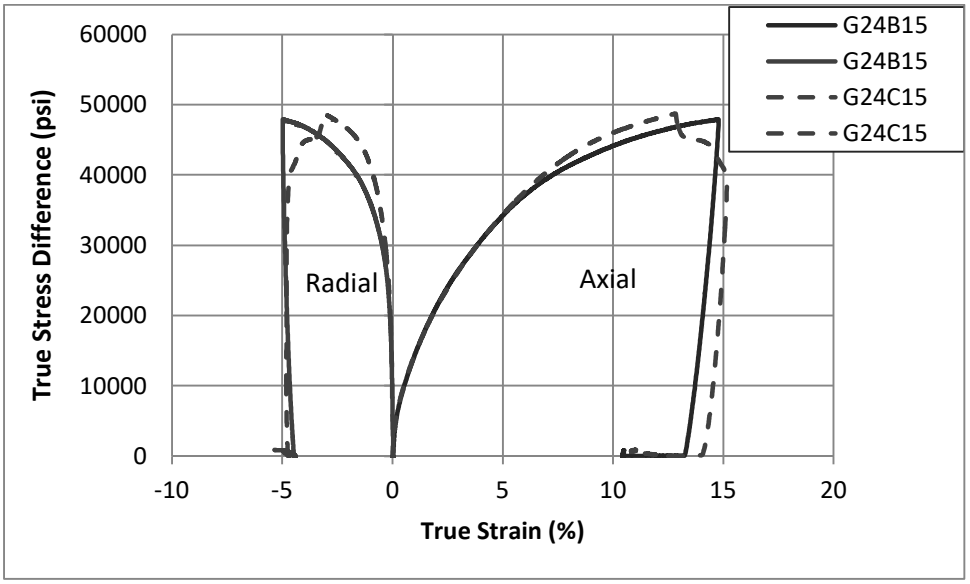

Figure 6. Stress Difference versus Strain for ARA Triaxial Tests with 21,750 psi Confining Pressure.

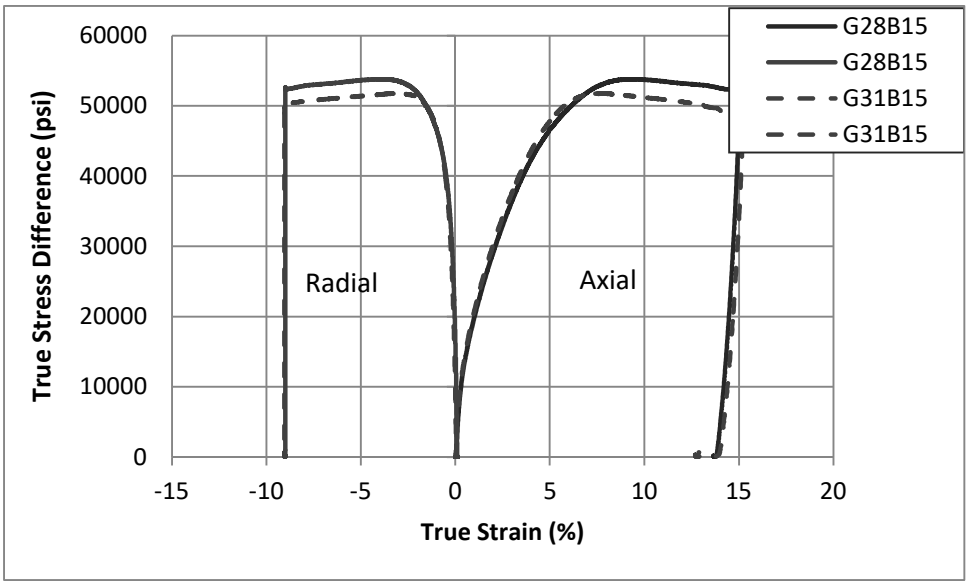

Figure 7. Stress Difference versus Strain for ARA Triaxial Tests with 43,500 Psi Confining Pressure.

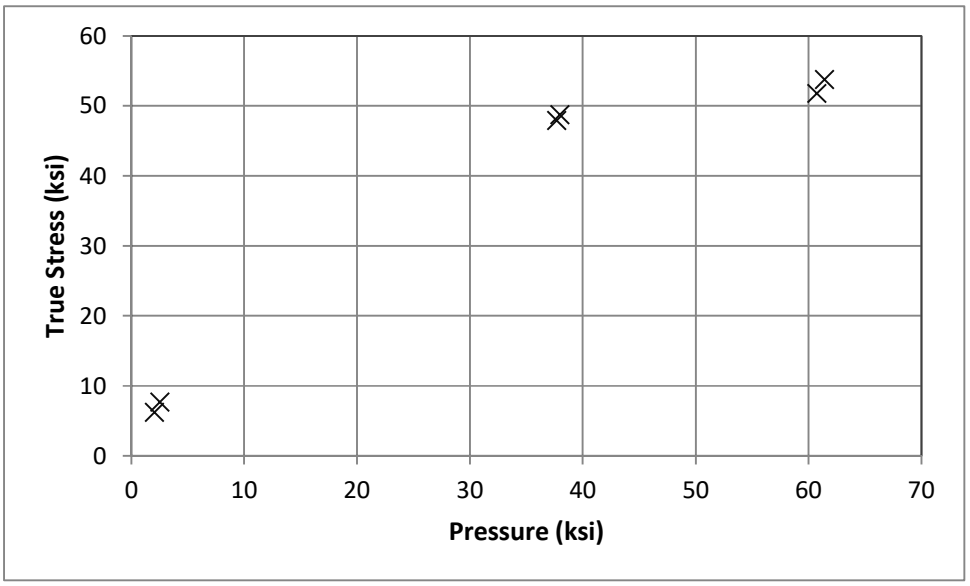

Figure 8. Shear Failure Surface from ARA Tests.

PENDULUM TEST SETUP

The test setup is shown in Figures 9 and 10. The column was positioned horizontally in the test fixture and struck on its side at the mid-point of the column. A 15x 15 x 1-inch cap-plate was mounted onto each end of the column specimens by inserting the rebar, which protruded out of the ends of the column, through 11/16-inch diameter holes drilled in the cap-plates; a washer and nut was welded onto each rebar to secure the column to the plates, as shown in Figure 11. The cap-plates were then bolted onto the test fixture using twenty-four 5/8-inch diameter bolts (i.e., twelve Grade 8 bolts on the front [tension] side of the fixture and fourteen Grade 5 bolts at remaining locations around the perimeter of the plates). An important aspect of the fixture design

was to ensure that it provided boundary constraints at the ends of the column that were rigid as feasible to ensure that all the kinetic energy transferred from the striker during the tests was absorbed solely by the concrete test specimens and not lost to deformations at the specimen boundaries. A 25-kip axial load was applied to the ends of the column to simulate a typical working load on the column (e.g., 15 percent of design strength). The load was applied using a hydraulic jack and was measured using a 100-kip load cell (refer to Figures 9 and 10).

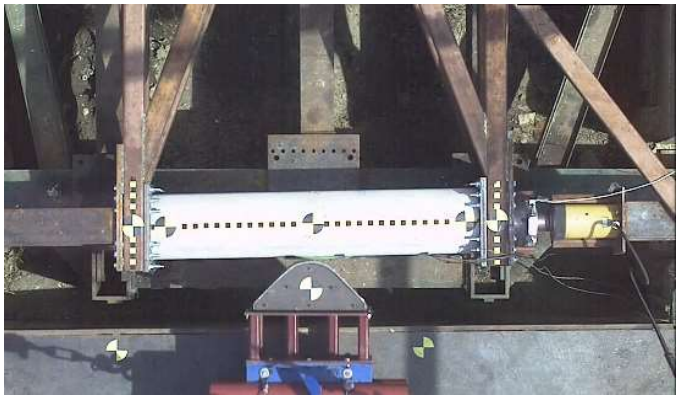

Figure 9. Overhead View of Test Setup for FOIL Test Series 15008.

Figure 10. Isometric View of Test Setup for FOIL Test Series 15008.

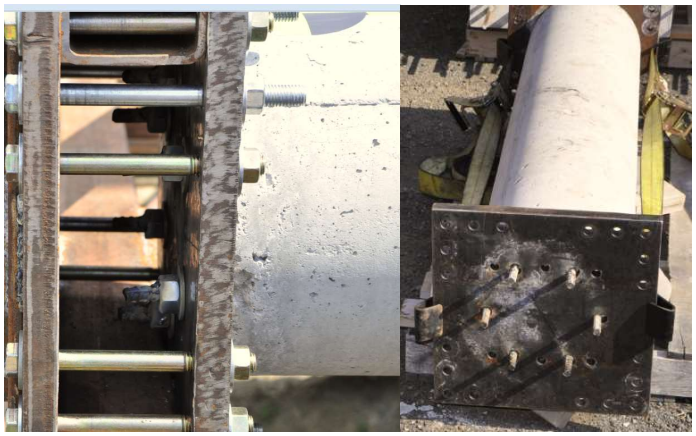

Figure 11. Column Cap-Plate.

IMPACT CONDITIONS AND TEST MATRIX

The columns were struck on their side at mid-span by a 4,360-lb rigid pendulum with a wooden nose. Accelerometers were mounted onto the back of the pendulum mass to measure accelerations of the striker during impact, and impact forces were back calculated from the accelerometer data. Three tests were performed for each design except for Design III which included only two tests. A nominal impact velocity of 10 mi/hr (14.67 ft/s) was performed for the first two tests for Designs I through III to assess repeatability of the tests. The third tests for Designs I and II were performed at a slightly higher nominal impact velocity of 12 mi/hr (17.6 ft/s). A higher impact speed was desired to ensure failure of the column but safety of the test equipment was a concern. For Design IV the impact conditions for the second and third tests were incrementally reduced to determine the threshold of failure for the column. The complete test matrix is shown in Table 10 excluding preliminary "shake-down" tests.

Table 10. Test matrix for Test Series 15008 – Lateral Impact into Scaled Pier Designs.

				Concrete			Long. Steel		Spiral/Shear Steel			Impact Conditions	
Design No.	Test No.	Test Date	Type	F'c	Maximum Aggregate Size (in)	Concrete Cover (in)	No. of Bars	Bar Size	Spiral Outside Diameter (in)	Bar Size	Pitch (Spacing) (in)	Weight (lb)	Speed (ft/s)
I	15008D	8/24/2015	12"-Spiral	7.88	0.75	1.125	6	#4	9.75	#3	1-3/8	4,360	14.42
	15008J	9/2/2015	12"-Spiral	7.88	0.75	1.125	6	#4	9.75	#3	1-3/8	4,360	14.36
	15008K	9/3/2015	12"-Spiral	7.88	0.75	1.125	6	#4	9.75	#3	1-3/8	4,360	16.90
II	15008F	8/27/2015	12"-Spiral	7.88	0.75	1.125	11	#3	9.75	#3	1-3/8	4,360	14.02
	15008I	9/1/2015	12"-Spiral	7.88	0.75	1.125	11	#3	9.75	#3	1-3/8	4,360	14.33
	15008L	9/4/2015	12"-Spiral	7.88	0.75	1.125	11	#3	9.75	#3	1-3/8	4,360	17.06
III	15008G	8/28/2015	12"-Spiral	7.88	0.75	1.125	11	#3	9.75	#3	8-5/8	4,360	14.22
	15008H	8/31/2015	12"-Spiral	7.88	0.75	1.125	11	#3	9.75	#3	8-5/8	4,360	14.39
IV	15008M	9/8/2015	12"-Tied	7.88	0.75	1.125	8	#4	-	#3	8	4,360	15.40
	15008N	9/9/2015	12"-Tied	7.88	0.75	1.125	8	#4	-	#3	8	4,360	12.73
	15008O	9/10/2015	12"-Tied	7.88	0.75	1.125	8	#4	-	#3	8	4,360	9.72

TEST RESULTS

A summary of the test results is shown in Table 11 which includes peak force, peak displacement, and the reserve elastic energy in the column specimens at peak displacement in terms of rebound energy of the pendulum. In all cases, there were radial cracks which originated on the tension side of the column near the impact location; and also shear cracks and spalling at the tension sided of the column at the boundaries. In most cases, the radial cracks at the center extended all the way through the column diameter but did not result in complete failure (i.e., complete dislocation of the top and bottom of the section) of the column as long as there was sufficient shear steel. For example, Figure 12 shows the damage to the column for Design I after Test 15008D which resulted in full-diameter cracks and the column retained much of its strength. When the columns did not have sufficient shear steel, the column rupture was very sudden and resulted in complete loss of capacity, such as for Design III and IV as shown in Figure 13.

Table 11. Summary of Results for Scaled-Column Impact Test Series 15008.

			Impact Conditions			Results				
No.	**Test No. and Date**	**Type**	**Weight (lbs)**	**Speed (ft/s)**	**Kinetic Energy (kip-in)**	**Peak Force (kips)**	**Peak Disp (in)**	**Rebound Velocity (ft/s)**	**Rebound Energy (kip-in)**	**Energy Ratio (rebound/ final)**
I	15008D 8/24/15	12"-Spiral	4,360	14.42	168.9	71.3	3.15	-5.46	24.2	14.3%
	15008J 9/02/15	12"-Spiral	4,360	14.36	167.5	87.9	3.20	-5.43	24.0	14.3%
	15008K 9/03/15	12"-Spiral	4,360	16.90	232.0	88.2	3.98	-5.99	29.1	12.6%
I	15008F 8/27/15	12"-Spiral	4,360	14.02	159.7	88.0	2.86	-6.87	38.3	24.0%
	15008I 9/01/15	12"-Spiral	4,360	14.33	166.8	88.5	3.00	-5.94	28.7	17.2%
	15008L 9/04/15	12"-Spiral	4,360	17.06	236.5	94.1	3.90	-6.02	29.4	12.5%
III	15008G 8/28/15	12"-Spiral	4,360	14.22	164.3	85.6	3.30	-2.91	6.9	4.2%
	15008H 8/31/15	12"-Spiral	4,360	14.39	168.2	73.3	3.74	-2.25	4.1	2.4%
IV	15008M 9/08/15	12"-Tied	4,360	15.40	192.7	76.3	4.24	-0.24	0.0	0.0%
	15008N 9/09/15	12"-Tied	4,360	12.73	131.7	88.3	2.38	-3.47	9.8	7.4%
	15008O 9/10/15	12"-Tied	4,360	9.72	76.8	75.5	2.08	-4.94	19.8	25.8%

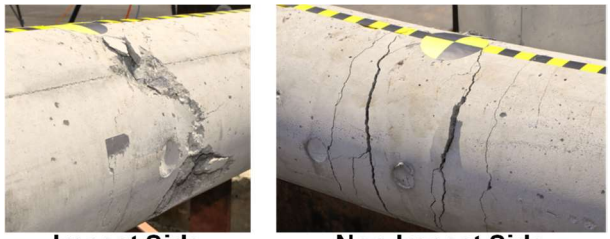

Figure 12. Damage to Design I under Baseline Test Conditions (Test 15008D)

Figure 13. Damage to Designs III and IV under Baseline Test Conditions.

The following sections discuss the capacity of the test columns in terms of force and energy. The differences in impact energy arise solely to changes in impact speed since the mass of the striker and the mass of the columns were constant for all tests.

FORCE CAPACITY

The force-time histories and the force-deflection plots (i.e., center deflection of the column) are shown in Figures 14 through 17.[1] The peak force in the tests ranged from 71.3 to 94.1 kips with no notable difference in the peak force for the different design cases. The minimum peak force occurred for Design I in Test 15008D, but this reduced force was likely due to the 4 rebar that failed at the boundaries prior to the column reaching its peak response. A similar reduction occurred for Design IV in test 15008M where two longitudinal bars were broken at the left boundary during impact. The relatively low peak force in Test 15008H for Design III was more difficult to understand. In this case the general response was essentially the same as the response in Test 15008G with the exception of the magnitude for the two peaks (refer to Figure 16).

[1] All time history data in this section from the pendulum tests were processed using an SAE Class 60 filter.

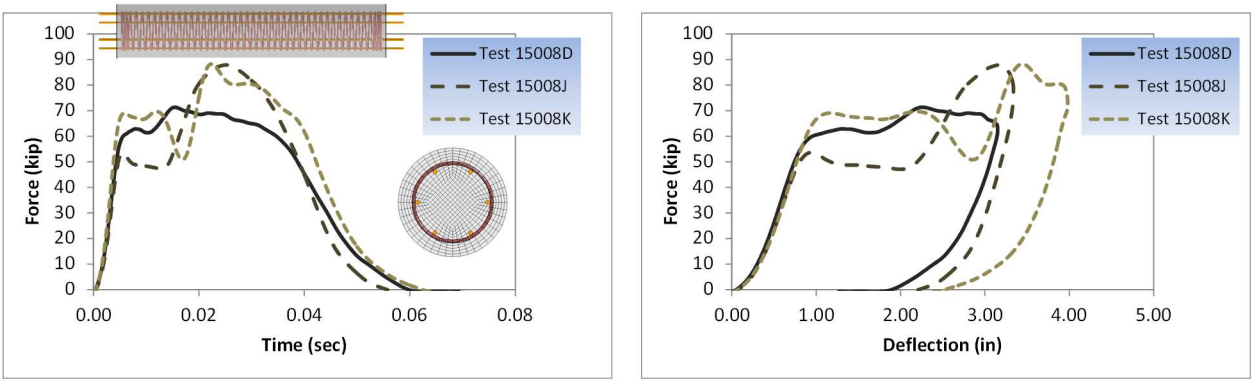

(a) (b)

Figure 14. Results for Design I Showing (a) Force-Time History and (b) Force-Displacement.

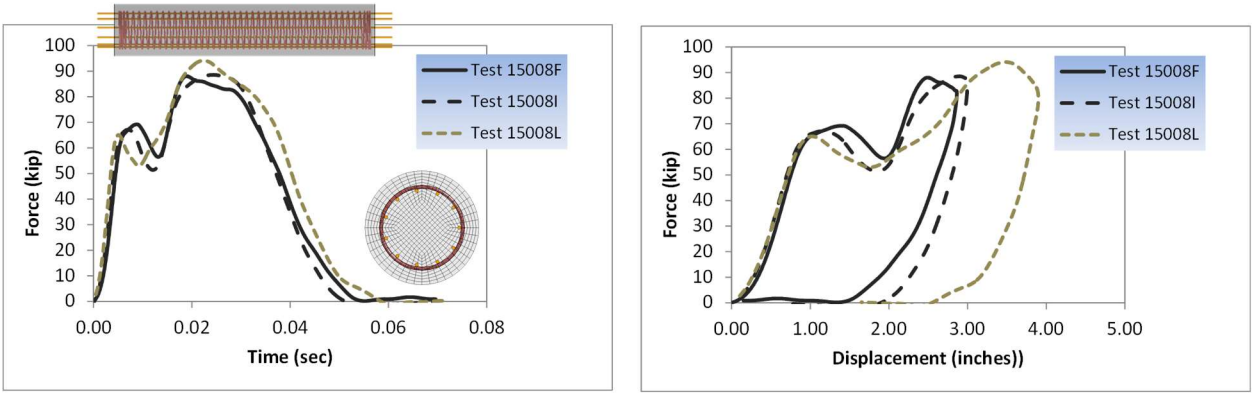

(a) (b)

Figure 15. Results for Design II Showing (a) Force-Time History and (b) Force-Displacement.

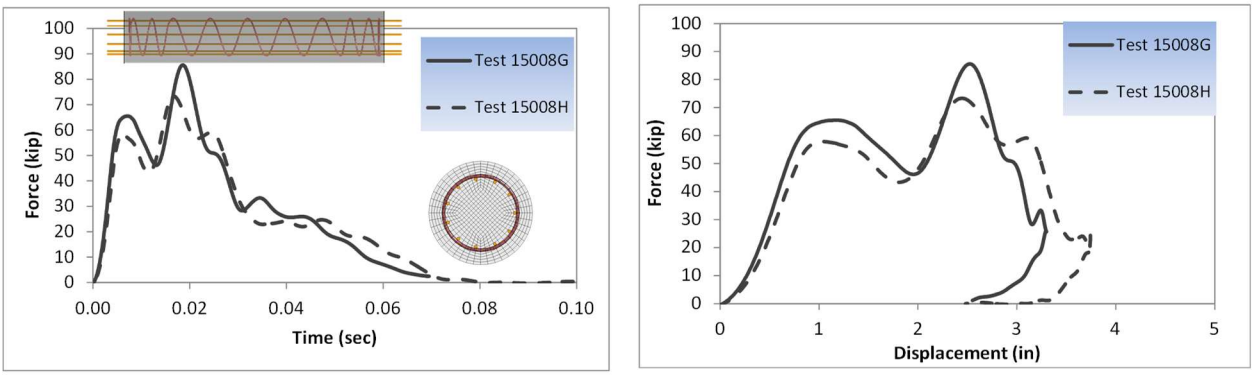

(a) (b)

Figure 16. Results for Design III Showing (a) Force-Time History and (b) Force-Displacement.

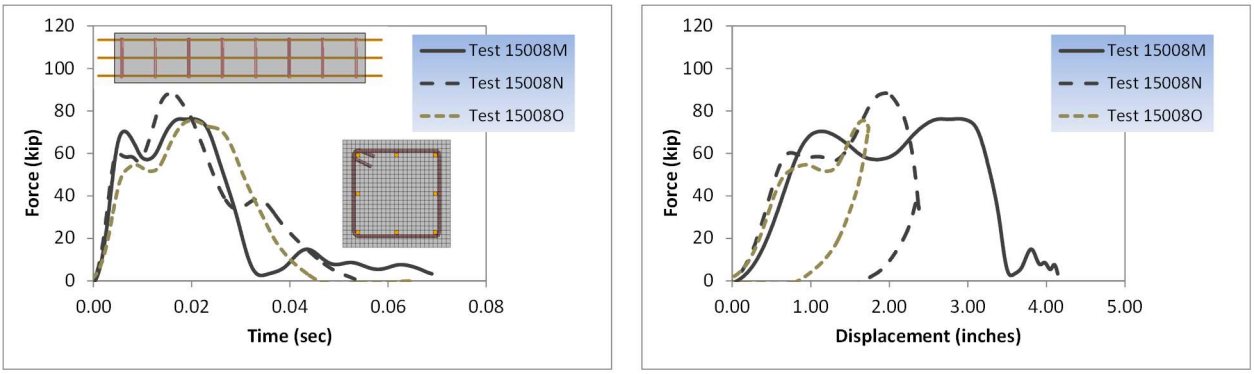

Figure 17. Results for Design IV Showing (a) Force-Time History and (b) Force-Displacement.

The results of these tests indicate that impact force is not a good indicator of the strength capacity of columns. It may be inferred from the results that failure is not likely unless the force reaches a magnitude of at least 88 kips for Designs I and II; 73 kips for Design III; and 76 kips for Design IV. However, once these minimum force levels are attained they must then be sustained until the deflection of the column reaches critical values. Generally speaking, the peak force for all the pendulum tests occurred about one inch of centerline lateral deflection as shown in Figure 14 to Figure 17. After the peak force is achieved there is generally a plateau in the force-deflection response. The width of this plateau is dependent on the amount of kinetic energy in the striking pendulum and represents a phase of the collision where the concrete is completely cracked from the tension face to the impactor and the plateau force results from the additional straining of the longitudinal steel.

STRAIN ENERGY CAPACITY

Designs I and II

In Tests 15008D and 15008J the impact energies were 169 and 168 kip-in, respectively. The rebound energy of the pendulum for these cases was around 24 kip-in (14 percent of the initial impact energy); thus, there was significant elastic energy in the column at the point of maximum displacement which was approximately 3.2 inches. When the impact energy was increased to 232 kip-in the rebound energy increased slightly to 29.1 kip-in. This implies that there was increased elastic energy in the column when it reached a max displacement of 3.9 inches. The fact that the reserve elastic energy in the column was still increasing as the impact energy increased, implies that there is likely considerable reserve strain energy capacity due to the longitudinal steel for these designs cases beyond those impact energies tested. No additional specimens were available for investigating higher impact energies.

Design III

In Tests 15008G and 15008H for Design III the baseline impact conditions resulted in complete rupture of the columns. The rebound energies for the pendulum in these two tests were 6.9 kip-in and 4.1 kip-in, respectively, with maximum displacements of 3.3 inches and 3.74 inches, in which Test 15008H had a slightly higher impact energy. Lower impact velocities were not investigated, thus the threshold for the onset of failure was not determined.

Design IV

This design was tested at three impact velocities resulting in energy values of 192.7, 131.7 and 76.8 kip-in for Tests 15008M, N and O, respectively. At 192.7 kip-in of impact energy the column failed completely with no rebound of the pendulum (i.e., with no reserve elastic energy in the column). Reducing the impact energy to 131.7 kip-in again resulted in complete rupture of the concrete in the column with a rebound energy of 9.8 kip-in of the pendulum (i.e., minimal elastic energy in the column at max displacement). Reducing the impact energy further to 76.8 kip-in resulted in minimal damage to the column and relatively high rebound energy of 19.8 kip-in for the pendulum. The threshold for onset of failure was therefore between 131.7 kip-in and 76.8 kip-in.

Capacity Assessment

The lateral load capacity based on the shear force and hinge moment discussed earlier can be used to assess the pendulum test results. The test results and the estimates from the simple plastic hinge model are shown below in Table 12 and the associated force-displacement plots are shown in Figure 18. The LRFD shear capacity shown in Table 12 is the nominal capacity (i.e., ϕ =1 rather than 0.9). A ϕ of 1 was used since the results are being compared to physical test results rather than being used as a design criterion. Similarly, there is no ϕ associated with the simple hinge model capacity either. In Table 12 cells colored red indicate that either failure was observed in the test or failure was predicted by the simple hinge model or nominal shear calculation.

Table 12. Capacity Assessment of Scaled Pendulum Tests.

Test Results				**Nominal LRFD Shear Capacity** (See Appendix E)	**Simple Hinge Model Capacity** (See Appendix E)	
Test	**Design**	**Force** (kips)	**Energy** (in-kips)	**Force** (kips)	**Force** (kips)	**Energy** (in-kips)
15008D	I	58	169	188	39	11
15008E		62	167		39	11
15008J		53	168		39	11
15008K		68	232		39	11
15008F	II	63	161	188	86	45
15008I		63	168		86	45
15008L		63	238		86	45
15008G	III	64	166	63	86	45
15008H		64	169		86	45
15008M	IV	70	193	90	63	46
15008N		60	132		63	46
15008O		56	77		63	46

Failure for the tests were generally based on the observed condition of the sample whereas failure for the simple hinge model implies that at least two layers of longitudinal bars have reached the fully plastic stress. Failure requires first that the lateral load capacity be achieved and second that there is more energy available after the lateral load capacity has been reached.

Figure 12, shown earlier, illustrates the damage to the test specimen in Test 15008D. As shown in Figure 12, there are tension cracks and shear crack as well as some spalling although the top and bottom of the section did not have any relative displacement. As such, the specimen was considered as not failing. The nominal LRFD shear capacity was 188 kips, much higher than the 58-kip peak load observed in the test. The simple hinge model predicted failure since the test load exceeded 39 kips and there was more than 11 in-kips of energy available. This may indicate that the specimen in Test 15008D may have been just over the failure limit or at the point of failure. This is confirmed from the upper left portion of Figure 18 where the peak lateral test forces just exceed the simple hinge prediction. The simple hinge model provided a conservative prediction whereas the LRFD shear capacity was still much higher. Similar results occurred for the other tests of Design I.

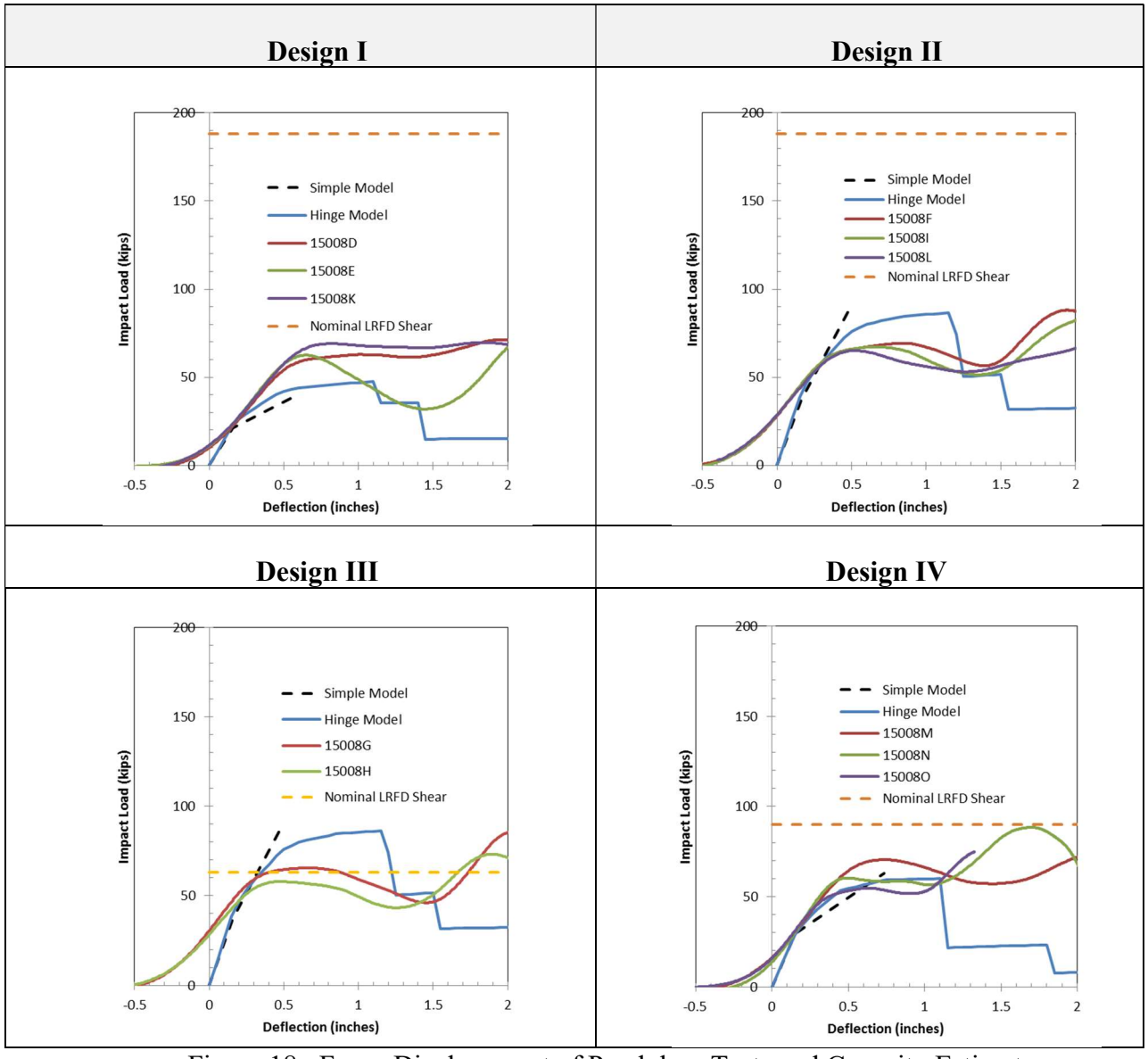

Figure 18. Force-Displacement of Pendulum Tests and Capacity Estimates

Designs II and III were identical except Design III was under-reinforced for shear as shown in Table 12. The damage to Design III in Test 15008G, shown earlier in Figure 13, included shear and tensile cracks, spalling and a very large shear dislocation that separated the section. As shown in Table 12, the nominal LFRD shear capacity predicted no failure for Design II (i.e., Tests 15008F, 15008I and 15008L) but failure for both Design III tests (i.e., Tests 15008G and 15008H) which agrees with the test results. The simple hinge capacity model does not account for shear steel at all and is based only on the longitudinal reinforcement. The simple hinge capacity method predicted that all the tests for Designs II and III were just under the hinge capacity limit. This is confirmed by the Design II tests but contradicted by the Design III tests. It appears that the failure limit state reached first (e.g., shear in Design III and plastic hinge in Design II) predicts the failure.

Design IV was a square column and the damage in Test 15008M was shown earlier in Figure 13. None of the three tests exceeded the nominal LRFD shear capacity but two tests (i.e., Tests 15008M and 15008N) exceeded the simple hinge model capacity. Both the physical tests and the simple hinge capacity model indicated that Tests 15008M and 15008N failed whereas Test 15008O did not. This is confirmed from the lower right portion of Figure 18 where the peak lateral test forces just exceed the simple hinge prediction for 15008M and 15008N but are just under for Test 15008O. The simple hinge model accurately predicted the failure of the specimens for Design IV.

CONCLUSIONS

Eleven dynamic tests were conducted using a 4,360-lb pendulum impacting four column designs and various impact speeds ranging from 9.72 ft/s to 15.4 ft/s. The primary purpose of these tests was to provide physical test data for validation of the finite element models of reinforced concrete columns. The validated models were then used to investigate static and dynamic strength capacity of various full-scale bridge pier columns as will be described in a subsequent section.

Regarding the response of the columns in these tests, the following conclusions have been drawn regarding lateral impact loading on the side of reinforced concrete columns with various types and amounts of shear steel:

1) Increasing the amount of shear reinforcement does not necessarily increase the lateral load capacity of the column.
2) Increasing the amount of shear reinforcement increases the ductility of the column.
3) Increasing the amount of shear reinforcement increases the strain energy capacity of the column.
4) In order to fail the column, the maximum lateral load capacity of the column must be attained and then sustained until the column reaches its critical deflection (e.g., bending or shear strain). Recall from bullet 2) that the ductility increases as the amount of shear steel increases.
5) Columns that do not have sufficient volume of shear steel and/or those that have too large of spacing between shear reinforcement will ultimately fail in shear.

Although, the column designs that had high shear reinforcement ratios did not undergo complete failure, they did result in several large radial cracks, some of which extended through

the full cross-section of the column. It is uncertain what the final failure mode would be for these column designs.

A comparison of the nominal LRFD shear capacity and the simple hinge model capacity showed that whichever value is exceeded first will determine the failure mode. Generally, the nominal LRFD shear capacity was much higher than the simple hinge lateral load except for Design III which was intentionally under-reinforced for shear. The simple hinge model appears to provide reasonable though slightly conservative predictions of the lateral impact load capacity of these scaled down experiments.

CALIBRATION OF CONCRETE MATERIAL MODEL

One of the purposes of performing the scaled impact experiments was to collect data for validating the concrete material model in LS-DYNA such that it could be used with confidence in full-scale simulations. The LS-DYNA *MAT_RHT (MAT272) material model was calibrated for 7.8 ksi (54 MPa) unconfined compression strength concrete using triaxial compression data at three confining pressures. The results of the triaxial tests were presented earlier in this report. The calibration consisted of modifying the shear failure and pressure versus volume strain parameters generated by MAT272 for a 54 MPa unconfined compression strength. Additional details of the concrete material model calibration are provided in Appendix 6.2D.

Detailed finite element models of the four test column designs and test fixture were developed and used to simulate the impact conditions performed in Test Series 15008. Figure 19 shows the finite element models of the four test-columns, where the concrete model is displayed in transparent mode. The mesh for the concrete is only shown for Column A in Figure 19 in order to facilitate visual comparison of the reinforcing steel in the different designs.

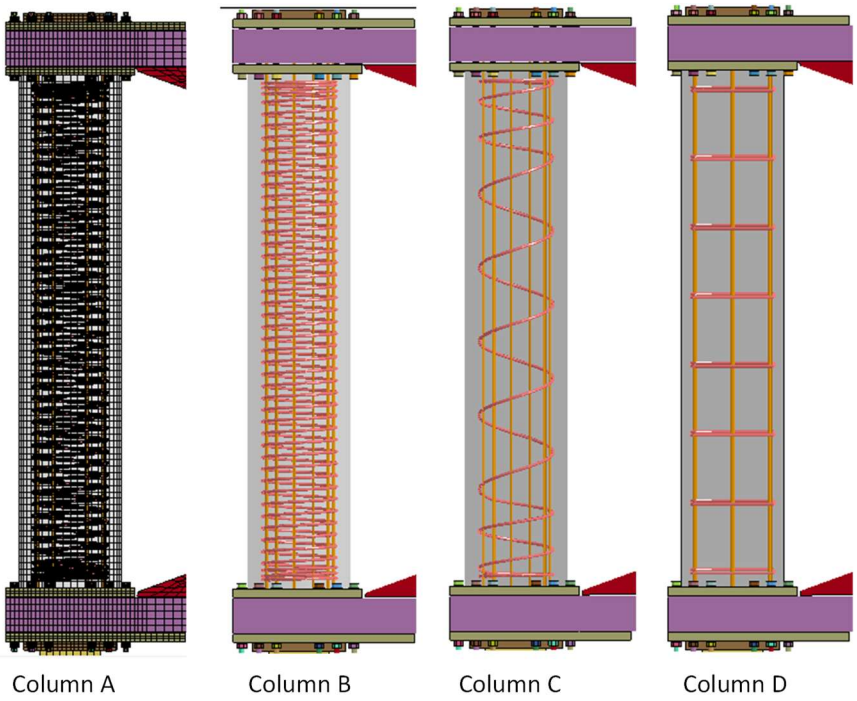

Figure 19. Finite Element Models for the Four Test-Column Designs.

The validity of the model results was assessed by direct comparison to the physical tests. The assessment included comparison of force vs. time, force vs. deflection, as well as qualitative

comparison of visual damages (e.g., concrete cracking, spalling and damage to the steel reinforcement).

The finite element model used for simulating Test Series 15008 is shown in Figures 20 through Figure 21. The concrete columns were modeled with 44,880 constant-stress brick elements (Type 1 in LS-DYNA) with nominal size of 19x22x10 mm. The rebar was modeled using the default Hughes-Liu beam element with nominal length of 1 inch. The nuts that fasten the 1-inch thick plate onto the ends of the column were restrained to the rebar using rigid nodal constraints. The cap-plates were modeled with 13,668 constant-stress brick elements with element lengths ranging from 0.314 to 0.472 inches (8-12 mm) with three elements through the thickness with side length 0.333 inches (8.5 mm). The fixture tubes were modeled with 15,000 thin-shell fully-integrated elements (type 16 in LS-DYNA) with nominal length of 1 inch. The wide-flange sections were modeled with 2,232 thin-shell elements with nominal length of 1 inch. The bolts fastening the cap-plates to the fixture were modeled using the Hughes-Liu beam element with nominal length of 0.43 inch (11 mm). All welds were modeled using the rigid-spot-weld option in LS-DYNA.

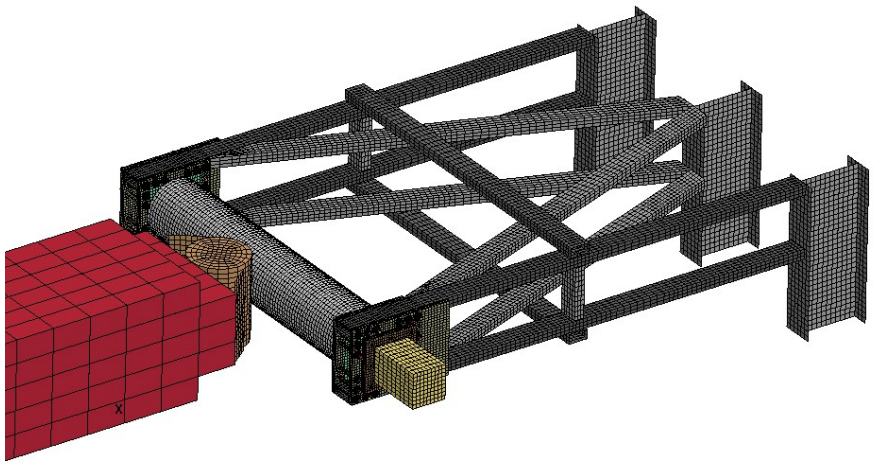

Figure 20. Isometric View of the Finite Element Model Used for Simulation of Test Series 15008.

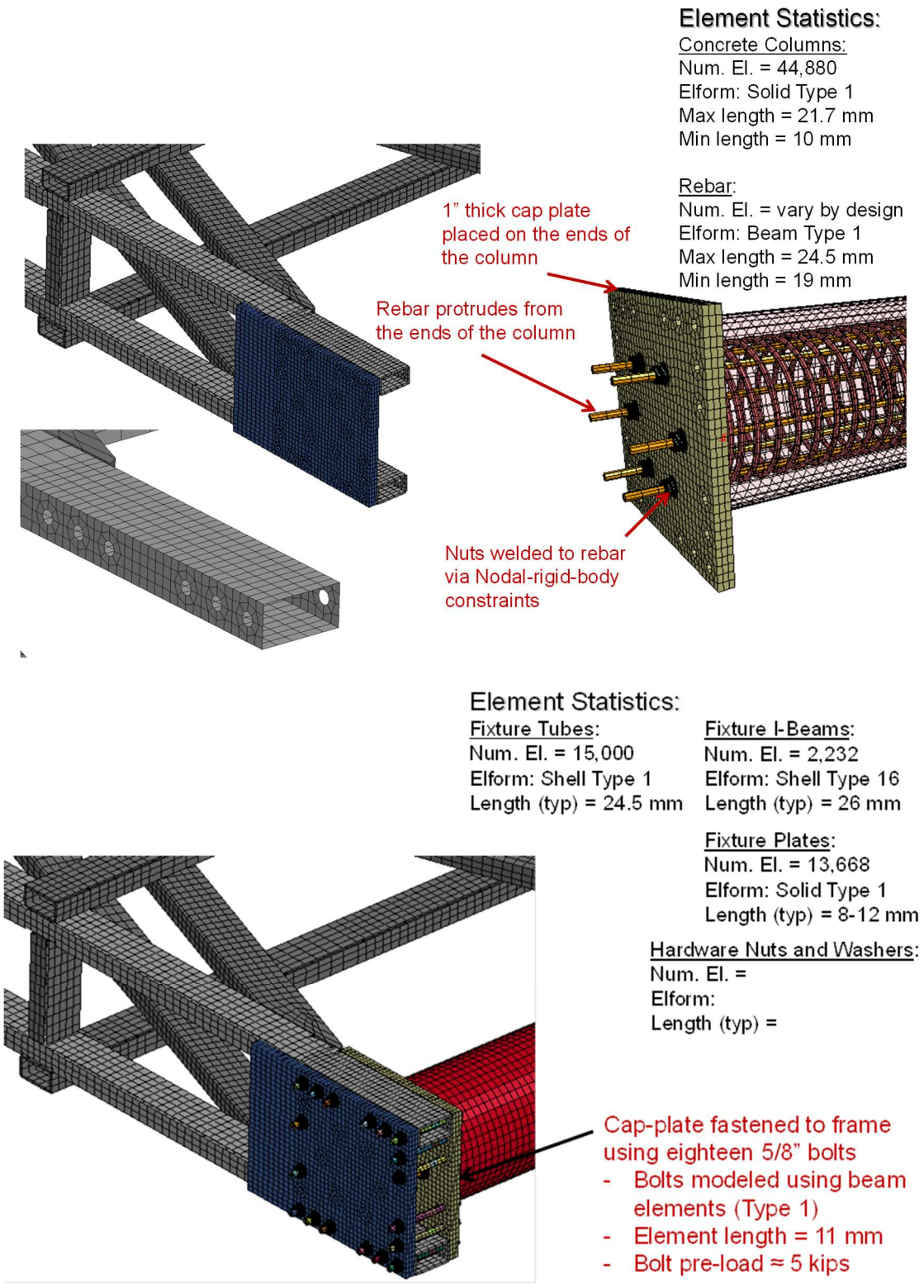

Figure 21. Model Details and Element Statistics for Simulation of Test Series 15008.

The 25-kip axial load was applied in the model by restraining the left-end of the fixture plate from translation in the axial direction of the column and applying a displacement-time history to the rectangular block (representing the hydraulic jack) at the right-end of the fixture until the target load was achieved. The position of the rectangular block was then held fixed during the simulated impact. The pendulum was modeled with elastic material properties consistent with concrete and the pendulum head was modeled with wood properties.

The bond-connection between the rebar and the concrete was modeled using the Constrained_Beam_in_Solid option in LS-DYNA. This is a new feature in LS-DYNA which is only available in the latest version (i.e., version R8.0.0) and side-steps certain limitations involving energy conservation that are inherent in other constraint formulations (e.g., Constrained_Lagrange_in_Solid). The material characterization for the rebar was based on tensile tests performed on ASTM A615 Grade 60 #4 bars. The engineering stress-strain curve and the corresponding true-stress versus true-strain curve for the rebar material are shown in Figure 22. Notice that while 60 ksi rebar steel has a yield stress of 60 ksi, the ultimate engineering stress increases to about 100 ksi. Incorporating this strengthening is an important feature of correctly modeling the pier columns in large deflections to failure.

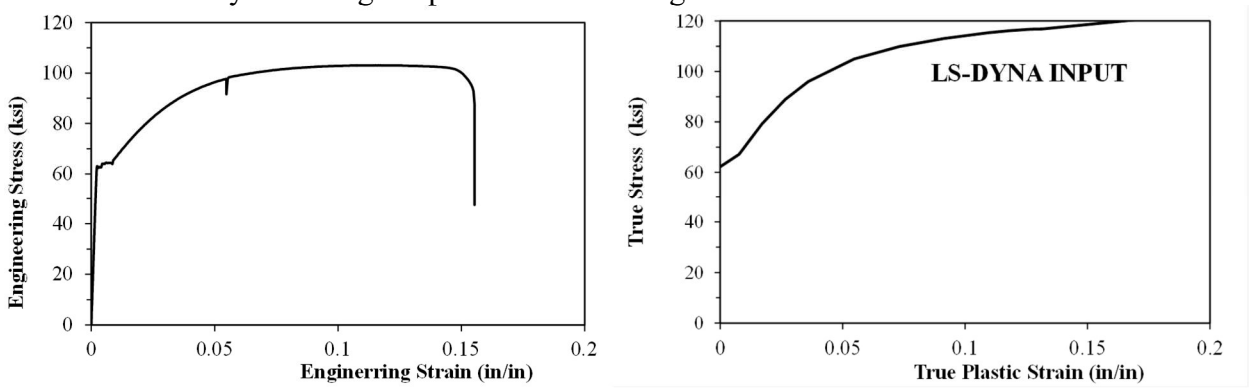

Figure 22. Stress-Strain Curves for ASTM A615 Grade 60 #4 Rebar.

A total of eight analyses were conducted and the complete analysis matrix is shown in Table 13. The finite element analyses were conducted with a time-step of 0.84 microseconds for a time period of 0.1 seconds. The impact location was at the center point of the column with impact velocities that varied depending on the test case being simulated. The force-time histories and the force-deflection response from the model are compared to the tests in Figures 23 through 30. The images in each of the figures show the deformation of the column at peak deflection. The damage to the column is in the finite element analysis is represented by a contour plot of 1st principle strain with the contour range cut off at a strain of 0.1. Yellow contours indicate that a crack has occurred in the concrete, and red contours indicate significant crack opening has occurred. Table 14 provides a summary of peak force, peak displacement, rebound velocity and energy for the striker and whether or not the impact resulted in "failure." In several of the cases, cracks extended all the way through the cross-section of the column; however, "failure" here was defined by an obvious displacement shift separation of the column at the failure plane.

Table 13. Simulation Matrix for the Concrete Validation Study.

Design No.	Analyses			Corresponding Tests	
	Case No.	Nominal Impact Speed (mph)	Impact Speed (ft/s)	Test No.	Impact Speed (ft/s)
I	1	10	14.37	15008D	14.42
				15008J	14.36
	2	12	16.87	15008K	16.9
II	3	10	14.37	15008F	14.02
				15008I	14.33
	4	12	17.01	15008L	17.06
III	5	10	14.37	15008G	14.22
				15008H	14.39
IV	6	10.5	15.4	15008M	15.4
	7	8.7	12.73	15008N	12.73
	8	6.6	9.68	15008O	9.72

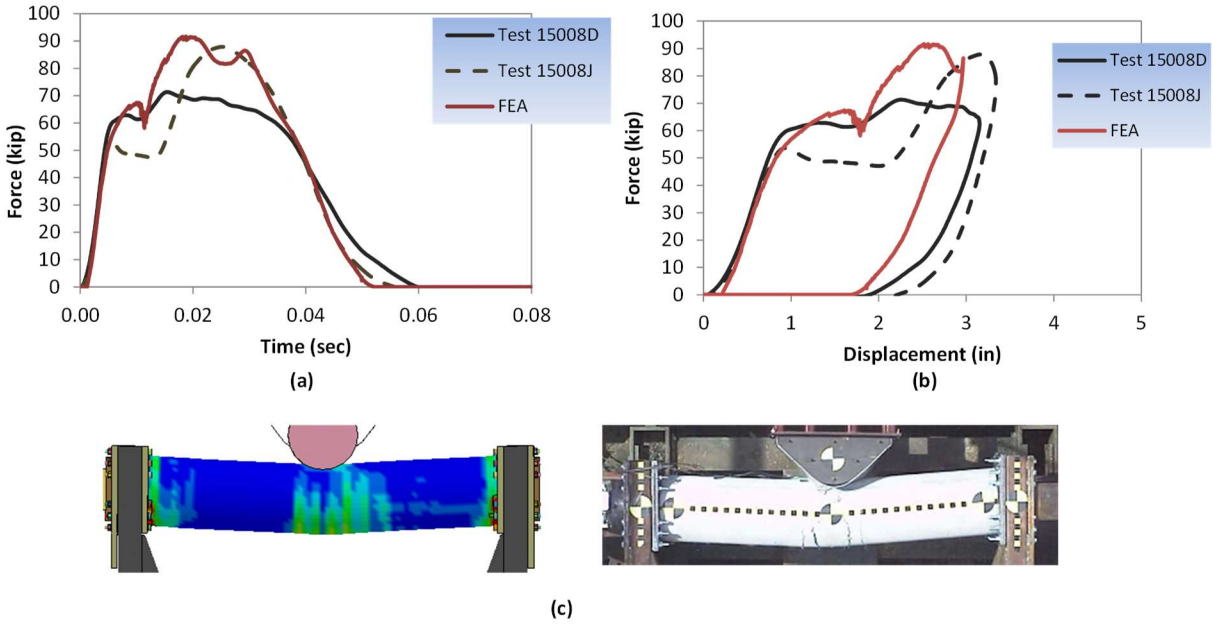

Figure 23. Comparison of FEA for Design I with Tests at 10 mi/hr (nominal) regarding (a) Force versus Time, (b) Force versus Deflection and (c) Concrete Damage.

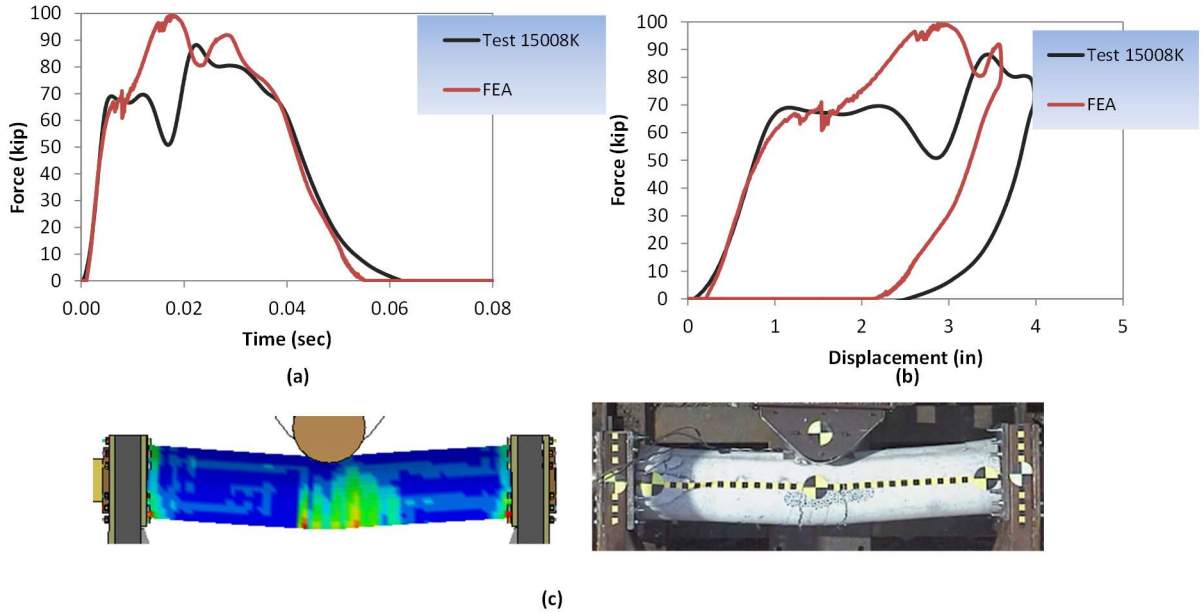

Figure 24. Comparison of FEA for Design I with Tests at 12 mi/hr (nominal) regarding (a) Force versus Time, (b) Force versus Deflection and (c) Concrete Damage.

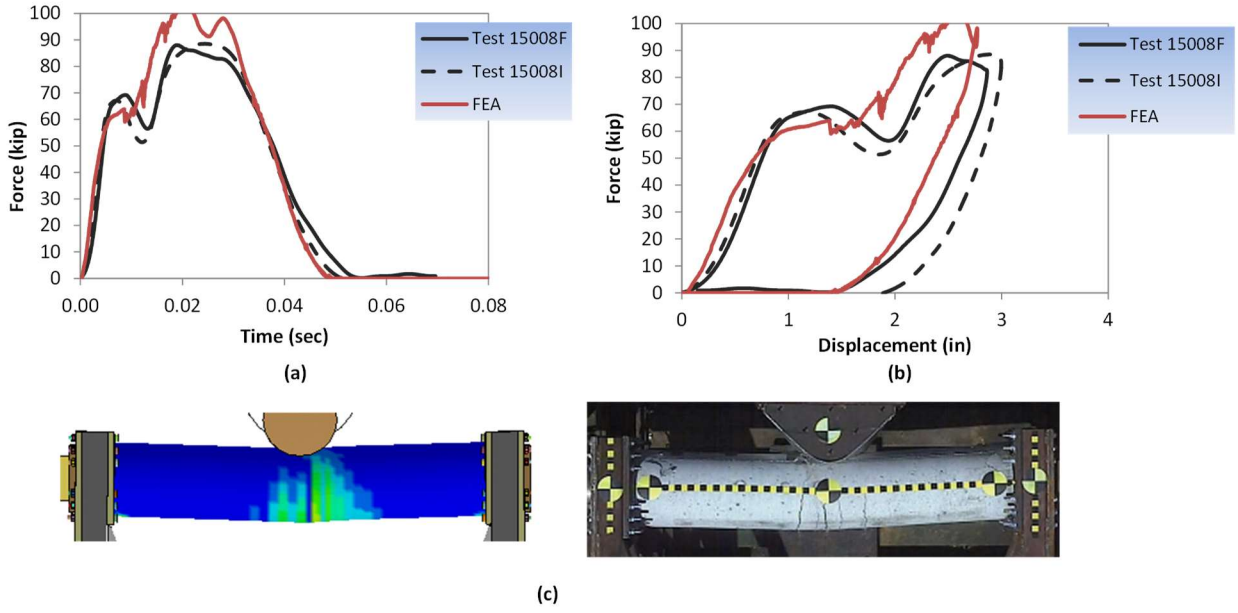

Figure 25. Comparison of FEA for Design II with Tests at 10 mi/hr (nominal) regarding (a) Force versus Time, (b) Force versus Deflection and (c) Concrete Damage.

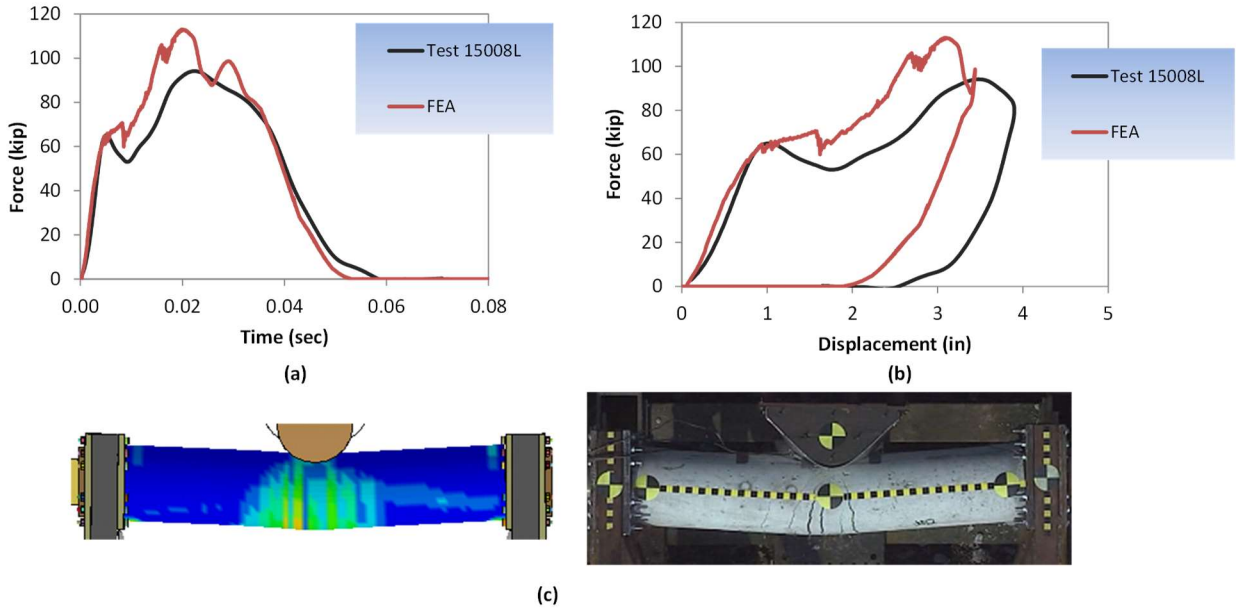

Figure 26. Comparison of FEA for Design II with Tests at 12 mi/hr (nominal) regarding (a) Force versus Time, (b) Force versus Deflection and (c) Concrete Damage.

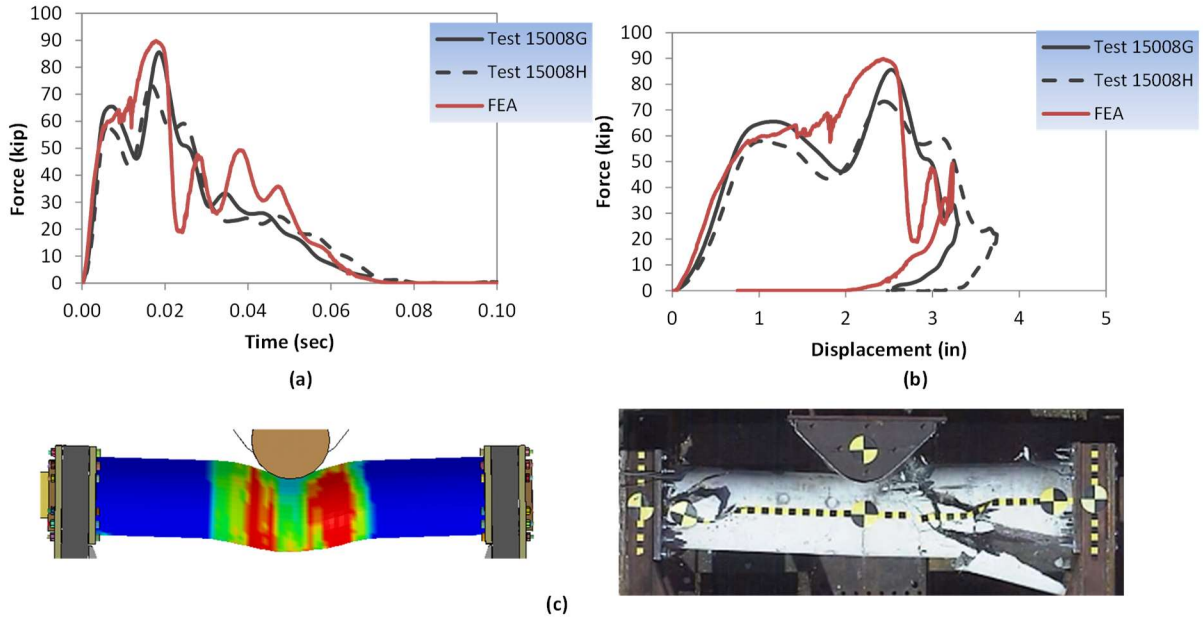

Figure 27. Comparison of FEA for Design III with Tests at 10 mi/hr (nominal) regarding (a) Force versus Time, (b) Force versus Deflection and (c) Concrete Damage.

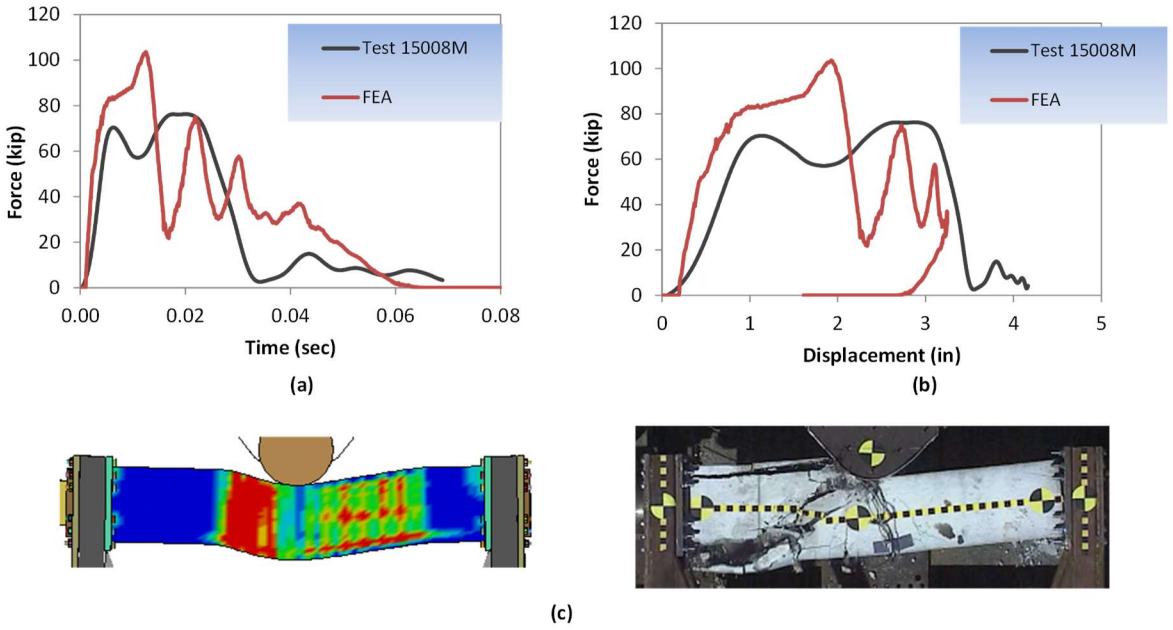

Figure 28. Comparison of FEA for Design IV with Tests at 10.5 mi/hr (nominal) regarding (a) Force versus Time, (b) Force versus Deflection and (c) Concrete Damage.

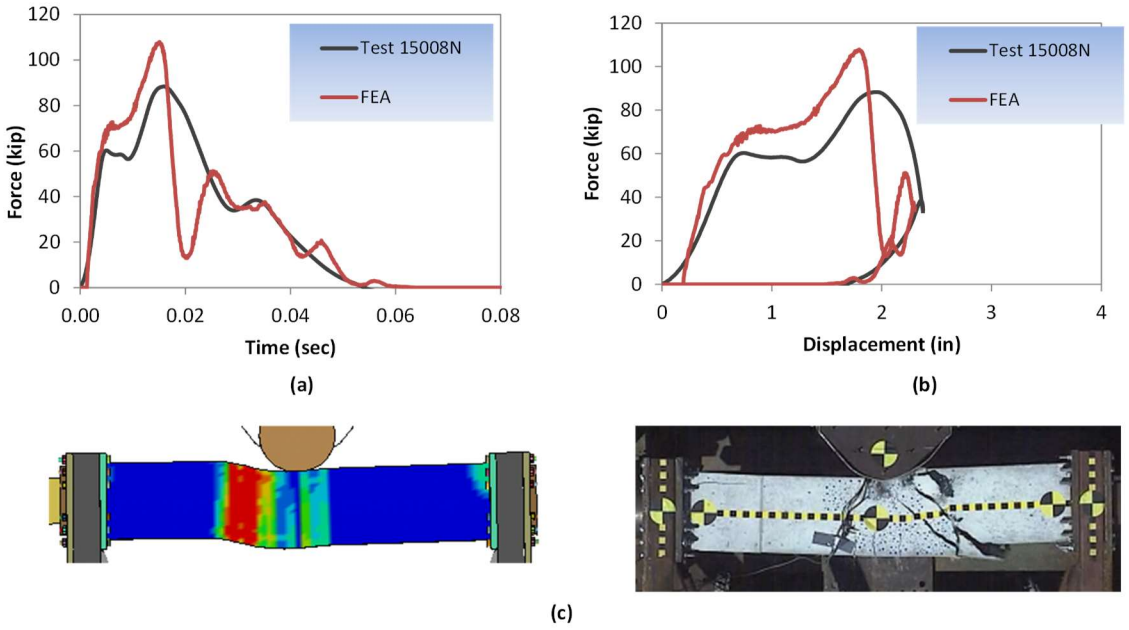

Figure 29. Comparison of FEA for Design IV with Tests at 8.7 mi/hr (nominal) regarding (a) Force versus Time, (b) Force versus Deflection and (c) Concrete Damage.

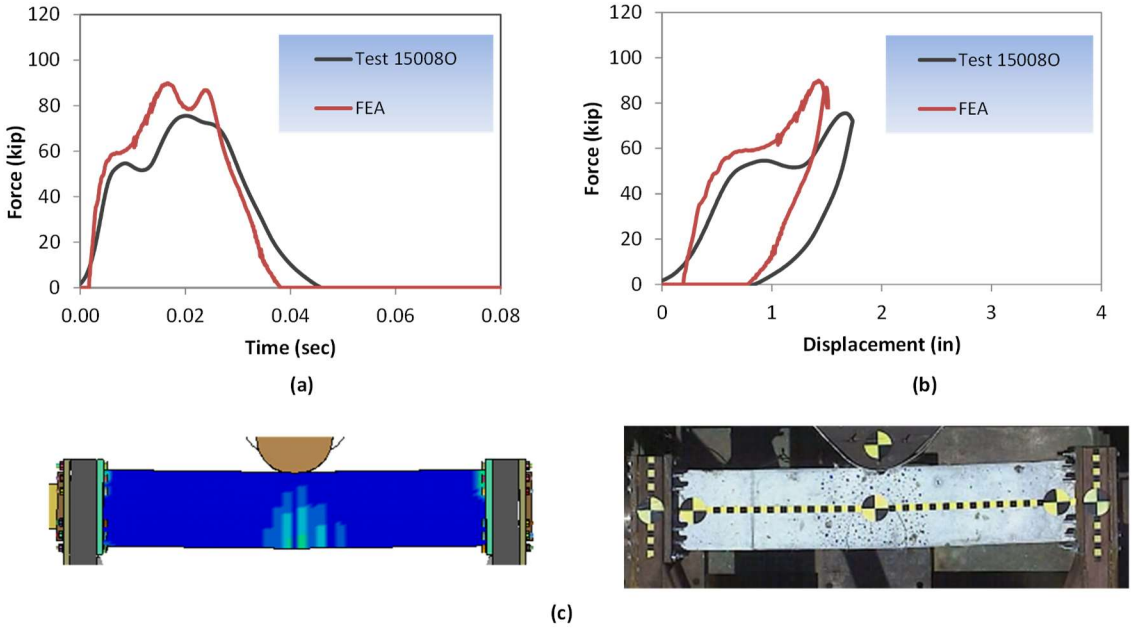

Figure 30. Comparison of FEA for Design IV with Tests at 6.6 mi/hr (nominal) regarding (a) Force versus Time, (b) Force versus Deflection and (c) Concrete Damage.

Table 14. Summary of Results for FEA versus the 15008 Test Series.

No.	Test No.	Impact Conditions			Results							
		Weight (lbs)	Speed (ft/s)	Kinetic Energy (kip-in)	Peak Force (kips)		Peak Disp (in)		Rebound Velocity (ft/s)		Rebound Energy (kip-in)	
					Test	FEA	Test	FEA	Test	FEA	Test	FEA
I	15008D	4360	14.42	168.9	71.3	92.1	3.15	2.96	-5.46	-6.36	24.2	32.9
	15008J	4360	14.36	167.5	87.9		3.20		-5.43		24.0	
	15008K	4360	16.9	232.0	88.2	100.0	3.98	3.58	-5.99	-6.97	29.1	39.5
II	15008F	4360	14.02	159.7	88.0	102.0	2.86	2.78	-6.87	-5.87	38.3	28.0
	15008I	4360	14.33	166.8	88.5		3.00		-5.94		28.7	
	15008L	4360	17.06	236.5	94.1	112.0	3.90	3.4	-6.02	-6.68	29.4	36.2
III	15008G	4360	14.22	164.3	85.6	89.0	3.30	4.4	-2.91	-1.96	6.9	3.1
	15008H	4360	14.39	168.2	73.3		3.74		-2.25		4.1	
IV	15008M	4360	15.4	192.7	76.3	100.0	4.24	3.83	-0.24	-1.80	0.0	2.6
	15008N	4360	12.73	131.7	88.3	107.0	2.38	2.3	-3.47	-2.48	9.8	5.0
	15008O	4360	9.72	76.8	75.5	89.0	2.08	1.56	-4.94	-3.95	19.8	12.7

The general shape for the force vs time curves and the force vs displacement curves from the FE analyses for Design Cases I and II were very similar to the tests. The models tended to over predict the peak force, and consequently under-predicted the peak displacements; however, the model predicted the severity of damage with reasonable accuracy. For example, the number and location of cracks were indicated in the FE analyses by relatively large principle strains.

The model for Design III, which involved significantly less shear reinforcement, resulted in good comparison with test 15008G regarding force magnitude and maximum dynamic displacement, but over predicted force magnitude for Test 15008H. The pitch spacing of the spiral steel for these test specimens was not uniform and ranged from approximately six to nine inches compared to the design pitch which was 8.6 inches. It is not known how this may have affected results between the two test cases. The model also accurately predicted that the column would fail under the simulated impact conditions.

The model for Design IV over-predicted the peak force in all three impact cases. The model did, however, accurately predict the severity of damage for each case, including failure of the columns in Tests 15008M and N.

The concrete material model used in the validation was calibrated based on unconfined compression tests and triaxial compression tests with three confinement levels. Additional analyses were also performed using default parameters for the material model (i.e., MAT_RHT) in the simulations. The results were very similar to those using the calibrated properties; and in some cases, compare slightly better with the tests (refer to Appendix 6.2G). This is important since it will be necessary to evaluate bridge piers with concrete strength ranging from 4 to 7 ksi and calibrated properties are not available for those cases.

The scaled column models used in simulating Test Series 15008 is considered valid for these impact conditions. The modeling methodology used herein is also considered valid for use in the finite element analyses of full-scale bridge pier impacts.

FULL-SCALE SIMULATED LOADING ON SELECT PIER COLUMN DESIGNS – DISPLACEMENT CONTROL LOADING

Finite element models were developed for the representative bridge pier designs in Appendix E. LS-DYNA was then used to simulate quasi-static and dynamic lateral loading on the columns. In these analyses, the columns were loaded to failure under quasi-static and dynamic loading rates so that capacity information could be determined. The modeling methodology described in the previous sections for modeling the concrete columns was adopted here for evaluating the full-scale bridge pier designs.

The study matrix included four column diameters (i.e., 24, 30, 36 and 48 inches); two shear-steel designs for the 24- through 36-inch diameter columns; and two column heights for the 48-inch diameter column. The analyses also included four concrete strengths (i.e., 4 ksi, 5.5 ksi, 6.5 ksi, and 7.8 ksi) and two impact speeds (i.e., 2 mi/hr and 20 mph). Based on the results of the 48-inch diameter column it was determined that analysis of the 54-inch column design for was not necessary; the 48-inch diameter column did not reach the failure conditions so the 54-inch diameter column would not do so either. Table 15 shows a summary of the various bridge pier design cases that were evaluated in this study. There were a total of 58 analyses performed.

Table 15. Bridge Pier Design Cases Evaluated to Determine Static and Dynamic Strength Capacity.

Design Case		Dia. (in)	Column Height (ft)	Concrete Strength (ksi)				Longitudinal Steel (num. and size)	Steel Ratio (%)	Shear Steel (size and pitch)	Concrete Cover (in)
Baseline Designs	24b	24	15	4	5.5	6.5	7.8	5 #9	1.10	#3 w/2.25" pitch	3
	30b	30	15	4	5.5	6.5	7.8	8 #9	1.13	#3 w/ 2.25" pitch	3
	36b	36	15	4	5.5	6.5	7.8	9 #10	1.12	#4 w/ 4.0" pitch	3
	48(15)	48	15	4	5.5	6.5	7.8	15 #10	1.05	#4 w/ 4.0" pitch	3
Increased Spacing of Shear Steel	24a	24	15	4	5.5	6.5	7.8	5 #9	1.10	#3 w/ 4.0" pitch	3
	30a	30	15	4	5.5	6.5	7.8	8 #9	1.13	#3 w/ 4.0" pitch	3
	36a	36	15	4	5.5	6.5	7.8	9 #10	1.12	#4 w/ 6.0" pitch	3
Increased Height	48(28)	48	28	-	-	-	7.8	15 #10	1.05	#4 w/ 4.0" pitch	3

BOUNDARY CONDITIONS

The concrete columns in pier cap designs are connected to the footer and the header using "cold" joints. For example, the footing is cast first with lap-steel protruding from the foundation to allow for connection to the columns. The steel reinforcement for the pier column is then fabricated and placed over the lap-steel and the concrete column is poured. The column also includes lap-steel which protrudes from the top end of the column for connection to the pier cap. To accurately capture the boundary conditions the model of the cold joints were modeled explicitly. The methodology described below was used to simulate the construction sequence to properly replicate the boundary conditions.

For the top and bottom boundaries of the column, a portion of the pier cap and footer was explicitly modelled with lap steel at the joints as illustrated in Figure 31. The pier cap and footer model for the 36-inch column designs was based on the Ohio Pier Plan and Elevation Drawing FRA-270-22.42. The cap is 36 inches wide and 40 inches tall and includes 8 #11 bars on the bottom, 5 #10 bars on top and 4 #5 bars on each side. A 5-ft length of the pier cap was modeled with fixed boundary conditions at the inside end of the cap. The stirrups in the pier cap were not modeled. The foundation was modeled after another Ohio design in which the column rested on pile footing with diameter equal to 1.375 times the column diameter. The modeled portion of the pile for the 36-inch diameter pier column model was 49.5 inches diameter and 4 feet deep with fixed boundaries on the perimeter and bottom sides. The reinforcement at the outer surface of the pile consisted of 16 #10 bars with #4 spiral steel with a concrete cover of 3 inches. The lap steel between the pier and the footer is of the same design as the pier column reinforcement; however, the lap steel is rotated (offset) such that the bars fit between the adjacent pier column reinforcement, as shown in Figure 31. For the joint at the pier cap, the longitudinal reinforcement of the pier column simply extends approximately 36 inches into the pier cap. These bars are typically curved at the ends (i.e., hooks), but were modeled without the curved ends. The footer and cap models for the remaining designs were based on this general methodology with concrete sized appropriate for each column design with similar steel ratio.

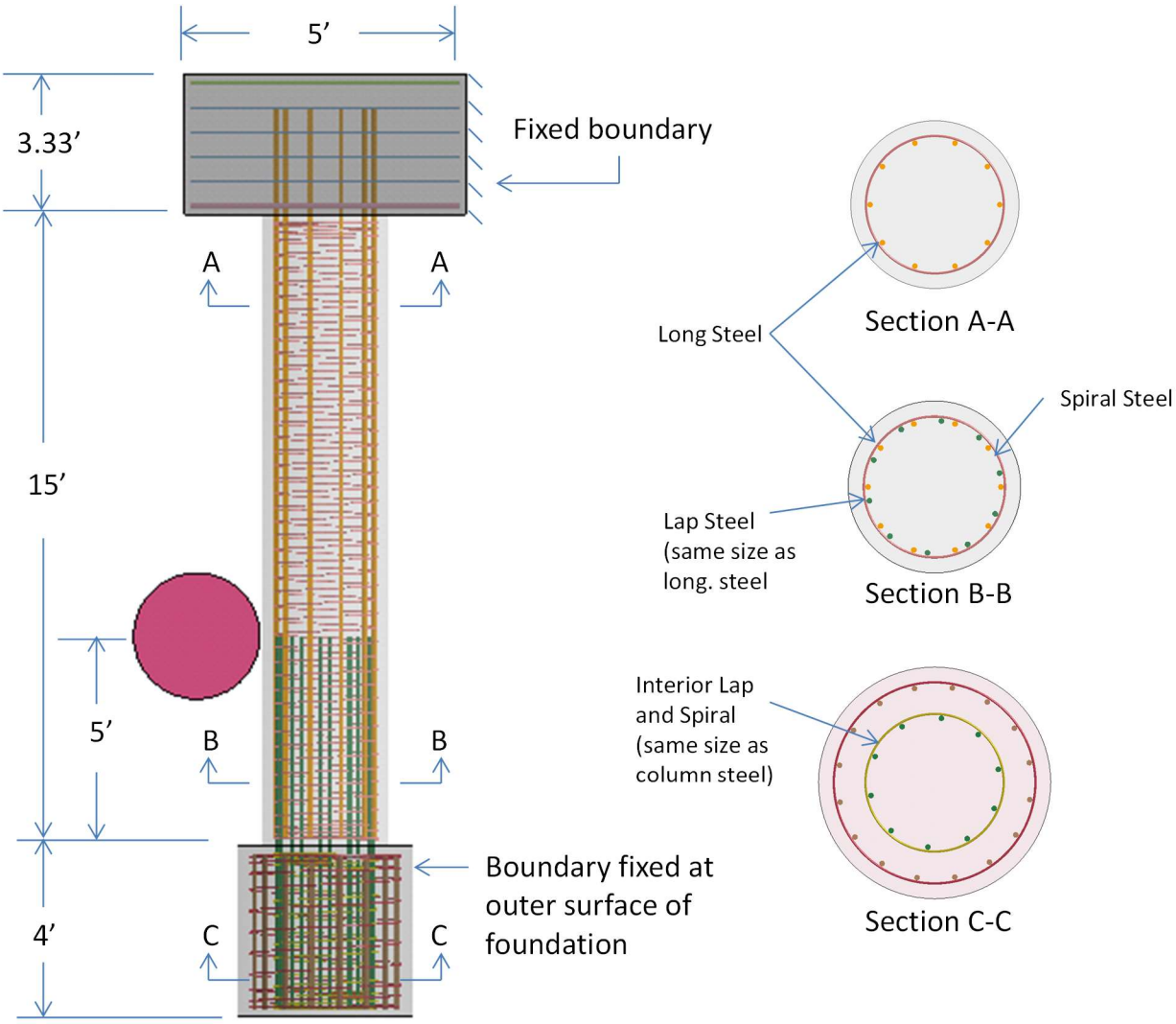

Figure 31. Column, Pier Cap and Footer Model.

LOADING

The loading was applied to the column by a 36-inch diameter rigid cylinder moving at constant velocity. The load was applied at 5 feet above ground at loading speeds of 2 and 20 mi/hr as illustrated in Figure 32. This loading arrangement does not conserve energy but, rather, maintains a constant loading rate such that the internal forces approaching failure can be observed consistently between the pier column designs.

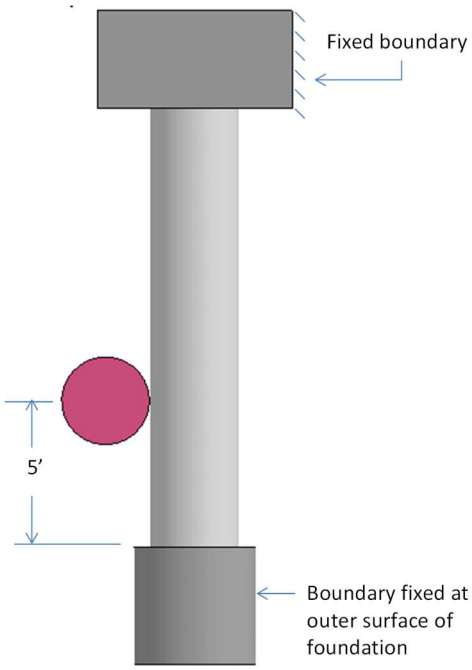

Figure 32. Loading and Boundary Conditions for Analyses.

RESULTS

A summary of the results from the analyses are provided in Table 16, which includes peak force; displacement and energy absorbed by column at peak force; dynamic magnification factor for peak force; and the deflection and energy at time of column "rupture." The column capacity in terms of peak force and energy absorption is discussed below, as well as how rupture is defined.

Force Capacity

The force-deflection plots for the baseline designs with 4, 5.5, 6.5 and 7.8 ksi concrete are shown in Figures 33 through 40.

Table 16. Summary of Results from the Column Capacity Analyses.

Design Case	f'_c (ksi)	Loading Rate (mph)	At Peak Force				At Initial Softening		At Secondary Softening	
			Force (kips)	DMF	Disp. (in)	Strain Energy (kip-in)	Disp. (in)	Strain Energy (kip-in)	Disp. (in)	Strain Energy (kip-in)
24a	4.0	2	289		0.66	105	1.29	267	4.33	754
		20	678	2.34	0.77	352			2.16	873
	5.5	2	365		0.95	218	1.21	302	4.81	975
		20	821	2.25	0.74	403			2.53	1119
	6.5	2	403		0.98	245	1.30	364	5.56	1193
		20	916	2.27	0.73	438			3.14	1374
	7.8	2	487		0.96	243	1.47	456	5.27	1340
		20	1001	2.06	0.44	211			2.69	1499
24b	4.0	2	311		0.97	194	1.18	255	3.73	748
		20	700	2.25	0.77	356			2.96	1182
	5.5	2	384		1.00	243	2.45	333	3.81	914
		20	839	2.19	0.77	436			2.50	1233
	6.5	2	417		0.96	245	1.35	397	3.92	1038
		20	937	2.25	0.75	465			2.73	1376
	7.8	2	487		1.38	445	1.46	474	3.86	1240
		20	1002	2.06	0.46	224			3.28	1814
30a	4.0	2	609		0.74	248	0.87	311	3.71	1129
		20	1057	1.74	0.69	394			2.80	1403
	5.5	2	717		0.73	285	0.10	405	4.50	1332
		20	1253	1.75	0.70	495			2.60	1563
	6.5	2	790		0.85	400	0.99	466	5.65	1454
		20	1251	1.58	0.73	524			2.90	1579
	7.8	2	950		1.00	537	1.13	617	5.87	2154
		20	1604	1.69	0.67	584			3.66	2540
30b	4.0	2	609		0.72	236	0.94	338	3.81	1139
		20	1057	1.73	0.69	394			2.84	1412
	5.5	2	727		0.73	287	0.99	435	3.33	1199
		20	1253	1.72	0.70	495			2.65	1575
	6.5	2	815		0.88	426	1.01	495	4.15	1542
		20	1251	1.54	0.71	516			0.87	1830
	7.8	2	1044		1.16	715	1.27	794	4.88	2465
		20	1551	1.49	0.56	419			2.78	2222
36a	4.0	2	816		0.87	378	1.02	466	4.78	1975
		20	1414	1.73	0.88	642			2.30	1918
	5.5	2	1059		1.00	570	1.14	677	3.96	1938
		20	1701	1.61	0.86	933			2.55	2328
	6.5	2	1165		1.06	693	1.20	800	5.40	2740
		20	1904	1.63	0.70	741			3.32	2925
	7.8	2	1473		1.43	1397	1.58	1530	6.54	4024
		20	2415	1.64	0.75	961			3.47	3969
36b	4.0	2	868		0.91	420	1.06	493	4.13	1842
		20	1431	1.65	0.89	665			2.73	2248
	5.5	2	1092		0.95	644	1.07	736	3.60	2006
		20	1727	1.58	0.78	802			2.17	2264
	6.5	2	1211		1.01	764	1.19	903	5.20	3017
		20	1930	1.59	0.70	746			3.63	3299
	7.8	2	1591		1.43	1418	1.58	1610	5.79	4480
		20	2419	1.52	0.74	935			5.79	4480
48 - 15ft	4.0	2	1491		1.27	1239	1.62	1706	4.48	3973
		20	2204	1.48	0.95	1201			3.68	4843
	5.5	2	1867		1.28	1479	1.71	2183	5.21	5888
		20	2687	1.44	0.84	1225			3.40	5661
	6.5	2	2056		1.35	1743	1.55	2105	4.50	6249
		20	3047	1.48	0.90	1551			3.12	6003
	7.8	2	2343		1.63	2480	2.66	4415	7.90	10996
		20	3641	1.55	1.09	2405			3.60	7913

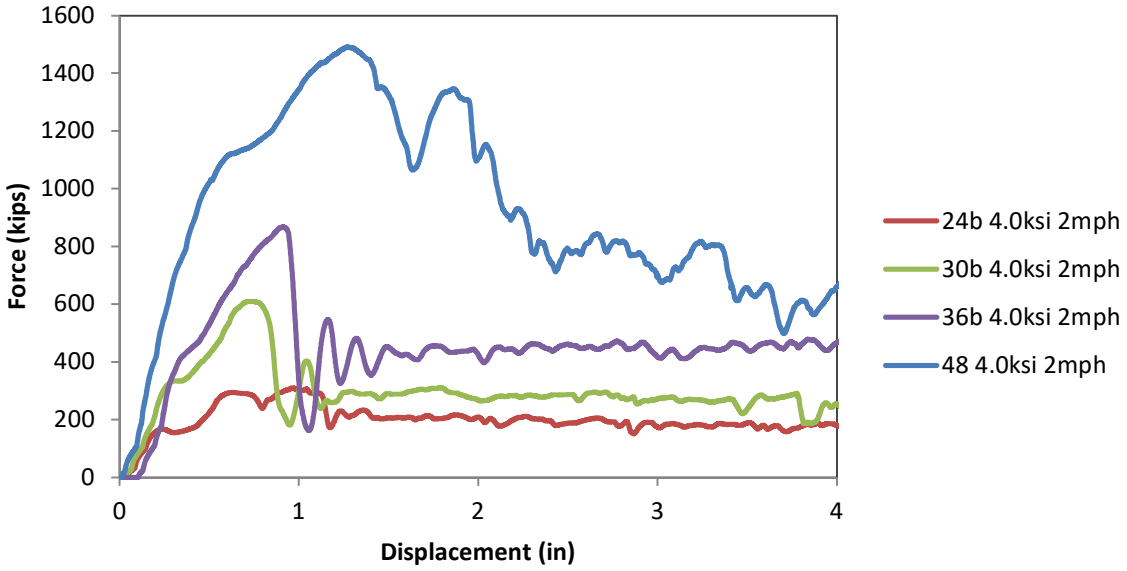

Figure 33. Force-Deflection Response for Baseline Column Designs with 4 ksi Concrete and 2 mi/hr (Quasi-Static) Loading Rate.

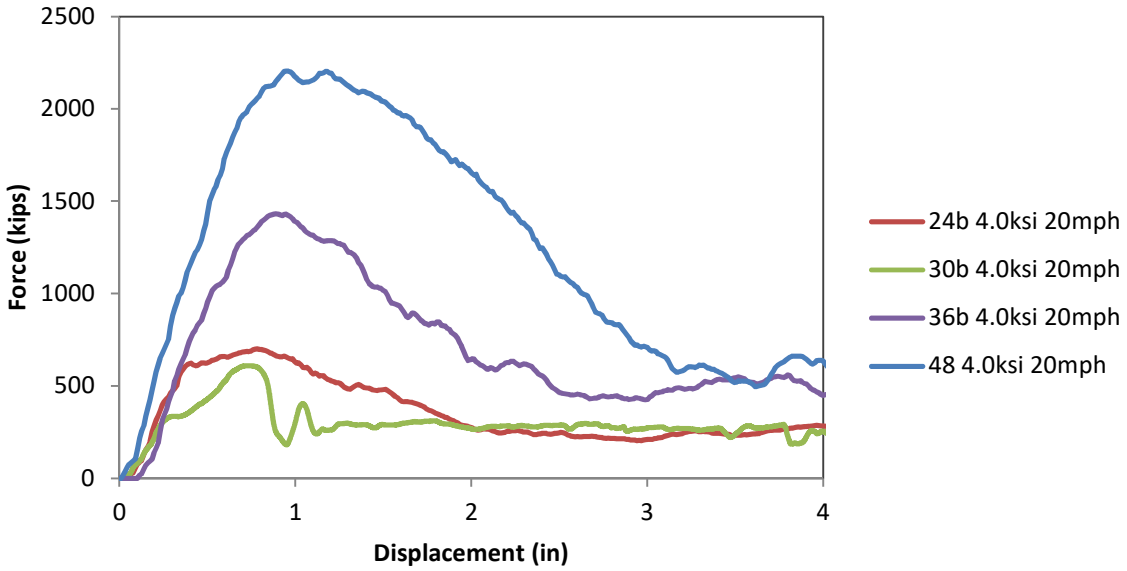

Figure 34. Force-Deflection Response for Baseline Column Designs with 4 ksi Concrete and 20 mi/hr (Dynamic) Loading Rate.

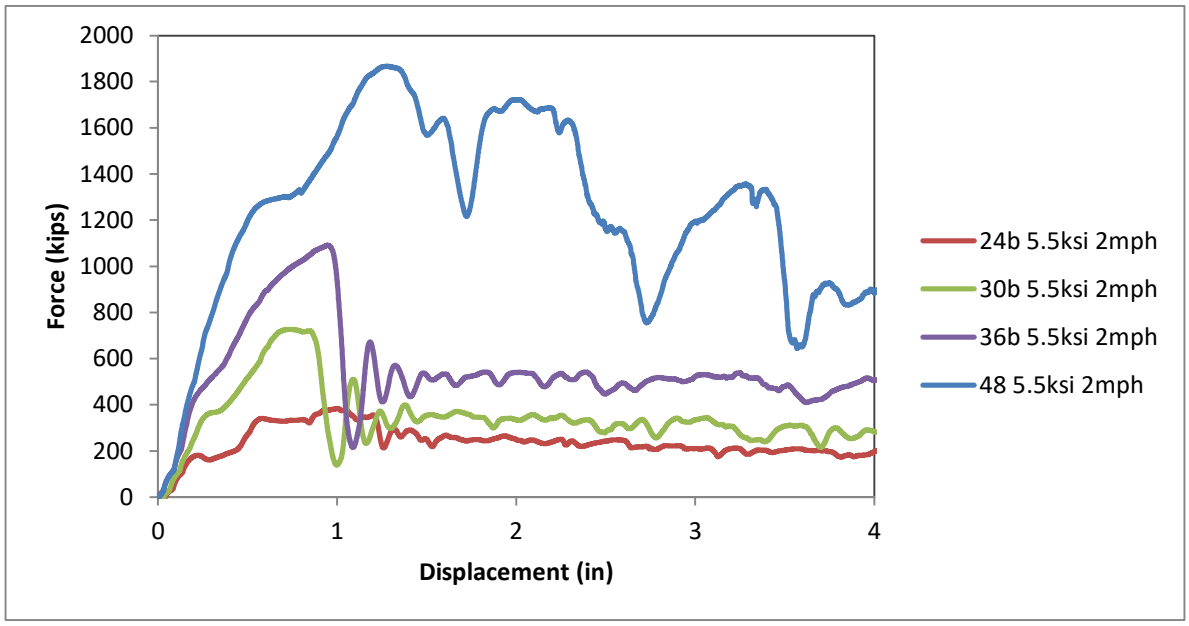

Figure 35. Force-Deflection Response for Baseline Column Designs with 5.5 ksi Concrete and 2 mi/hr (Quasi-Static) Loading Rate.

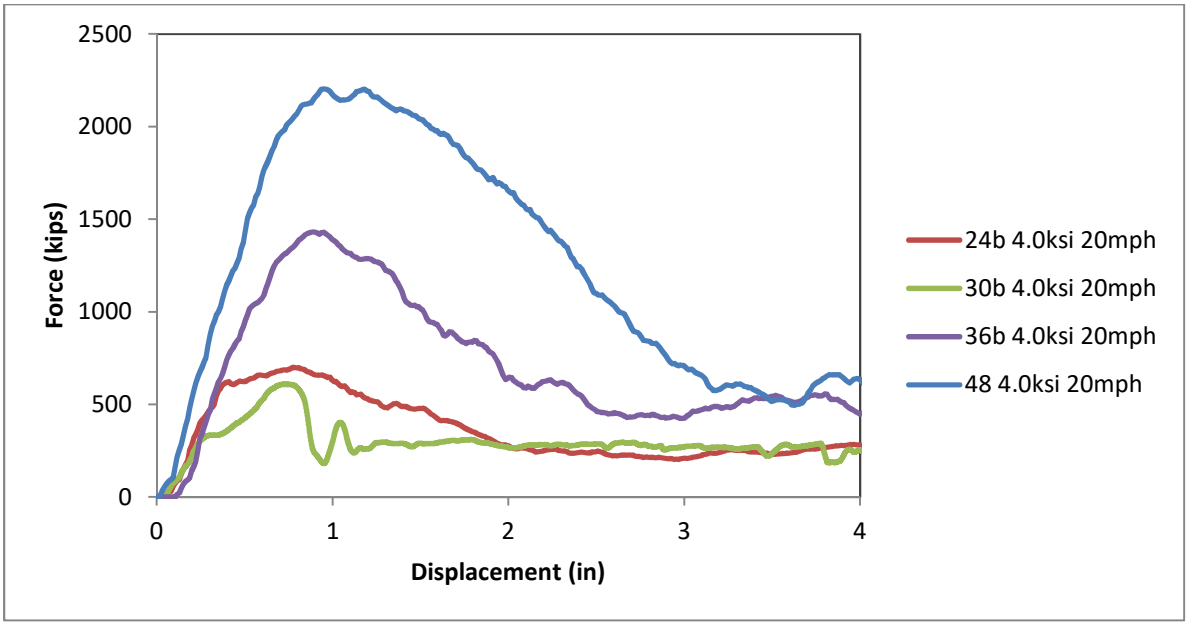

Figure 36. Force-Deflection Response for Baseline Column Designs with 5.5 ksi Concrete and 20 mi/hr (Dynamic) Loading Rate.

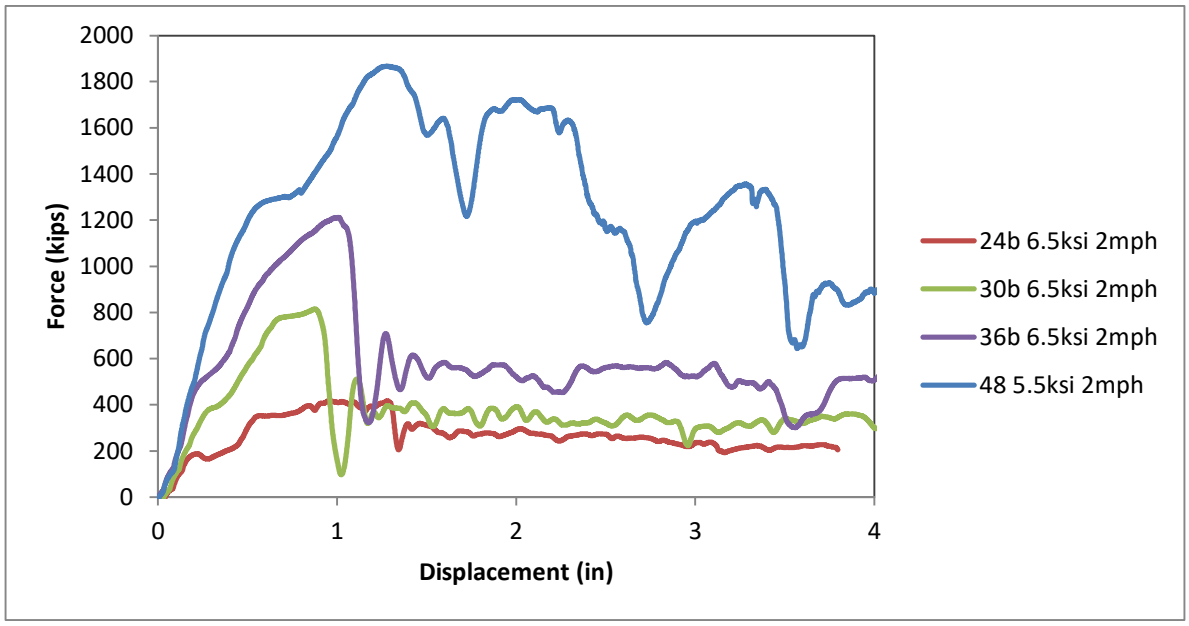

Figure 37. Force-Deflection Response for Baseline Column Designs with 6.5 ksi Concrete and 2 mi/hr (Quasi-Static) Loading Rate.

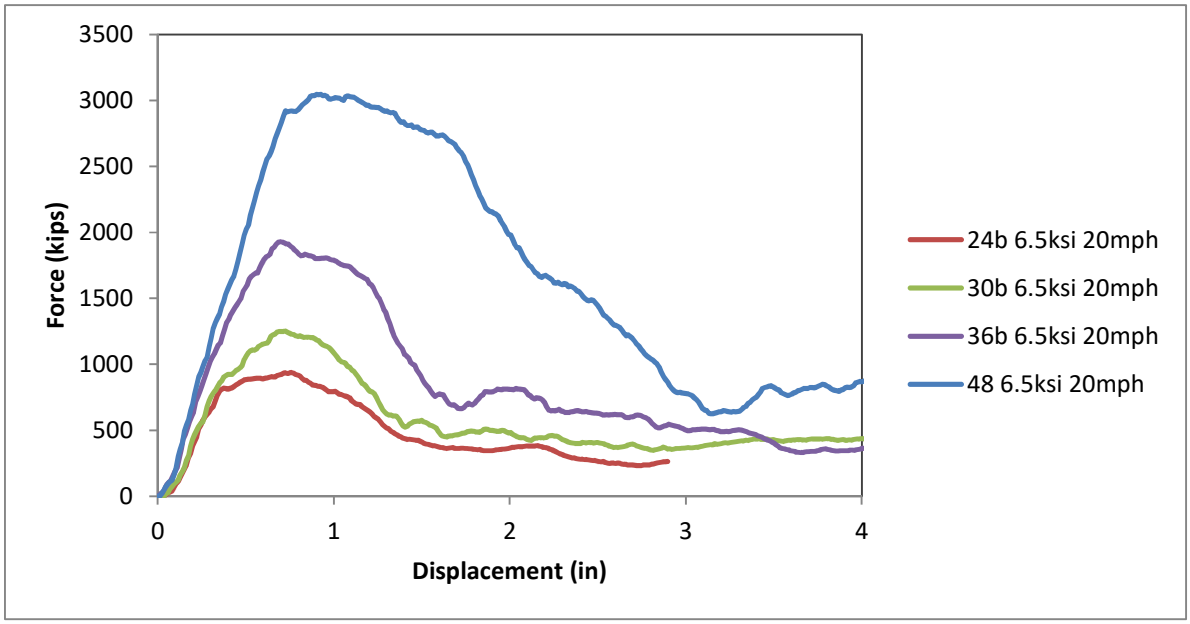

Figure 38. Force-Deflection Response for Baseline Column Designs with 6.5 ksi Concrete and 20 mi/hr (Dynamic) Loading Rate.

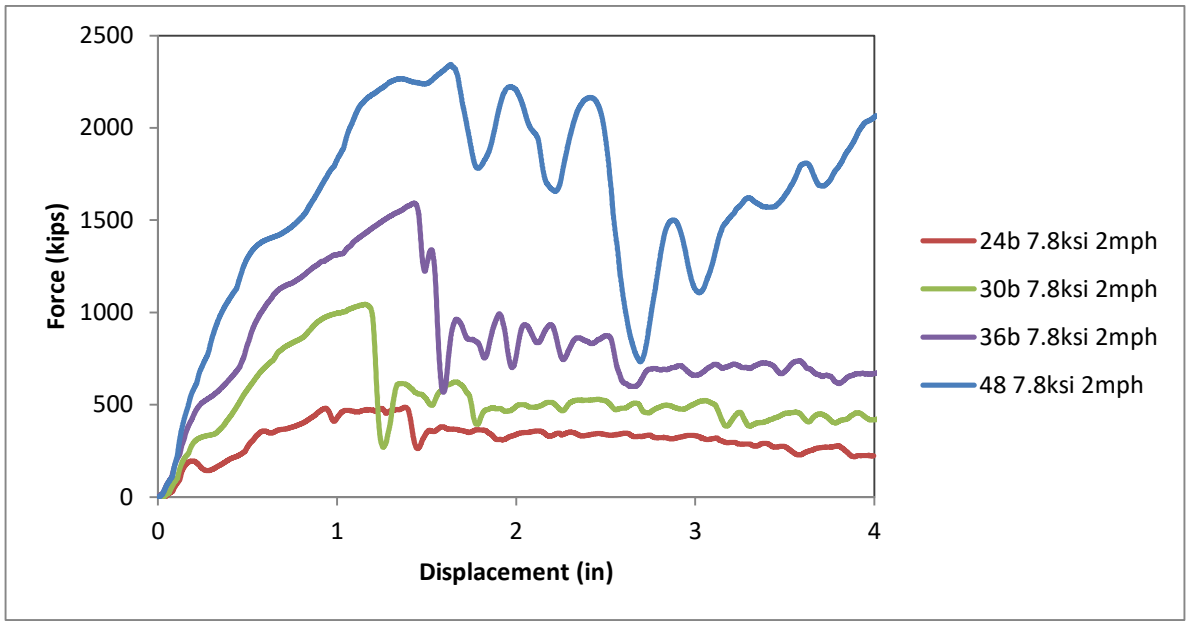

Figure 39. Force-Deflection Response for Baseline Column Designs with 7.8 ksi Concrete and 2 mi/hr (Quasi-Static) Loading Rate.

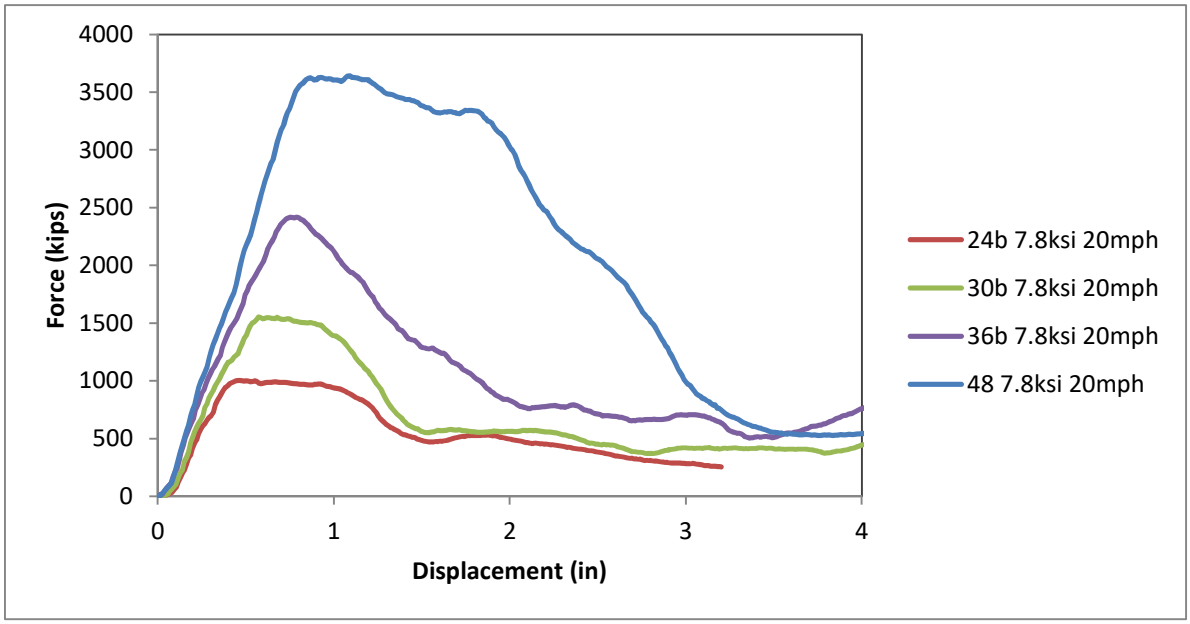

Figure 40. Force-Deflection Response for Baseline Column Designs with 7.8 ksi Concrete and 20 mi/hr (Dynamic) Loading Rate.

Figures 41 through 44 show plots of peak force versus column diameter for each of the four concrete strength cases. Results for the baseline designs are labeled with solid-diamond markers, and the results for the designs with reduced shear steel are labeled with x's. The plots show a linear relationship between peak force and column diameter for both the static and dynamic loading conditions, as indicated by the trend line plots on each chart. The results also show that peak force is not affected by the amount of shear steel in the column (e.g., the x-labels overlay the solid labels). Recall that this was also concluded from the physical test program for the scaled column designs presented earlier.

The peak force values computed for the dynamic load cases were significantly higher than those computed for the static load cases. The dynamic magnification factor (DMF) ranged from 1.44 to 2.34 and was found to be dependent on both f'c and column diameter, as shown in Figure 45. The DMF decreases with respect to both variables; but its sensitivity to concrete strength decreases as column diameter increases. For a given column diameter the DMF tended to decrease linearly as f'_c increased. For a given concrete strength, however, it was difficult to develop accurate trend plots for DMF versus column diameter. The DMF increased significantly for the 24-inch column diameter with values ranging from 2.06 to 2.34; for column diameters of 30, 36, and 48 inches the DMF appeared to be relatively flat with values ranging from 1.48 to 1.75 and approaching an asymptote of 1.5 as column diameter increased. It is important to keep in mind that although the model was "validated" for the scaled column tests (see previous sections) it was not possible to fully evaluate the accuracy of the model results regarding loading rate. Thus, the conclusions made here are dependent on the accuracy of the constitutive model in LS-DYNA and the accuracy of the default parameters used for the material model.

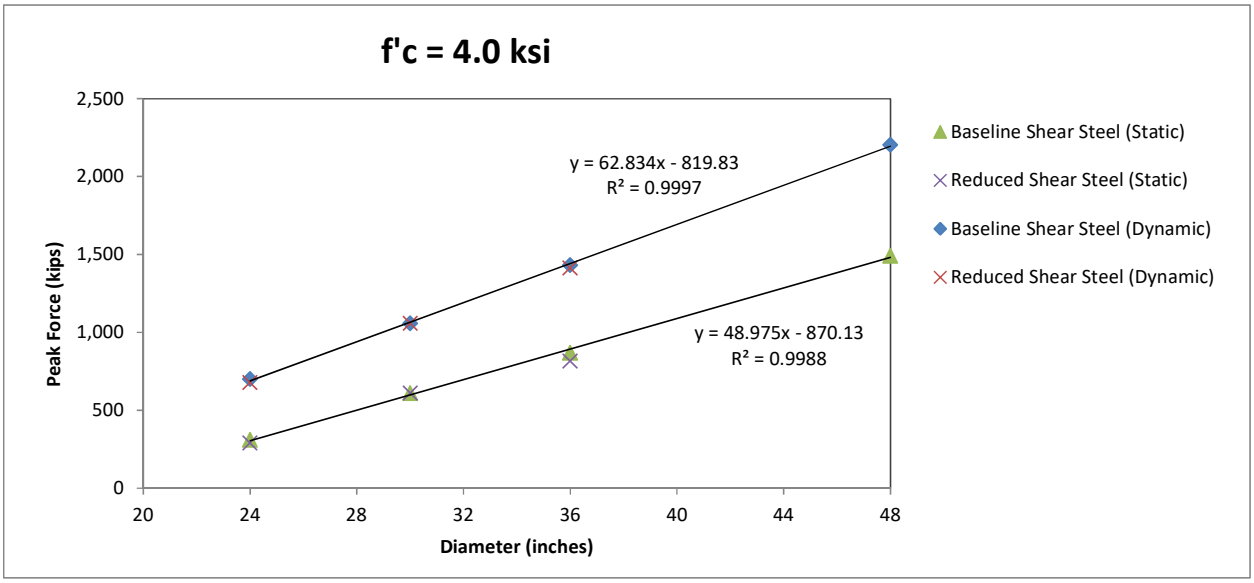

Figure 41. Peak Force versus Column Diameter for Baseline and Reduced Shear Steel Cases with F'c = 4 ksi and Both the Static and Dynamic Loading Rates.

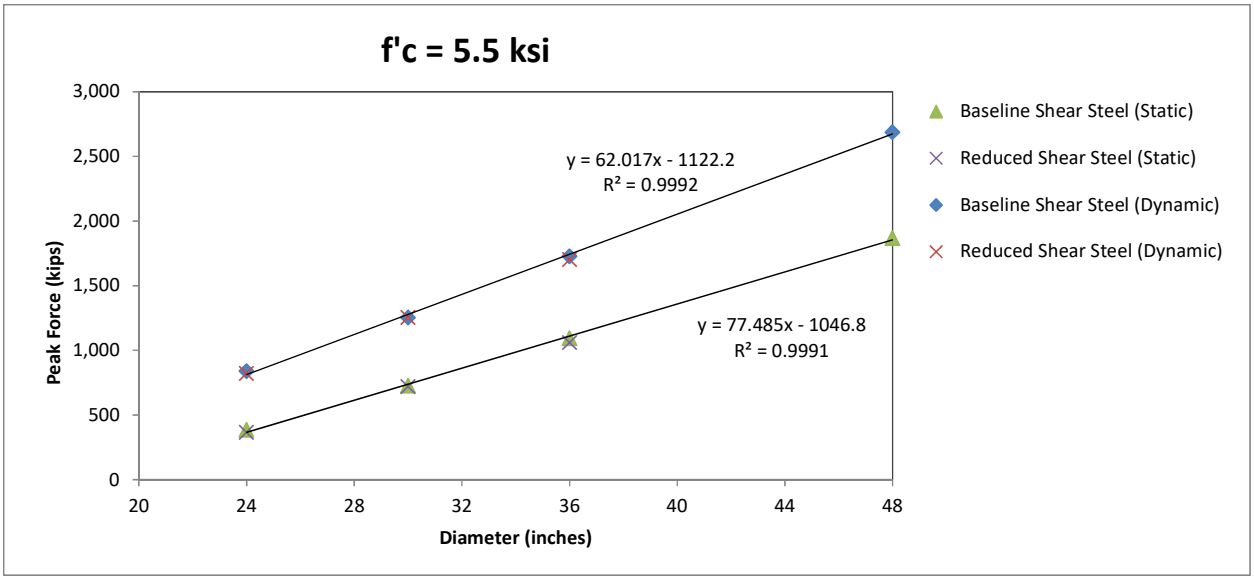

Figure 42. Peak Force versus Column Diameter for Baseline and Reduced Shear Steel Cases with f'c = 5.5 ksi and Both the Static and Dynamic Loading Rates.

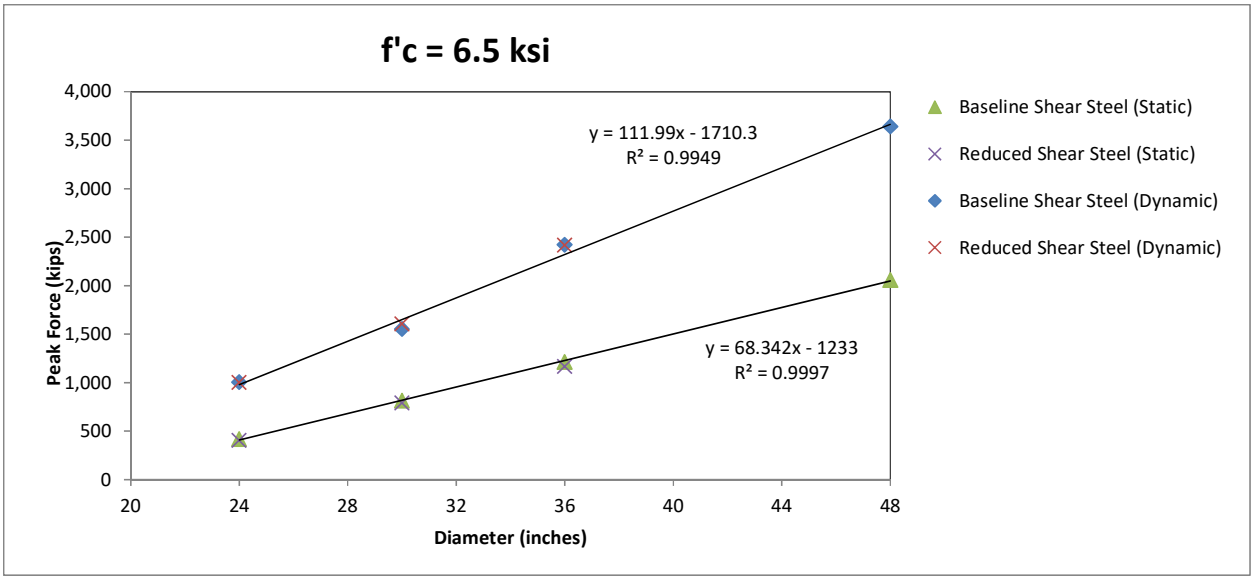

Figure 43. Peak Force versus Column Diameter for Baseline and Reduced Shear Steel Cases with f'c = 6.5 ksi and Both the Static and Dynamic Loading Rates.

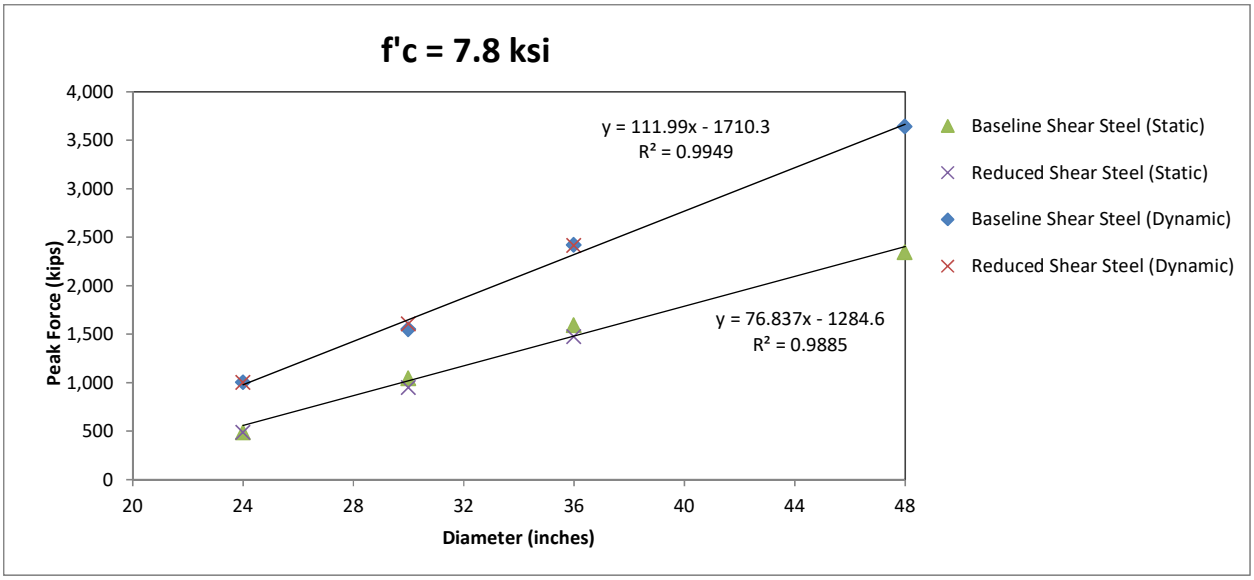

Figure 44. Peak Force versus Column Diameter for Baseline and Reduced Shear Steel Cases with f'c = 7.8 ksi and Both the Static and Dynamic Loading Rates.

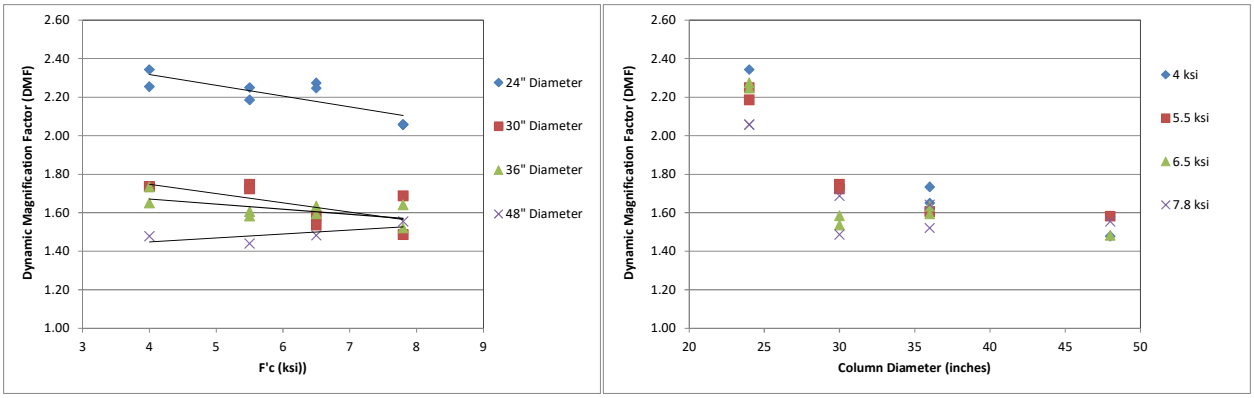

Figure 45. Dynamic Magnification Factor versus Concrete Strength and Column Diameter.

Figure 41through Figure 44 indicate that for the quasi-static case (i.e., 2 mi/hr loading), a 600 kip peak force is achieved for a 24-inch diameter column using 7.8 ksi concrete and a 30-inch diameter column for 4 ksi concrete.

Energy Capacity

The peak force capacity was evident from the force-deflection plots shown in Figures 33 through 40; however, the point of "complete column failure" was not. The material model for the concrete does not accurately simulate full loss of concrete strength after failure (i.e., the material model formulation yields a reduced strength after failure rather than complete loss of strength). Also, the steel reinforcing continued to provide resistance after the concrete had failed, although at a much lower magnitude of force. As a result, the point of "complete failure" could not be accurately ascertained from the plots, particularly for the quasi-static cases. The energy absorbed by the column during quasi-static loading was reported in Table 16 at three possible failure points: (1) at peak force, (2) at the change in slope after initial softening stage and (3) at

the change in slope after the secondary softening stage. For the dynamic loading cases, the energy was reported only at peak force and at the end of the secondary softening stage. Figure 46 shows and example illustrating the data collection points for the static and dynamic cases.

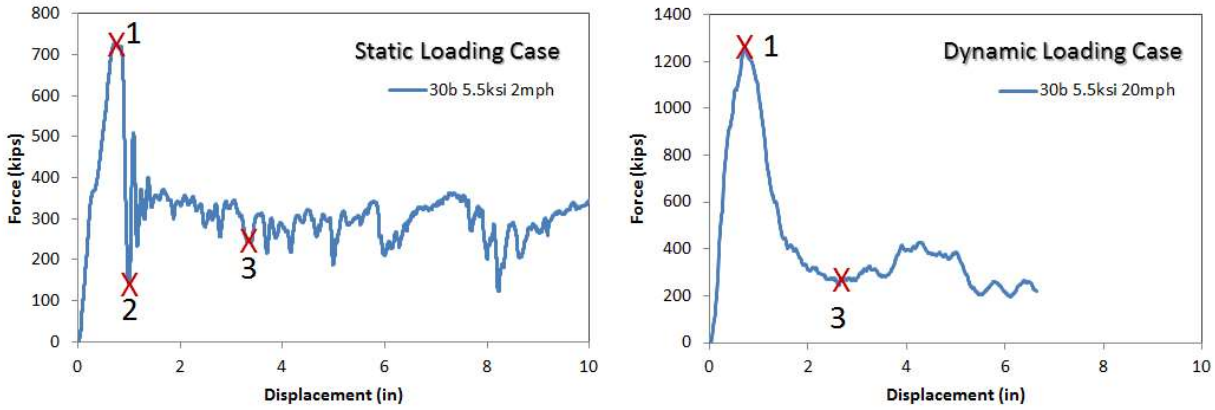

Figure 46. Example Illustrating the Points Where Energy Data was Collected for Table 16.

Figures 47 through 50 show plots of the energy at peak force versus column diameter for the baseline and reduced shear steel cases under static and dynamic loading for each of the four concrete strengths. Figure 51 through Figure 54 show plots of energy at the points of initial and secondary softening of the column versus column diameter for the baseline and reduced shear steel cases under static and dynamic loading for each of the four concrete strengths. Note that the end of the secondary softening stage was much easier to determine for the dynamic cases.

As was the case for peak forces, there were also trends relating energy to column diameter. The energy data fit reasonably well to exponential trend curves generated in Microsoft Excel, particularly for the energies computed at the initial and secondary softening stages. Also interesting is that, although the peak forces were much higher for the dynamic load case, the total energy absorbed was very similar between the static and dynamic cases regarding the energies calculated at the secondary softening stage; the differences started to become indistinguishable as concrete strength increased.

The analysis results indicated that the reduction in shear steel did not have a noticeable effect of the energy capacity of the columns. So even though the amount of shear steel was reduced (i.e., pitch spacing of shear steel), the resistance to lateral loading remained sufficient to force the column to fail in flexure for all cases evaluated.

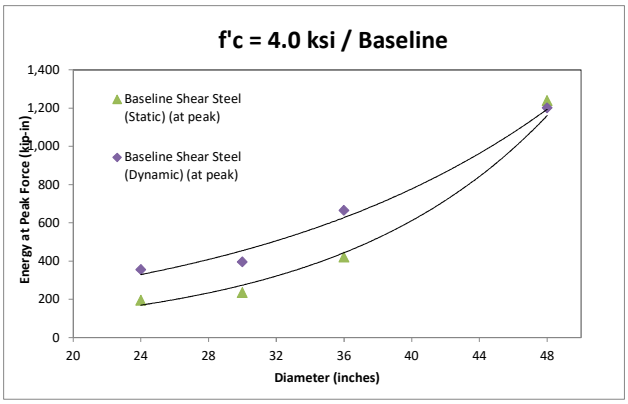

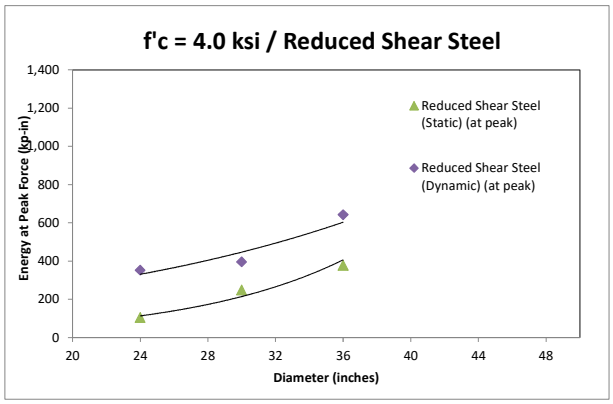

Figure 47. Energy at Peak Force for Baseline and Reduced Shear Steel Cases with f'c = 4 ksi.

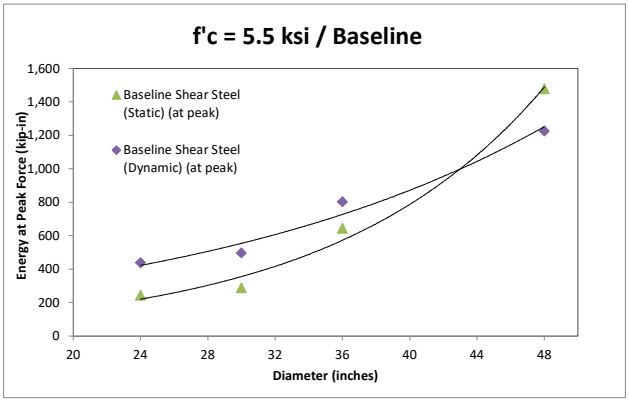

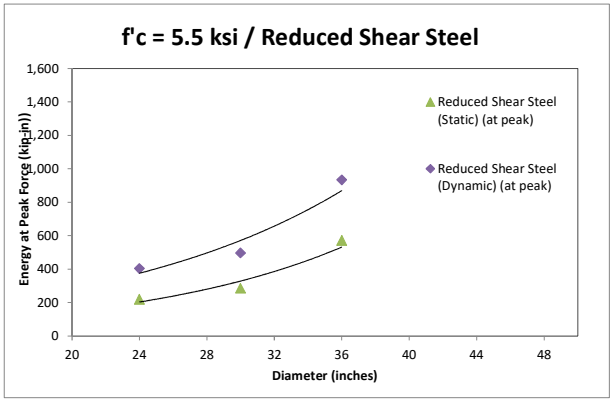

Figure 48. Energy at Peak Force for Baseline and Reduced Shear Steel Cases with f'c = 5.5 ksi.

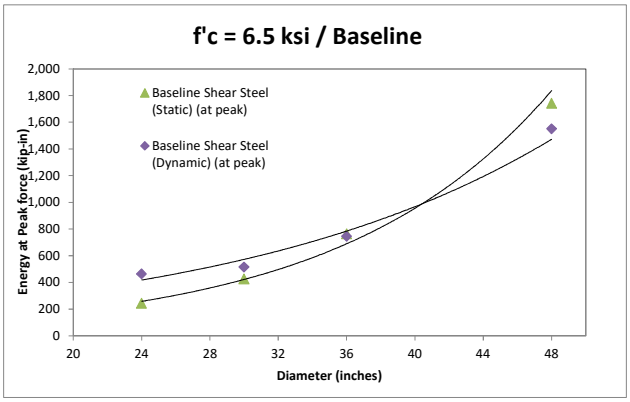

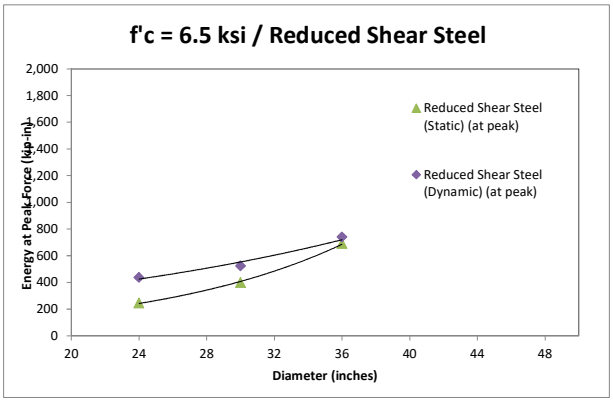

Figure 49. Energy at Peak Force for Baseline and Reduced Shear Steel Cases with f'c = 6.5 ksi.

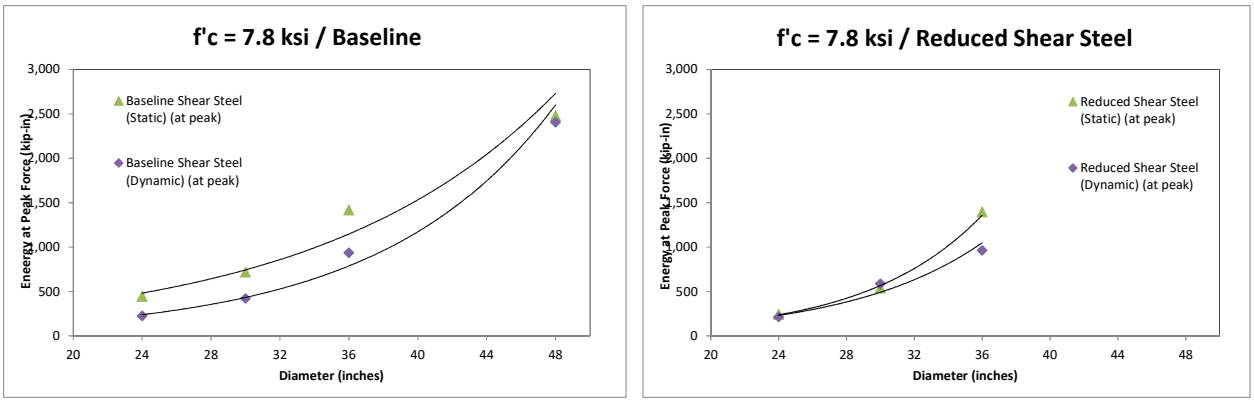

Figure 50. Energy at Peak Force for Baseline and Reduced Shear Steel Cases with f'c = 7.8 ksi.

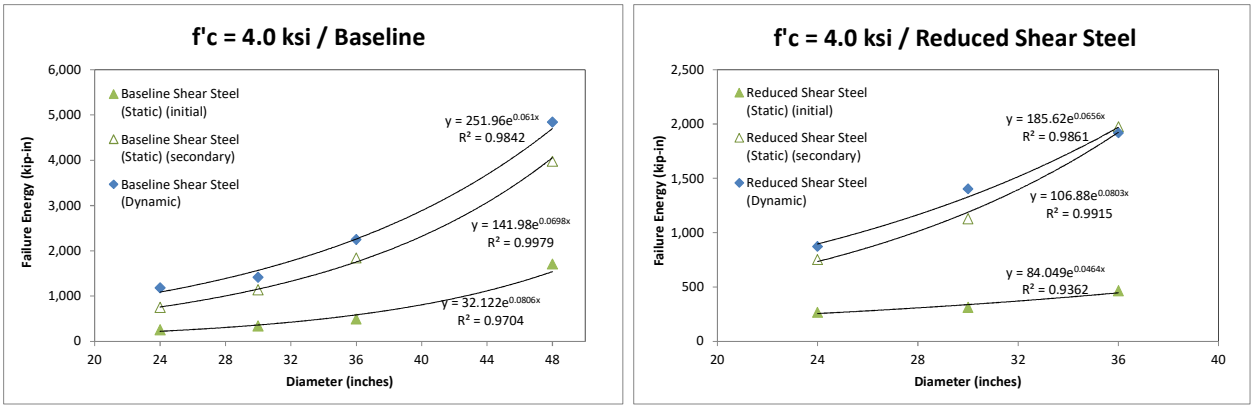

Figure 51. Energy at Initial and Secondary Softening Points for Baseline and Reduced Shear Steel Cases with f'c = 4 ksi.

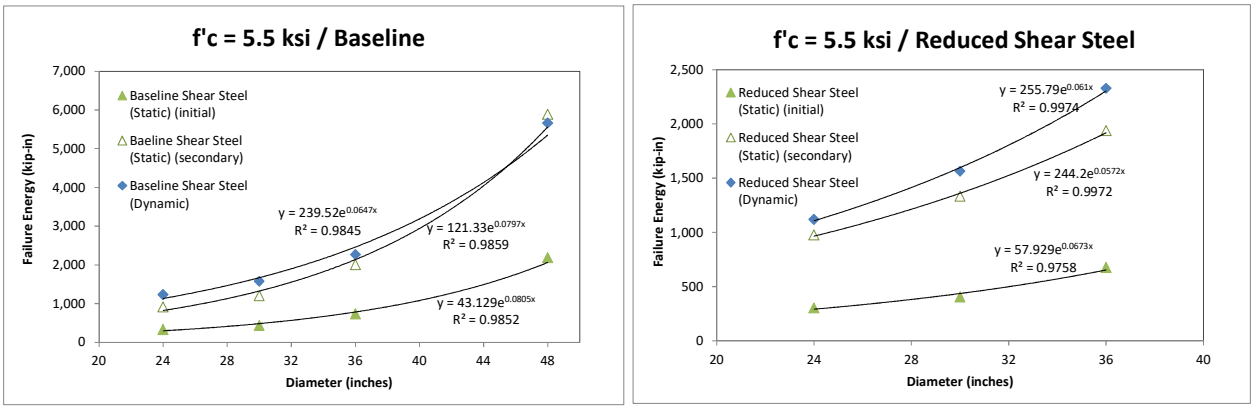

Figure 52. Energy at Initial and Secondary Softening Points for Baseline and Reduced Shear Steel Cases with f'c = 5.5 ksi.

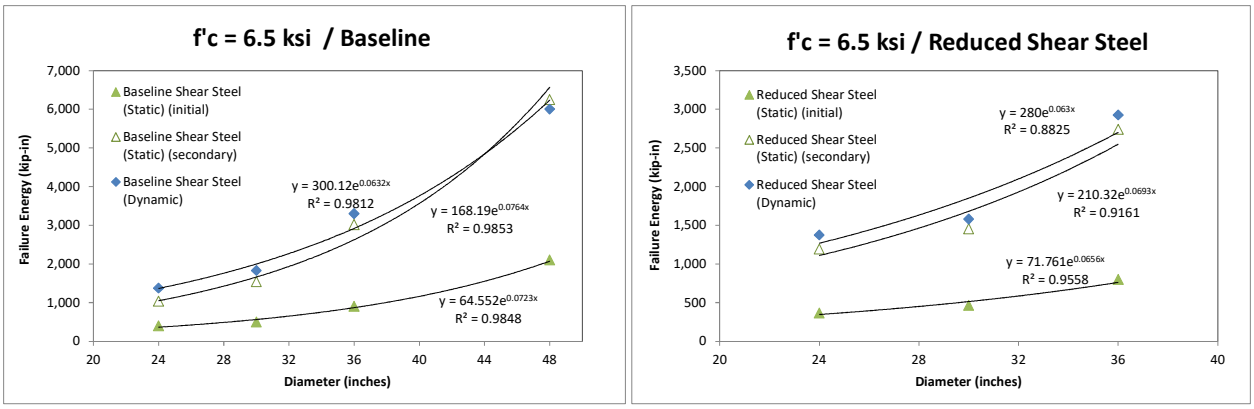

Figure 53. Energy at Initial and Secondary Softening Points for Baseline and Reduced Shear Steel Cases with f'c = 6.5 ksi.

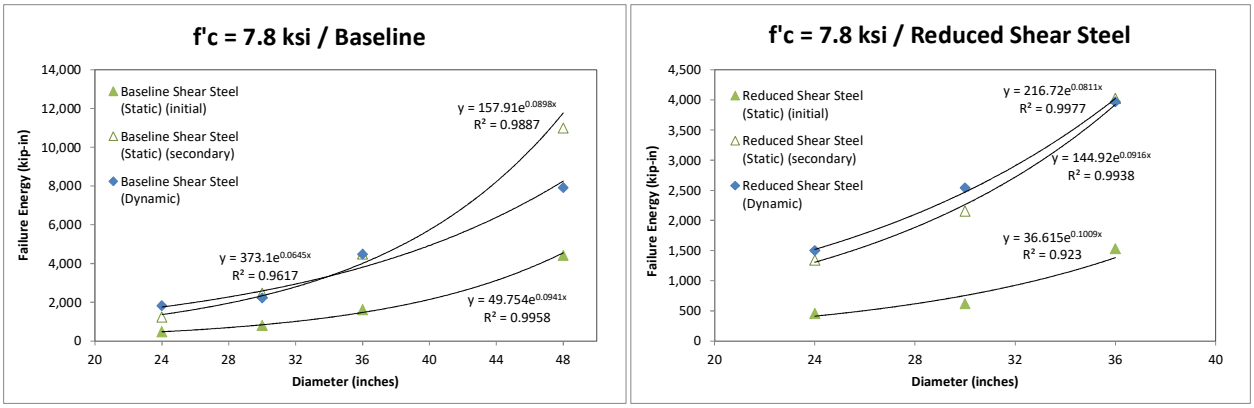

Figure 54. Energy at Initial and Secondary Softening Points for Baseline and Reduced Shear Steel Cases with f'c = 7.8 ksi.

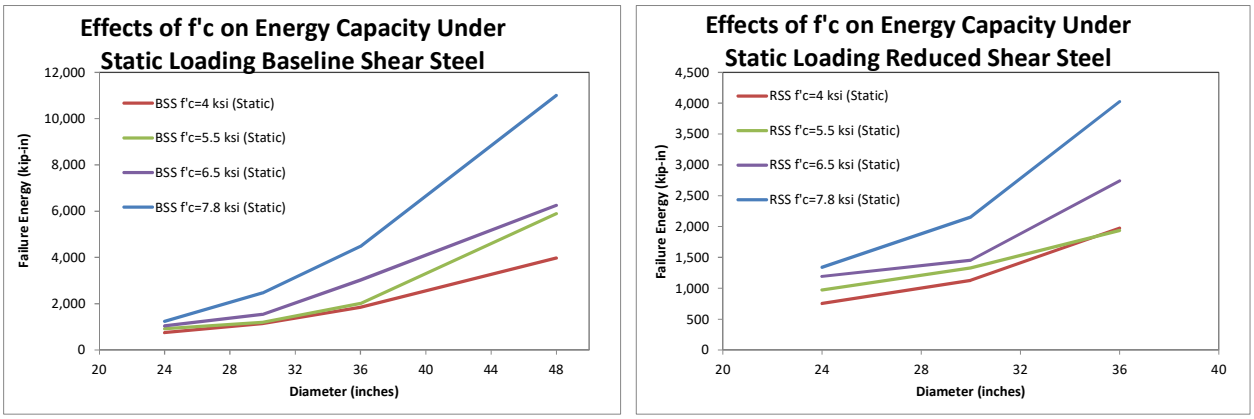

Figure 55. Energy at Secondary Softening Points for Baseline and Reduced Shear Steel Cases for Various Concrete Strengths under Static Loading.

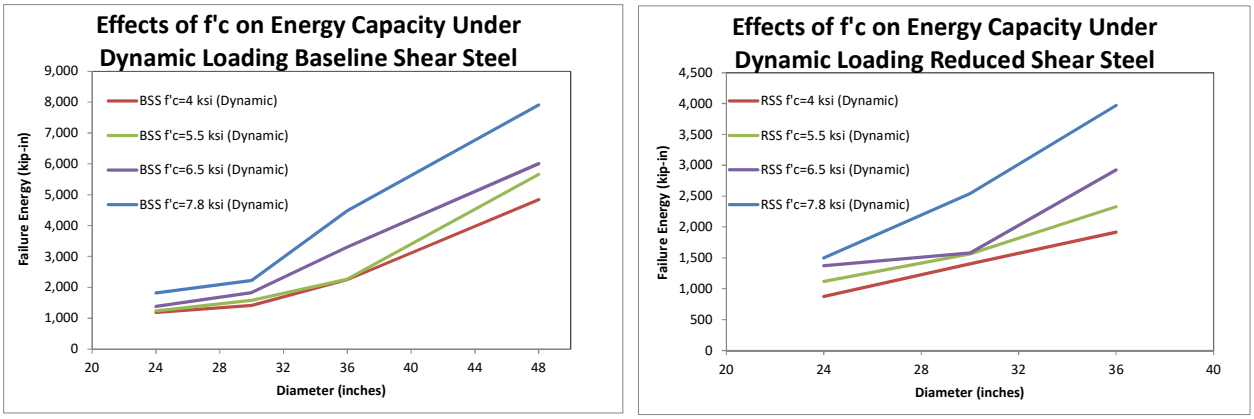

Figure 56. Energy at Secondary Softening Points for Baseline and Reduced Shear Steel Cases for Various Concrete Strengths under Dynamic Loading.

CONCLUSIONS REGARDING RESULTS OF THE STRENGTH CAPACITY ANALYSES

Finite element models were developed for the representative bridge pier designs shown in Appendix E. LS-DYNA was then used to simulate quasi-static and dynamic lateral loading on the columns to determine strength capacity and to also evaluate various trends relating bridge pier design parameters to strength capacity. Table 17 provides a summary of the column capacities computed for the baseline representative column designs identified in Appendix E.

Table 17. Summary of Strength Capacities for the Baseline Representative Column Designs (see Appendix E).

Column Diameter (in)	f'c (ksi)	Loading Rate*	Force Capacity (kips)	Energy Capacity (kip-in)		
				At Peak Force	Initial Softening Response	Secondary Softening Response
24	4.0	static	311	194	255	748
		dynamic	700	356		1182
30	4.0	static	609	236	338	1139
		dynamic	1057	394		1412
36	4.0	static	868	420	493	1842
		dynamic	1431	665		2248
48	4.0	static	1491	1239	1706	3973
		dynamic	2204	1201		4843

* static = 2 mi/hr and dynamic = 20 mph

Based on the results of these analyses the following conclusions were made regarding the effects of various design parameters on column capacity:

1) Peak force for the columns increased linearly with respect to column diameter for both static and dynamic loading conditions.
2) Increasing the amount of shear reinforcement did not necessarily increase the force capacity of the column.

3) Decreasing the amount of shear reinforcement also did not noticeably affect the ductility of the column, which contradicted the conclusions from the scaled column tests. However, it is assumed that for the shear steel designs evaluated, the amount of reinforcement was sufficient to force the column to fail in flexure rather than shear. Additional reductions in shear reinforcement were not evaluated to determine the threshold of the shear-to-flexure failure mode.
4) Loading rate significantly affected the magnitude of the peak force on the columns with the dynamic magnification factor (DMF) ranging from 1.44 to 2.34 for the dynamic load rate of 20 mph.
5) The DMF decreases with respect to both concrete strength (f'c) and column diameter, but its sensitivity to concrete strength decreases as column diameter increases.
6) The energy capacities of the columns were found to increase exponentially with respect to column diameter.
7) The total energy absorbed was very similar between the static and dynamic cases regarding the energies calculated at the secondary softening stage (i.e., when defining complete column rupture as the point when the softening stage of the force-deflection response reaches a plateau).
8) The differences in the energy capacity between the static and dynamic cases started to become indistinguishable as concrete strength increased.

FULL-SCALE SIMULATED LOADING ON SELECT PIER COLUMN DESIGNS – DISPLACEMENT CONTROL LOADING ANALYSES

The lateral impact strength of the four baseline representative bridge pier column designs shown in Table 15 were evaluated using an 80,000-lbs tractor-trailer truck striking the leading pier column head-on at 50 mi/hr using finite element analysis. The finite element model of the 80,000-lb tractor trailer model validated earlier was used for these analyses. For each column design, the tractor-trailer model struck the column head-on at 49.7 mi/hr (80 km/hr). The centerline of the vehicle was aligned with the centerline of the column as shown in Figure 57.

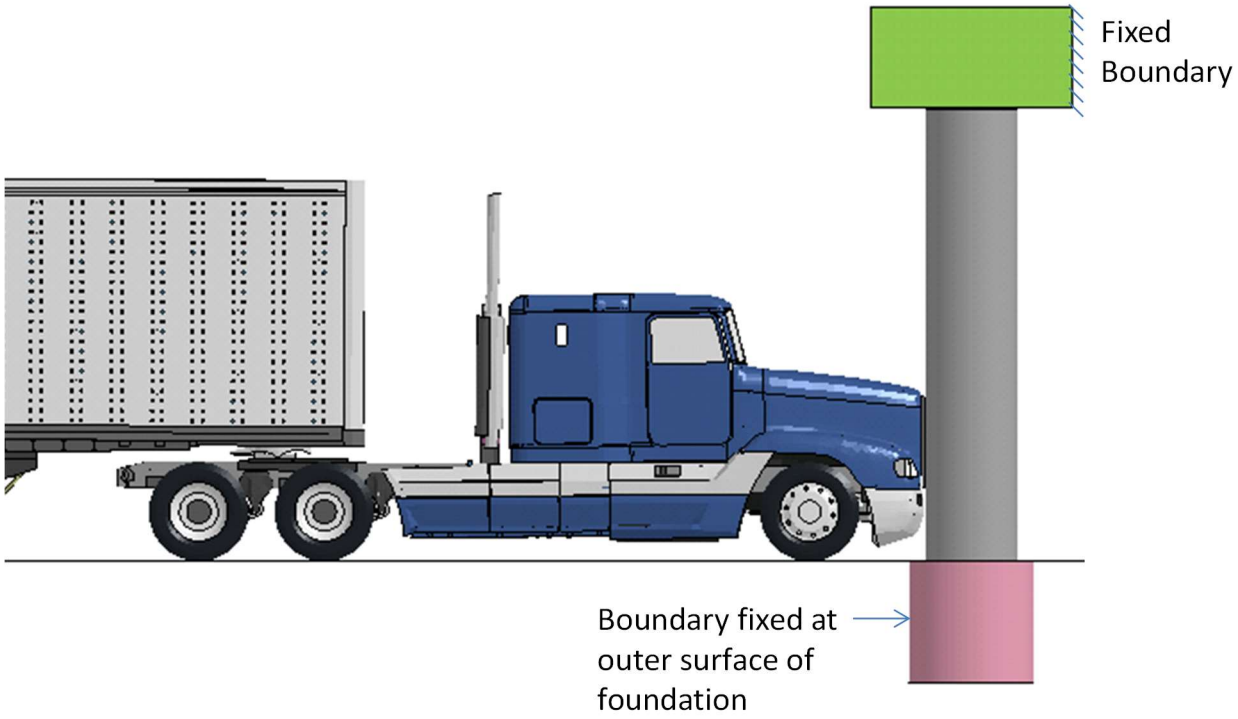

Figure 57. FE Model for an 80,000-lbs Tractor Trailer Truck Striking the Leading Pier Column Head-On at 50 mi/hr (36-inch column design).

The impact force between the tractor and the column was computed for each case from the contact forces. The contact between the tractor and the column was defined using the surface-to-surface contact option in LS-DYNA and the resulting contact forces in the global x, y and z directions were written to the RCFORC database file by LS-DYNA. The forces were collected at a sampling rate of 30 kHz. The displacement of the column was also collected during the analysis. These measurements were taken at 25 inches above grade which corresponded to the maximum deflection point of the column during the initial impact stage and the height of the tractor trailer truck bumper (e.g., resulting from the engine impacting against the bridge pier). The displacement data was collected from a node on the front-most longitudinal rebar element. It was not possible to collect displacement data from the concrete elements since they often eroded (i.e., elements are removed from the analysis once the failure condition is reached) during the analysis as the strains in those elements reach critical values.

TRACTOR-TRAILER MODEL VALIDATION

The tractor-trailer model developed by NCAC/Battelle/ORNL (version 10-0308) was used to simulate full-scale crash test 429730-2 conducted at the Texas Transportation Institute (TTI) discussed earlier. [Buth11] This FEA simulation was performed in order to validate the truck model for use in full-scale finite element simulations of pier impacts to be discussed later in this section

Finite Element Model

The model used in this analysis was a modified version of the NCAC/Battelle/ORNL tractor-trailer model (model versions tractor_10-0308 and trailer_10-0521).[Miele10] The tractor model was the sleeper-cab version validated by Battelle for use in simulations involving impact of the vehicle into rigid longitudinal barriers at impact speed and angle of 50 mi/hr and 15 degrees.[Miele10] The damage to the vehicle, however, is generally low to moderate for such impact cases and rarely results in material or component failures other than the u-bolts connecting the front axle to the front leaf-spring suspension. Accordingly, the majority of the tractor and trailer components were modeled using an elasto-plastic constitutive material law (i.e., MAT24 in LS-DYNA) with no failure condition defined.

In the case of a head-on impact into a rigid column, on the other hand, the deformations of the tractor are very severe, as evidenced in the post-tests photo shown Figure 3. During the test, all the component connections on the frame-rails back to the rear tandem axels, failed during the impact. The model was modified to account for these failures by modeling the bolted connections as “generalized-spotwelds-with-failure” and setting the effective plastic failure strain for all the structural steel components to 0.2. Also, most of the brackets fastened to the frame rails were re-meshed to reduce element length by half in order to improve accuracy of the deformation response.

The geometric and inertial properties of the model are compared to those of the test vehicle in Figure 2. The most notable differences were that (1) the wheelbase length of the tractor model was 16.2 inches shorter than the test vehicle; (2) the empty weight of the tractor trailer truck model was 6.3 kip less than the test vehicle (i.e., 17 percent); and (3) the ballast in the model was 6.6 kip greater than the test vehicle (i.e., 15 percent). Also, the fifth-wheel was positioned approximately eight inches forward in the model relative to position in the test vehicle. All other differences in vehicle dimensions were considered to be inconsequential to this particular impact scenario.

The column and fixture were modeled as a structural steel tube filled with concrete, consistent with the full-scale test. Fixed translational constraints were placed on the backside of the column at the locations of the two load cells in the full-scale test; the constraints were modeled using the SPC option in LS-DYNA. Figure 58 shows a comparison of the column test fixture and the model.

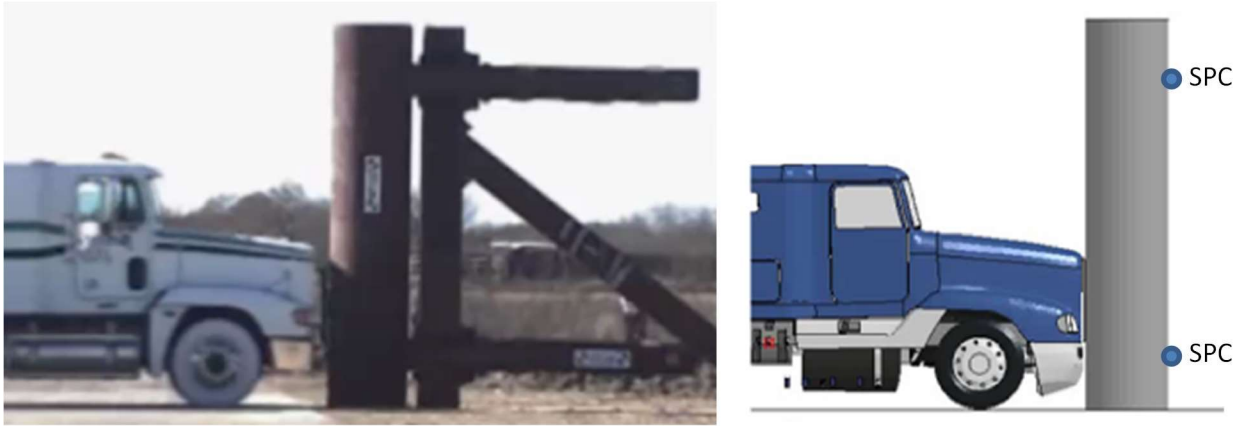

Figure 58. Comparison of Column Test Fixture and FE Model Illustrating the Location of SPC Constraints.

The test vehicle was ballasted with unrestrained sand in paper bags which were stacked five to six rows high on wooden pallets. The model included sand bags placed directly on the trailer floor. The sand was modeled using MAT_Soil_and_Foam in LS-DYNA with properties based on calibration tests provided in Fasanella, *et al*. [Fasanella09]

Figure 59. Test and FE Model Ballast.

Simulation of Test 429730-2

The model was used to simulate the impact conditions of Test 429730-2. A qualitative assessment was made by comparing the 10- and 25-ms average force-time histories on the column, as well as sequential views of the impact event to verify vehicle kinematic response as well as sequence and timing of key phenomenological events. The force-time history plot is shown in Figure 61 and sequential views of the crash event are compared in Figure 62. The results from the finite element analysis compare reasonably well with the results from full-scale crash test. The model appears to simulate the basic kinematic behavior of the tractor-trailer vehicle and adequately captures the basic phenomenological events that occur during impact.

The model compared particularly well until approximately 0.28 seconds of the impact, which corresponded to the time when the front wall of the trailer ruptured in the test. The following is a summary of the key phenomenological events from the analysis and their effects on the column loading compared to those from the full-scale test.

At 0.03 seconds the engine impacted against the column resulting in the highest force spike of the impact event. The magnitude of the 10-msec rigid pole force was 11 percent higher in the analysis compared to the test (i.e., 830 kips vs 928 kips), as shown in Figure 61. Similarly, the magnitude of the 25-msec rigid pole force was 12 percent higher in the analysis compared to the test (i.e., 626 kips vs 560 kips), as shown in Figure 61. The 25-msec peak rigid pole force of about 600 kips is believed to be the basis for the 600 kips design load used in the current LRFD Bridge Design Specifications. [AASHTO12]

At 0.1 seconds the cabin mounts failed in both the analysis and the test resulting in a sudden drop in load on the column. At 0.17 seconds the load on the column again drops as the cabin is at rest (waiting on impact from the trailer). At 0.23 seconds the trailer contacts the back of the cabin and the load increases as the cabin is being crushed between the column and the trailer. At 0.276 seconds of the test it appears that the engine becomes wedged between the rigid column and the rear tandem axle on the tractor, resulting in a force spike of 500 kips. The sudden stop of the fifth wheel caused high stresses on the riveted connections between the trailer side walls and the kingpin box, which subsequently failed and released the front wall of the trailer. In the analysis, the engine wedged between the column and the left-side wheel-set of the tandem axle resulting in a peak force of approximately 480 kips. The trailer wall did not fail in the model. After the trailer failed there was a sudden drop in force on the column during the test. The force then reached a second peak at approximately 0.39 seconds when the front of the trailer made contact with the column. The column loading dropped significantly after this peak as the sand in the trailer begin to spill out onto the ground. In the analysis the tractor and trailer continued to press forward under relatively constant load as the sand ballast continued to slide forward against the front of the trailer. The analysis terminated at 0.52 seconds due to excessive deformations of the elements modeling the sand. Although, the loading on the column was still at significant load levels at this time (e.g., greater than 200 kips), it is believed that the majority of the impact event was completed. The peak force caused from the secondary impact from the trailer reached a magnitude of 462 kips in the analysis compared to 513 kips in the test (e.g., 10 percent less).

A quantitative validation assessment of the model's results was based on validation procedures of NCHRP Web Document 179 (W179). [Ray10] The purpose of these guidelines is to establish accuracy, credibility, and confidence in the results of crash test simulations that are intended to support policy decisions, and to be used for approval of design modifications to roadside safety devices that were originally approved with full-scale crash testing.

RSVVP (Roadside Safety Verification and Validation Program) software, which was developed as part of W179, was used to compute the comparison metrics between analysis and full-scale test data. RSVVP computes fifteen different metrics that quantify the differences between a pair of curves. Since many of the metrics share similar formulations, their results are often identical or very similar. Because of this, it is not necessary to include all of the variations. The metrics recommended in Report W179 for comparing time-history traces from full-scale crash tests and/or simulations of crash tests are the Sprague-Geers metrics and the ANOVA metrics. The Sprague-Geers metrics assess the magnitude and phase of two curves while the

ANOVA examines the differences of residual errors between them. The definitions of these metrics are shown below:

Sprague-Geers:

$$\text{Magnitude}\,(M) = \sqrt{\frac{\Sigma c_i^2}{\Sigma m_i^2} - 1}$$

$$\text{Phase}\,(P) = \frac{1}{\pi}\cos^{-1}\frac{\Sigma c_i m_i}{\sqrt{\Sigma c_i^2 \Sigma m_i^2}}$$

$$\text{Comprehensive}\,(C) = \sqrt{M^2 + P^2}$$

ANOVA:

$$\text{Residual Error}\,(\bar{e}^r) = \frac{\Sigma(m_i - c_i)}{m_{\max}} \cdot \frac{1}{n}$$

$$\text{Standard Deviation}\,(\sigma) = \sqrt{\frac{1}{n}\Sigma(m_i - c_i - \bar{e}^r)^2}$$

where,

c_i = calculated quantities

m_i = measured quanties

$m_{\max}$ = maximum measured experimental value

$\bar{e}^r$ = relative average residual error

σ = relative standard deviation

The quantitative evaluation was based on comparison of force-time history on the column in the analysis to those measured in the full-scale crash test. The RSVVP computer program was used to compute the Sprague-Geer metrics and ANOVA metrics using time-history data from the full-scale test (i.e., true curve) and analysis data (i.e., test curve). The default metrics evaluation options in RSVVP were used, which included the Sprague -Geers and the ANOVA. The curves were evaluated over 0.52 seconds of the impact event, corresponding to the termination time of the analysis.

Based on the validation metrics shown in Figure 60 the force-time history computed in the analysis was in good agreement with the test. The values for the Sprague-Geers magnitude and phase metrics were 1.6 and 19.4, respectively, which were well below the limit of 40 recommended in W179. The values for the ANOVA mean and standard deviation were 0.7 and 19, respectively, which were also well below the recommended limits of 5 and 35 for those corresponding metrics.

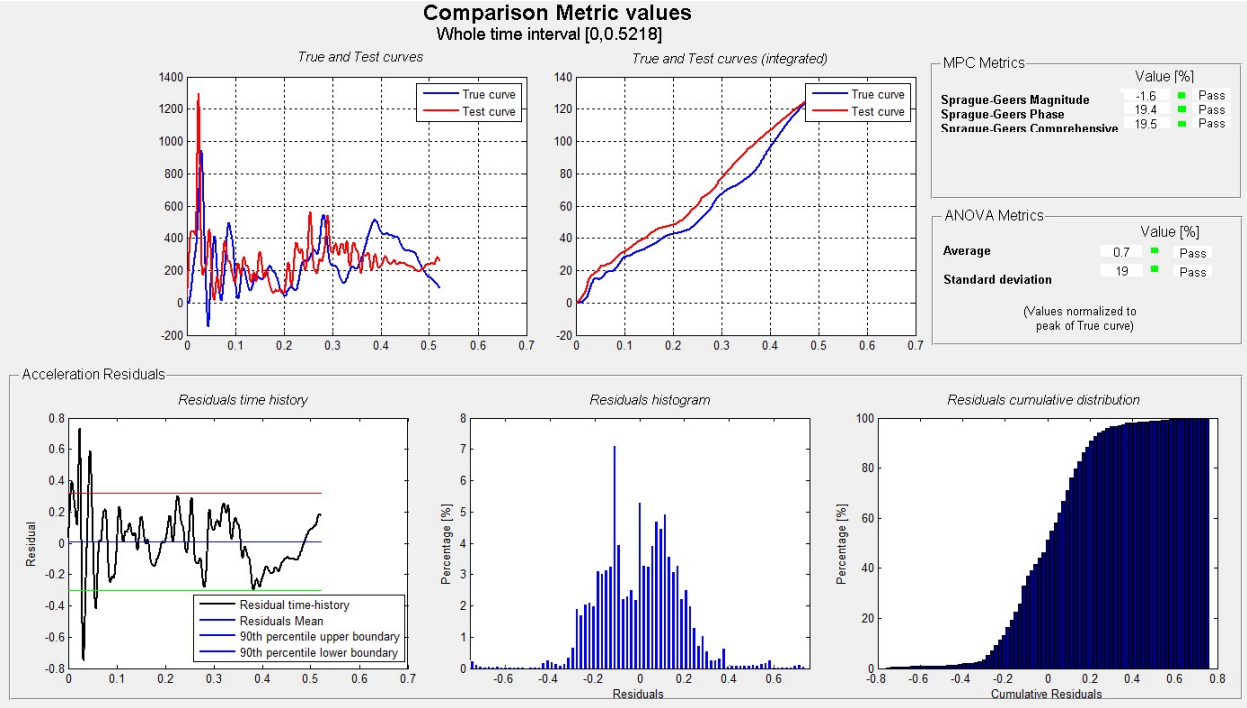

Figure 60. Results from the Program RSVVP Showing Quantitative Comparison Metrics for the FE Model Results and the Full-Scale Test.

Validation Results

Figure 61 shows the total force time histories for Test 429730-2 and the finite element analysis results, annotated with timing of key impact events. Figure 62 shows sequential views of the test from the high-speed video and the FE simulation.

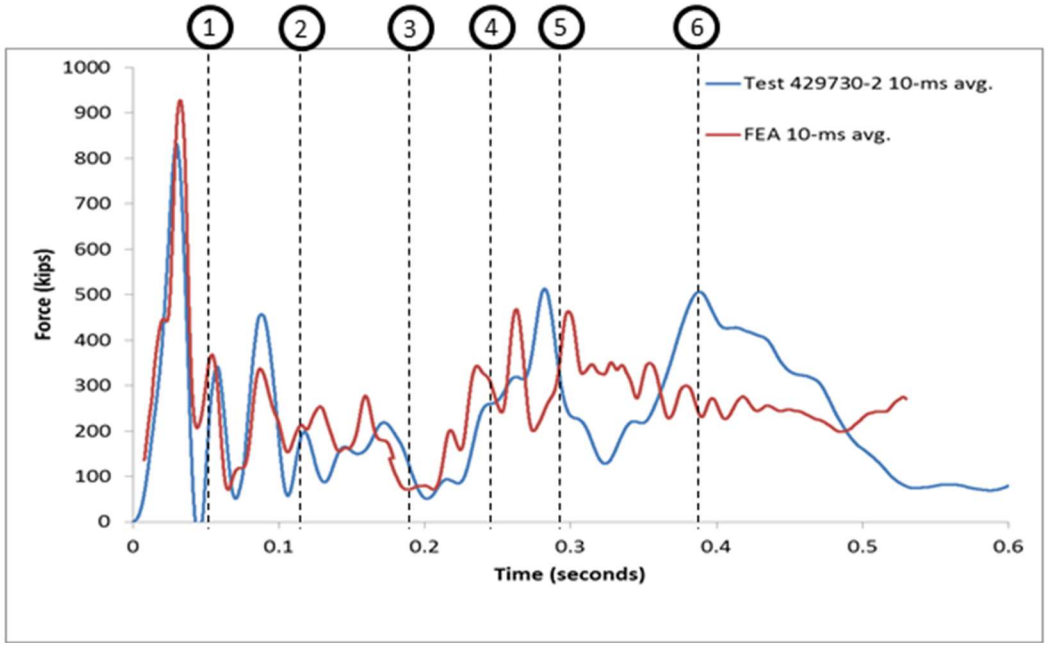

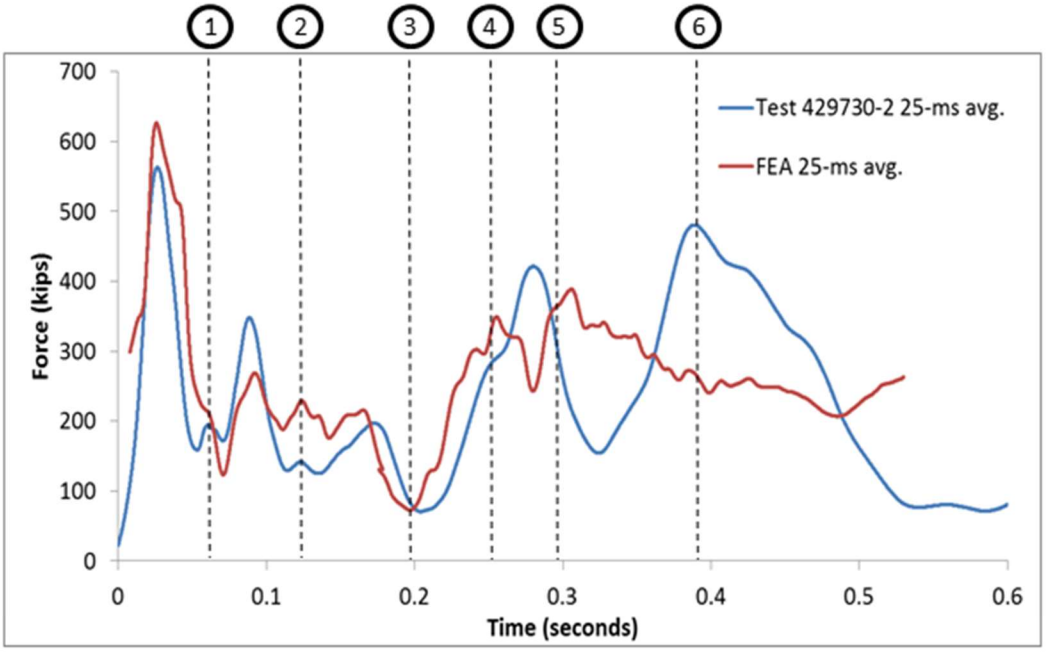

1 – Engine impacts against column
2 – Cabin mounts fail
3 – Resistance drops as cabin is stationary
4 – Truck sleeper contacts trailer and starts crushing
5 – Assume that engine wedges between the column and the rear tandem axle
– Front wall of trailer fails (kingpin does not fail)
6 – Front of trailer contacts column

Figure 61. Total Force for Test No. 429730-2 and FEA Results with Annotations.

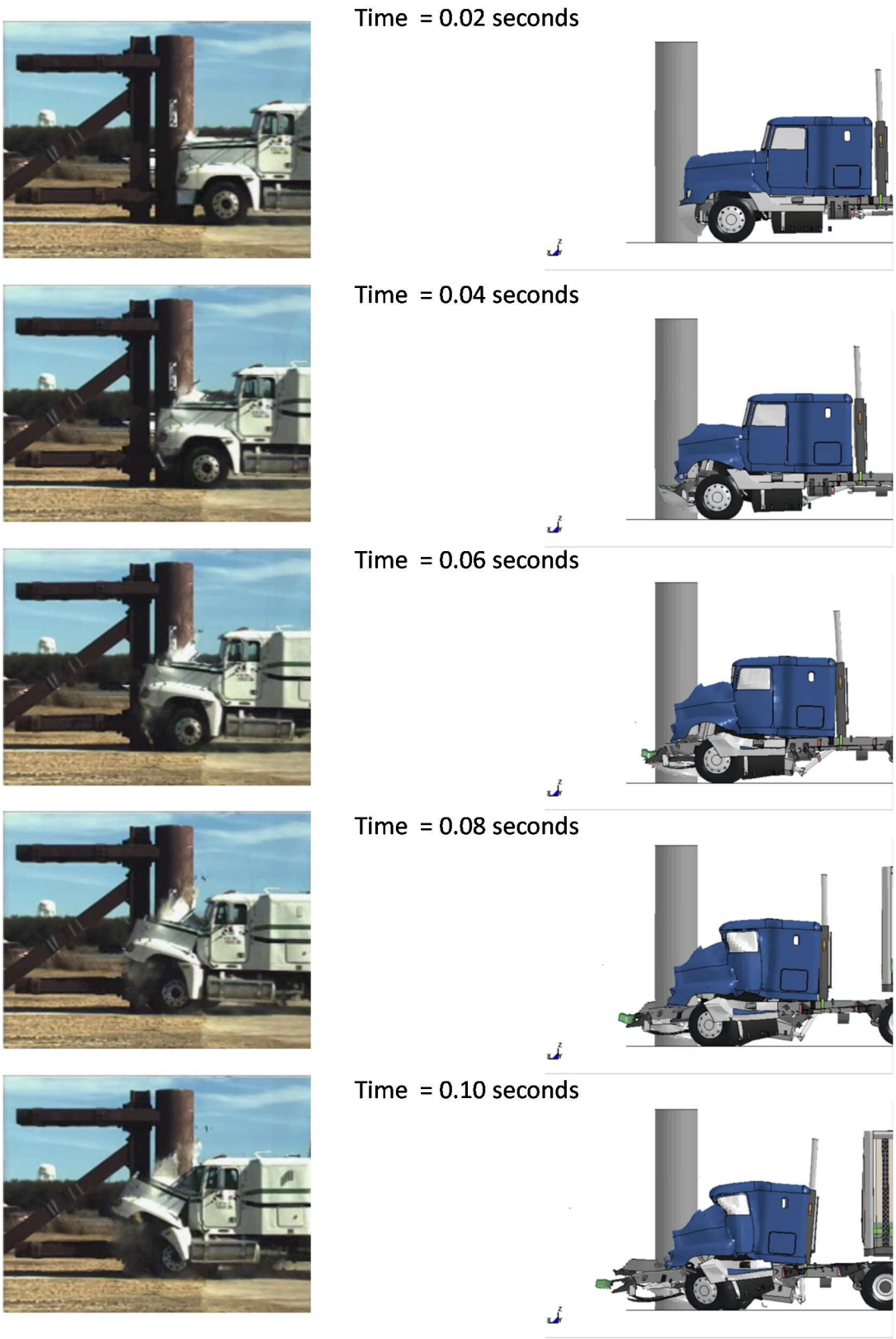

Figure 62. Sequential Views of Test 429730-2 and the FEA Results.

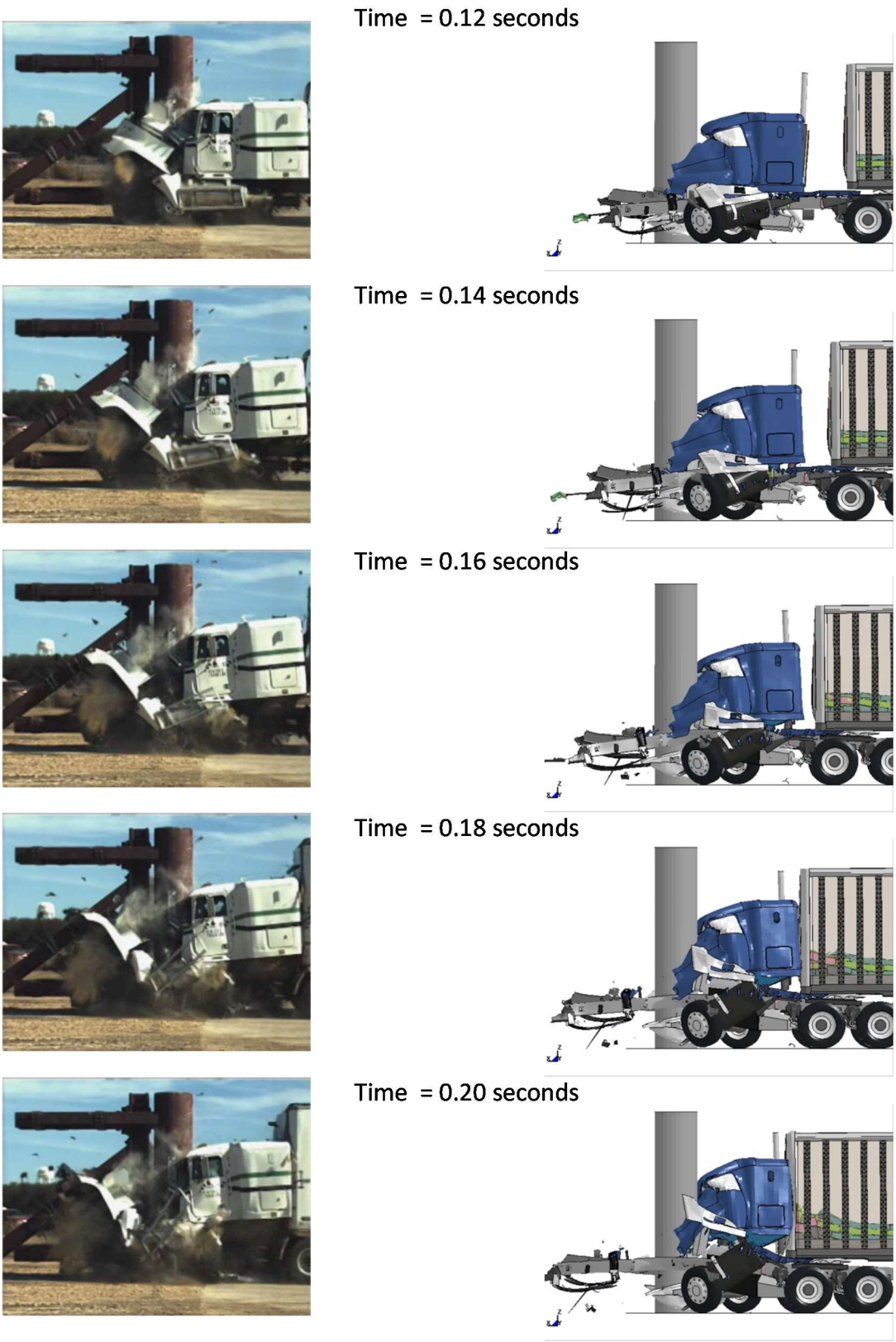

Figure 62. [CONTINUED] Sequential Views of Test 429730-2 and the FEA Results.

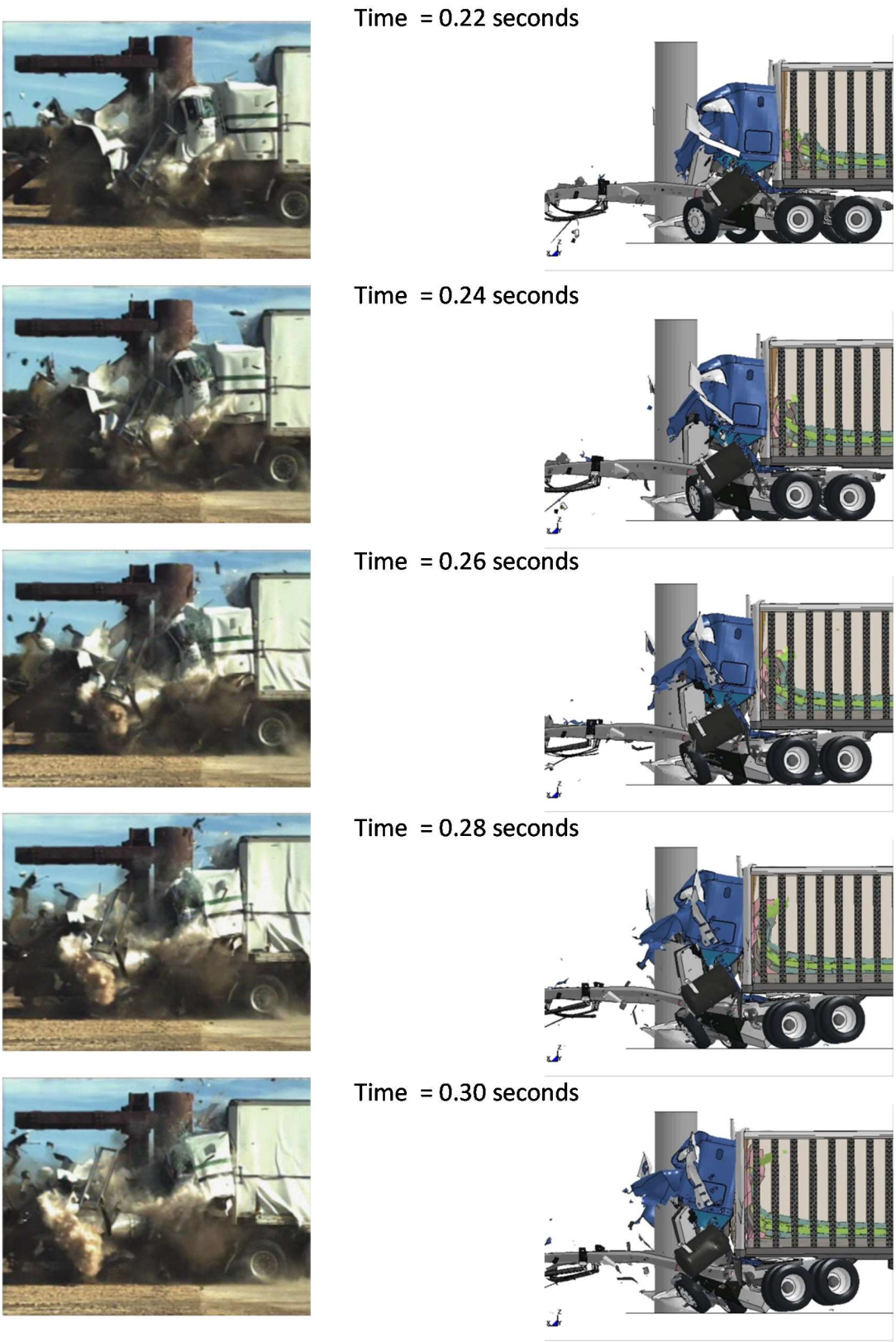

Figure 62. [CONTINUED] Sequential Views of Test 429730-2 and the FEA Results.

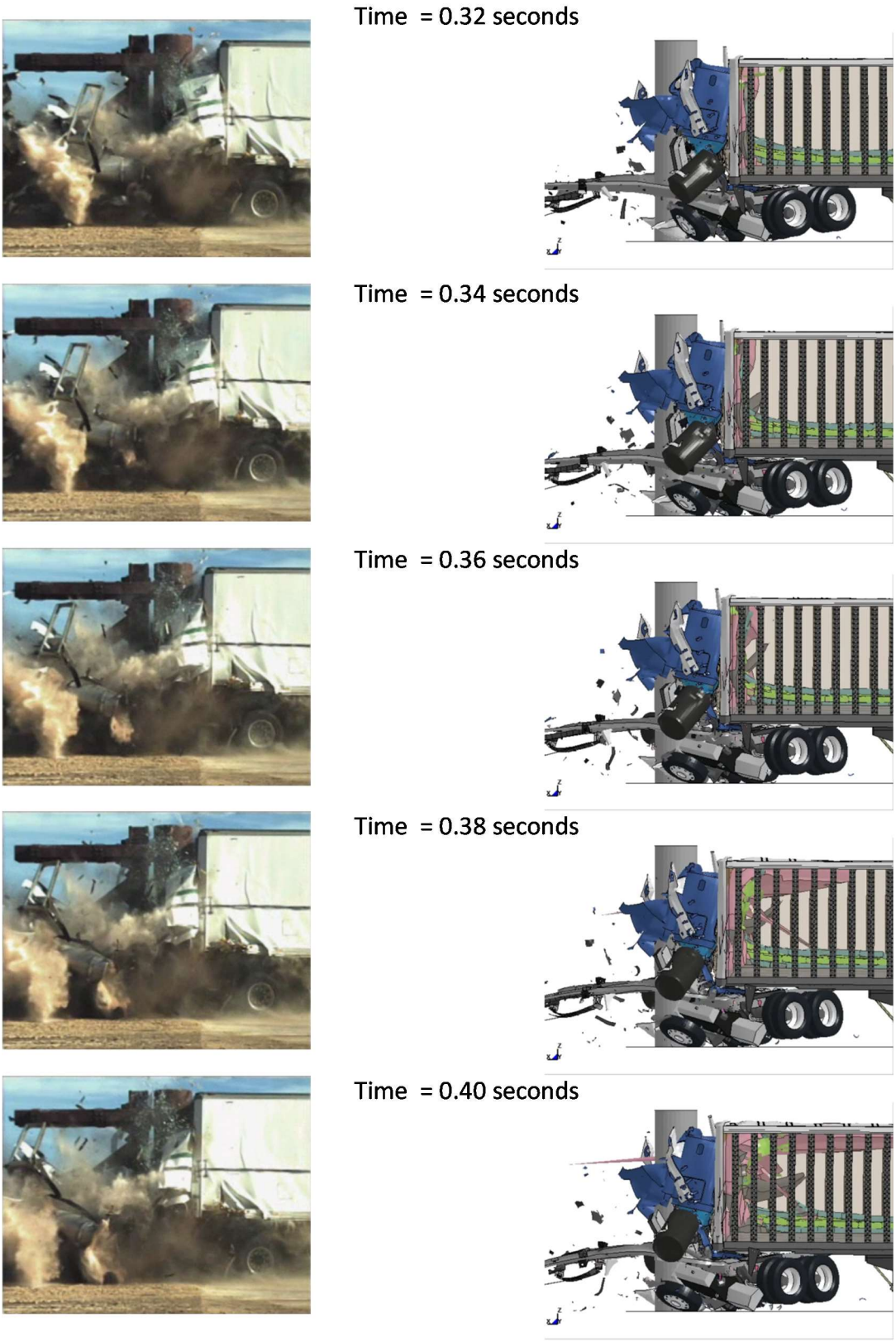

Figure 62. [CONTINUED] Sequential Views of Test 429730-2 and the FEA Results.

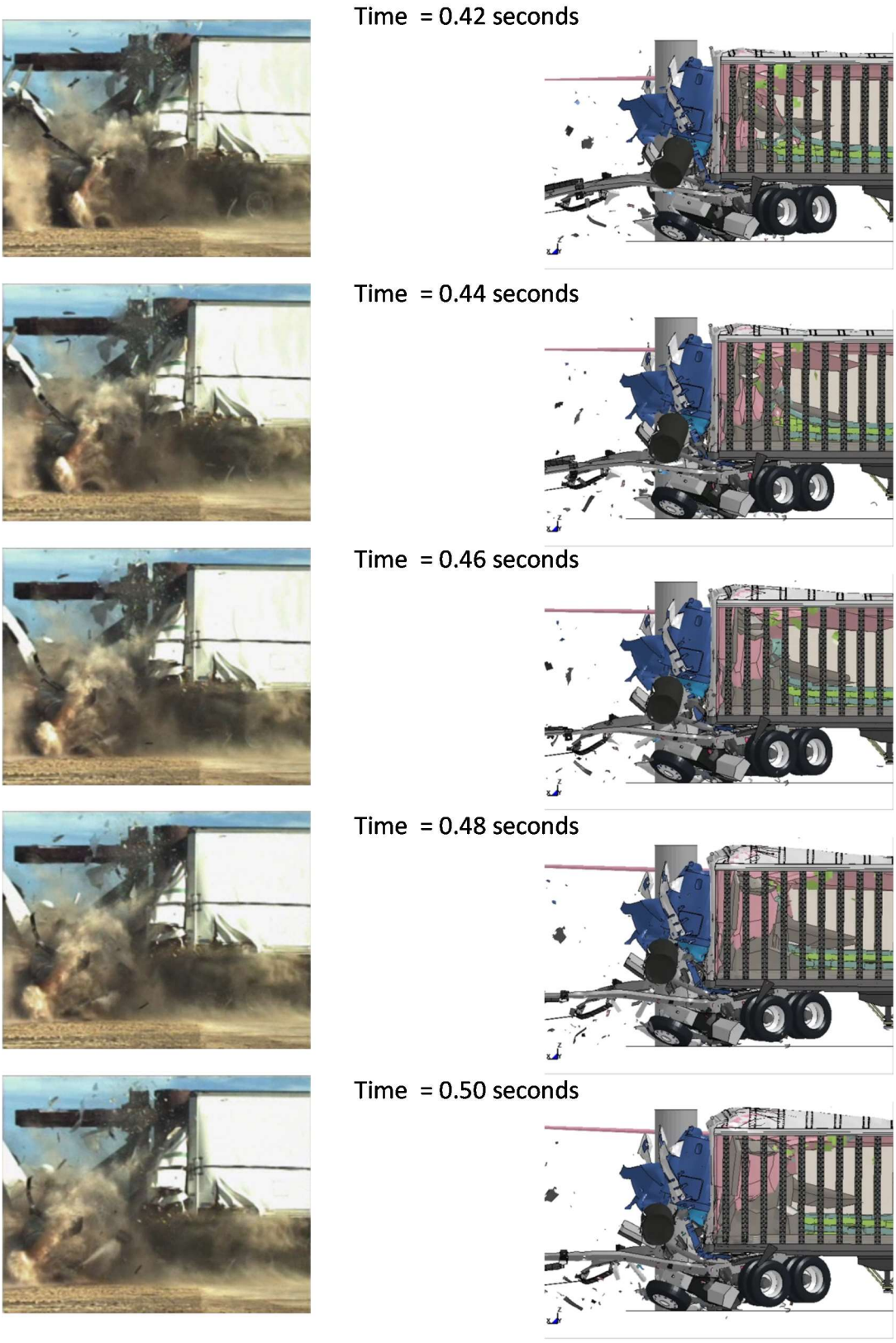

Figure 62. [CONTINUED] Sequential Views of Test 429730-2 and the FEA Results.

In general, the results of the simulated impact indicated that the finite element model of the tractor-trailer replicated the basic phenomenological behavior of the impact event with reasonable accuracy in comparison with the physical crash test. Although the model did not capture the failure of the trailer's front wall (in part because failure was not included in the material definitions for the trailer), there was good agreement between the test and the simulations with respect to event timing, overall kinematics of the vehicle, and loading on the column. The quantitative comparison of the force-time history data also indicated that the finite element model accurately replicates the tests. Based on these comparisons, the model is considered to be sufficient for simulating the impact load on concrete columns. The model will be used to investigate the strength/capacity of various bridge pier designs for lateral impact loading where an 80,000-lbs tractor-trailer truck strikes the pier at 50 mi/hr head-on.

As shown in Figure 61, the loading on the column under these types of impacts occurs in two phases. The first phase occurs when the engine strikes the column. The peak force from this event is generally very high but then drops off quickly as the engine is brought to rest. The secondary peak results from the trailer impacting the column. This stage of the loading generally occurs at lower forces than the initial stage (i.e., from the engine impact); however, the loads in this stage are sustained for a much longer time as the contents of the trailer continue to move toward the front of the trailer and load the column.

The rigid pole time history results shown in Figure 61 also show the origins of the 600 kips design load used in the 6th edition of the LRFD Bridge Design Specification. While Buth does not explicitly state it, the 600-kip design load was apparently determined from the peak 25 msec average rigid pole force. [Buth10, AASHTO12] In essence, Buth is assuming that the 25-msec average dynamic load is essentially equivalent to a quasi-static design loading.

RESULTS

In all cases the analysis terminated prematurely due to numerical instabilities caused by excessive local forces on various individual components during the impact event. The termination generally occurred during the second loading phase as the engine was wedged between the column and the tractor tandem axle as illustrated in Figure 63. In most cases the peak forces had occurred prior to or just at the termination time.

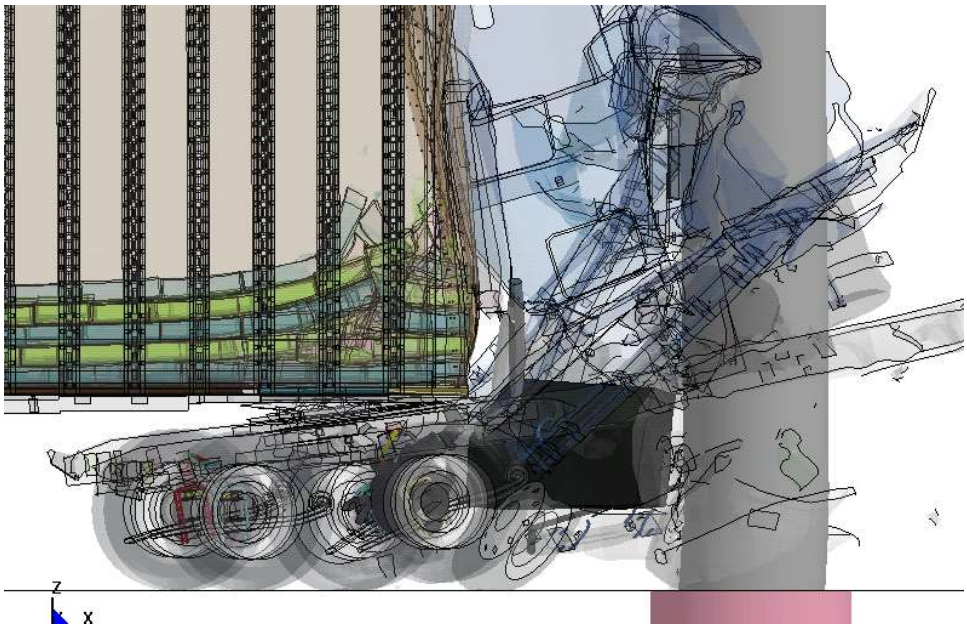

Figure 63. Image from FE Analysis Showing Engine Wedging Between Column and Tractor Tandem Axle During Column Impact.

The force-time histories and the force-displacement curves from the impact simulations are shown in Figures 64 through 71. The force values represent the overall total force between the vehicle and the bridge pier which was spread out over a relatively large contact area. Although, the force during the initial stage of the impact was generally concentrated at the location where the deflection data was collected, the location of the effective load point generally moved up the column during later stages of the impact. An image of the final damaged state of the column at the termination time of the analysis is shown on the each of the plots (note: the lateral displacement is artificially magnified for illustration purposes). These images also include the location where the lateral deflection was measured.

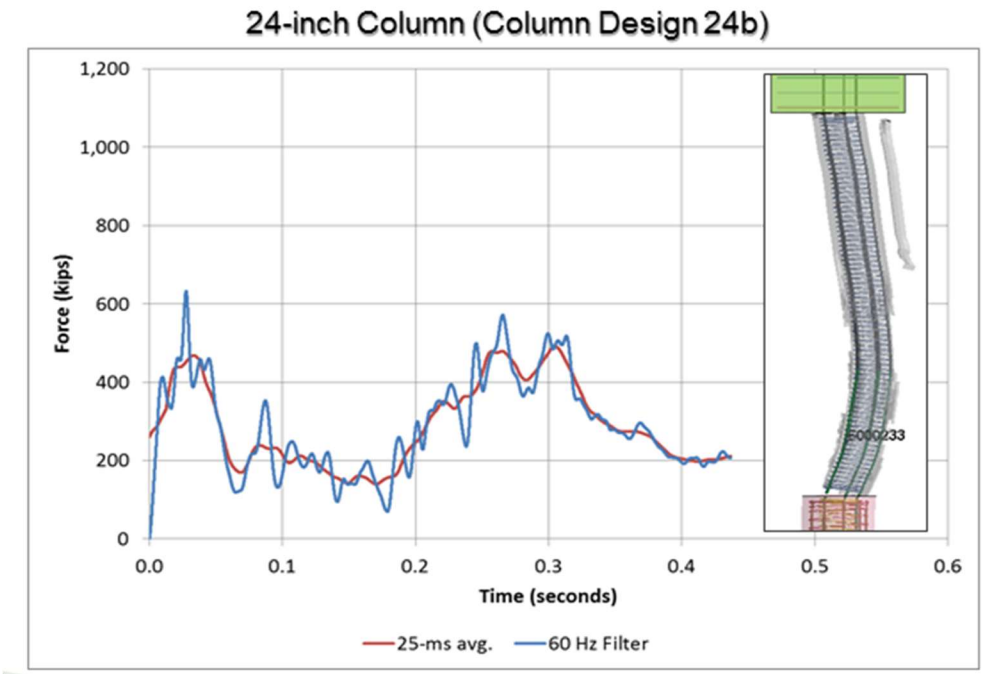

Figure 64. Force-Time History Resulting from 80,000-lb Tractor-Trailer Impacting 24-inch Diameter Bridge Pier (FEA).

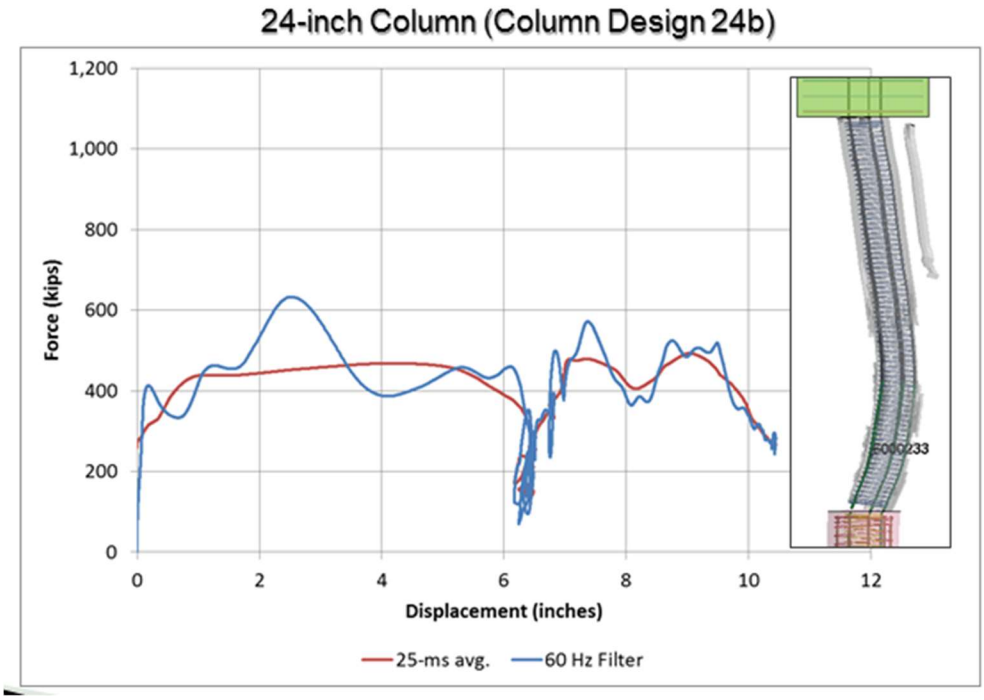

Figure 65. Force-Deflection Plot Resulting From 80,000-ib Tractor-Trailer Impacting 24-inch Diameter Bridge Pier (FEA).

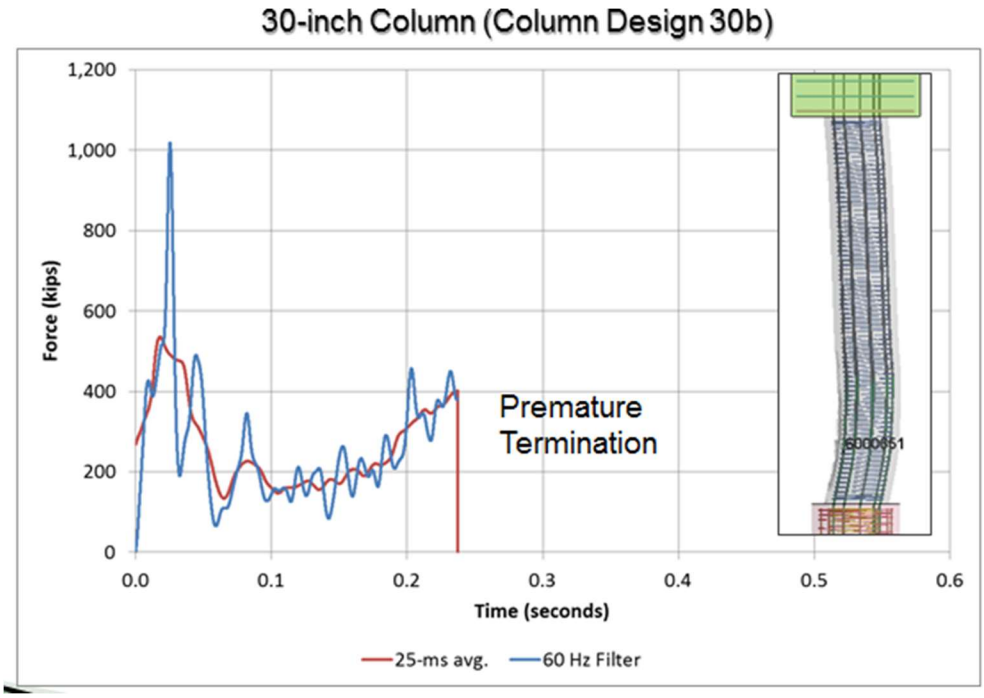

Figure 66. Force-time History Resulting From 80,000-lb Tractor-Trailer Impacting 30-inch Diameter Bridge Pier (FEA).

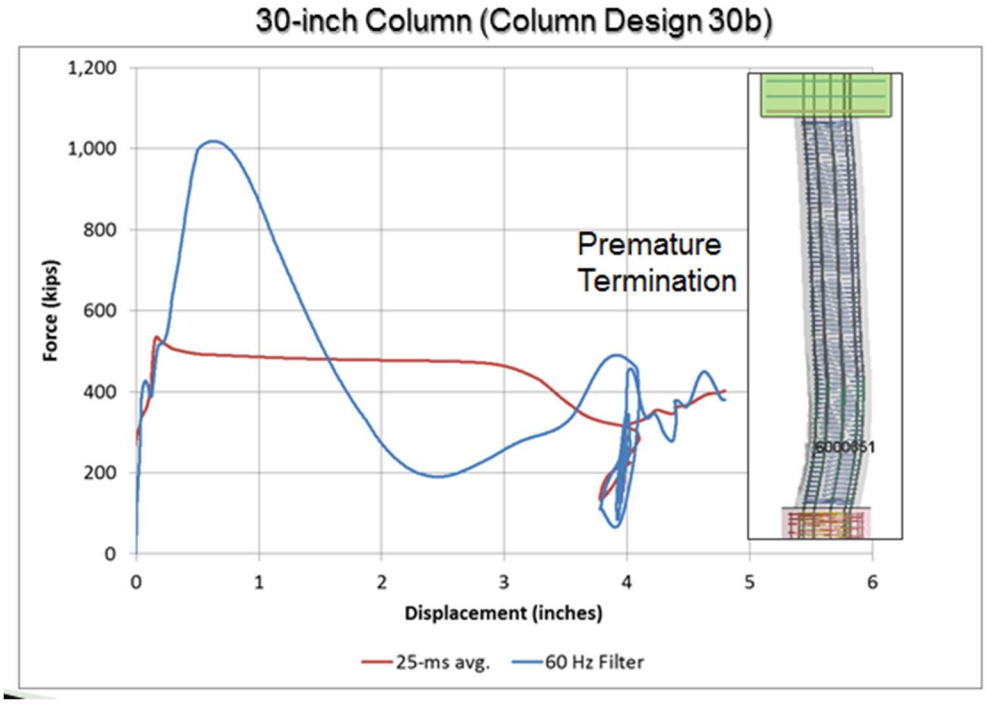

Figure 67. Force-Deflection Plot Resulting From 80,000-lb Tractor-Trailer Impacting 30-inch Diameter Bridge Pier (FEA).

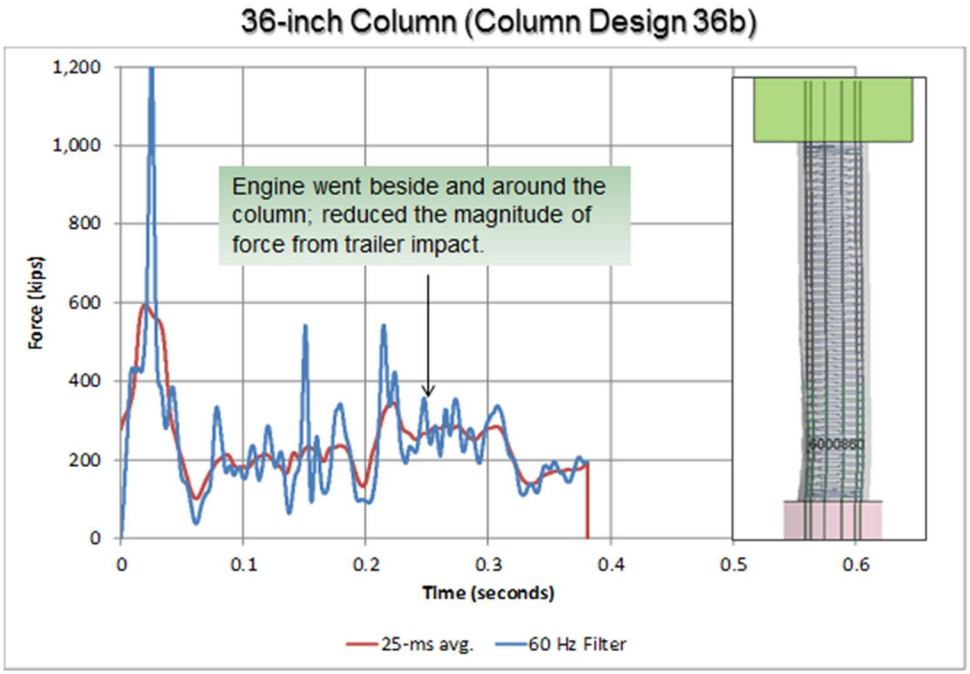

Figure 68. Force-Time History Resulting From 80,000-lb Tractor-Trailer Impacting 36-inch Diameter Bridge Pier (FEA).

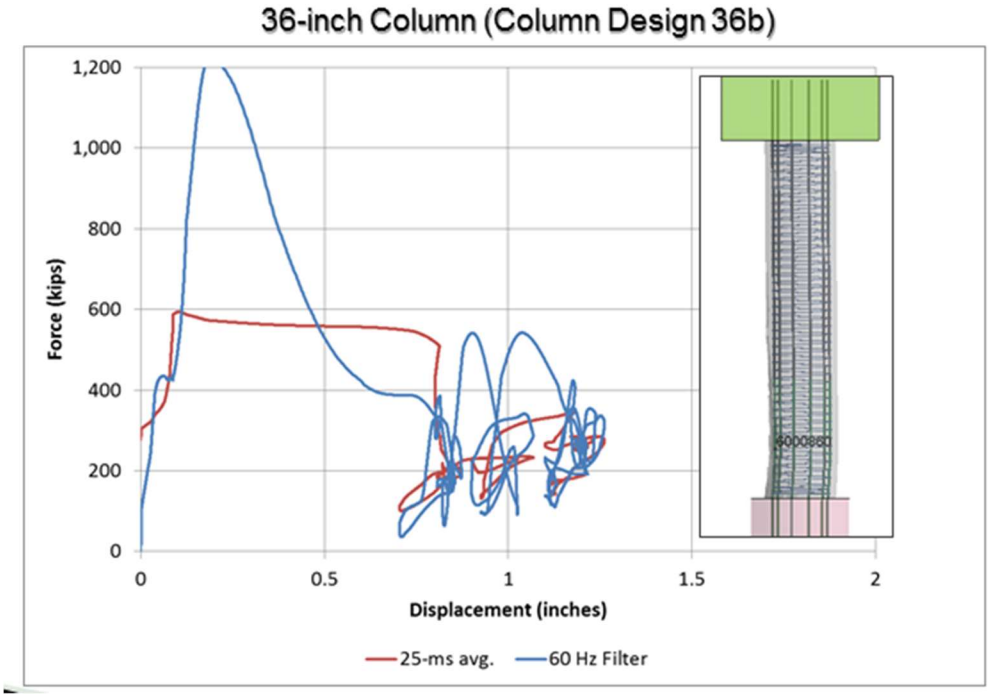

Figure 69. Force-Deflection Plot Resulting From 80,000-lb Tractor-Trailer Impacting 36-inch Diameter Bridge Pier (FEA).

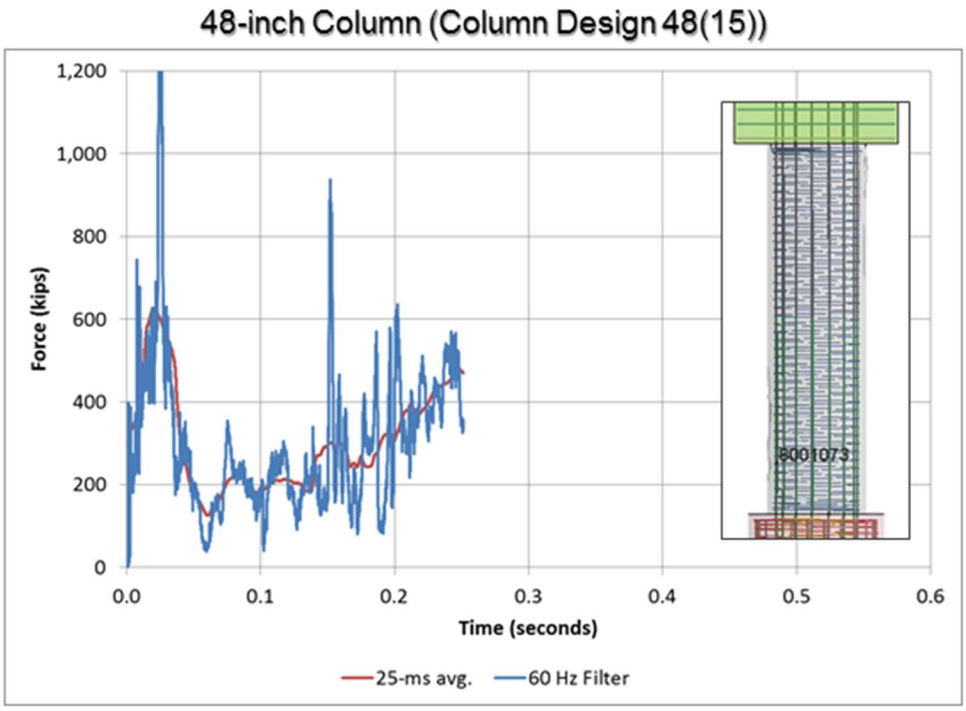

Figure 70. Force-Time History Resulting From 80,000-lb Tractor-Trailer Impacting 48-inch Diameter Bridge Pier (FEA).

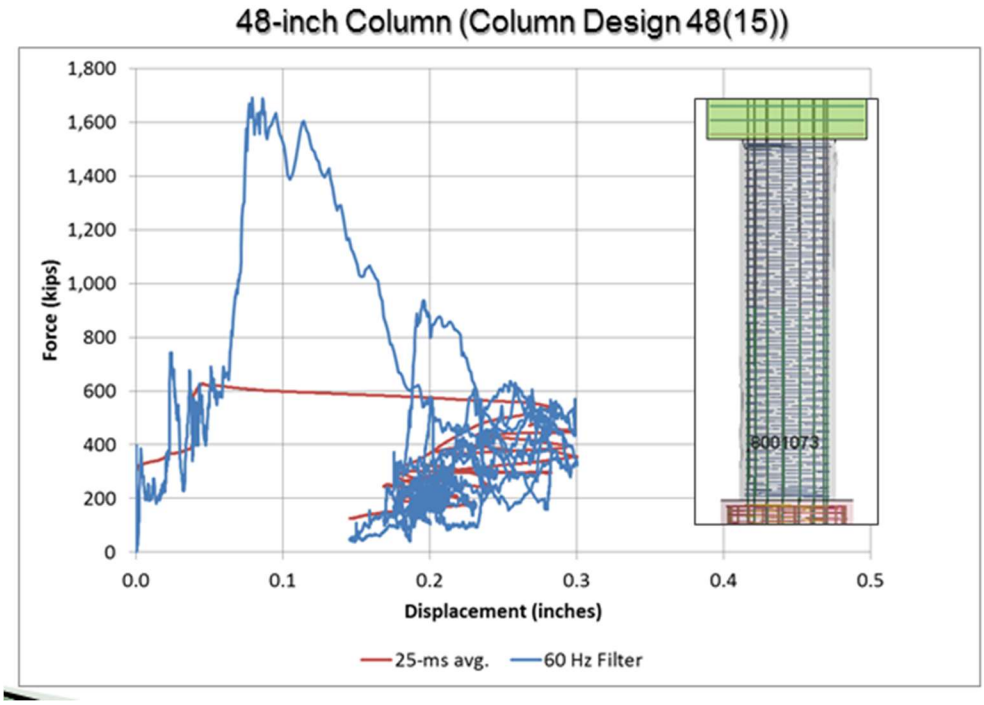

Figure 71. Force-Deflection Plot Resulting From 80,000-lb Tractor-Trailer Impacting 48-inch Diameter Bridge Pier (FEA).

Table 18 shows a summary of results from the 80,000-lbs tractor-trailer truck, 50 mi/hr, head-on impact simulations. The peak 25-ms average impact force for the 24-inch diameter column was 456 kips and increased to 623 kips for the 48-inch diameter column. The failure of the column was apparent for the 24-inch and 30-inch diameter bridge pier cases under the 80,000-lbs, 50-mi/hr head-on impact conditions. From visual inspection (see Figures 64 through 67), as well as from the summary table below, the deflection and damage to the column was excessive for those cases. The force-deflection plots also indicated that the columns were still deflecting at the termination of the analysis. It was also apparent that the 48-inch diameter case did not fail under these conditions. The maximum deflection was only 0.3 inches and had rebounded to 0.11 inches at termination of the analysis indicating that the impact had been contained.

Table 18. Summary of Results for the 80,000-lbs, 50 mi/hr, Head-On Tractor-Trailer Truck Impact Simulations.

Design Case	f'_c (ksi)	Initial Peak Force (kips)		Second Peak Force (kips)		Column Deflection (in)		Failure Yes / No
		60 Hz Filter	25-ms avg.	60 Hz Filter	25-ms avg.	Peak	Final	
24b	5.5	632	456	560	487	10.4+	10.4+	Yes
30b	5.5	1020	534	*	400	4.8+	4.8+	Yes
36b	5.5	1220	592	541	343	1.25	1.11	No++
48(15)	5.5	1690	623	567	472	0.3	0.14	No

* Premature termination of analysis

\+ The column was still deflecting at termination of the analysis

++ There was notable damage to the column including spalling but no through cracks

The results from 36-inch diameter column case, on the other hand, could not be decisively determined from the force-deflection plots and visual inspection. The peak 25-msec impact force was 592 kips and the deformation of the column was approximately 1.25 inches. However, from contour plots of 1st principle strain, it appears that the strains in the column did not reach magnitudes that would indicate that a crack had occurred in the column. Figure 72 shows the contour plots of 1st principal strain for a front view of the column and also for a vertical cross-section view from the left side of the column. The contour range in Figure 72 is cut off at a strain of 0.1. Recall from the validation study for the concrete model shown earlier, strain values of 0.07 to 0.08 (yellow contours) indicated initial crack openings in the concrete when correlated to the scaled column impact tests; likewise strains from 0.08 to 0.1 (red contours) corresponded to significant crack openings. The analysis results for the 36-inch column impact case resulted in strain values approaching only 0.05 (light green contours) at the base of the column, which were below the critical thresholds. There was, however, significant spalling of the concrete on the front side of the column, as shown in Figure 72. Although the column was significantly damaged during the impact, it was concluded that it did not fail when struck at 50 mi/hr, head-on with an 80,000-lbs tractor-trailer truck although it was very close to its capacity. Interestingly, the peak 25-msec lateral load was 592 kips, just under the 600 kips LRFD design recommendation. [AASHTO12]

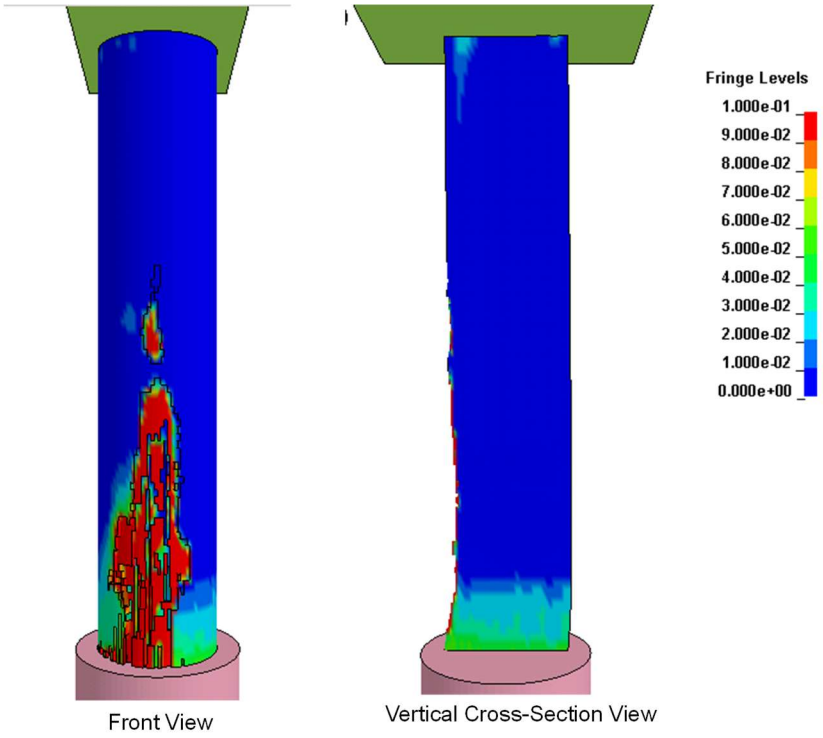

Figure 72. Contours of 1st Principle Strain for the 36-inch Diameter Column (Case 36b).

Figure 73 shows a plot of peak impact force versus column diameter. Recall from the column capacity study that the column capacity increased linearly with respect to column diameter (although in the capacity study the load was applied at 5 ft above grade, whereas in these analyses the load point varies throughout the analysis depending on the stage of the impact and which components are in contact with the column at any given time). Thus, it was concluded that the 24-inch and 30-inch column cases reached capacity and a trend line was generated using those two data points. The 36-inch diameter case was near the estimated capacity threshold line but did not reach the critical load value. The 48-inch diameter case, on the other hand, was well below the estimated capacity threshold line. This further supports the original conclusion that the 36-inch case was damaged but did not fail.

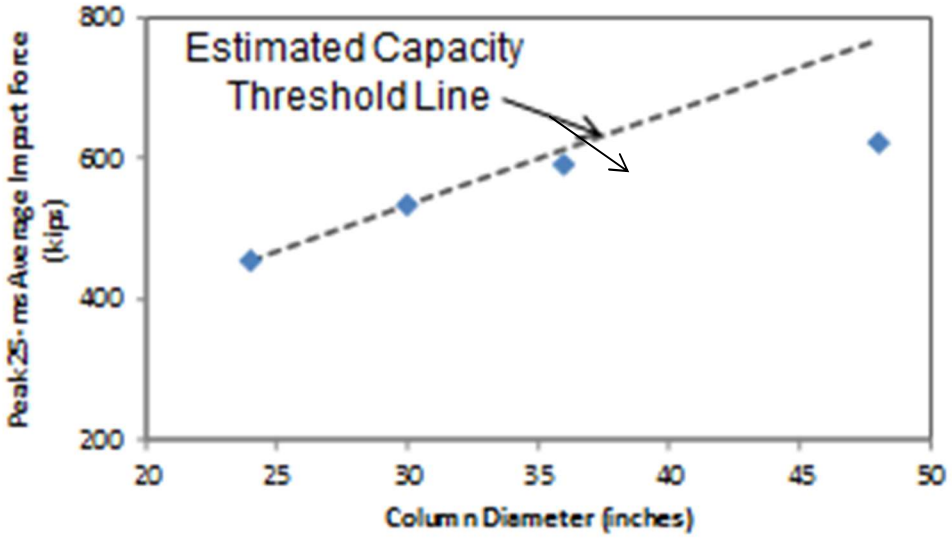

Figure 73. Peak Impact Force versus Column Diameter for the 50 mi/hr, Head-On, 80,000-lbs Tractor-Trailer Truck Impact Simulations.

Capacity ***Assessment***

The lateral load capacity based on the shear and hinge moment discussed earlier in this section can be used to assess the finite element simulations of the full-scale tractor-trailer impacts with the representative column designs in the same manner as previously used to assess the pendulum test results. The test results and the estimates from the simple plastic hinge model are shown below in Table 19 and the associated force-displacement plots are shown Figure 74. The LRFD shear capacity shown in Table 19 is the nominal capacity (i.e., ϕ =1 rather than 0.9). A ϕ of 1 was used since the results are being compared to simulated impact events rather than being used as a design criterion. Similarly, there is no ϕ associated with the simple hinge model capacity either. In Table 19 cells colored red indicate that either failure was observed in the finite element simulation or failure was predicted by LRFD shear capacity or simple hinge model.

Table 19. Capacity Assessment of Tractor-Trailer Truck Finite Element Analyses.

Finite Element Analyses			**Nominal LRFD Shear Capacity**	**Simple Hinge Model Capacity**	
Design	**Force**	**Energy**	**Force**	**Force**	**Energy**
	(kips)	(in-kips)	(kips)	(kips)	(in-kips)
24b	456	1,020	297	277	64
30b	534	607	413	554	162
36b	592	300	548	924	214
48b	623	270	855	2052	321

Failure for the tests were generally based on the observed damage in the model with particular attention to dislocations between the top and bottom of the section whereas failure for the simple hinge model implies that at least two layers of longitudinal bars have reached the fully

plastic stress. Failure requires first that the lateral load capacity be achieved and second that there is more energy available after the lateral load capacity has been reached.

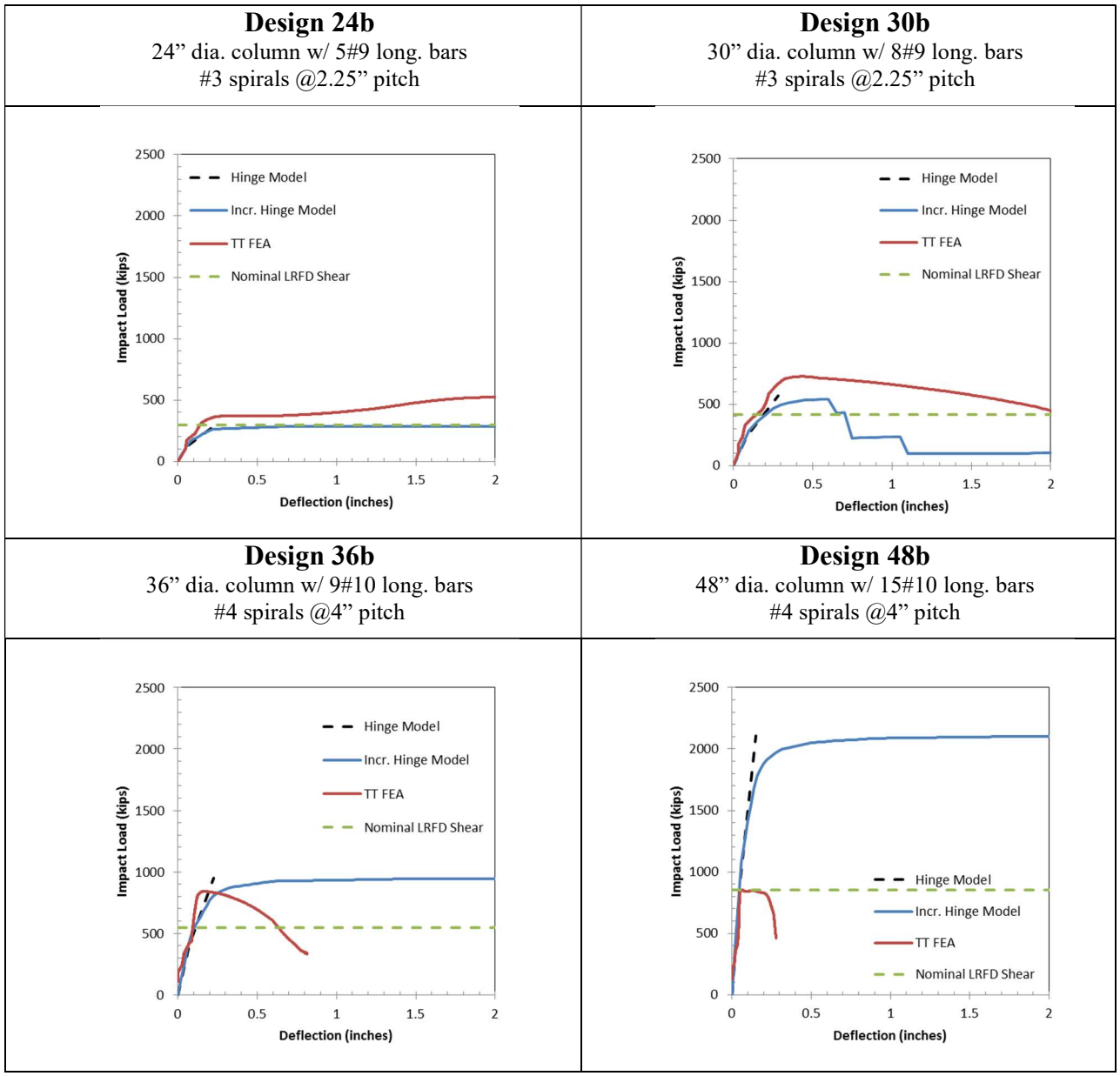

Figure 74. Force-Displacement of Tractor-Trailer Impact Finite-Element Analyses and Capacity Estimates

The force-displacement curve for representative column design 24b was shown earlier in Figure 65 and the results are summarized in Table 18. Based on the deformations and damaged shown in Figure 65 the column was judged to have catastrophically failed in the tractor-trailer truck impact simulation. As shown in Table 19, the nominal LFRD shear capacity of 297 kips was exceeded as was the simple hinge load of 277 kips so both the nominal LRFD shear and hinge moment correctly predicted a failure in this 50 mi/hr impact with an 80,000-lbs tractor trailer truck. This is also evident in the upper left side of Figure 74 where the impact load exceeds both the nominal LRFD shear and the hinge load.

The force-displacement curve for representative column design 30b was shown earlier in Figure 67 and the results are summarized in Table 18. Based on the deformations and damaged shown in Figure 67 the column was judged to have catastrophically failed in the tractor-trailer truck impact simulation. As shown in Table 19, the nominal LFRD shear capacity of 413 kips was exceeded the 534 kips impact load was just under the simple hinge load of 554 kips so both the nominal LRFD shear and hinge moment correctly predicted a failure in this 50 mi/hr impact with an 80,000-lbs tractor trailer truck. This is also evident in the upper right side of Figure 74 where the impact load exceeds both the nominal LRFD shear and the hinge load.

The force-displacement curve for representative column design 36b was shown earlier in Figure 69 and the results are summarized in Table 18. In this case, the displacements and damage, shown in Figure 69, appear very close to failure. As described earlier and shown in Figure 72, a careful examination of the strains in the column indicated that the finite element analysis showed the column had not reached the failure limit although it was very close. As shown in Table 19, the nominal LFRD shear capacity of 548 kips was exceed but the impact load was still less than the simple hinge load of 924 kips so the nominal LRFD shear capacity estimated failure but the hinge moment predicted the column was under the failure limit for this 50 mi/hr impact with an 80,000-lbs tractor trailer truck. This is also evident in the lower left side of Figure 74.

The force-displacement curve for representative column design 48b was shown earlier in Figure 71 and the results are summarized in Table 18. In this case, the displacements and damage, shown in Figure 71, show that the column had not failed and, in fact, had quite a bit of additional capacity left. As shown in Table 19, the nominal LFRD shear capacity of 855 kips was over the impact lateral load of 623 and well under the simple hinge load of 2,052 kips so both criteria indicated no failure for this 50 mi/hr impact with an 80,000-lbs tractor trailer truck. This is also evident in the lower right side of Figure 74 where the finite element analysis curve does not exceed either the nominal LRFD shear capacity or the simple hinge lateral load capacity.

CONCLUSIONS

Based from the results of the 50 mi/hr, head-on, 80,000-lbs tractor-trailer truck impact simulations discussed in the previous sections, bridge piers with diameters of 30-inches or less may fail catastrophically at these impact conditions. Bridge piers with diameter of 36 inches or greater likely not fail under these conditions when conventionally reinforced; however, the 36-inch diameter columns are susceptible to significant damage, including spalling, on the impact side of the column. Columns larger than 36 inches appear unlikely to fail.

The assessment of capacity indicated that for failure to be observed in the finite element analyses, the simple hinge lateral load capacity had to be exceeded. The simple hinge method, therefore, appears to adequately predict the lateral load failure capacity of these representative columns.

Based on the scaled model impact tests, the finite element capacity analysis of the representative piers, the full-scale tractor trailer finite element analyses of the representative piers and the capacity analysis, the research team recommends that the current LRFD Bridge Specification recommendation of a 600 kips lateral load capacity be retained. This value, however, should be interpreted not as the shear capacity of the column but as the hinge capacity of the column.

The foregoing analyses showed that circular columns 30-inches in diameter and smaller are likely to fail in an impact with an 80,000-lbs tractor trailer truck striking the column head-on at 50 mi/hr. Such columns generally have a simple hinge lateral impact load capacity of under 600 kips so they are at high risk of catastrophic failure in the field.

The simple hinge lateral impact load capacity should be calculated for circular or square reinforced concrete columns using the following equations as presented earlier:

$$x_{H2} = \left[\frac{AB}{A+B}\right]\left[\frac{\varepsilon_p}{\varepsilon_s}\right]\frac{y_{crit}}{(d_2 - a)}$$

$$P_{H2} = \left[f_p A_b \left(n_1(d_1 - a)\sum_{i=2}^{N} n_i A_b n_i \left[\frac{d_i^2}{d_1}\right]\right)\right]\left[\frac{(A+B)^2}{AB}\right]$$

$$E_{HINGE} = \left[\frac{P_{H2}x_{H2}}{2}\right]$$

The 6th Edition of the LRFD Bridge Design Specifications recommends that this impact load be applied to the column five feet above the grade but the finite element analysis showed clearly that the peak load is associated with the impact of the engine of the tractor which is located much lower, typically at the bumper level of 25 inches. The research team recommends that the impact load be applied at 25 inches rather than 5 ft. The guidelines user should check not only the impact load capacity at the level of impact but also the resulting moments at the pier cap and foundation to ensure that the connections have sufficient strength to resist the impact.

The research team recommends the following for use in step two of the guidelines:

- The critical lateral load capacity will be 600 kips,
- The capacity of the column is based on the moment that causes complete failure of the column,
- The impact lateral load will be applied to the column 25 inches above the grade.
- The impact angle should be between zero and 15 degrees.

Appendix E. Nominal Resistance to Lateral Impact Loads on Pier Columns

PIER COMPONENT LATERAL RESISTANCE TO IMPACT

The objective of this section was to determine the quasi-static capacity of each representative pier for use in the probabilistic risk analysis of pier protection or strengthening alternatives. The nominal design capacity of each of the representative pier designs selected in Section 6.2A were determined using conventional design methods according to the current LRFD Bridge Design Specifications. [AASHTO12] These procedures have also been summarized in a recent study by Buth *et al* to evaluate bridge pier protection recommendations included in AASHTO's LRFD Bridge Design Specifications [Buth10]. These procedures were further refined to provide the best available first principles analyses of the shear capacity of a bridge pier to survive an impact with heavy vehicles of various sizes and configurations. It is important to note that first principles analyses are based upon a static analysis and cannot accurately evaluate the stiffening effects associated with dynamic loading. The capacities developed herein are analogous to the capacity (i.e., nominal resistance) a designer would calculate prior to using the pier protection guidelines.

The resulting quasi-static design capacity of the representative bridge pier components (e.g., circular columns, square columns, pier walls, etc.) can be included directly into RSAPv3 or the design guidelines to be developed in Phase III Task 10. RSAPv3 already allows each type of roadside feature to have a load and strain energy capacity where the feature fails and allows the vehicle to pass through. Currently, RSAPv3 sets the bridge pier capacity to a very large value to represent essentially rigid conditions. Instead of having just one bridge pier hazard in RSAPv3, as is the case now, additional bridge piers will be added to the hazard list in Phase III Task 10 and the appropriate capacities included as describe herein.

SHEAR CAPACITY

In conventional bridge design, the minimum shear capacity of the bridge piers is generally determined based on the contribution of shear strength from the concrete and the shear strength of the transverse or spiral reinforcement. Shear strength contributions from the longitudinal steel are generally neglected. Some specific design requirements from the AASHTO LRFD Bridge Design Specifications for transverse reinforcement steel in bridge piers are: [AASHTO12]

- Article 5.10.6 – Transverse Reinforcement for Compression Members
  - 5.10.6.2 – Spirals
    - "Spiral reinforcement for compression members … shall consist of one or more evenly spaced continuous spirals … with a minimum diameter of 0.375 in [#3 bar].
    - Longitudinal reinforcement located on inside of, and in contact with spiral steel.
    - Clear spacing between the bars of the spiral [pitch spacing minus bar diameter] shall not be less than 1.0 inch or 1.33 times the maximum size of the aggregate. [The ACI code A7.10.4 states that the clear spacing of spirals may not be less than 1 inch or greater than 3 inches.]
    - The center-to-center spacing shall not exceed 6.0 times the diameter of the longitudinal bars or 6.0 in."
  - 5.10.6.3 - Ties

        - "In tied compression members, all longitudinal bars or bundles shall be enclosed by lateral ties that shall be equivalent to:
            - No. 3 bars for No. 10 or smaller bars
            - No. 4 bars for No. 11 or larger bars, and
            - No. 4 bars for bundled bars.
        - The spacing of ties along the longitudinal axis of the compression member shall not exceed the least dimension of the compression member or 12.0 in. Where two or more bars larger than No. 10 are bundled together, the spacing shall not exceed half the least dimension of the member of 6 in."
- Article 5.7.4.6 – Spirals and Ties

    "Where the area of spiral and tie reinforcement is not controlled by seismic requirements, shear or torsion as specified in Article 5.8, or minimum requirements as specified in Article 5.10.6, the ratio of spiral reinforcement to total volume of concrete core, measured out-to-out of spirals, shall satisfy:

    $$\rho_s \geq 0.45\left(\frac{A_g}{A_c} - 1\right)\frac{f'_c}{f_{yh}} \qquad (5.7.4.6-1)$$

    Where:
    A_g = gross area of concrete section (in^2)
    A_c = area of core measured to the outside diameter of the spiral (in^2)
    f'_c = specified strength of concrete at 28 days, unless another age is specified (ksi)
    f_{yh} = specified yield strength of spiral reinforcement (ksi)"
- Article 5.8.2.7 – Maximum Spacing of Transverse Reinforcement
    - "The spacing of the transverse reinforcement shall not exceed the maximum permitted spacing, s_{max}, determined as:

    $$If\ v_u < 0.125f'_c, then$$
    $$s_{max} = 0.8d_v \leq 24\ in. \qquad (5.8.2.7-1)$$
    $$If\ v_u \geq 0.125f'_c, then$$
    $$s_{max} = 0.4d_v \leq 12\ in. \qquad (5.8.2.7-2)$$

    Where:
    v_u = the shear stress calculated in accordance with Article 5.8.2.9 (ksi)
    d_v = effective shear depth as defined in Article 5.8.2.9 (inches)"

Rectangular Columns

Shear capacity calculations were also developed for square columns. Appendix 6.2B shows an example of the structural analysis calculations for a 30 x 30-inch square column. The design includes: 4 ksi concrete, #4 shear ties with minimum yield strength of 60 ksi, a spacing of 12 inches for the ties, 1.5 inches clear cover for the outer concrete shell, and a maximum aggregate size of 1 inch. The maximum spacing of the ties was based on Article 5.7.4.6 of the LRFD. The contribution of the longitudinal steel to the shear capacity of the column was not included in the calculations. The resulting capacity was 179 kips using the general procedure with a maximum value of strain of 0.002 for the reinforcing steel compared to a capacity of 363 kips for the 30-inch diameter spiral column (see Table 2).

Table 1. Summary of Shear Strength Calculations for Four Bridge Pier Designs from Accident Cases Collected by Buth Compared to Current Design Practice (uses ϵ_s=0.006).

	Case	Column Dia. (in)	Concrete			Longitudinal Steel				Spiral Steel						Shear Capacity (kips)	Max Pitch A5.7.4.6	Min Pitch A5.10.6.2	Min. Clear Space A5.10.6.2
			f'_c (ksi)	D_{ag} (in)	Cover (in)	f_y (ksi)	Size	Dia (in)	No. of Bars	f_{yt} (ksi)	size	Dia (in)	Pitch (in)	Clear Space (in)	Vol. (in3/ft)				
Out-Dated Design Practice	Case 1 (Accident #10)	24	4	2	2.25	60	#9	1.128	8	40	#2	0.25	6.00	5.75	5.94	**61**	0.43	2.91	2.66
	Case 2a - (Accident #1 - #7, #19)	30	4	2	2.25	60	#9	1.128	8	40	#2	0.25	6.00	5.75	7.79	**88**	0.44	2.91	2.66
	Case 2b (Accident #8, #18)	30	4	2	2.25	60	#9	1.128	8	60	#3	0.375	6.00	5.63	17.44	**146**	1.48	3.04	2.66
	Case 3 (Accident #17)	32	4	2	2.25	60	#9	1.128	9	60	#4	0.5	6.00	5.50	33.31	**231**	2.64	3.16	2.66
Current Design Practice	Case 1 (Min LRFD)	24	4	1	1.5	60	#9	1.128	8	60	#3	0.375	2.25	1.87	38.21	**216**	2.25	1.71	1.33
	Case 2 (Min LRFD)	30	4	1	1.5	60	#9	1.128	8	60	#3	0.375	2.25	1.88	49.27	**286**	2.29	1.71	1.33
	Case3 (Min LRFD)	32	4	1	1.5	60	#9	1.128	8	60	#3	0.375	2.25	1.88	52.97	**310**	2.30	1.71	1.33

Table 2. Minimum Shear Strength vs. Column Diameter Comparing Results Using AASHTO LRFD Bridge Design Specifications for the Simplified and General Procedures.

Procedure	Column Dia. (in)	Concrete			Longitudinal Steel						Spiral Steel							Shear Capacity (kips)	Checks		
		f'_c (ksi)	D_{ag} (in)	Cover (in)	f_y (ksi)	Size	Dia (in)	No.	Steel Ratio	Min Check	f_{yt} (ksi	size	Dia (in)	Pitch (in)	Suggested pitch	Clear Space	Vol. (in3/ft		Max Pitch A5.7.4.6	Min Pitch A5.10.6.2	Min. Clear Space A5.10.6.2
General Procedure LRFD 5.8.3.4.2 with $\varepsilon_s = 0.006$	24	4	1	1.5	60	#9	1.1	5	1.10%	OK	60	#3	0.375	2.25	2.25	1.88	38.2	**216**	2.250	1.705	1.330
	24	4	1	1.5	60	#9	1.1	5	1.10%	OK	60	#3	0.375	4.00	2.25	3.63	21.5	**141**	2.250	1.705	1.330
	30	4	1	1.5	60	#9	1.1	8	1.13%	OK	60	#3	0.375	2.25	2.25	1.88	49.3	**286**	2.293	1.705	1.330
	30	4	1	1.5	60	#9	1.1	8	1.13%	OK	60	#4	0.5	4.00	4.00	3.50	49.0	**289**	4.057	1.830	1.330
	36	4	1	1.5	60	#10	1.3	9	1.12%	OK	60	#4	0.5	6.00	4.00	5.50	40.1	**274**	4.110	1.830	1.330
	36	4	1	1.5	60	#10	1.3	9	1.12%	OK	60	#4	0.5	4.00	4.00	3.50	60.1	**363**	4.110	1.830	1.330
	48	4	1	1.5	60	#10	1.3	16	1.12%	OK	60	#4	0.5	4.00	4.00	3.50	82.3	**528**	4.176	1.830	1.330
	54	4	1	1.5	60	#11	1.4	16	1.09%	OK	60	#5	0.625	6.50	6.50	5.88	89.6	**606**	6.542	1.955	1.330
	60	4	1	1.5	60	#14	1.7	14	1.11%	OK	60	#5	0.625	6.50	6.50	5.88	100.3	**699**	6.570	1.955	1.330
General Procedure LRFD 5.8.3.4.2 with $\varepsilon_s = 0.002$	24	4	1	1.5	60	#9	1.1	5	1.10%	OK	60	#3	0.375	2.25	2.25	1.88	38.2	**266**	2.250	1.705	1.330
	24	4	1	1.5	60	#9	1.1	5	1.10%	OK	60	#3	0.375	4.00	2.25	3.63	21.5	**190**	2.250	1.705	1.330
	30	4	1	1.5	60	#9	1.1	8	1.13%	OK	60	#3	0.375	2.25	2.25	1.88	49.3	**363**	2.293	1.705	1.330
	30	4	1	1.5	60	#9	1.1	8	1.13%	OK	60	#4	0.5	4.00	4.00	3.50	49.0	**368**	4.057	1.830	1.330
	36	4	1	1.5	60	#10	1.3	9	1.12%	OK	60	#4	0.5	6.00	4.00	5.50	40.1	**387**	4.110	1.830	1.330
	36	4	1	1.5	60	#10	1.3	9	1.12%	OK	60	#4	0.5	4.00	4.00	3.50	60.1	**476**	4.110	1.830	1.330
	48	4	1	1.5	60	#10	1.3	16	1.12%	OK	60	#4	0.5	4.00	4.00	3.50	82.3	**727**	4.176	1.830	1.330
	54	4	1	1.5	60	#11	1.4	16	1.09%	OK	60	#5	0.625	6.50	6.50	5.88	89.6	**860**	6.542	1.955	1.330
	60	4	1	1.5	60	#14	1.7	14	1.11%	OK	60	#5	0.625	6.50	6.50	5.88	100.3	**1011**	6.570	1.955	1.330
Simplified Procedure LRFD 5.8.3.4.1	24	4	1	3	60	#9	1.1	5	1.10%	OK	60	#3	0.375	2.25	1.00	1.88	32.6	**254**	1.030	1.705	1.330
	24	4	1	3	60	#9	1.1	5	1.10%	OK	60	#3	0.375	4.00	1.00	3.63	18.3	**182**	1.030	1.705	1.330
	30	4	1	3	60	#9	1.1	8	1.13%	OK	60	#3	0.375	2.25	1.00	1.88	43.7	**352**	1.074	1.705	1.330
	30	4	1	3	60	#9	1.1	8	1.13%	OK	60	#4	0.5	1.75	1.75	1.25	99.4	**625**	1.899	1.830	1.330
	36	4	1	3	60	#10	1.3	9	1.12%	OK	60	#4	0.5	6.00	1.75	5.50	36.4	**379**	1.950	1.830	1.330
	36	4	1	3	60	#10	1.3	9	1.12%	OK	60	#4	0.5	1.75	1.75	1.25	124.8	**794**	1.950	1.830	1.330
	48	4	1	3	60	#10	1.3	16	1.12%	OK	60	#4	0.5	2.00	2.00	1.50	153.6	**1070**	2.012	1.830	1.330
	54	4	1	3	60	#11	1.4	16	1.09%	OK	60	#5	0.625	3.00	3.00	2.38	182.6	**1298**	3.167	1.955	1.330
	60	4	1	3	60	#14	1.7	14	1.11%	OK	60	#5	0.625	3.00	3.00	2.38	205.8	**1504**	3.192	1.955	1.330

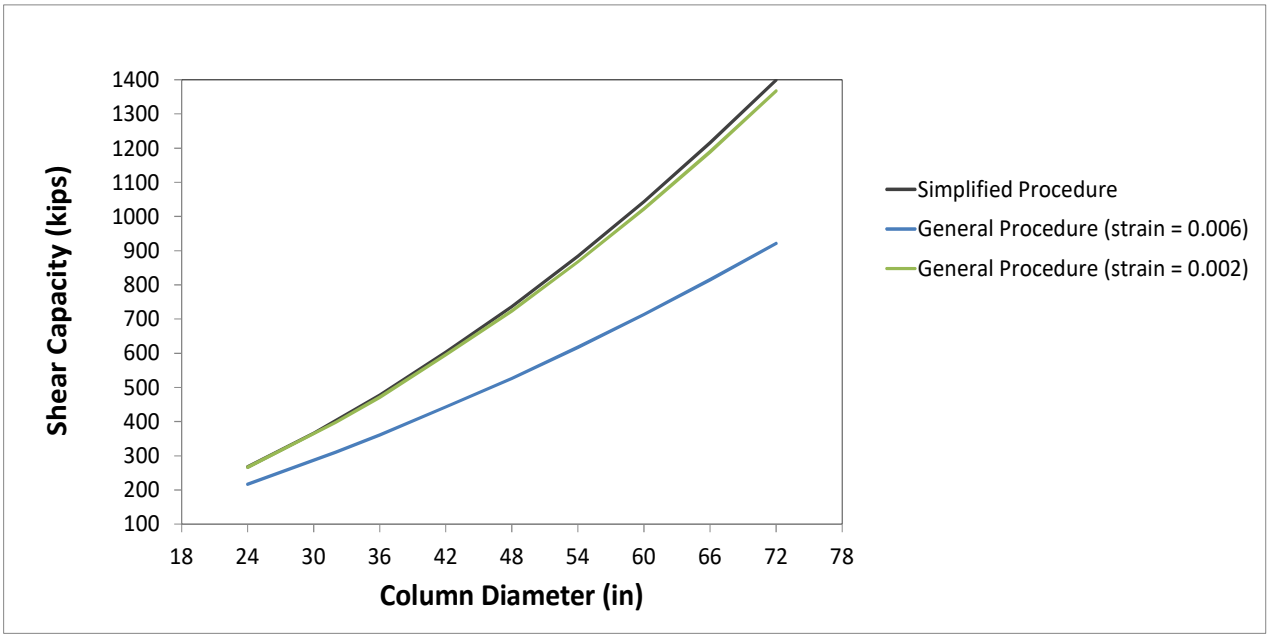

Figure 1. Minimum Shear Capacity vs. Column Diameter Based on AASHTO LRFD Bridge Design Specifications for the Simplified and General Procedures.

Circular Columns

The calculation for minimum reinforcement ratio of the volume of spiral steel to the volume of the concrete core as specified in Article 5.7.4.6, which is also the same calculation used in the ACI code, generally governs the spiral design. [ACI11] Table 3 which was taken from Design of Concrete Structures Appendix A was developed based on this minimum ratio. [Nilson10] For example, entering the table with a 30-inch diameter column, f_y = 60 ksi and f'_c = 4 ksi yields a pitch spacing of 2.25 inches for the spiral ties (note: the values in Table 3 are also based on a concrete cover of 1.5 inches).

Of all the bridge pier crashes investigated by Buth *et al*, none of the piers met the 6th Edition LRFD Bridge Design Specifications in regard to the spiral steel. [Buth10] As a result, the design shear strength of those columns was significantly lower than that of current design practice. In the upper portion of Table 1 a summary of the shear strength calculations for the four bridge pier designs from the accident cases investigated by Buth *et al* is provided. These capacities are based on two failure planes resisting the impact force as illustrated in the accident photo shown in Figure 2. Of these four designs, two involved the use of #2 spiral steel bars, which does not meet current LRFD specifications, and all four designs used a pitch spacing of 6 inches which exceeds the current specifications for pitch spacing. The design parameters from those cases that directly conflict with current practice are identified in a red font in the table.

The lower section of Table 1 shows the design parameters for these same size columns using current design practices in accordance with AASHT0 LRFD Bridge Design Specifications, 6th Edition. [AASHTO12] The values of shear capacity shown here are based on an assumed maximum strain of 0.006 for the reinforcing steel and using the general procedure specified in LRFD Article 5.8.3.4.2 for computing the parameters β and θ. The pitch spacing used in the calculations was based on the maximum pitch (i.e., LRFD Article 5.7.4.6) and rounded down to

the nearest 0.25 inch to be consistent with current practice. All the designs include spiral reinforcement steel with minimum yield strength of 60 ksi, the maximum allowable pitch spacing of the spiral steel according to Article 5.7.4.6 of the LRFD, 1.5 inches clear cover over the spiral steel for the outer concrete shell, and a maximum aggregate size of 1 inch. These designs meet the LRFD requirements for maximum pitch (LRFD Article 5.7.4.6), minimum pitch (LRFD Article 5.10.6.2), and minimum clear space between spirals (LRFD Article 5.10.6.2). Note that the pitch spacing for the spiral steel also meets the ACI design specifications shown in Table 3. These revised designs result in a significant increase in shear strength, particularly for those cases that used #2 size bars for the spiral steel in the Buth *et al* study. [Buth10]

Table 3. Size and Pitch of Spirals According to the ACI Code. [Nilson10, ACI11]

Column Diameter (in)	**Spiral Out to Out (in)**	f'_c			
		2500	**3000**	**4000**	**5000**
Fy = 40,000					
14-15	11-12	#3@2.00”	#3@1.75”	#4@2.50”	#4@1.75”
16	13	#3@2.00”	#3@1.75”	#4@2.50”	#4@2.00”
17-19	14-16	#3@2.25”	#3@1.75”	#4@2.50”	#4@2.00”
20-23	17-20	#3@2.25”	#3@1.75”	#4@2.50”	#4@2.00”
24-30	21-27	#3@2.25”	#3@2.00”	#4@2.50”	#4@2.00”
Fy = 60,000					
14-15	11-12	#2@1.75”	#3@2.75”	#3@2.00”	#4@2.75”
16-23	13-20	#2@1.75”	#3@2.75”	#3@2.00”	#4@3.00”
24-29	21-26	#2@1.75”	#3@3.00”	#3@2.25”	#4@3.00”
30	27	#2@1.75”	#3@3.00”	#3@2.25”	#4@3.25”

As previously mentioned, the shear capacities shown in Table 1 were determined using the procedure specified in LRFD Article 5.8.3.4.2 for calculating the parameters β and θ using an assumed maximum strain of 0.006 for the reinforcing steel. This maximum strain value was adopted from Buth *et al* and corresponds to “the maximum strain from severe impact conditions.” [Buth10] Since the revised designs all meet the minimum amount of shear reinforcement specified in LRFD Article 5.8.2.5, the simplified procedure of LRFD Article 5.8.3.4.1 may be used for determining β and θ (i.e., β=2 and θ=45°). The resulting shear capacity values computed using the simplified procedure are significantly higher than those computed using the general procedure. The primary difference seems to be related to the value of maximum strain, ε_s, for the reinforcing steel. Setting $\varepsilon_s = 0.002$ results in shear capacity values computed from the general procedure that are similar to those computed using the simplified procedure.

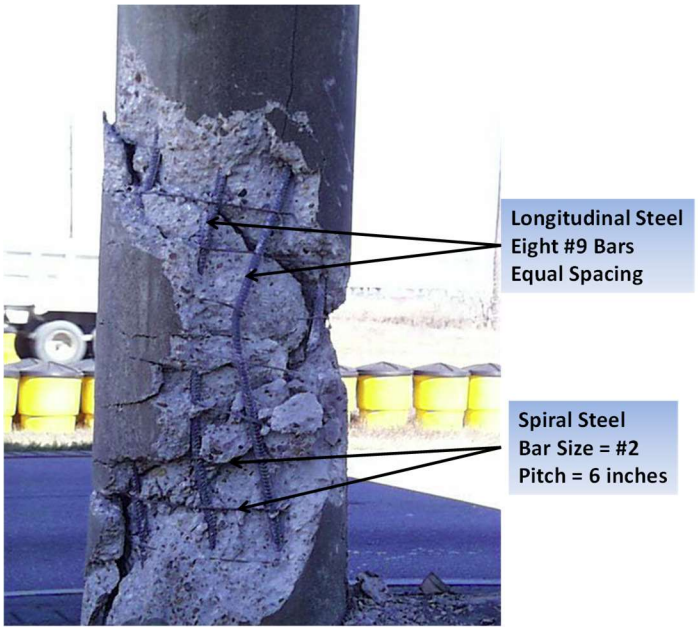

Figure 2. Accident Case #1 Illustrating Typical Two-Plane Shear Failure Mode and Typical Design of Steel Reinforcement in the Column.[Buth10]

FLEXURE CAPACITY OF CIRCULAR COLUMNS

Appendix D (Lateral Impact Loads on Pier Columns) showed that the LRFD calculated shear capacity generally can be overly conservative since columns tend to have additional bending capacity in lateral impacts beyond the point where the shear capacity is exceeded. A review of the literature was unable to find a design method for circular columns in flexure so this section describes an approach for estimating the moment capacity of a circular reinforced concrete pier column based on the balanced moment in the column at the impact point.

Typical design parameters like the nominal shear capacity do not appear to correlate very well with the lateral loads at which bridge columns fail as shown in Appendix D (Lateral Impact Loads on Pier Columns). Failure, in this context, is reaching some maximum lateral load where if the column is deflected further, the column may collapse. The reason typical design shear calculations do not predict the failure capacity is partly due the following factors that are substantially different than the usual quasi-static analysis used to design for service loads:

- Heavy vehicle impacts are dynamic events rather than static events,
- Impact causing failure of the column are large displacement events,
- The steel reinforcing in particular has substantial additional capacity past the yield point of the material and
- Typical nominal shear capacity calculation procedures are based on the shear resulting from axial loading of the column due to gravity loads rather than from lateral impact loads.

For these reasons, a different methodology was developed to more accurately estimate the lateral shear capacity of typical reinforced concrete bridge pier columns in an impact event.

Bridge pier columns are generally intermediate slenderness (i.e., $L/r < 30$) with heights of 15-ft or more and thickness of more than two feet. Early in the impact event, the column responds as a beam and a crack forms on the non-impact face in line with the impact and starts to

propagate through the section. Similar cracks may form at the connection to the bent and foundation creating a hinge mechanism. These cracks quickly propagate to a location where the compression forces in the concrete will be balanced by the tensile forces in the steel. This point is analogous to the balance point in typical beam bending analysis although since columns are reinforced at about the 1 percent level, the location of the neutral axis tends to be very close to the impact face. It is assumed in this analysis that a hinge forms at the location of the neutral axis such that the concrete on the impact side is crushing and the steel on the non-impact side is in tension. The following nomenclature will be used below:

a	=	Distance from the impact face to the neutral axis.
A	=	Distance from the impact plane to the top of the column (e.g., pier cap).
A_b	=	Area of one longitudinal steel bar.
A'_c	=	Area of concrete in the compression zone
b	=	Diameter of a circular column or the width and height of a square column.
B	=	Distance from the impact plane to the bottom of the column (e.g., foundation)
d_c	=	Distance from the neutral axis to the centroid of the compressive concrete.
d_i	=	Distance from the impact face to bar level i such that d_1 is the distance from impact face to the longitudinal bars farthest from the impact face.
f'_c	=	Compressive strength of concrete.
f_p	=	Fully plastic stress of reinforcing steel
f_y	=	Yield strength of reinforcing steel
M_b	=	Balanced moment.
M_{H1}	=	First plastic hinge moment.
M_{H2}	=	Second plastic hinge moment.
n_i	=	Number of bars in a level
P_{H1}	=	Lateral impact load at the first plastic hinge moment.
P_{H2}	=	Lateral impact load at the second plastic hinge moment.
x	=	Displacement in the direction of the impact load.
x_b	=	Displacement associated with the balanced moment.
x_{H1}	=	Displacement associated with the first plastic hinge moment.
x_{H2}	=	Displacement associated with the second plastic hinge moment.
y_{cr}	=	The pseudo crack width on the non-impact face of the column.
y_{crit}	=	The crack width at a particular bar layer associated with yielding the steel.

The resisting moment at the balance point can be estimated as follows. The concrete is cracked through to the neutral axis so a compressive force is generated on the compression (i.e., impact) side of the column only. The tensile forces from the longitudinal steel act on the non-impact side of the neutral axis. The first displacement of interest is the moment at which the concrete reaches its full compression strain (i.e., 0.003) and the steel farthest from the impact reaches its yield stress (e.g., typically 0.00207 for 60 grade reinforcing steel). The other longitudinal bars will also develop tension in proportion to their distances from the impact face. In order to find the moment at the balanced strain condition, the location of the neutral axis (i.e., "a") must be determined based on the vertical equilibrium and the assumption that the crushing strain of the concrete is achieved at the same time as the yield strain in the outer most layer of longitudinal reinforcement. This results in the following expression:

$$\sum F_y = 0 = -0.85 f_c' A_c' + \sum_{i=1}^{N} n_i A_b f_y \left[\frac{d_i - a}{d_1}\right]$$

In the above expression, the summation involves the characteristics of the longitudinal steel at each layer of bars. The above expression is used to solve for the location of the neutral axis, a, and then used in the following equation to calculate the balanced moment:

$$M_b = -0.85 f_c' A_c' d_c + \sum_{i=1}^{N} n_i A_b f_y \left[\frac{d_i - a}{d_1}\right](d_i - a)$$

For circular columns, the area of concrete in compression and the moment arm of the compression concrete are:

$$A_c = \left[\frac{b}{2}\right]\cos^{-1}\left(\frac{b-2a}{b}\right) - \left[\frac{b-2a}{2b}\right]\sqrt{ba - a^2}$$

$$d_c = \frac{\left[\frac{4b}{6}\right]\sin\left[\cos^{-1}\left(\frac{b-a}{b}\right)\right]}{3\left[\cos^{-1}\left(\frac{b-a}{b}\right) - \sin\left[\cos^{-1}\left(\frac{b-a}{b}\right)\right]\right]}$$

For square columns, the area of concrete in compression and the moment arm are:

$$A_c = ba$$
$$d_c = \mathrm{ba}/2$$

Unfortunately for circular columns, the vertical equilibrium equation must be solved iteratively since the concrete area is dependent on the location of the neutral axis but this is relatively easily accomplished. The balanced moment provides the first key point on the force-displacement curve in assessing the capacity of the column.

Unlike designing for service loads, designing for the failure of the column involves allowing the column to undergo large plastic strains. The column has considerable energy capacity beyond the balance point that should be considered. For example, while the yield stress of grade 60 reinforcing steel is 60 ksi, the maximum plastic stress is 100 ksi, so there is a considerable amount of strain energy in the material after the yield point has been. The 6th Edition of the LRFD Bridge Design Specifications allow a maximum strain in the steel of 0.006 to be used and this corresponds to a plastic stress of 100 ksi for grade 60 reinforcement. Analogous to the balance point, the point when the first longitudinal bars reach the fully plastic stress is given by:

$$M_{H1} = -0.85 f_c' A_c' d_c + \sum_{i=1}^{N} n_i A_b f_p \left[\frac{d_i - a}{d_1}\right](d_i - a)$$

where the only difference between this expression and the one above for the balanced moment is the replacement of the plastic stress f_p for the yield stress f_y. This value is referred to as the first plastic hinge moment since a plastic hinge will form at the neutral axis. Likewise, the moment when the second layer of bars from the non-impact side reach the plastic stress defines the second plastic hinge moment and can be written as:

$$M_{H2} = -0.85 f_c' A_c' d_c + f_p A_b \left[n_1(d_1 - a) \sum_{i=2}^{N} n_i A_b n_i \left[\frac{d_i - a}{d_2}\right](d_i - a)\right]$$

As will be shown in later sections, the second plastic hinge moment appears to be associated with the ultimate bending capacity of the column. The lateral load associated with the second plastic hinge moment is:

$$P_{H2} = \left[-0.85 f_c' A_c' d_c + f_p A_b \left(n_1 (d_1 - a) \sum_{i=2}^{N} n_i A_b n_i \left[\frac{d_i - a}{d_2}\right] (d_i - a) \right)\right] \left[\frac{1}{(A+B)\beta}\right]$$

where β represents the end conditions of the column.

While columns are generally joined to the caps and footings using cold-formed joints, the end conditions are actually better represented as pinned-pinned connections. This is because only a small amount of rotation is required to reach a pinned end condition and the cracking in the column in an impact will allow such small rotations. The load-moment relationship for a pinned-pinned beam with unequal distances between the ends and the load is given by:

$$M = \frac{PAB}{L} = PL\left[\frac{AB}{(A+B)^2}\right]$$

where the bracketed term corresponds to β for a pinned-pinned beam with unequal distances to the load (i.e., A is the distance from the load to the foundation and B is the distance from the load to the pier cap). The second hinge load based on the pinned-pinned end condition assumption is therefore:

$$P_{H2} = \left[-0.85 f_c' A_c' d_c + f_p A_b \left(n_1 (d_1 - a) \sum_{i=2}^{N} n_i A_b n_i \left[\frac{d_i - a}{d_2}\right] (d_i - a) \right)\right] \left[\frac{(A+B)^2}{AB}\right]$$

In addition to the load and moment caused by the lateral impact force, it is also useful to know the deflection when these particular lateral loads occur so that the strain energy absorbed by the deforming column can be calculated. Since the column is relatively long with respect to its width the geometry of a pseudo crack at the impact level can be approximated by straight lines even though in actuality the column would be curved at the ends and at the impact point. The basic geometry of the column is shown in Figure 3.

The following relationships can be derived based on similar triangles:

$$\frac{y_t}{b-a} = \frac{x}{A} \qquad \frac{y_b}{b-a} = \frac{x}{B}$$

$$y_{cr} = y_t + y_b = \left[\frac{A+B}{AB}\right] (b-a)x$$

The pseudo crack opening at each bar level is simply proportional to the ratio of the distance from the neutral axis to the bars divided by the section width minus the neutral axis.

$$y_i = \left[\frac{(d_i - a)}{(b-a)}\right] y_{cr} = \left[\frac{A+B}{AB}\right] (d_i - a)x$$

The pseudo crack width at any deflection x and any bar level can be found from the geometry of the cracking column as follows:

$$y_i = \left[\frac{A+B}{AB}\right] (d_i - a)x \;\rightarrow\; x = \left[\frac{AB}{A+B}\right] \frac{y_i}{(d_i - a)}$$

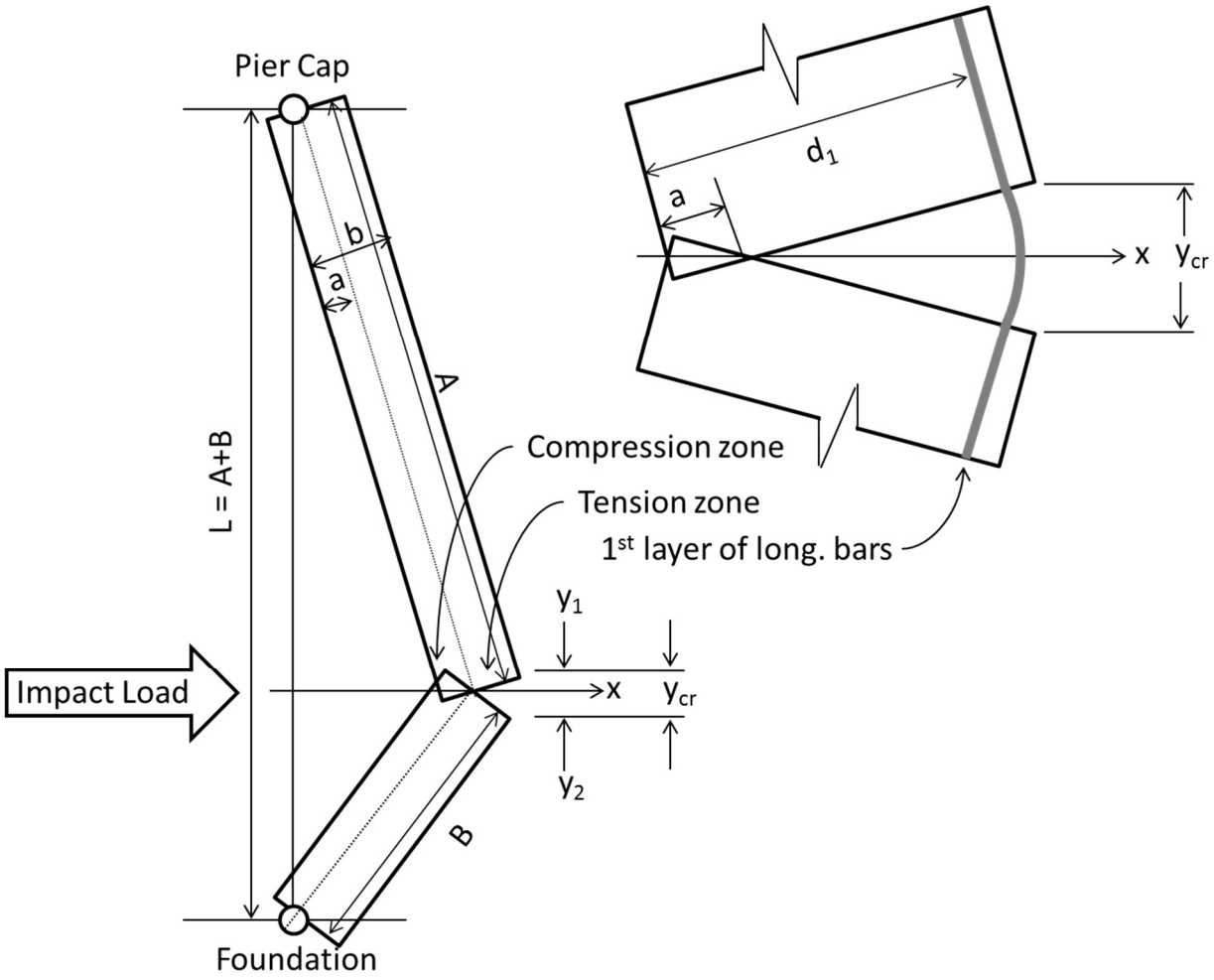

Figure 3. Assumed Column Geometry.

The x displacement of the pseudo crack associated with yielding the first layer of tension bars when the balanced condition occurs is found as follows based on the crack geometry:

$$x_b = \left[\frac{AB}{A+B}\right] \frac{y_{crit}}{(d_{max} - a)}$$

Where y_{crit} is the critical crack width that is associated with yielding in the steel. For example, when the crack width at the outer most bar layer reaches y_{crit}, it is assumed that the strain in the steel has reached 0.00207, the strain corresponding to the yield point. The column will continue to rotate when a hinge will start to form when the outer longitudinal bars reach the plastic strain of 0.006. The x displacement of the column at the level of the impact load using the expressions above can be written as:

$$x_b = \left[\frac{AB}{A+B}\right] \frac{y_{crit}}{(d_1 - a)}$$

The first plastic hinge moment occurs when the first layer of longitudinal steel farthest from the impact point reaches the plastic strain, therefore:

$$x_{H1} = \left[\frac{AB}{A+B}\right] \left[\frac{\varepsilon_p}{\varepsilon_s}\right] \frac{y_{crit}}{(d_1 - a)}$$

And the second plastic hinge moment occurs when the second layer of longitudinal steel farthest from the impact point reaches the plastic strain:

$$x_{H2} = \left[\frac{AB}{A+B}\right]\left[\frac{\varepsilon_p}{\varepsilon_s}\right]\frac{y_{crit}}{(d_2-a)}$$

The above equations can be used to develop an incremental model where equilibrium is enforced for each increment of the displacement subject to the conditions for yielding the tensile enforcing steel and the formation of the plastic moments in each longitudinal bar layer. This method would be too laborious to use in design but it does illustrate that the basic method reasonably predicts the lateral load capacity of the impacted column and the displacements when these loads occur.

A simpler version of the incremental hinge model was also developed which simply uses the lateral force when the balanced moment occurs (i.e., P_b), the lateral force when the second layer of bars reach the plastic strain (i.e., P_{H2}) and the displacements when these forces are achieved. If it is assumed that the distance to the neutral axis is very small (i.e., the neutral axis is very near the impact point) then the neutral axis can be assumed to be zero. Likewise, the area of concrete in compression is very small and can likewise be ignored. With these assumptions, the equations above reduce to:

$$x_b = \left[\frac{AB}{A+B}\right]\frac{y_{crit}}{(d_1-a)} \qquad P_b = \left[\sum_{i=1}^{N} n_i A_b f_y \left[\frac{d_i^2}{d_1}\right]\right]\left[\frac{(A+B)^2}{AB}\right]$$

$$x_{H2} = \left[\frac{AB}{A+B}\right]\left[\frac{\varepsilon_p}{\varepsilon_s}\right]\frac{y_{crit}}{(d_2-a)} \qquad P_{H2} = \left[f_p A_b \left(n_1(d_1-a)\sum_{i=2}^{N} n_i A_b n_i \left[\frac{d_i^2}{d_1}\right]\right)\right]\left[\frac{(A+B)^2}{AB}\right]$$

It will be shown later that these assumptions result in a slightly conservative estimation which is thought to be beneficial. The strain energy using these two points on the force-displacement curve estimate the strain energy absorbed as follows:

$$E_{HINGE} = \left[\frac{P_b x_b}{2}\right] + \left[\frac{(P_b + P_{H2})}{2}(x_H - x_b)\right]$$

An even simpler method is to simply calculate only one point, the load and displacement for the second plastic hinge as follows:

$$x_{H2} = \left[\frac{AB}{A+B}\right]\left[\frac{\varepsilon_p}{\varepsilon_s}\right]\frac{y_{crit}}{(d_2-a)}$$

$$P_{H2} = \left[f_p A_b \left(n_1(d_1-a)\sum_{i=2}^{N} n_i A_b n_i \left[\frac{d_i^2}{d_1}\right]\right)\right]\left[\frac{(A+B)^2}{AB}\right]$$

$$E_{HINGE} = \left[\frac{P_{H2} x_{H2}}{2}\right]$$

Predictions using the above outlined method are compared to experimental results in Appendix D (Lateral Impact Loads on Pier Columns).

APPENDIX F. HEAVY VEHICLE TRAFFIC MIX AND PROPERTIES

1.1 HEAVY VEHICLE MIX

1.1.1 Background

Developing the appropriate vehicle mix for analysis is a critical first step in assessing the risk to bridge piers posed by errant vehicles. Piers are massive structural elements of a bridge system so they are most in danger of being subjected to failure inducing impacts from the heaviest vehicles. Passenger vehicles, for example, would rarely have the combination of mass and speed necessary to represent enough kinetic energy to cause the failure of a bridge pier component. On the other hand, tractor-trailer trucks can sometimes weigh over 100,000 lbs so when travelling at interstate highway speeds they generally have a large amount of kinetic energy. This was borne out anecdotally by Buth where of the 23 bridge pier crash investigated, none of the cases involved passenger vehicles, two involved intercity buses, one involved a single-unit truck and the remaining 19 all involved tractor-trailer trucks. [Buth10] At least one column was severely damaged or completely failed in 18 of the 23 crashes and all but one of these failures were caused by impacts with tractor trailer trucks and the other was a single-unit truck. Determining the mix and characteristics of heavy vehicles in the traffic stream is, therefore, an important first step in the analysis of the risk of failure in bridge pier crashes.

Traffic engineers often characterize the traffic stream in terms of the percentage of each vehicle type in the traffic flow. The percentage of each type of vehicle in the traffic flow is called the traffic mix. The sum of the percentages of all the heavy vehicles in the mix is called the percent trucks (PT). While detailed traffic mix data can be found for some locations, the designer in most typical design situations may only know the AADT and the percent trucks based on typical traffic engineering data. The objective of this section is to select traffic mixes that can be used in developing guidelines for the design and shielding of bridge piers.

1.1.2 FHWA Vehicle Classification System

In the 1980's FHWA developed a 13-vehicle classification system and asked the states to report data using these classifications when possible in the future. [FHWA01] The FHWA vehicle classification with definitions is shown below in Figure 1 from the FHWA Traffic Monitoring Guide. [FHWA01] The classifications are based on configuration (i.e., single body, articulated tractor and trailer, etc.) and the number of axles. The FHWA requires each State Highway agency to conduct "continuous classification counters to measure truck travel patterns and provide the factors to convert short classification counts to annual averages." [FHWA01] Figure 1 is a pictographic representation of each vehicle classification.[TXDOT12]

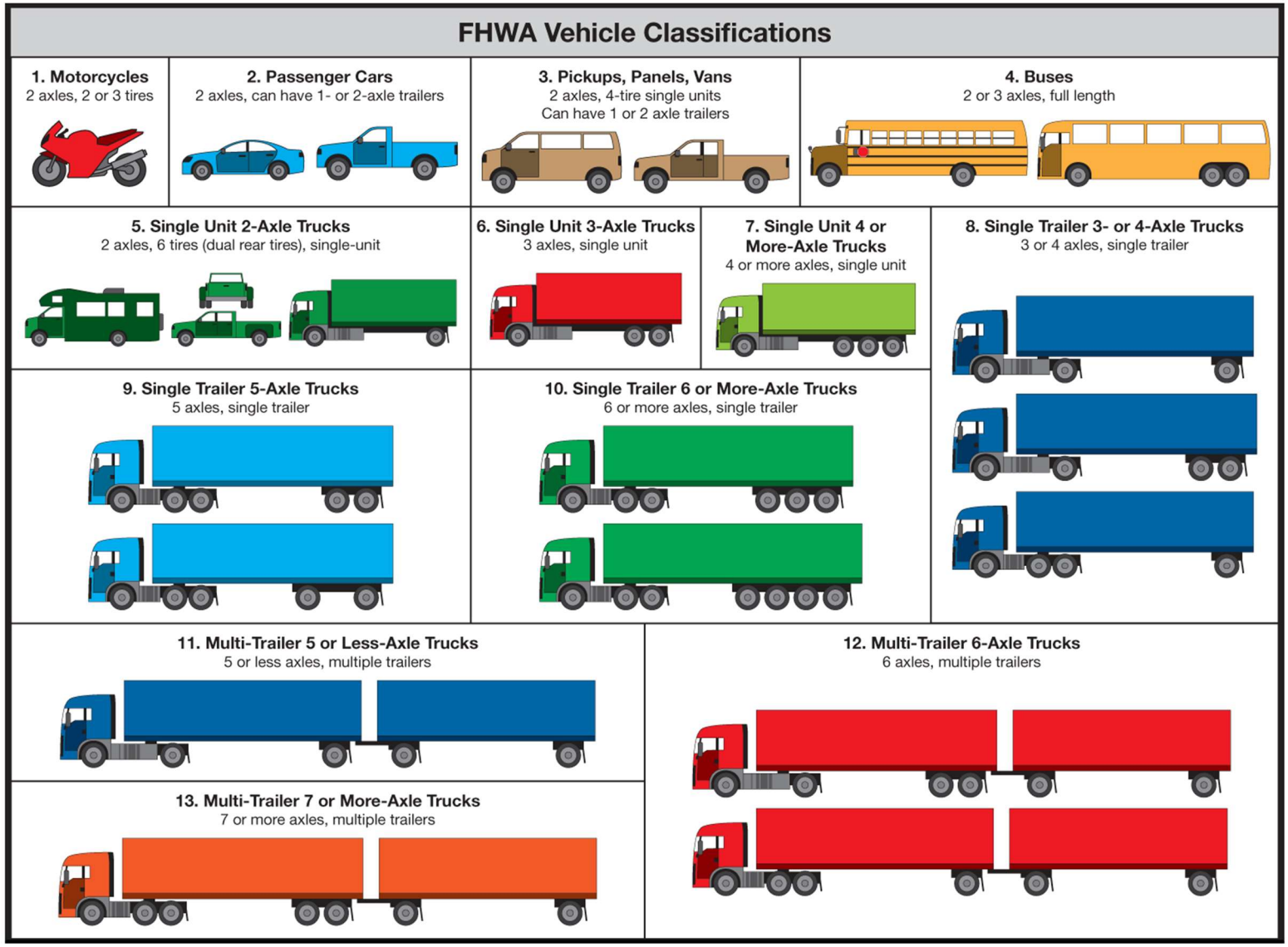

Figure 1. FHWA Vehicle Classifications.[FHWA01]

1.1.3 Data Sources

There are two types of data that can be used to determine traffic mix characteristics: (1) summary data from the FHWA and States and (2) specific vehicle counts at particular locations. The first has the advantage that it represents broad average conditions over a large geographical area and the second has the advantage that particular sites can be subject to conditions well above or below the mean conditions. Both types of data were examined herein.

1.1.3.1 FHWA Data

The FHWA annually publishes the "Highway Statistics Series" which includes reports of motor vehicle miles traveled by vehicle type and highway type. [FHWA14a] The 2012 statistics have been compiled for both rural and urban areas. A distribution of this data has been calculated and the results presented in Table 1. Unfortunately, FHWA does not use its own vehicle classification system in this report but the data were reformulated in Table 1 to list the vehicles by the presumed FHWA vehicle classification.

As expected, the percent of trucks is highest (i.e., 24.25 percent) on the rural interstate system and lowest (i.e., 5.82 percent) on the off-interstate urban system. The percentage of tractor-trailer trucks likewise is highest (i.e., 19.80 percent) on the rural interstate system and lowest (i.e., 2.32 percent) on the urban off-interstate system.

The lower part of Table 1 shows the traffic mix within the passenger vehicle and truck categories. For all highway types, the percentage of passenger cars of the passenger vehicle mix is between 69 and 79 percent with somewhat higher percentages on the more urban roadways. Motorcycles are seldom above one percent of the passenger vehicle mix. In general, passenger cars represent about 75 percent of the passenger vehicle mix and pickup trucks, SUVs and vans represent approximately 25 percent. This ratio, while increasing somewhat in urban areas, remains more or less constant because passenger cars, pickup trucks, vans, and SUVs are all used in much the same way on most types of roadways.

There is much more variation in the heavy truck fleet mix shown in the lowest portion of Table 1. There are generally five times more tractor trailer trucks on rural interstates than single unit trucks (i.e., 81.68/15.51=5.26) whereas there are about 30 percent more (i.e., 52.46/39.95=1.31) single-unit trucks on urban off-interstate roadways than tractor trailer trucks. The type of roadway and land use, therefore, can have an effect on the traffic mix. The reason for this variation in mix is that different types of trucks use different types of roads for different purposes. Tractor-trailer trucks hauling goods over large distances will prefer Interstate and other principal arterials. In urban areas, the mix is dominated more by local delivery vehicles and regional movement of goods typical of single-unit delivery trucks. Similarly, buses are twice as common in the heavy vehicle mix on local urban routes as on rural interstates due to the nature of the trips being generated.

Table 1. FHWA 2012 Percentage of Vehicle-miles Traveled by Vehicle and Highway Type.

Vehicle Type	Presumed FHWA Vehicle Class	RURAL			URBAN			Total Rural and Urban (%)
		Interstate (%)	Other (%)	All (%)	Interstate (%)	Other (%)	All (%)	
Motorcycles	1	0.53	0.93	0.77	0.58	0.73	0.69	0.72
Passenger Cars	2	57.38	63.20	61.35	71.22	74.23	73.50	69.50
Pickups, Vans, SUVs	3	17.85	26.30	23.25	17.36	19.23	18.77	20.25
Buses	4	0.68	0.57	0.59	0.49	0.44	0.45	0.50
Single-Unit Trucks	5-7	3.76	5.01	4.55	3.00	3.05	3.04	3.54
Tractor-Trailer Trucks	8-13	19.80	3.99	9.49	7.35	2.32	3.55	5.50
	Total	100.00	100.00	100.00	100.00	100.00	100.00	100.00
	Percent Trucks	24.24	9.57	14.63	10.84	5.81	7.04	9.54
Traffic Mix within Passenger Vehicle Classes								
Motorcycles	1	0.69	1.03	0.90	0.65	0.77	0.74	0.79
Passenger Cars	2	75.75	69.89	71.86	79.88	78.82	79.07	76.83
Pickups, Vans, SUVs	3	23.56	29.08	27.24	19.47	20.41	20.19	22.38
Traffic Mix within Truck Classes								
Buses	4	2.81	5.92	4.02	4.49	7.59	6.43	5.21
Single-Unit Trucks	5-7	15.51	52.35	31.09	27.69	52.46	43.18	37.08
Tractor-Trailer Trucks	8-13	81.68	41.73	64.89	67.82	39.95	50.39	57.71

1.1.3.2 State Data

Summary mix data can be obtained from most States to examine the types of vehicles common on their road systems. Data from New Jersey, Maryland, Kansas and Washington State are presented below as examples of the types of mix data commonly available in the States.

For example, the state of New Jersey publishes an annual traffic report where State-wide traffic volumes are summarized by the FHWA vehicle classification system. These data are broken into the complete 13-class FHWA system and typical Green Book roadway functional classifications. Recall the FHWA values are a distribution of vehicle miles traveled while these state data are distributions of traffic volumes (i.e., point-in-time counts) which may vary by direction and are not normalized by the mileage of urban or rural roads in these states. In New Jersey, the highest percent of trucks occurs on the rural interstates (i.e., 13.73 percent) and the lowest on the urban minor arterials (i.e., 3.07 percent). Similar to the national data summarized in Table 1, the middle portion of Table 2 shows that within the passenger vehicle fleet, motorcycles are less than one percent for all highway types and overall the passenger cars represent about 80 percent and the pickup trucks, SUV and vans represent about 20 percent of passenger vehicle fleet. The mix within the heavy vehicle fleet is also similar to the national data. Buses account for between about 1 and 5 percent of the heavy vehicles with somewhat higher percentages on the urban roads. Single and multi-trailer trucks account for almost 80 percent of the rural interstate heavy vehicle traffic in New Jersey whereas single-unit trucks dominate the urban principal arterials.

The 2012 traffic mix distributions by highway functional classification for the States of New Jersey, Maryland, Washington and Kansas are shown in Table 2 through Table 5. [MDDOT14] [WSDOT14] [KSDOT12] The New Jersey, Kansas and Maryland distributions are based on traffic volumes whereas the Washington distribution is based on vehicle miles traveled as is the FHWA data shown earlier. The highest percent of trucks in these four States occurs on the rural interstates and varies between a high of 26 percent in Kansas and a low of just over 13 percent in New Jersey and Maryland. The lowest percent trucks in all four States occur on the urban arterials varying between three and six percent.

The passenger vehicle fleet distribution in these States is similar with the ratio between passenger cars and pickup, vans and SUVs varying between 3:1 and 5:1 on rural and 3:1 to 7:1 on urban principal arterials. The higher ratio of passenger cars is more common both in urban areas and more eastern States. As shown in Figure 2, passenger cars (i.e., Class 2) account for between 68 and almost 90 percent of the passenger vehicle traffic volume across highway types and pickup trucks, vans and SUVs (i.e., Class 3) account for between 12 and 23 percent. The proportion of passenger cars to passenger vehicles on the urban interstate system approaches almost 90 percent in Maryland and is somewhat lower on the rural interstate system. Motorcycles (Class 1) represent a negligible percentage of the passenger vehicle volume in all four States for all highway functional classifications.

The truck mix distributions in these States are consistent with the national findings discussed earlier. Tractor trailers account for between 70 and 80 percent of the truck volume on rural principal arterials whereas single-unit trucks are more prevalent on more local roads. Multi-trailer trucks accounted for about 10 percent of the truck volume in the two western States whereas the multi-trailer truck volume in the two eastern States was around five percent on the principal arterials. Aside from the principal arterials, there are relatively few multi-trailer trucks travelling on other functional classification roadways. The same pattern of larger tractor trailer proportions of the truck mix on the rural interstate system to the urban system holds in each State

shown. Similarly, the mix of tractor trailer and single-unit trucks reverses on more locally oriented functional classification roadways.

As shown in Figure 2b, there is much more variation in the heavy vehicle classes by highway functional class. Single- and multi-trailer trucks (i.e.., Classes 8 through 13) average just under10 percent on rural interstates according to the FHWA but less than 4 percent on urban roadways. None of the data sources summarized in Figure 2b have buses (i.e., Class 4) accounting for more than 1 percent of the total traffic mix. The ratio between tractor trailers and SUTs is generally about 65 percent on rural roads and about 50 percent on more urban roadways. Of course, these mix values represent broad average conditions across an entire State and particular routes can have a mix and percent trucks much higher or lower. Unfortunately, the Washington data could not be included in this figure because the data is not summarized by individual vehicle class.

NCHRP Report 505, "Review of Truck Characteristics as Factors in Roadway Design," provides a review of truck characteristics of the US truck fleet and also summarizes the general vehicle fleet characteristics. Recommendations for changes to highway geometric design policy to ensure that highway designs reasonably accommodate trucks were the ultimate objective of this study. [Harwood03] Harwood *et al.* found that five-axle tractor-trailer trucks (i.e., Class 9) alone account for 46.1 percent of the trucks by the vehicle miles traveled and two-axle single-unit trucks (i.e., Class 5) account for 29.5 percent. [Harwood03] After Class 5 and 9, the next highest class is three-axle single-unit trucks (i.e., Class 6) at 5.3 percent. Class 5 (i.e., two-axle single-unit trucks) and Class 9 (i.e., five-axle tractor trailer trucks) together account for more than 75 percent of the truck vehicle-miles travelled.

Table 2. 2012 Average New Jersey Traffic Mix by Highway Type. [NJDOT12]

FHWA Vehicle Class	Vehicle Category		RURAL				URBAN			
			Principal arterial Interstate (%)	Principal arterial Other (%)	Minor Arterial (%)	Major Collector (%)	Principal arterial Interstate (%)	Principal arterial Other (%)	Principal arterial Other (%)	Minor Arterial (%)
1	Passenger Vehicles		0.05	0.23	0.34	0.16	0.04	0.15	0.11	0.12
2			71.17	74.19	73.42	65.85	75.81	74.90	76.31	77.23
3			15.05	19.27	22.48	29.01	16.12	19.20	19.58	19.57
4	Buses	Trucks	0.43	0.12	0.17	0.04	0.28	0.28	0.16	0.07
5	Single-Unit Trucks		1.60	1.94	1.74	1.96	1.68	2.08	1.85	1.70
6			0.57	0.73	0.63	0.57	0.64	0.72	0.57	0.38
7			0.18	0.32	0.22	0.16	0.19	0.23	0.10	0.07
8	Single-Trailer Trucks		0.58	0.25	0.14	0.12	0.42	0.27	0.16	0.15
9			9.68	2.90	0.83	2.12	4.61	2.12	1.12	0.69
10			0.09	0.05	0.03	0.00	0.06	0.03	0.02	0.01
11	Multi-Trailer Trucks		0.42	0.01	0.00	0.00	0.11	0.02	0.01	0.00
12			0.17	0.00	0.00	0.00	0.04	0.00	0.00	0.00
13			0.01	0.00	0.00	0.00	0.00	0.00	0.00	0.00
Total			100.00	100.00	100.00	100.00	100.00	100.00	100.00	100.00
Percent Trucks			13.73	6.32	3.76	4.97	8.03	5.75	3.99	3.07
Vehicle Mix within Passenger Vehicle Category										
1	Motorcycles		0.06	0.25	0.35	0.17	0.04	0.16	0.11	0.12
2	Pass. Cars		82.50	79.20	76.29	69.29	82.43	79.47	79.48	79.68
3	PU, Vans,		17.45	20.57	23.36	30.53	17.53	20.37	20.39	20.19
Vehicle Mix within Truck Category										
4	Buses		3.13	1.90	4.52	0.80	3.49	4.87	4.01	2.28
5-7	Single-Unit		17.12	47.31	68.88	54.12	31.26	52.70	63.16	70.03
8-10	Single-		75.38	50.63	26.60	45.07	63.39	42.09	32.58	27.69
11-13	Multi-Trailer		4.37	0.16	0.00	0.00	1.87	0.35	0.25	0.00

Table 3. 2012 Average Maryland Traffic Mix by Highway Functional Class. [MDDOT14]

FHWA Vehicle Class	Vehicle Category		RURAL						URBAN					
			Interstate	Other Principal arterial	Minor Arterial	Major Collector	Minor Collector	Local	Interstate	Other Principal arterial	Minor Arterial	Major Collector	Minor Collector	Local
1	Passenger Vehicles		0.4	0.37	0.45	0.65	0.72	1.33	0.19	0.18	0.34	0.29	0.52	0.48
2			72.35	73.53	69.17	69.93	68.07	60.13	81.28	80.81	78.84	80.34	77.64	73.08
3			13.68	18.57	21.76	21.4	22.69	26.94	11.23	13.73	15.53	14.31	16.29	18.03
4	Buses	Trucks	0.73	0.62	0.68	0.79	0.79	1.05	0.77	0.61	0.61	0.79	0.62	0.89
5	Single-Unit Trucks		2.72	3.16	3.76	4.61	5.82	8.53	2.11	2.47	3.03	2.76	3.16	4.34
6			0.65	0.75	0.88	0.8	0.57	0.65	0.57	0.44	0.51	0.45	0.47	0.73
7			0.18	0.09	0.61	0.32	0.12	0.02	0.12	0.15	0.13	0.08	0.06	0.03
8	Single-Trailer Trucks		1.02	0.51	0.41	0.69	0.73	0.93	0.51	0.42	0.4	0.47	0.46	0.81
9			7.56	2.19	2.19	0.79	0.47	0.38	3.04	1.1	0.54	0.45	0.72	1.37
10			0.23	0.11	0.06	0.03	0.03	0.03	0.06	0.03	0.03	0.05	0.03	0.22
11	Multi-Trailer Trucks		0.27	0.04	0.02	0.01	0.00	0.00	0.09	0.03	0.01	0.01	0.01	0.00
12			0.12	0.01	0.01	0.00	0.00	0.00	0.03	0.01	0.00	0.00	0.00	0.00
13			0.08	0.05	0.01	0.00	0.00	0.03	0.01	0.01	0.01	0.01	0.02	0.01
	Percent Trucks		13.56	7.53	8.63	8.04	8.53	11.62	7.31	5.27	5.27	5.07	5.55	8.40
Vehicle Mix within Passenger Vehicle Category														
1	Motorcycles		0.46	0.40	0.48	0.69	0.78	1.48	0.19	0.20	0.38	0.30	0.55	0.53
2	Pass. Cars		83.70	79.52	75.70	76.04	74.42	68.04	87.69	85.31	83.23	84.63	82.20	79.78
3	PU, Vans, SUV		15.84	20.08	23.82	23.27	24.81	30.48	12.12	14.49	16.39	15.07	17.25	19.68
Vehicle Mix within Truck Category														
4	Buses		5.38	8.23	7.88	9.83	9.26	9.04	10.53	11.57	11.57	15.58	11.17	10.60
5-7	Single-Unit		26.18	53.12	60.83	71.27	76.32	79.17	38.30	58.06	69.64	64.89	66.49	60.71
8-10	Single-Trailer		64.97	37.32	30.82	18.78	14.42	11.53	49.38	29.41	18.41	19.13	21.80	28.57
11-13	Multi-Trailer		3.47	1.33	0.46	0.12	0.00	0.26	1.78	0.95	0.38	0.39	0.54	0.12

Table 4. 2012 Average Washington State Vehicle Miles Travelled Mix by Highway Functional Class. [WSDOT14]

FHWA Class	WSDOT Class		Rural					Urban				
			Interstate	Principal Arterial	Minor Arterial	Collector	Total	Interstate	Principal Arterial	Minor Arterial	Collector	Total
1-3	Passenger Vehicles		81.06	83.66	85.49	85.47	83.03	90.99	92.87	92.80	86.56	91.80
4-7	SUTs and Buses 2-4 or more Axles	Trucks	5.57	7.94	8.67	8.79	7.16	4.17	4.50	5.24	8.48	4.31
8-10	Trucks 4-6 or more Axles		11.55	6.91	4.81	4.79	8.30	4.28	2.37	1.66	4.68	3.45
11-13	Trucks 5-7 or more Axles		1.82	1.49	1.03	0.95	1.51	0.56	0.26	0.30	0.28	0.43
	Percent Trucks		18.94	16.34	14.51	14.51	16.97	9.01	7.13	7.20	13.44	8.20
Vehicle Distribution within the Heavy Vehicle Category												
4-7	SUTs and Buses 2-4 or more Axles		29.41	48.59	59.74	60.47	42.20	46.24	63.11	72.77	63.10	52.62
8-10	Trucks 4-6 or more Axles		60.98	42.28	33.16	32.99	48.91	47.56	33.25	23.03	34.79	42.15
11-13	Trucks 5-7 or more Axles		9.60	9.13	7.10	6.54	8.89	6.20	3.64	4.20	2.11	5.23

Table 5. 2012 Average Kansas Traffic Mix by Highway Functional Class. [KSDOT12]

FHWA Vehicle-Class	Vehicle Category		Rural						Urban				
			Interstate	Freeway \ Expressway	Principal Arterial	Minor Arterial	Major Collector	Minor Collector	Interstate	Freeway \ Expressway	Principal Arterial	Minor Arterial	Major Collector
1	Passenger Vehicles		0.6	0.8	0.8	0.9	1.1	0.0	0.5	0.8	0.6	0.5	0.9
2			53.0	58.5	54.2	54.8	62.5	25.6	65.2	74.5	73.3	73.6	81.8
3			20.3	25.5	25.5	29.6	30.8	55.6	23.3	19.5	20.6	22.7	15.9
4	Buses	Trucks	0.2	0.1	0.1	0.1	0.0	0.0	0.1	0.0	0.1	0.2	0.2
5	Single-Unit Trucks		1.9	1.9	1.2	1.4	1.6	1.1	2.3	1.1	1.3	1.7	0.9
6			0.7	0.7	1.2	1.6	0.8	5.6	1.0	0.6	0.5	0.4	0.1
7			0.2	0.1	0.2	0.2	0.1	0.0	0.2	0.1	0.1	0.1	0.0
8	Single-Trailer Trucks		1.4	1.1	1.3	1.3	0.6	0.0	0.6	0.7	0.4	0.2	0.1
9			18.5	10.2	14.1	9.1	2.0	8.9	6.0	2.2	2.9	0.6	0.0
10			0.4	0.3	0.7	0.6	0.2	0.0	0.2	0.1	0.1	0.0	0.0
11	Multi-trailer trucks		1.8	0.6	0.4	0.2	0.1	0.0	0.5	0.1	0.0	0.0	0.0
12			0.7	0.1	0.2	0.0	0.0	2.2	0.1	0.1	0.0	0.0	0.0
13			0.3	0.1	0.1	0.1	0.1	1.1	0.1	0.1	0.0	0.0	0.0
Percent Trucks			26.1	15.2	19.5	14.6	5.5	18.9	11.1	5.1	5.4	3.2	1.3
Vehicle Mix within Passenger Vehicle Category													
1	Motorcycles		0.8	0.9	1.0	1.1	1.2	0.0	0.6	0.8	0.6	0.5	0.9
2	Pass. Cars		71.7	69.0	67.3	64.2	66.2	31.5	73.3	78.6	77.6	76.0	83.0
3	PU, Vans, SUV		27.5	30.1	31.7	34.7	32.6	68.5	26.2	20.6	21.8	23.5	16.1
Vehicle Mix within Truck Category													
4	Busses		0.8	0.7	0.5	0.7	0.0	0.0	0.9	0.0	1.8	6.3	15.4
5-7	Single-Unit		10.7	17.8	13.3	21.9	45.5	35.4	31.5	35.3	35.4	68.8	76.9
8-10	Single-Trailer		77.8	76.3	82.6	75.3	50.9	47.1	61.3	58.8	62.7	25.0	7.7
11-13	Multi-trailer		10.7	5.3	3.6	2.1	3.6	17.5	6.3	5.9	0.0	0.0	0.0

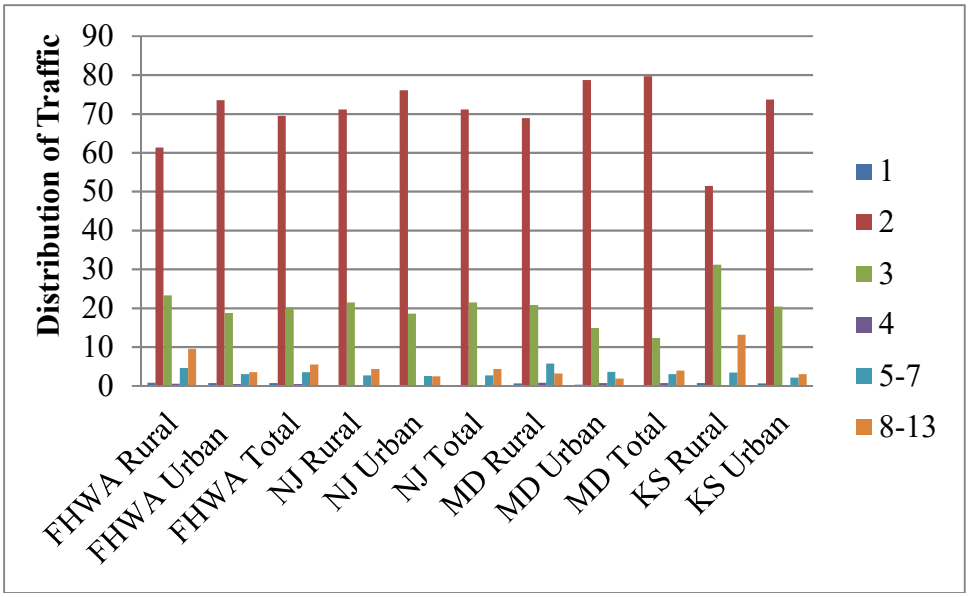

a) Summary of All Vehicles.

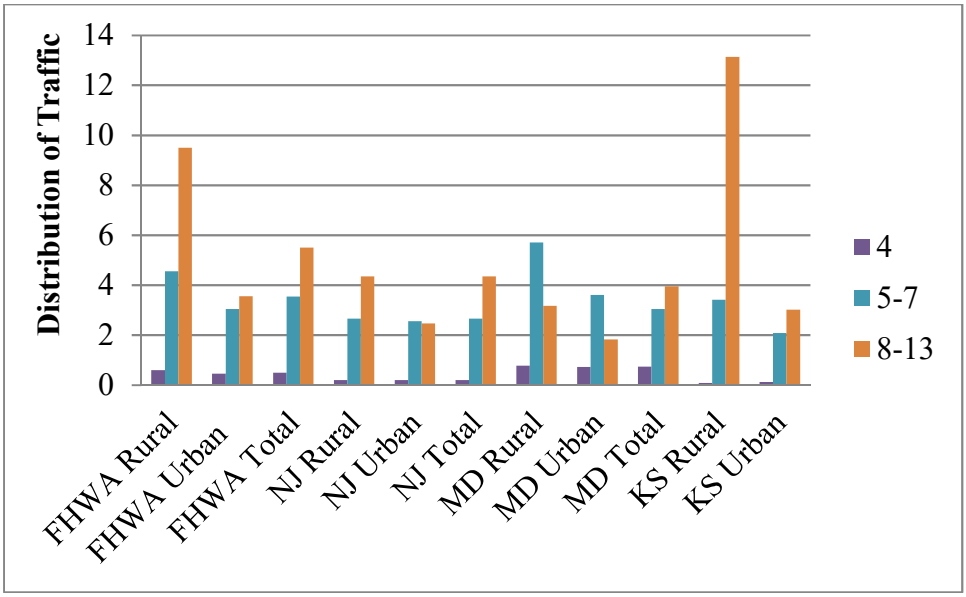

b) Summary of Heavy Vehicles.

Note: FHWA distribution calculated from VMTs and State distributions calculated from ADTs.

Figure 2. Traffic Mix on Rural and Urban Highways.

1.1.3.3 Site Specific Mix Data

Many states maintain weigh-in-motion (WIM) data collection stations to collect the axle loadings of heavy vehicles in order to assist in formulating pavement designs. WIM data were obtained from NCHRP Project 12-76(01) which is documented in NCHRP Report 683, "Protocols for Collecting and Using Traffic Data in Bridge Design." [Sivakumar11]

While the project collected data from numerous WIM site, two specific WIM stations were selected because data was available for at least 10 months of the year and included all lanes of the cross-section. The first WIM station is WIM site number 1 in Lodi, California. The data were collected for 10 months between June 2006 and March 2007. This WIM data collection station is a four-lane divided highway with two lanes in each direction on Interstate 5 and data was collected for all four lanes. The AADT for this roadway during the data collection period was 53,000 veh/day with 21 percent trucks. The posted speed limit on the section of I-5 including the WIM station had a posted speed limit of 70 mi/hr. This particular WIM station represents a fairly typical four-lane rural interstate highway.

The second WIM station is WIM site number 9919 in Brevard County, Florida. The data were collected for the 12 months of 2005. This WIM data collection station is a four-lane divided highway with two lanes in each direction on Interstate 95 and data was collected for all four lanes. The AADT for this roadway during the data collection period was 39,616 veh/day with 17.5 percent trucks. The posted speed limit on the section of I-95 including the Brevard County WIM station had a posted speed limit of 70 mi/hr. This site also is representative of typical rural four-lane divided highways.

Both of these sites are rural principal arterials. Like the rural principal arterials in New Jersey, Maryland, Kansas and Washington States summarized in Table 2 through Table 5, these two WIM stations have tractor trailer truck (i.e., Classes 8-13) volumes that account for between 70 and 80 percent of the truck traffic with the dominant truck type being a Class 9, 5-axle tractor trailer truck. Similar to the other States, the percent of buses is about one percent and the single unit truck volume accounts for between 14 and 25 percent of the truck traffic. These two WIM sites, therefore, have vehicle mix properties that are consistent with the heavy vehicle mix averages observed in the States listed in Table 2 through Table 5.

Table 6. Heavy Vehicle Mix from Two WIM Counting Stations.

FHWA Vehicle Truck Class	Heavy Vehicle Traffic Mix (%)	
	2006/2007 Lodi CA	2005 Brevard Co. FL
4	0.78	1.12
5	22.75	10.29
6	2.01	3.64
7	0.03	0.61
8	3.28	4.39
9	57.52	72.36
10	0.47	0.71
11	9.25	2.67
12	1.05	0.84
13	0.09	0.16
Unknown	2.77	3.20
Total	100.00	100.00
4	0.78	1.12
5-7	24.79	14.54
8-10	61.27	77.47
11-13	10.39	3.67
Unknown	2.77	3.20
Total	100.00	100.00

1.2 PERCENT TRUCKS

The percentage of trucks on any particular route can vary widely from one site to the next. As shown in the earlier tables, typical values are from 10 to 20 percent on the rural Interstate system and 3 to 10 percent on more local roadways. These values, however, are average values and the percent trucks can vary between essentially zero on residential and local streets to up to 60 percent or more on roadways with industrial or shipping facilities. Table 7 was developed to further review the variation of percent trucks around the mean values generally reported as "PT". It shows the range of percent trucks in three States: North Carolina, Washington and Ohio. The percent of trucks on each functional classification of roadway was determined using the FHWA's Highway Safety Information System (HSIS) for the years 2002 through 2007.

Table 7. Sample of Percent Trucks on Highways in Three States.

	Functional Classification	Min.	25th	50th	75th	Max.
2002-2007 North Carolina HSIS Data						
Rural	Principal arterial - Interstate	0	19	19	22	97
	Principal arterial – Other	0	8	13	13	30
	Minor Arterial	0	9	9	9	41
	Major Collector	0	7	7	7	91
	Minor Collector	0	6	6	6	10
	Local	0	9	9	9	99
Urban	Principal arterial – Interstate	0	16	16	20	97
	Principal arterial – Freeway	0	8	9	9	21
	Principal arterial – Other	0	8	8	8	99
	Minor Arterial	0	4	4	4	92
	Collector	0	4	4	6	92
	Local	0	3	6	9	95
2002-2007 Washington State HSIS Data						
Rural	Freeways	0	0	4	8	52
	Freeways with less than 4 lanes	19	19	21	23	24
	2-Lane Undivided Roads	0	9	14	20	73
	Multi-lane Divided	0	7	11	18	67
	Multi-lane Undivided	0	7	12	16	34
Urban	Freeways	0	0	6	11	34
	Freeways with less than 4 lanes	0	0	8	11	30
	2-Lane Undivided Roads	0	0	7	11	31
	Multi-lane Divided	0	0	3	5	34
	Multi-lane Undivided	0	0	4	8	34
2002-2007 Ohio HSIS Data						
Rural	Principal arterial - Interstate	7	28	32	36	56
	Principal arterial – Other	2	9	16	26	67
	Minor Arterial	1	6	8	11	57
	Major Collector	0	4	6	9	56
	Minor Collector	1	4	6	9	51
	Local	1	4	5	9	30
Urban	Principal arterial – Interstate	2	10	15	24	55
	Principal arterial – Freeway	1	6	10	14	57
	Principal arterial – Other	0	3	5	8	55
	Minor Arterial	0	3	4	6	28
	Collector	1	3	4	6	46
	Local	1	3	5	12	23

Table 8 shows the recommended traffic mix for performing pier protection and shielding research. Examination of Table 1 through Table 5 as well as Figure 2 indicate that it is not necessary to replicate all functional classifications. The data appear most strongly affected by the land use (i.e., rural versus urban) and whether the roadway is an arterial or a collector/local road. The four highway functional classifications shown in Table 8 will provide sufficient description of the traffic mix to be able to represent the most typical situations while not including a large number of repetitive categories that would make use of the guidelines cumbersome. Likewise, as will be discussed at greater length in the next section, the vehicle classifications have been compressed in Table 8 from the 13 recommended by the FHWA to just seven for generation of the guidelines. Some of these classifications can be further compressed and, of course, the motorcycle class has no significant traffic volume associated with it so it can be eliminated.

When considering passenger vehicles alone, sedans and pickups appear to share the traffic mix within the passenger vehicle category in a roughly 3 to 1 ratio (i.e., 75 percent of passenger vehicles are cars and 25 percent are SUVs, vans and pickup trucks) on rural highways as shown earlier in Figure 2a. This ratio generally increases to about 4 to 1 in more urban areas (i.e., 80 percent passenger cars). These ratios have been included in Table 8.

The most important features of the vehicle mixes shown in Table 2 through Table 5 and Figure 2 are the variations and distributions of heavy vehicles on different types of roadways. All the State mix data examined showed that single-trailer trucks generally account for about 70 percent of the truck volume on rural interstate roadways. This is particularly important for assessing the risk of failure of bridge piers and components because this class of vehicles, as will be shown in the next section, carries the heaviest loads and represents the largest kinetic energy on the roadways. Multi-trailer trucks also account for a small percentage (i.e., around 5 percent) on rural interstates so the tractor trailer classes (i.e., Classes 8 through 13) often account for 75 percent of the rural arterial and interstate truck volume. The tractor trailer truck percentage decreases somewhat on urban arterials due to an increase in single-unit trucks. For collectors and local roads and streets, single-unit trucks account for a higher percentage of the truck volume; about 60 percent on rural collectors and local roads and about 70 percent on urban collectors and local roads. These values have been used in Table 8 to represent the likely mix of trucks on these basic functional classifications of roadways. Using these four types of roadways should provide measurable discrimination between traffic conditions appropriate for assessing the risk of impacts to piers from heavy vehicles.

Table 8. Recommended Traffic Mix for Pier Design and Shielding Guidelines.

		Rural		Urban	
FHWA Vehicle Class	Vehicle Category	Interstates and Arterials	Collectors and Locals	Interstates and Arterials	Collectors and Locals
1	Motorcycles	0.00	0.00	0.00	0.00
2	Pass. Cars	0.75(1-PT)	0.75(1-PT)	0.80(1-PT)	0.80(1-PT)
3	Pickups, Vans and SUVs	0.25(1-PT)	0.25(1-PT)	0.20(1-PT)	0.20(1-PT)
4	Buses	0.05(PT)	0.10(PT)	0.05(PT)	0.10(PT)
5-7	Single-Unit Truck	0.20(PT)	0.60(PT)	0.30(PT)	0.70(PT)
8-10	Single-Trailer Truck	0.70(PT)	0.30(PT)	0.60(PT)	0.20(PT)
11-13	Multi-Trailer Truck	0.05(PT)	0.00	0.05(PT)	0.00

The percent trucks is the other traffic characteristic examined in this section. As shown in Table 7, while most rural and urban arterials have a percentage of trucks between 8 and 25 percent, there are some unusual arterials that can have percentages of trucks as high as 97 percent. Similarly, while non-arterials generally have a percentage of trucks around 10 percent, some unusual roads in these categories can have values of over 60 percent. Since there is a wide variation in the percent trucks, it is recommended that the percent trucks be retained as a basic input variable (i.e., the percent trucks will be an input that can vary from zero to 40). This means that the user of the guidelines can use the actual or projected percent of trucks explicitly in the guidelines. A maximum value of 40 is recommended because the underlying encroachment data for heavy vehicles is reliable between zero to 40 as discussed in Carrigan. [Carrigan14] When a user has a value of percent trucks greater than 40, a value of 40 should be used. This will result in conservative findings, as the larger the percent trucks, the lower the number of encroachments.

1.3 HEAVY VEHICLE PROPERTIES

1.3.1 Background

Section 1.1 provided a recommended traffic mix including the percentage of each FHWA class of vehicles to use in developing bridge pier risk and protection guidelines for several highway types. Knowing which types of vehicles are likely to strike piers is the first step in assessing the risk; the second step is to determine the properties and distribution of those properties in order to be able to evaluate the likelihood of a collision and the likely distribution of the impact conditions for those vehicles. Determining the typical characteristics of vehicles in the traffic mix is important since some vehicle properties like weight and dimensions have an

effect on the likely impact performance of both bridge pier components and barriers used to shield them. In particular, the following characteristics are needed by RSAPv3 to represent vehicles:

- Gross vehicle weight,
- Length and width and
- Center of gravity location.

RSAPv3 uses these properties in several different ways. First, basic dimensions (i.e., length and width) are used by RSAPv3 to determine if the vehicle footprint on the vehicle path will intersect a hazard like a bridge pier or shielding barrier. Second, the vehicle properties are also used in the penetration and rollover algorithms to determine if the vehicle has sufficient force or energy to break through the hazard (e.g., catastrophically fail the bridge pier or break through a shielding barrier) or rollover the hazard (e.g., the barrier shielding the bridge pier). RSAPv3's penetration and rollover algorithms are simple point-mass models so the dimensions, location of the center of gravity and weight are the only properties needed. .

Weight is a particularly important property for designing bridge piers for impacts since the vehicle weight is one of the two basic components of kinetic energy. The heaviest vehicles travelling at the highest speeds will create the highest risk of failure for impacted bridge piers. Selecting a distribution of vehicle weights within each vehicle class to accurately reflect the loading conditions experienced on the nation's roadways is necessary in order to accurately assess the risk of pier failure and bridge collapse. For example, if only the average Class 9 tractor trailer were used, the heaviest Class 9 trucks would be excluded and it is precisely these heavier vehicles in the distribution that are most likely to pose the highest risk for a pier failure in a collision. This section will examine the distribution of vehicles weights within each of the FHWA heavy vehicle classifications.

1.3.2 Heavy Vehicle Weight

1.3.2.1 Gross Vehicle Weight Limits

Each State imposes a maximum vehicle gross weight for their highways. A vehicle can only be loaded above this weight if it is specially permitted. As shown in Table 9, 35 States have a maximum gross vehicle weight (GVW) of 80,000 lbs. Alaska has the highest limit at 150,000 lbs, Montana and Nevada have limits of 129 Kips and six States have limits between 95,000 and 105,000 lbs. Vehicles with weights above the legal limit will also be considered since vehicles can be specially permitted to operate above the normal legal limit but the legal limit is likely a rough indicator of the highest loads that can normally be expected.

Table 9. Maximum Legal Load for Selected State.

Maximum Unpermitted Legal Load (kips)												
150	132	129	105	100	95	90	88	86.4	85.5	85	80.608	80
States												
AL	MT	NV	ID ND OR WS	ME	NE	OK	HI	NM	KS	CO	SC	All Others

1.3.2.2 Distribution of Vehicle Weights from the VTIS

The FHWA Office of Highway Policy Information (OHPI) publishes the Vehicle Travel Information System (VTIS) website which can be queried for data on the average time heavy vehicles spend both empty and loaded. VTIS data from Nevada for the year 2013 was evaluated to determine the average (i.e., 50th percentile) weight of each of the 13 FHWA vehicle classifications on urban and rural roadways. [FHWA14] Recall from above that Nevada has a maximum gross vehicle weight limit of 129 kips. The results are summarized in Table 10.

Table 10. Heavy Vehicle Gross Vehicle Weight Distributions by FHWA Vehicle Classification from the 2013 VTIS Data for Nevada.

Vehicle Type	FHWA Vehicle Class	Samples	50th Percentile Weight (kips)
Urban			
Single-Unit Trucks	5	82	24.08
	6	237	14.26
	7	77	17.91
Single-Trailer Trucks	8	154	21.59
	9	117	24.95
	10	428	34.67
Multi-Trailer Trucks	11	27	36.94
	12	88	36.02
	13	39	36.61
All SUTs Combined		396	15.09
All Single-Trailer		699	28.80
All Multi-Trailers Combined		154	34.34
All Tractor Trailers Combined		853	35.42
Rural			
Single-Unit Trucks	5	34	22.35
	6	8	38.10
	7	107	28.99
Single-Trailer Trucks	8	466	41.04
	9	11	39.18
	10	34	39.62
Multi-Trailer Trucks	11	10	38.45
	12	50	9.90
	13	63	18.96
All SUTs Combined		149	27.94
All Single-Trailer		511	40.79
All Multi-Trailers Combined		123	16.15
All Tractor Trailers Combined		634	35.96

1.3.2.3 Distribution of Class 9 Trucks from 15 States

Class 9 trucks (i.e., five axle single-trailer trucks) are one of the most important types of vehicles from a pier design and protection stand point since they are both common on the roadways and tend to carry some of the heaviest loads. The National Academy of Sciences and FHWA collaborated to publish "Technologies and Approaches to Reducing the Fuel Consumption of Medium and Heavy-Duty Vehicles" in 2010.[NAS10] Data from 2008 were gathered and analyzed from the following 15 States: California, Connecticut, Florida, Georgia, Hawaii, Iowa, Minnesota, Missouri, Montana, North Carolina, Oregon, Pennsylvania, South Dakota, Texas, and Washington. The analysis includes the consideration of on-road vehicle weight for five-axle tractor-trailer trucks (i.e., class 9). Using the data presented in that report, a cumulative distribution of gross vehicle weight (GVW) was generated for Class 9 vehicles as

shown in Figure 3. Some of the key percentiles for the Class 9 weight distribution are shown in Table 11. While the median Class 9 vehicle has a GVW of about 53,000 lbs, the 99th percentile Class 9 vehicle weighs almost 90,000 lbs as shown in Table 11. In Table 11 as well as most of the rest of the tables in this section, GVWs that are above 80,000 lbs are highlighted with a red color. Interestingly, according to the data summarized in Table 11, the 99th percentile Class 9 vehicle weight exceeds the legal GVW limit in 35 States shown in Table 9.

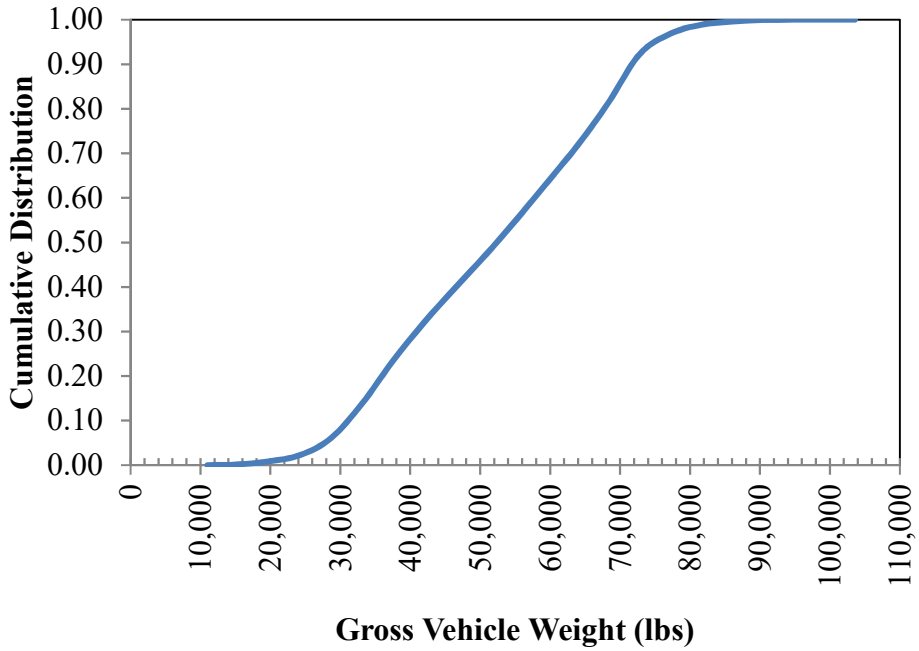

Figure 3. 2008 Cumulative Distribution of Class 9 Vehicles for 15 States.

Table 11. Class 9 Vehicle Weight Distribution from 15 States.

		Gross Vehicle Weight Percentile (kips)				
Vehicle Type	**FHWA Vehicle Class**	**50th**	**85th**	**90th**	**95th**	**99th**
Single-Trailer Trucks	9	52.90	69.80	71.90	76.32	86.00

† Red cells indicate GVWs greater than 80,000 lbs which is the maximum legal limit in 35 States.

1.3.2.4 Distribution of Vehicle Weights from the VIUS

The FHWA Vehicle Inventory and Use Survey (VIUS) data from 2002 was evaluated to determine the GVW of different vehicle classes. [Alam07] The data provides the physical and operating characteristics of the heavy vehicle population for each State. The data is gathered through surveys, not field measurements. The average payload and empty weights were calculated from the survey data and reported for each State. These calculated values were then used to generate a national average distribution for each heavy vehicle class. Since the VIUS is a trucking company survey, Class 4 vehicles (i.e., buses) were not included in the data.

Unfortunately, the VIUS data is reported using a different vehicle classification system than the usual FHWA classification system, therefore the equivalency table shown in Table 12 was used to convert the data to the equivalent FHWA vehicle classification for consistency. A summary of the resulting national distribution is shown in Table 14.

Table 12. Equivalency Table for VIUS and FHWA Vehicle Classifications.

VIUS Vehicle Classification	FHWA Vehicle Classification
Class 1 – Single Unit: 2-axle	5
Class 2 – Single Unit: 3-axle	6
Class 3 – Single Unit: 4-axle or more	7
Class 4 – Truck/Tractor Trailers: 4-axle or less	8
Class 5 – Truck/Tractor Trailers: 5-axle	9
Class 6 – Truck/Tractor Trailers: 6-axle or more	10
Class 7 – Combination Trucks: 5-axle or less	11
Class 8 – Combination Trucks: 6-axle	12
Class 9 – Combination Trucks: 7-axle or more	13

Table 13. Heavy Vehicle Gross Vehicle Weight Distributions by FHWA Vehicle Classification from the VIUS Data.

			Gross Vehicle Weight Percentile (kips)				
Vehicle Type	**FHWA Vehicle Class**	**No. States Responding**	**50th**	**85th**	**90th**	**95th**	**99th**
Single-Unit Trucks	5	33	17.52	21.86	22.05	22.80	31.44
	6	34	33.03	36.21	36.25	37.38	40.45
	7	35	47.52	54.82	57.05	59.20	68.74
Single-Trailer Trucks	8	35	35.43	40.39	41.73	43.09	54.42
	9	36	55.24	60.63	61.37	61.55	64.83
	10	35	65.01	69.03	71.77	79.10	89.38
Multi-Trailer Trucks	11	32	55.85	63.03	64.67	65.46	66.10
	12	24	61.03	69.25	71.78	73.18	74.61
	13	27	79.78	98.00	100.42	107.48	127.00

† Red cells indicate GVWs greater than 80,000 lbs which is the maximum legal limit in 35 States.

1.3.2.5 Distribution of Vehicle Weights from the MEPDG

Figure 4 shows a cumulative distribution of single-axle weights and Figure 5 shows a similar cumulative distribution of tandem-axle weights for each of the heavy vehicle classes from the Mechanistic-Empirical Pavement Design Guide (MEPDG). [MEPDG04] Unfortunately, the MEPDG does not list the distributions of vehicle weights but only the distribution of axles but this data was used to estimate the GVW distribution by combining the single and tandem axle distributions according to the number and axle configuration for each of the heavy vehicle types in the FHWA classification system. This data was used to develop the vehicle GVW distribution statistics shown in Table 14. The 22,000-lbs single-unit truck used in MASH appears to be a good representation of the 85th percentile two-axle single unit truck

whereas the 80,000-lbs tractor trailer is more representative of the 95th percentile Class 9 truck weight based on the MEPDG. [MEPDG04]

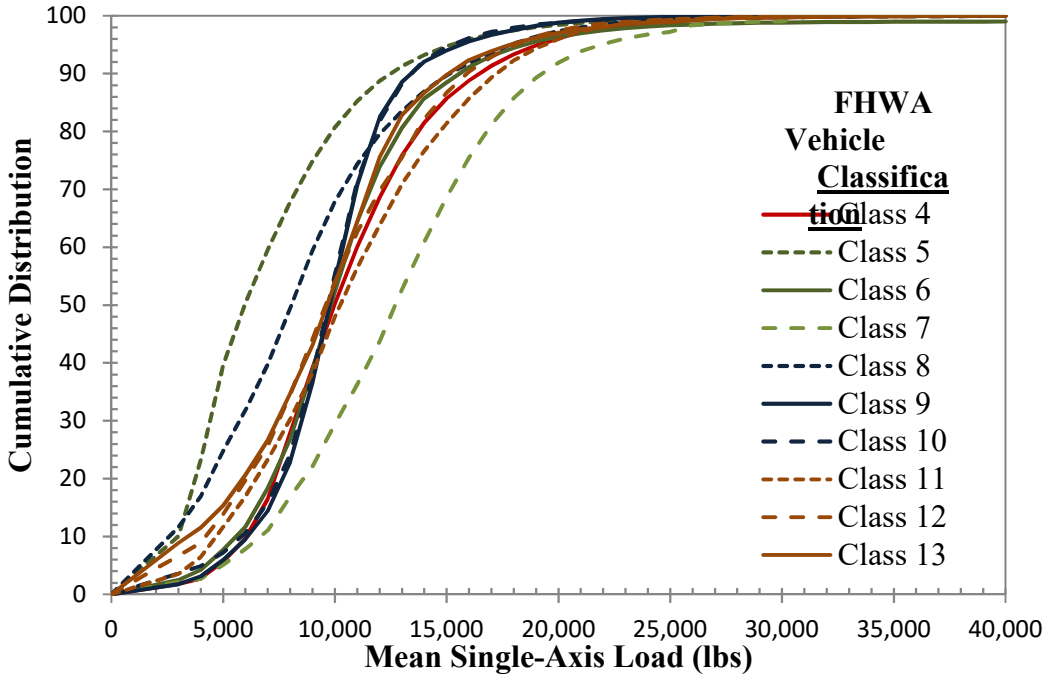

Figure 4. Mean Single-Axle Load by Vehicle Classification. [after MEPDG04]

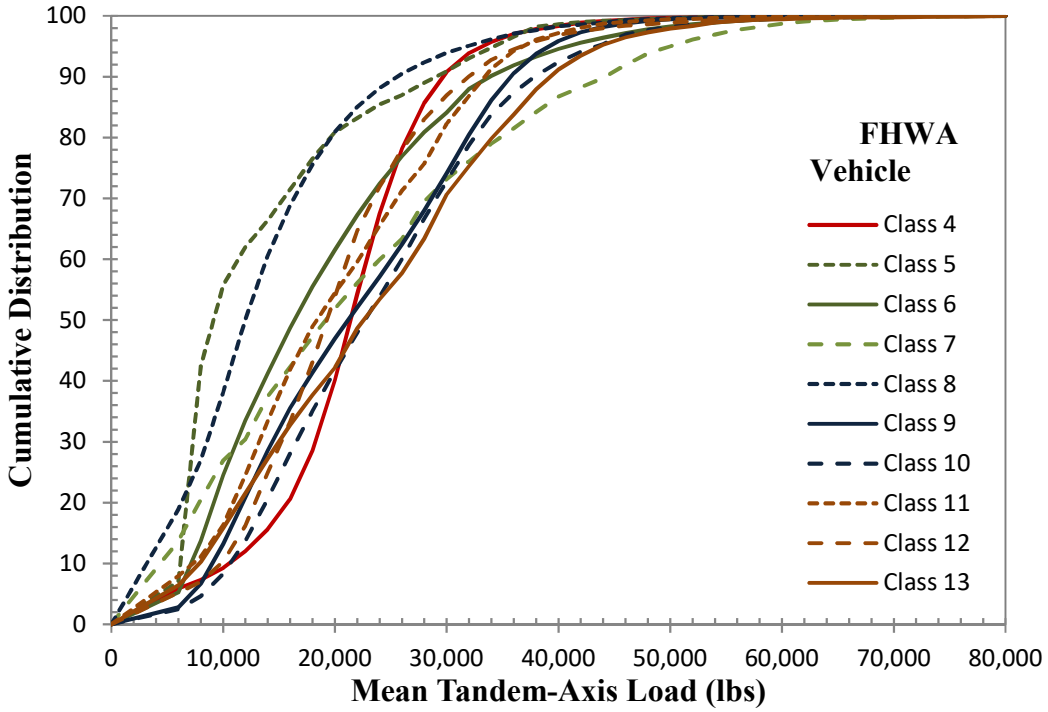

Figure 5. Mean Tandem-Axle Load by Vehicle Classification. [after MEPDG04]

Table 14. Heavy Vehicle Gross Vehicle Weight Distributions by FHWA Vehicle Classification from the MEPDG. [after MEPDG04]

Vehicle Type	FHWA Vehicle Class	Gross Vehicle Weight Percentile (kips)				
		50th	85th	90th	95th	99th
Buses	4	24.51	34.87	38.25	43.90	56.59
Single-Unit Trucks	5	11.94	21.89	25.00	30.44	43.68
	6	26.25	44.29	49.43	59.31	93.62
	7	33.62	59.95	67.44	76.42	96.37
Single-Trailer Trucks	8	27.20	46.68	53.19	63.82	85.87
	9	51.90	78.88	84.12	93.28	114.08
	10	56.45	83.54	90.96	104.12	131.74
Multi-Trailer Trucks	11	49.80	77.91	84.63	94.96	117.33
	12	56.90	86.29	94.37	107.70	143.44
	13	76.71	119.89	129.82	146.85	189.48

† Red cells indicate GVWs greater than 80,000 lbs which is the maximum legal limit in 35 States.

1.3.2.6 Distribution of Vehicles Weights from WIM Data

As discussed in the last section, weigh-in-motion data (WIM) from two rural arterial sites were examined to determine the distribution of the vehicle mix as well as the weight, speed and energy distribution by class. Summary statistics for the heavy vehicle weights by class are shown in Table 15.

Table 15. Heavy Vehicle Gross Vehicle Weight Distributions by FHWA Vehicle Classification from WIM Data.

Vehicle Type	FHWA Vehicle Class	Samples	Gross Vehicle Weight Percentile (kips) 50th	85th	90th	95th	99th
Lodi, CA WIM Site							
Buses	4	31,738	35.40	45.90	47.40	49.40	53.30
Single-Unit Trucks	5	923,192	11.20	19.20	21.30	24.90	30.40
	6	81,671	20.00	36.50	40.60	45.20	53.60
	7	1,077	62.60	67.00	67.80	69.50	74.40
Single-Trailer Trucks	8	133,074	31.40	43.40	46.30	50.90	59.90
	9	2,334,096	58.70	76.80	78.00	79.70	83.60
	10	18,879	60.60	77.90	79.70	82.70	102.60
Multi-Trailer Trucks	11	375,456	57.20	78.40	79.80	81.80	86.30
	12	42,648	56.00	73.50	76.80	80.50	86.10
	13	3,515	100.50	177.20	188.50	204.00	224.60
All SUTs Combined		421,619	12.1	20.3	22.8	27.2	39.5
All Single-Trailer		2,486,049	56.5	76.6	77.9	79.6	83.6
All Multi-Trailers Combined		1,005,940	57.2	78.3	79.8	81.9	87.7
All Tractor Trailers Combined		3,491,989	56.60	76.85	78.18	79.93	84.19
Brevard Co., FL WIM Site							
Buses	4	25,285	28.91	37.85	39.40	41.70	46.00
Single-Unit Trucks	5	232,322	15.64	20.63	22.02	24.09	27.78
	6	82,296	23.61	35.03	38.89	44.80	52.46
	7	13,716	53.30	59.13	60.69	63.07	68.03
Single-Trailer Trucks	8	99,175	30.10	39.48	41.98	45.87	54.03
	9	1,633,972	44.81	62.59	65.24	68.62	74.61
	10	16,071	48.84	70.69	74.62	80.92	91.63
Multi-Trailer Trucks	11	60,334	50.91	59.73	61.54	64.18	69.36
	12	18,869	46.62	60.43	63.29	67.06	73.30
	13	3,717	68.00	101.47	106.95	115.07	130.64
Unknown		72,254	25.03	45.70	51.31	59.03	72.67
All SUTs Combined		328,334	17.28	26.23	30.86	43.88	57.52
All Single-Trailer		1,749,218	43.56	62.21	64.98	68.47	74.71
All Multi-Trailers Combined		82,920	50.28	60.53	62.89	66.98	94.40
All Tractor Trailers Combined		1,832,138	43.86	62.13	64.89	68.40	75.60

† Red cells indicate GVWs greater than 80,000 lbs which is the maximum legal limit in 35 States.

1.3.3 Recommended Weight Distributions and Categories

Table 10 through Table 15 show data from a variety of sources regarding heavy vehicle weight distributions. While all the data are fairly similar it is certainly not identical. Each different study includes its own assumptions and definitions such that there are some nuances between all the different data sources. The results are summarized in Figure 6 through Figure 8. Figure 6 summarizes all SUT data, Figure 7 summarizes all the single-trailer truck data and

Figure 8 summarizes all the multi-trailer truck data. In these figures, each marker style represents a different percentile of the GVW distribution for that vehicle class and the box indicates the range between the 50th and 99th percentile.

The MEPDG data generally shows the widest range (i.e., lowest average and highest 99th percentile) which is due to the way the data had to be re-aggregated to estimate the vehicle GVW. Since only axle weight distributions were provided an assumption about how to combine them had to be made. The assumption was that the appropriate single and tandem axles would come from the same percentile in the distribution presuming the trucking companies attempted to balance their loads. This certainly would not always be the case so it should be recognized that the 50th percentile of the MEPDG is probably on the low side while the 99th percentile is probably over-estimated. At the other extreme are the VTIS and VIUS data which are compiled from surveys of trucking companies. Based on a careful examination of the data it is highly likely that loads are sometimes incorrectly reported and there is likely often confusion among the survey takers about the loaded and unloaded configurations. As a result, the VIUS and VTIS data tend to have higher mean values and lower 99th percentiles. The WIM data is a highly accurate measurement of the GVW of each vehicle passing since it is explicitly measured but it only represents those two particular highways sections rather than a national distribution. Each data source, then, has certain inherent advantages and disadvantages such that there is no single absolutely correct distribution. What needs to be done is to select reasonable values that are consistent with each of these databases while not necessarily exactly matching them. In general, the WIM data will be preferred since it is an actual measure of specific vehicles.

Recommended weights for each vehicle class for developing the pier design and protection guidelines are shown in Table 16. The passenger and pickup truck (i.e., Classes 2-3) weights shown in Table 16 correspond to the MASH vehicle weights. [AASHTO09] The mix percentages are taken from the last section. Passenger and pickup vehicle weights are needed when considering the vehicle-barrier interaction and the probability of the vehicle penetrating the barrier. The MASH weights provide some linkage to the barrier testing guidelines. As in the previous section, motorcycles (i.e., Class 1) are excluded since they are not an important vehicle in assessing risk of pier failure.

Buses (i.e., Class 4) account for between 5 and 10 percent of the truck traffic depending on the functional classification of the roadway. The WIM data indicates that even the heaviest buses weight less than 60,000 lbs and the mean is about 30,000 lbs. One of the aspects of vehicle loading described by Buth indicates that the rigidity of the load is also a feature of the risk for piers. [Buth10] Vehicles where most of the mass is essentially rigid pose a greater risk than vehicles with distributed uncoupled masses. For example, a bus is composed of mass that is accounted for by dozens of people and their baggage. In a crash, each person and each piece of baggage act within the vehicle independently. On the other hand, a tractor trailer truck hauling a single large machine may act as one single 80,000 lbs mass in the impact. While a large intercity bus is at some risk of striking a pier, it is unlikely that the bus can seriously damage a pier since the vehicle is very deformable and filled with uncoupled independently acting masses. It is recommended that buses (Class 4) not be included in the vehicle mix for developing bridge pier design and protection guidelines but that their share of the vehicle mix be assigned to the other heavy vehicles. Some further justification for dropping buses will be provided in a later section where speed and energy data are presented.

The SUT classes (i.e., Classes 5-7) summarized in Figure 6 represent the most varied group of heavy vehicles with many different body styles, configurations and uses. Class 5 in

particular can be difficult because the differences between a heavy Class 3 pickup truck and a light Class 5 delivery truck can be very difficult to detect with vehicle counting equipment. The SUT used in Report 350 and MASH crash tests is a Class 6 vehicle. Class 7 is very similar to Class 6 except it has a triple rather than tandem axle in the rear. RSAPv3 only considers the overall dimensions, weight and c.g. location so all three SUT Classes are very similar in terms of their RSAPv3 properties so they all can be grouped into one SUT Class in developing the guidelines. If all SUTs are grouped together as shown in Table 15, the 50th percentile GVW is around 15 kips, the 85th around 22 kips and the 99th about 50 kips. These values generally fall around the ranges in Figure 6. The 85th percentile SUT at 22 kips is representative of the MASH 10000S SUT used in test level four crash tests. These weight recommendations are shown in Table 16.

The single-trailer truck classes (i.e., Classes 8-10) are all articulated tractor-trailer trucks that only differ in the number of axles at the king-pin or the rear of the trailer. As with the SUTs, RSAPv3 does not model the number of axles or configuration so it is reasonable to group all single-trailer trucks into one category sharing one weight distribution. As shown in Table 15, the average Class 9 single-trailer truck has a GVW of about 59 kips, the 85th percentile is about 77 kips and the 99th percentile is just over 83 kips. The MASH 36000V crash test vehicle is an 80-kip tractor trailer so it represents a truck at about the 99th percentile of Class 9 single-trailer truck GVWs. Based on crash test data, an empty MASH 36000V generally weighs 27 kips which is the 15th percentile in Figure 3. The legal load limit in 35 States is also 80,000 lbs so a 99th percentile tractor trailer truck weighing 80,000 lbs is a good choice for representing the upper end of the weight distribution for this class.

Multi-trailer trucks (i.e., Classes 11-13) are either not allowed or only allowed by special permit in many States. As shown in Table 15, the weight distribution of multi-trailer trucks is a little higher than that for single-trailer trucks although not dramatically higher. This is likely due to several factors. First, a multi-trailer may be required for both geometric as well as weight reasons. Sometimes multi-trailer trucks are used to carry large though not particularly heavy loads like wind turbine blades or bridge components. Second, the power available in the typical tractor is limited so even though there is more cargo volume available, there is a limit to how much load the tractor can pull. As shown in Table 15, the heaviest (i.e., 99th percentile) multi-trailer trucks have GVWs of about 90,000 lbs.

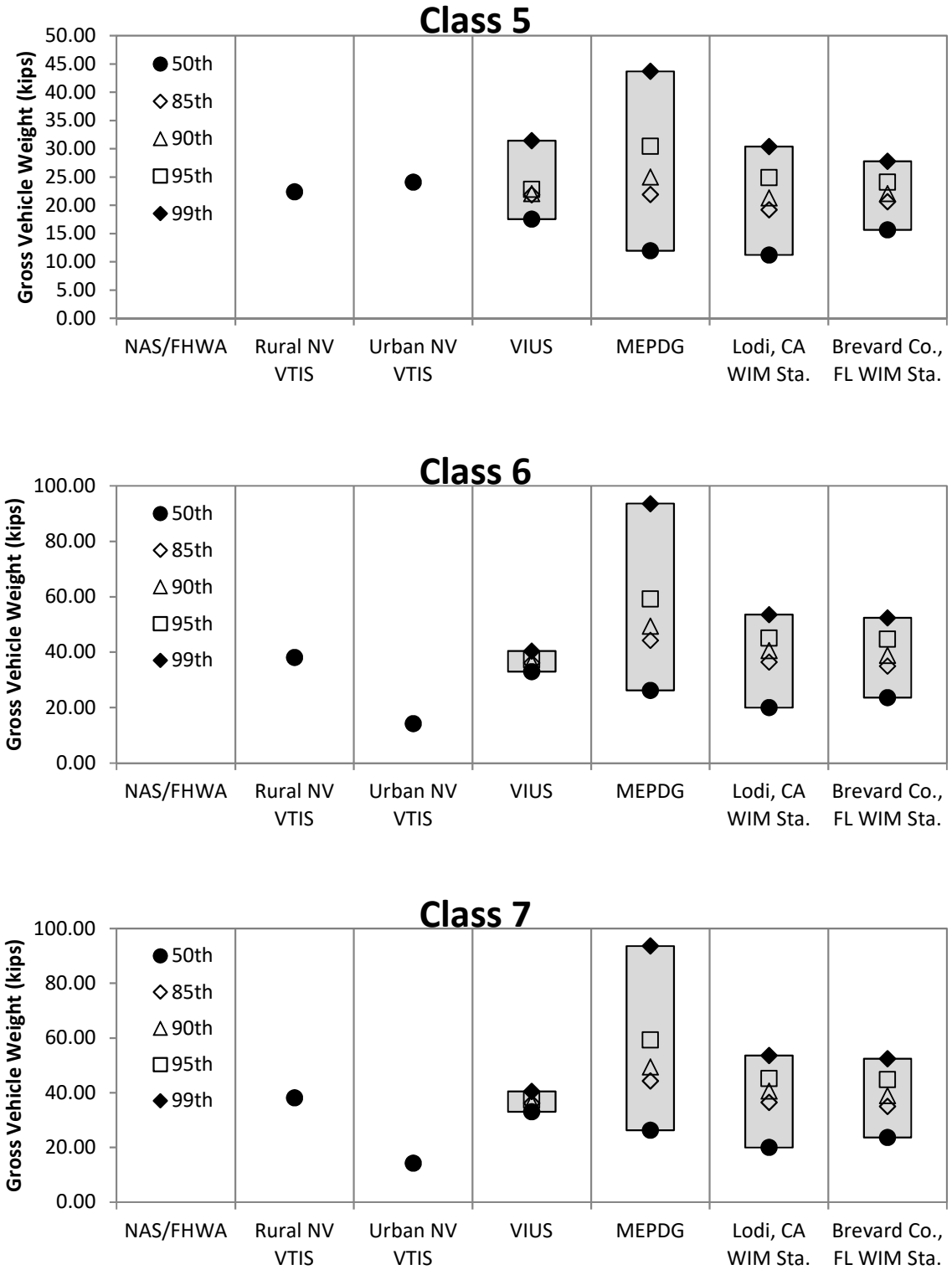

Figure 6. Comparison of SUT GVWs from all data sources.

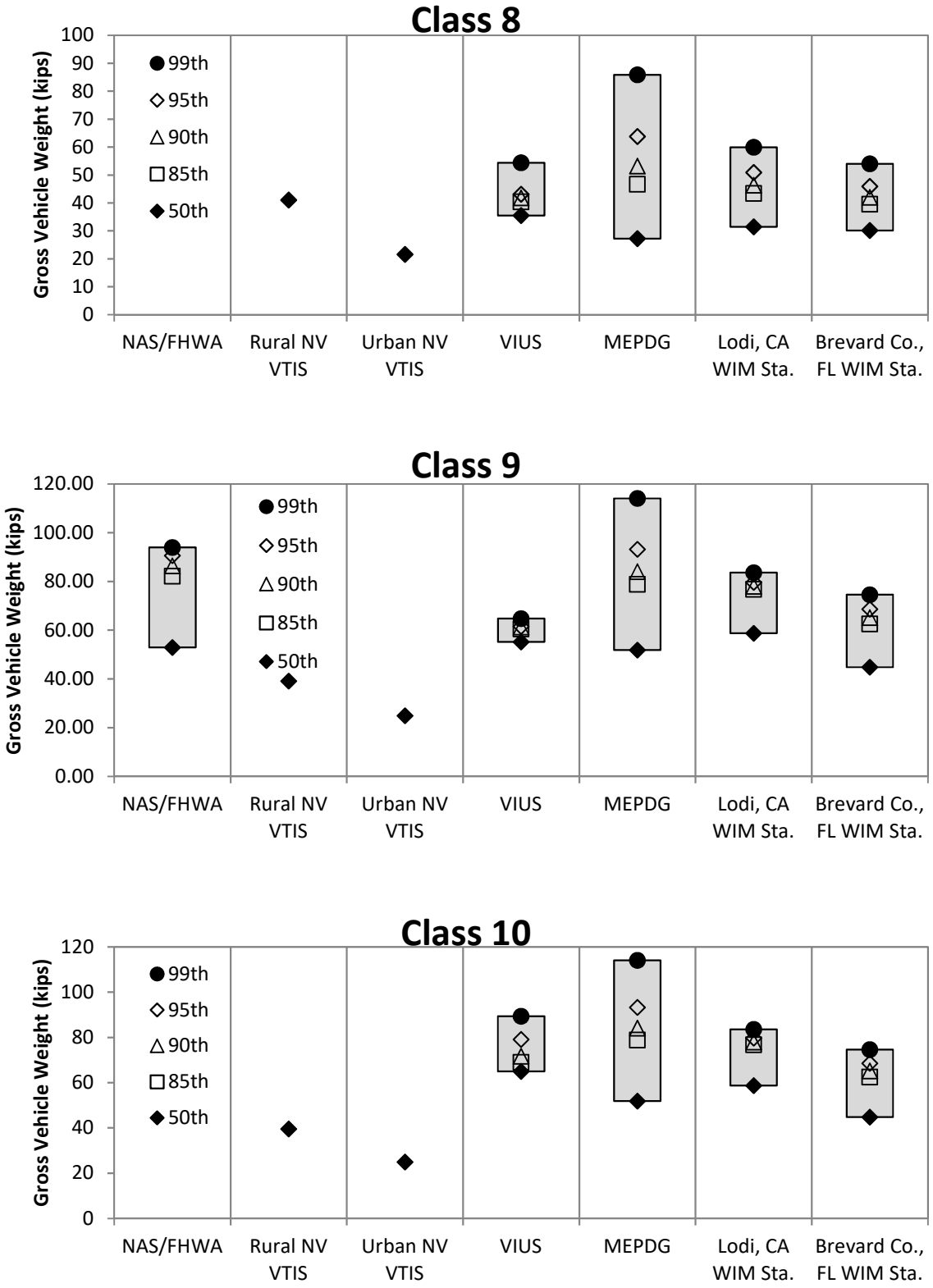

Figure 7. Comparison of Single-Trailer Truck GVWs from all data sources.

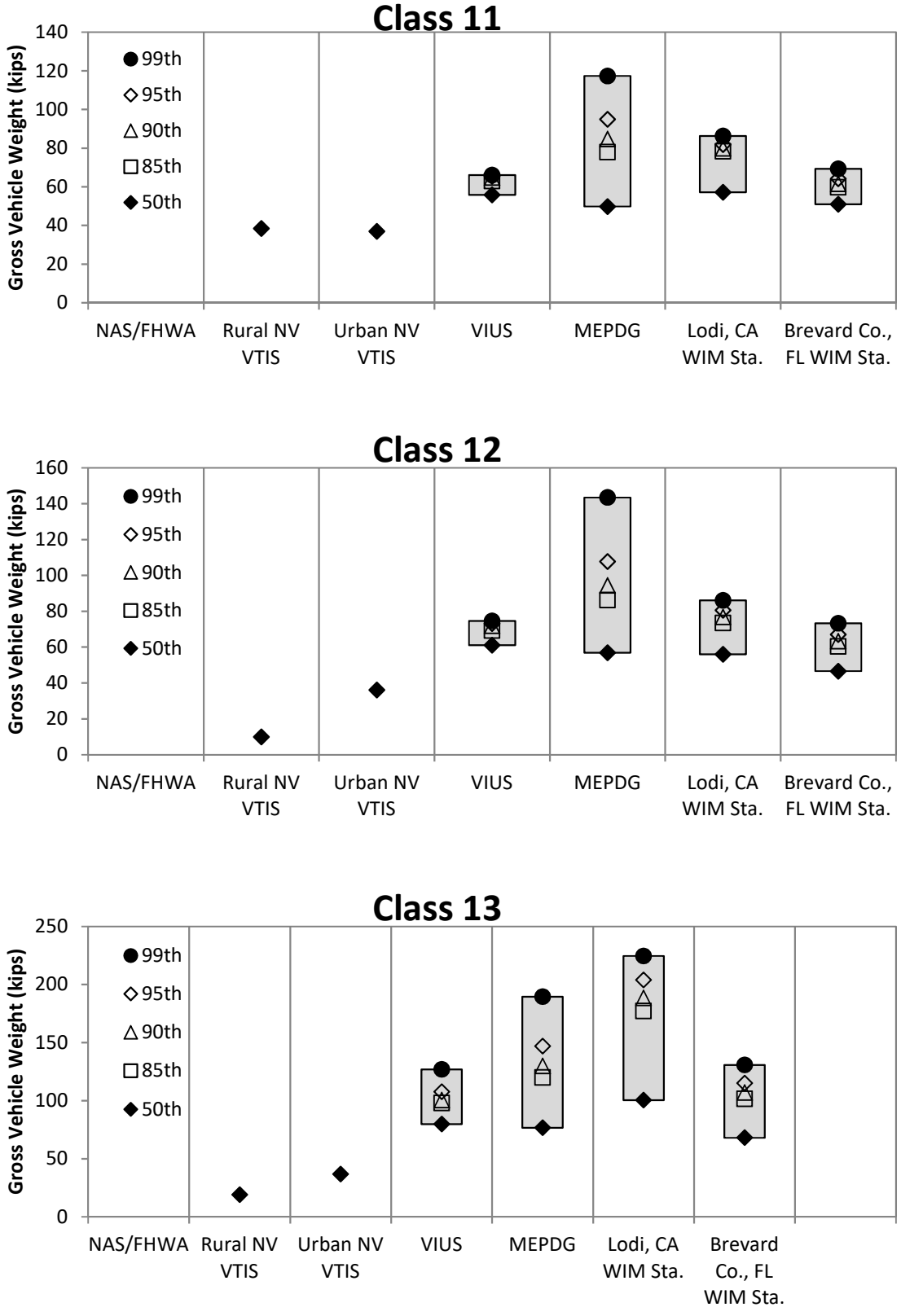

Figure 8. Comparison of Multi-Trailer Truck GVWs from all data sources.

RSAPv3 does not account for multi-articulated vehicles so modeling a multi-trailer truck in RSAPv3 would be identical to modeling a single-trailer truck. Instead of including more classes of vehicles it would be better to have a broader range of vehicle weights. It is recommended that the multi-trailer and single-trailer groups be combined for developing the guidelines. The 85th percentile weight of this combined group should be 80,000 lbs as discussed earlier for the single-trailer truck. The 99th percentile weight for the combined multi- and single-trailer truck group should be 105,000 lbs which represents the load limit in six States. This distribution, therefore, would encompass all the legal loads in 41 of the 50 States. The recommended vehicle weights for use in the development of the guidelines are shown in Table 16.

Table 16. Recommended Vehicle Weights for Use in Guideline Development.

Vehicle Groups	Percentile	RSAP Vehicle Type	FHWA Vehicle Class	Weight (lbs)	Percent of Group (%)
Passenger Vehicles		C	2	3,300	75
Pickup Truck		PU	3	5,000	25
					100
Light SUT	15	LSUT	5	11,500	25
Average SUT	50	ASUT	6	15,000	50
Heavy SUT	85	HSUT	7	22,000	20
Extra Heavy SUT	99	EHSUT	5-7	50,000	5
					100
Light TT	15	LTT	8-9	27,000	25
Average TT	50	ATT	8-13	50,000	50
Heavy TT	85	HTT	8-13	80,000	20
Extra Heavy TT	99	EHTT	8-13	105,000	5
					100

The empty SUT and TT weights shown in Table 16 were based on the empty weights of MASH crash test SUT and TT vehicles and verified using the finite element models of those two crash test vehicles. In both cases, the empty weight of the vehicles corresponds to the 15th percentile of all vehicles in that group.

1.3.4 Vehicle Dimensions

Vehicle dimensions are used in a variety of ways in RSAPv3. First, the length and width are needed in order to determine if a vehicle path intersects with a hazard on the roadside like a bridge pier or barrier. Length and width also play a role in predicting rollover and penetration probabilities for barriers. Harwood, *et al.* found in NCHRP Report 505 the AASHTO *Policy for the Geometric Design of Highways* (i.e., Green Book) published vehicle lengths and widths are reasonably accurate for the modern vehicle fleet. [Harwood03; AASHTO04] These vehicle characteristics have been summarized in Table 17.

Table 17. Green Book Vehicle Dimensions [AASHTO04]

Vehicle Type	Length (ft)	Width (ft)
Passenger Car	19	7
Single Unit Truck	30	8
Intercity Bus	45	8.5
City Transit Bus	40	8.5
Conventional School Bus	36	8
Large School Bus	40	8
Articulated Bus	60	8.5
Intermediate Semitrailer	55	8.5
Interstate Semitrailer	74	8.5
Motor Home	30	8
Car and Camper Trailer	49	8
Car and Boat Trailer	42	8
Motor Home and Boat Trailer	53	8
Farm Tractor	16	10

Table 18. Vehicle Properties Used in NCHRP 22-12(03). [Ray14b]

VEHICLES	FHWA Vehicle Class	RSAPv3 Vehicle Type	LENGTH (ft)			WIDTH (ft)
Passenger Cars	2	C	15.00			5.40
Pickup Truck	3	PU	19.75			6.50
Single Unit Truck	5-7	LSUT	35.00			7.77
		ASUT	35.00			7.77
		HSUT	35.00			7.77
		EHSUT	35.00			7.77
			Total	**Tractor**	**Trailer**	
Tractor Trailer Truck	8-13	LTT	61.30	13.3	48.00	8.50
		ATT	61.30	13.3	48.00	8.50
		HTT	61.30	13.3	48.00	8.50
		EHTT	61.30	13.3	48.00	8.50

After a review of the crash test literature, the NCHRP 22-12(03) project team summarized the geometric properties of the various vehicle classes for the development of bridge rail guidelines as shown in Table 18.[Ray14b] The vehicle dimensional properties shown in Table 18 were determined primarily from the typical crash test vehicles specified by AASHTO MASH. [AASHTO09, Ross93] The values used in Table 18 are consistent with those in Table 17 especially considering the Green Book values are used primarily to ensure appropriate lane widths and turning radii so they tend to represent the larger end of the vehicle dimensional

spectrum. These dimensions shown in Table 18 which were used in NCHRP 22-12(03) are recommended for developing the pier design and protection guidelines.

There are a variety of tractor-trailer configurations that could be included. While an earlier generation of trailers tended to be about 48 ft and these have been the most common in crash tests, 53-ft trailers are now more common on the roadways. The tractor can also be configured as either a day-cab or a sleeper cab which would increase its overall length. Shorter vehicles tend to be more critical when using the point-mass algorithms used in RSAPv3 so the properties in Table 18 for the tractor trailer use the shorter 48-ft trailer and assume the tractor is a day-cab configuration.

1.3.5 Center of Gravity

The height of the center of gravity is needed by RSAPv3 in its rollover algorithm. While weights can be determined from a variety of sources like WIM data discussed earlier, there is no on-the-road measurement of the height of the center of gravity. The height of the center of gravity for passenger cars and pickup trucks were obtained from a review of crash test data where the c.g. height was measured experimentally. The c.g. height of single unit trucks and tractor trailer trucks is known for some crash tested configuration (i.e., the 22-kip SUT and the 80-kip single-trailer truck) but not for the full range of weight distributions included in Table 16.

Table 19. Recommended Center of Gravity Heights for use in Guideline Development.

Vehicle Groups	RSAP Vehicle Type	FHWA Vehicle Class	C.G. Longitudinal (ft)	C.G. Height (ft)
Passenger Vehicles	C	2	6.00	2.00
Pickup Truck	PU	3	8.50	2.30
Light TT	LSUT	8-9	11.60	3.40
Average TT	ASUT	8-13	12.25	3.83
Heavy TT	HSUT	8-13	14.17	4.70
Extra Heavy TT	EHSUT	8-13	16.50	6.19
Light SUT	LTT	5	24.58	3.73
Average SUT	ATT	6	28.75	4.83
Heavy SUT	HTT	7	30.88	5.42
Extra Heavy SUT	EHTT	5-7	31.75	6.00

The SUT and TT center of gravity heights were determined using finite element models of the SUT and TT. Cargo was added to each of the models until the weight corresponded to each of the values shown in Table 16. The height to the center of gravity and longitudinal distance from the front bumper to the center of gravity was then calculated by the finite element program. As discussed in the last section, the shorter length configurations were recommended for the tractor trailer so the c.g. heights will likewise tend to be on the higher end of the range. This is a conservative but reasonable assumption for developing general purpose guidelines. The

results recommended for use in the development of pier design and protection guidelines are shown in Table 19.

1.3.6 Recommended vehicle properties

The vehicle properties recommended for use in development of the bridge pier risk assessment and protection guidelines based on the discussions in the previous sections are shown in Table 20.

Table 20. Recommended Vehicle Properties for use in Guideline Development.

Vehicle Type	FHWA Class	RSAP Vehicle Type	VEHICLE CHARACTERISTICS				
			Weight	Length	Width	C.G. Long.	C.G. Height
			lbs	ft	ft	ft	ft
Passenger Cars	2	C	3,300	15.00	5.40	6.00	2.00
Pickup Trucks	3	PU	5,000	19.75	6.50	8.50	2.30
Light Single Unit Truck†	5-7	LSUT	11,500	35.00	7.77	11.60	3.40
Average Single Unit Truck	5-7	ASUT	15,000	35.00	7.77	12.25	3.83
Heavy Single Unit Truck	5-7	HSUT	22,000	35.00	7.77	14.17	4.70
Extra-Heavy Single Unit Truck	5-7	EHSUT	50,600	35.00	7.77	16.50	6.19
Light Tractor Trailer†	8-10	LTT	27,000	61.30	8.50	24.58	3.73
Average Tractor Trailer	8-13	ATT	50,000	61.30	8.50	28.75	4.83
Heavy Tractor Trailer	8-13	HTT	80,000	61.30	8.50	30.88	5.42
Extra-Heavy Tractor Trailer	8-13	EHTT	105,000	61.30	8.50	31.75	6.00

† Represents the empty weight